UNIVERSITAT DE
BARCELONA

Syntheses of (S)-Bicalutamide and Somatostatin analogs, and development of Green procedures for Peptide synthesis

Joan Antoni Matarín Morales

Organic Chemistry PhD program

Syntheses of (*S*)-Bicalutamide and Somatostatin analogs, and development of Green procedures for Peptide synthesis

Joan Antoni Matarín Morales

Organic Chemistry PhD Program

Joan Matarín

Firmado digitalmente por Joan Matarín
Nombre de reconocimiento (DN): cn=Joan
Matarín, o=BCN Peptides, ou=UGQ,
email=jamatarin@bcnpeptides.com, c=ES
Fecha: 2021.09.23 12:43:07 +02'00'

Thesis directors

Dr. Antoni Riera Escalé

Departament de Química Orgànica

Universitat de Barcelona

IRB Barcelona

Dr. Josep Farrera Sinfreu

Departament de Recerca i

Desenvolupament

BCN Peptides

Memòria presentada per Joan Antoni Matarín Morales per a optar al grau de DOCTOR en Química per la Universitat de Barcelona.

Joan A. Matarín Morales

Revisada per:

Dr. Josep Farrera Sinfreu

Dr. Antoni Riera Escalé

Barcelona, Setembre 2021

One dream, one soul, one prize, one goal

One golden glance of what should be

It's a kind of magic

Queen

Agraïments

Ja han passat quatre anys des que vaig començar la tesi, el temps vola! Quatre anys de recerca, experiments, molt treball, moltes hores i molts canvis. Durant aquest temps m'he creuat amb infinitat de persones que m'han ajudat, animat, aconsellat o fet riure, i voldria agrair-los-hi en aquesta secció.

En primer lloc m'agradaria donar les gràcies al Dr. Antoni Riera que ha estat el meu supervisor des de fa cinc anys, per la oportunitat de treballar a URSA i l'IRB, per tot el que m'ha ensenyat, pels bons moments al laboratori i, sobretot, per tenir sempre la porta del despatx oberta per parlar de qualsevol cosa. En segon lloc, estic també molt agraït al Dr .Josep Farrera, el meu co-director de tesi a BCN Peptides, el qual m'ha ensenyat tot el que sé de síntesi de pèptids. Les seves idees, consells i recomanacions m'han permès desenvolupar els projectes que hem dut a terme durant aquests quatre anys. Toni i Josep, us estic molt agraït per l'oportunitat de fer la tesi amb vosaltres.

Als membres de la meva comissió de seguiment/TAC: Dr. Xavier Salvatella, Dra. Gemma Triola i Dra. Anna Grandas, moltes gràcies pels vostres consells, preguntes i recomanacions durant aquests quatre anys que m'han permès millorar i explicar millor els resultats obtinguts. Moltes gràcies a la Dra. Judit Tulla-Puche per haver sigut membre de la meva comissió de seguiment durant els primers dos anys.

A la Dra. Anna Escolà per haver sigut la meva antecessora en la síntesi de nous anàlegs de SOM. Sense els descobriments i les conclusions de la teva tesi no podria haver arribat fins on hem arribat en aquest projecte. A part d'això, t'estic molt agraït per ser la meva amiga i per totes les converses, consells, recomanacions i sobretot pels bons moments viscuts a URSA i a BCN. M'has ajudat moltíssim i t'estaré sempre agraït! Baby, I don't need dollar bills to have fun tonight (I love cheap thrills)!

Al Dr. Craig Donoghue, it all began when we met on summer of 2015 to help you with the Guaymoxifen project. We worked hard and had a good laugh for three months. Thank you for what you thaught me that summer and the years that we worked together in URSA. Hope you have an amazoning future Craig! URUGUASHO!

A ex-membres d'URSA com l'Ernest, Dan, Javi, Enric, Marta, Sílvia, Marc R., Edgar, Marc F., Helena com als membres actuals Marina B., l'home dels tres noms, Guillem, Pep, Mireia moltíssimes gràcies pels riures, consells i bones estones que hem passat al Lab. No podía dejarme a los miembros de mi pasillo: a la presi, al vice y a Caro, sois los mejores, no hay palabras para describir el vínculo que tenemos. Amparo, sin nuestra Presi estaríamos totalmente perdidos. Te agradezco muchísimo todo lo que me enseñaste todo el tiempo que fuimos compañeros de pasillo. Albert C., per tots els riures, per tots els berenars, per molts moments viscuts al teu costat, ets un crack d'investigador i de persona! Carolina trátame bien, la señora rotavapores, que ratos pasamos haciendo síntesis a gran escala, eres un pozo de sabiduría, tienes una anécdota para todo y muchísimos amigos perdidos por el mundo, ¡he aprendido mucho de ti y te estoy muy agradecido!

També vull agrair les seves recomanacions i consells al Dr. Xavier Verdaguer, al Dr. Arnald Grabulosa i a l'Albert G. durant les diferents reunions de grup de recerca que hem tingut al llarg d'aquests anys.

Table of contents

Abbreviations and units

(Benzotriazol-1-yloxy)tripyrrolidinophosphonium hexafluorophosphate (PyBOP)

1,4-Diazabicyclo[2.2.2]octane (DABCO)

1-ethyl-3-(3-dimethylaminopropyl)- carbodiimide (EDC)

2,2,4,6,7-pentamethyldihydrobenzofuran-5-sulfonyl (Pbf)

2,2,5,7,8-pentamethylchromane-6-sulfonyl (Pmc)

2,6-lutidine (LUT)

2-chlorotrityl chloride (CTC)

2-methyltetrahydrofuran (2-MeTHF)

4-Methylbenzhydrylamine (*p*MBHA)

Acetate counterion (AcO$^-$)

Acetic acid (AcOH)

Acetonitrile (ACN)

Acetyl (Ac)

Adrenocorticotropic hormone (ACTH)

Anhydrous (anh.)

Area under the curve (AUC)

Atomic Mass Unit (amu)

Benzyl (Bzn)

Carboxybenzyl (Cbz)

Celsius degree (ºC)

ChemMatrix resin (CM)

Cushing's Disease (CD)

Cyclopentyl methyl ether (CPME)

Dichloromethane (DCM)

Diethyl ether (DEE)

Diethylaminosulfur trifluoride (DAST)

Diisopropylcarbodiimide (DIPCDI)

Diisopropylethylamine (DIEA)

Diketopiperazine (DKP)

Dimethyl carbonate (DMC)

Dimethylamino pyridine (DMAP)

Dimethylsulfoxide (DMSO)

Diphenylphosphoryl azide (DPPA)

Dodecanethiol (DCT)

Enantiomeric excess (ee)

Enzyme replacement therapy (ERT)

Equivalents (eq)

Et alia (et al.)

Ethanol (EtOH)

Ethyl acetate (EtOAc)

European Medicines Agency (EMA)

Fluorenylmethoxycarbonyl (Fmoc), Fluorenylmethyl (Fm)

Food and Drug Administration (FDA)

Gastroenteropancreatic (GEP)

Gastrointestinal (GI)

Glycosaminoglycans (GAGs)

Good Manufacturing Practices (GMP)

G-protein-coupled receptor (GPCR)

Gram (g)

Growth Hormone (GH)

Haematopoietic stem cell transplantation (HSCT)

Half-life ($t_{1/2}$)

Hexafluoroisopropanol (HFIP)

High Performance Liquid Chromatography (HPLC)

High Resolution Mass Spectroscopy (HRMS)

Hours (h)

Hydroxybenzotriazole (HOBt)

Hydroxysuccinimide (HOSu)

Identification (ID)

Inhibition constant (K_i)

Isopropanol (IPA)

Kilogram (kg)

Leuprolide (LP)

Liquid Chromatography (LC)

Liter (L)

Long-acting release (LAR)

Lysosomal Storage Diseases (LSDs)

Mass spectrum (MS)

Mass/charge ratio (m/z)

m-chloroperoxybenzoic acid (*m*CPBA)

Mesityl alanine (Msa)

Methanol (MeOH)

Microliter (µL)

Micromolar (µM)

Microwave (MW)

Milligram (mg)

Milliliter (mL)

Millimeter (mm)

Millimol (mmol)

Millimolar (mM)

Minutes (min)

Model peptide (MP)

Molecular Weight (MW)

N,N-dimethylformamide (DMF)

Nanometer (nm)

Nanomolar (nM)

N-butylpyrrolidone (NBP)

N-carboxyanhydrides (NCA)

Neuroendocrine differentiation (NED)

Neuroendocrine Tumors (NETs)

N-formylmorpholine (NFM)

N-hydroxy-5-norbornene-2,3-dicarbocyclic acid imide (HONB)

N-methylmorpholine (NMM)

N-methylpiperidine (NMPip)

N-methylpyrrolidone (NMP)

Nuclear Magnetic Resonance (NMR)

Nuclear overhauser effect spectroscopy (NOESY)

Parts per million (ppm)

Pentafluorophenol (PFP)

Peptide receptor imaging (PRI)

Peptide-receptor radiotherapy (PRRT)

Phase analyzer reactor (PA)

Phenyl (Ph)

Polyethylene glycol (PEG)

Polystyrene (PS)

Positron emission tomography (PET)

Propylene carbonate (PC)

Protecting groups (PGs)

p-toluenesulfonic acid (*p*TSA)

Retention time (t$_R$)

Rink amide linker (RAM)

Room temperature (RT)

Seconds (s)

Single-photon emission computed tomography (SPECT)

Solid-Phase Peptide Synthesis (SPPS)

Solvent volumes (vol)

Somatostatin (SST or SST14)

Somatostatin analogs (SSAs)

Somatostatin Receptor (SSTR)

Substrate reduction therapy (SRT)

██████

████████

Temperature (T)

TentaGel resin (TG)

Tert-butyl (*t*Bu)

Tert-butyl methyl ether (MTBE)

Tert-butoxycarbonyl (Boc)

Tetrahydrofuran (THF)

Thin-layer chromatography (TLC)

Thioanisole (TAN)

Threoninol (Throl)

Time (t)

Total correlated spectroscopy (TOCSY)

Transmembrane Domains (TMDs)

Triethylbenzylammonium chloride (TEBAC)

Trifluoroacetate counterion (TFA$^-$)

Trifluoroacetic acid (TFA)

Trifluoroethanol (TFE)

Triisopropylsilane (TIS)

Trityl (Trt)

Tyr^3-octreotide (TOC)

Ultra Performance Liquid Chromatography (UPLC)

Ultraviolet (UV)

Urinary free-cortisol (UFC)

Visible (vis)

Wavenumber (λ)

γ-valerolactone (GVL)

Chapter 1

Introduction and objectives

1 Introduction and objectives

1.1 Introduction

1.1.1 Principles of Peptide Chemistry

Peptides are defined as compounds that contain between two and fifty amino acids connected together by amide bonds[1] (Figure 1.1). Inside our body, peptides are the natural biological messengers that play critical roles in human physiology acting as hormones, neurotransmitters, growth factors or antibacterial agents[2]. Because of these functions, peptides represent a unique class of pharmaceutical compounds, molecularly between small molecules and proteins, yet biochemically and therapeutically distinct from both[3].
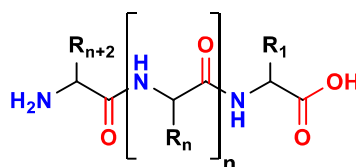
Figure 1.1 General peptide structure

Currently, synthetic peptides are produced industrially for the treatment of cancer, diabetes, as well as cardiovascular and neurodegenerative diseases, among others. In addition, these compounds are also used in cosmetics, diagnostics, and medicinal technology products, as well as in veterinary medicine, agrochemistry, or as dietary supplements[4].

The inherent properties of peptides define their strengths and weaknesses as drug molecules[2]. In general, peptides are membrane impermeable, thus their therapeutic application is restricted to extracellular and transmembrane targets[2]. In addition, their administration needs to be mainly parenteral in detriment to the comfort and convenience of the patient because peptides are unable to permeate the intestinal mucosa[2]. Related to this, peptides are also generally unable to cross the blood-brain barrier which eliminates central nervous system targets[2]. Furthermore, as natural peptides are the principal biological messengers in our body, they are also unstable displaying short plasma half-lives, which permits them to perform their physiologic function and be rapidly metabolized. Proteolytic degradation and renal filtration are the two main methods of peptide clearance in our body[5]. Nevertheless, peptides show a predictable metabolism in contrast to small molecules. As a consequence, they have a low incidence of side effects, because their metabolites are rarely toxic, which is often the reason for small molecules to fail in clinical trials[5]. Only in some cases, peptides can cause an immunogenic response.

Overall, natural peptides represent viable and validated leads for drug discovery, which permits to synthesize more potent and selective analogs with minimal side effects[2,5,6]. Because of this

reason, peptides have greatly impacted the development of modern pharmaceutical industry presenting opportunities for therapeutic intervention that closely mimic natural pathways. In fact, several peptide drugs are essentially replacement therapies that supplement peptide hormones in cases where endogenous levels are inadequate or absent[3]. Under this point of view, the discovery and development of the 51-amino acid hormone insulin (Figure 1.2), stands as one of the principal scientific achievements of the 20th century[2]. Following its initial isolation in 1921, this "miracle drug" reached diabetic patients only one year later becoming the first commercially available peptide drug in 1923[2]. Nowadays, the global Peptide Therapeutics market size is projected to reach US$ 42 billion by 2026, from US$ 33 billion in 2020[7].
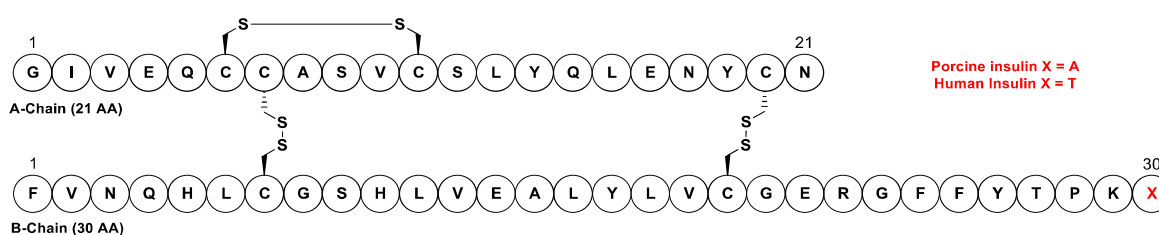
Figure 1.2 Chemical structures of porcine (X = A) and human insulin (X = T)

1.1.2 Green Peptide Synthesis

The first efforts on peptide synthesis date from the 1900s, when Curtius and Fischer presented early procedures for the chemical synthesis of oligopeptides. Introduction of cleavable protecting groups (PGs) enabled the condensation of amino acids with a great variety of functional groups in their sidechains. Thus solution-phase synthetic methods allowed the production of impressively long peptides. However, the real breakthrough in the field was the concept of solid-phase peptide synthesis (SPPS) reported in 1963 by Bruce Merrifield, who envisaged the use of a polymeric insoluble resin to make the peptide chain grow without having to isolate every synthetic intermediate as in solution-phase strategies. This idea owned the American researcher the Chemistry Nobel Prize in 1984. Since then, peptide synthesis has been significantly developed in terms of more efficient synthetic procedures, having taken advantage of novel protection methodologies (*e.g.* Fmoc/*t*Bu strategy), automation, microwave assistance and advanced analytics[4,5]. Moreover, smaller teams of medicinal chemists are needed to perform peptide drug optimization thanks to the relative simplicity and increasing automation of peptide synthesis in comparison to equivalent optimization efforts on small molecules[2].

To date, Fmoc/*t*Bu SPPS (Figure 1.3) has gained almost optimal efficiency in terms of coupling yields and duration in detriment to solvent consumption, which has been recognized as an economic and environmental issue. In addition, the solvents that are currently used in SPPS such as *N,N*-dimethylformamide (DMF), *N*-methylpyrrolidone (NMP) or dichloromethane (DCM) are

classified as substances of very high concern because of their carcinogenic, mutagenic, or toxic properties[4,8].
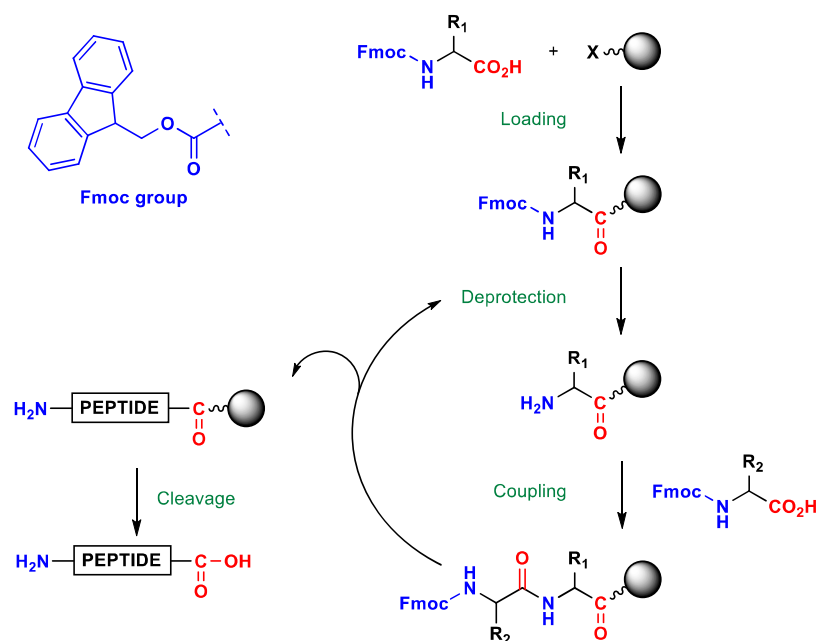
Figure 1.3 Experimental scheme of Fmoc/tBu SPPS[9]

In the 1990s, the field of Green Chemistry emerged to increase sustainability by reducing pollution and using less hazardous substances. In 1998, the 12 principles of Green Chemistry were introduced[10], considering all aspects of the chemical process, the toxicity of the products, solvents, reagents, and catalysts, safety issues, and the energy required. As current SPPS procedures are not green in terms of solvent consumption and use of hazardous substances, great research efforts have been performed in the last decade to bring closer SPPS to Green Chemistry.

The **first objective** of this doctoral thesis was to chemically explore new green SPPS methodologies that permit: i) the reduction of hazardous organic solvents using water as the main one; and ii) the minimization of PGs using N-α-unprotected amino acids. The results obtained during the exploration of green SPPS methods and procedures will be described in **Chapter 2**.

Fmoc/tBu SPPS has been established since the end of the 1970s as the most convenient strategy to synthesize peptides. The use of orthogonal PGs such as the base-labile Fmoc N-protecting group and the acid-labile PGs of the amino acid sidechains (*e.g.* Trt, Boc, *t*Bu, Pbf) permitted to use trifluoroacetic acid (TFA) only once, specifically, in the last cleavage/deprotection step of the synthesis after all the desired amino acids have been already coupled to the peptide chain. In addition, once the acidic peptide solution is separated from the polymeric resin, the peptide must be precipitated with great volumes of diethyl ether (DEE).

Under a green perspective, TFA is an aggressive and extremely corrosive acid capable of inflicting harm to our body by inhalation or skin contact leaving hard to heal chemical burns. Furthermore, it is relative expensive, both for the initial purchase and for ultimate disposal. Considering DEE, it is also a high concern substance due to its extreme volatility, flammability and may produce narcotic effects and drowsiness after exposure. As great amounts of TFA and DEE are needed in the cleavage/deprotection process of peptides, especially in industrial peptide synthesis, the reduction or substitution of these substances in these cleavage/deprotection procedures is very desirable[11].

The **second objective** of this doctoral thesis was to study the possible use of ███████ ████████ ███ █ ████ ████ in peptide cleavage and deprotection procedures. Methodologies using ████ as a green solvent will be explored with the purpose of █████████ ████████ █ ███ ███ ███ ██ normally used in this step. The results of the cleavage/deprotection experiments using ████ will be discussed in **Chapter 3**. The experiments shown in this chapter correspond to a research project of BCN Peptides.

1.1.3 Somatostatin

Somatostatin (SST14) is a 14-amino acid cyclopeptide hormone that was discovered in 1973 from ovine hypothalamus extracts[12] (Figure 1.4). In the human body, SST14 acts as a neuromodulator and a neurotransmitter, as well as a potent inhibitor of various secretory processes and cell proliferation[13]. This peptide accomplishes its activity through direct binding to its five receptors subtypes (SSTR1-5), which are G-protein-coupled receptors (GPCRs)[14,15]. Under a structural point of view, its pharmacophore consists in the β-turn formed by Phe^7-Trp^8-Lys^9-Thr^{10}, in which Trp^8-Lys^9 are essential for its interaction with SSTRs. Because of its broad modulatory activity, SST14 has been traditionally conceived as an interesting peptide for clinical applications. However, its full therapeutic potential could not be exploited because of its short plasma half-life ($t_{1/2}$ < 3 min)[16,17]. Therefore, since the 1980s researchers put a great effort on finding new somatostatin analogs (SSAs) with different selectivity profiles and improved stability to enhance their *in vivo* efficiency. The first analogs that reached the market were octapeptides that incorporated D-amino acids and conserved the pharmacophore of SST14. These shorter derivatives were octreotide[18], vapreotide[19] and lanreotide[20], which displayed high nanomolar binding affinity for SSTR2 and SSTR5. In addition to these, the last analog that reached the market was pasireotide[21], a cyclic hexapeptide with affinity for SSTR1,2,3,5.
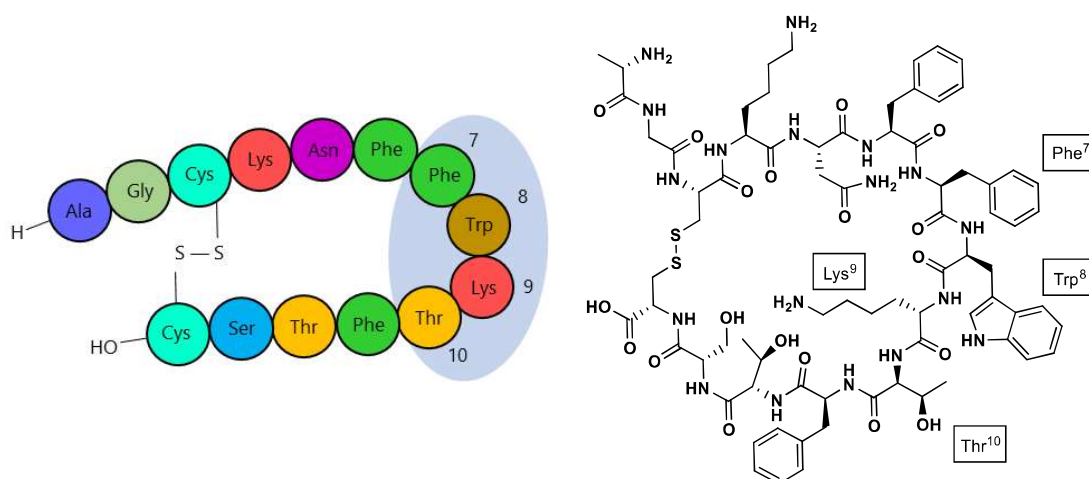
Figure 1.4 SST14: H-Ala¹-Gly²-c(Cys³-Lys⁴-Asn⁵-Phe⁶-Phe⁷-Trp⁸-Lys⁹-Thr¹⁰-Phe¹¹-Thr¹²-Ser¹³-Cys¹⁴)-OH

The strategy of BCN Peptides and Riera Lab in the development of these analogs consisted in the modification of the original SST14 sequence with unnatural aromatic amino acids while maintaining the 14-residue structure. By doing this, both the conformation of the synthesized analogs and their biological activity could be effectively modulated. In collaboration with Maria Macias group and following this strategy, a great number of SSAs have been synthesized and characterized in detail throughout different doctoral theses[22–26], publications[27–32] and a patent[33]. At present, BCN Peptides is conducting veterinary clinical trials with one of these analogs, which is coded as **A64**.

The **third objective** of this doctoral thesis was to design and develop new stable analogs maintaining the 14-amino acid structure of the parent peptide. Unnatural (*e.g.* Msa[28]) and D-amino acids[34] will be used for the design of these new analogs, whose synthesis and characterization will be described in **Chapter 4**.

1.1.4 (*S*)-Bicalutamide

Bicalutamide is an oral non-steroidal anti-androgenic drug that is used in the treatment of prostate cancer and that was firstly administered in 1995[35]. Bicalutamide displays anti-androgen activity by competing with testosterone and dihydrotestosterone for binding sites of androgen receptors, as well as by preventing their activation[36]. Bicalutamide is administered clinically in its racemic form, although the anti-androgenic activity is exclusively found in the (*R*)-enantiomer, being (*S*)-bicalutamide inactive and non-toxic[35] (Figure 1.5).

Recently, Farrera and co-workers[35] at BCN Peptides demonstrated the potential use of (*S*)-bicalutamide as an exocytosis activating compound that could be used to treat Lysosomal Storage Diseases (LSDs). This type of diseases are genetic disorders that involve the accumulation of macromolecules inside the cells, concretely in the lysosomes. This abnormal accumulation

might initiate a cascade of secondary effects, ultimately leading to irreversible cellular damage, cell death, organ dysfunction and/or organ degeneration[37]. In general, current therapies for LSDs such as haematopoietic stem cell transplantation (HSCT), enzyme replacement therapy (ERT) or substrate reduction therapy (SRT) offer limited benefits because of incompatible donors, possible graft failure and inability to cross the blood-brain barrier. (*S*)-bicalutamide proved to be effective *in vitro* in all the tested LSDs and demonstrated to be a potential universal treatment for prevention of the damaging clinical symptoms of these diseases. Despite the *in vitro* results, the effectiveness of (*S*)-bicalutamide must be confirmed *in vivo* in preclinical and clinical studies before submitting it to the corresponding pharmaceutical regulatory agencies.
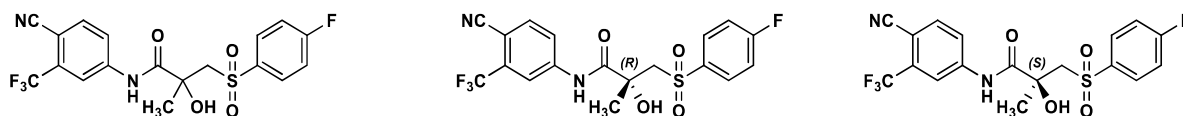
Figure 1.5 Chemical structures of bicalutamide, (R)-bicalutamide and (S)-bicalutamide

Therefore, the **fourth objective** of this doctoral thesis was to design and develop an enantioselective route to obtain (*S*)-bicalutamide, as well as its precursors using large-scale procedures and methodologies. In addition, the developed synthesis will be adapted to follow Good Manufacturing Practices (GMP) to produce (*S*)-bicalutamide according to the required quality standards to use it in preclinical and clinical trials. The large-scale synthesis of (*S*)-bicalutamide and its precursors will be described in **Chapter 5**.

1.2 Objectives

To summarize, the main objectives of the present Doctoral Thesis were:

- Exploration of Green SPPS methodologies that permit to: reduce the use of hazardous organic solvents (*e.g.* DMF or DCM) in favor of water and use *N*-α-unprotected amino acids to improve the atom economy of the process (**Chapter 2**).

- Development of a methodology using ▮▮▮▮▮▮▮▮▮▮▮▮▮▮▮▮▮▮▮ as a green solvent to ▮▮▮▮▮▮▮▮▮▮▮▮▮▮▮▮▮▮▮▮▮ employed in standard cleavage and deprotection procedures (**Chapter 3**).

- Design, synthesis and characterization of new stable 14-amino acid somatostatin analogs using unnatural (*e.g.* Msa) and D-amino acids in determined key positions of the structure (**Chapter 4**).

- Design and development of a large-scale synthetic route to obtain (*S*)-bicalutamide and its precursors according to the required quality standards to employ it in preclinical and clinical trials (**Chapter 5**).

Chapter 2

Green Solid-Phase Peptide Synthesis

2 Green Solid-Phase Peptides Synthesis

2.1 Introduction

2.1.1 Standard Solid-Phase Peptide Synthesis

Solid-Phase Peptide Synthesis (SPPS) has received increasing attention by the industrial sector since the pioneering report of Bruce Merrifield in 1963[38]. The use of a polymeric support as a permanent protecting group (PG) for the first amino acid simplified the procedure and scale-up, outperforming previous solution phase strategies. Because of these reasons, SPPS has been adopted as the strategy of choice for the production of peptides in both the industrial and research contexts[39–41]. The SPPS protocol consists in three main steps in each reaction: i) addition of reagents; ii) filtration; and iii) washing. This straightforward protocol permits the synthesis of peptides with up to 50 amino acid residues[6] with satisfactory yields[1].
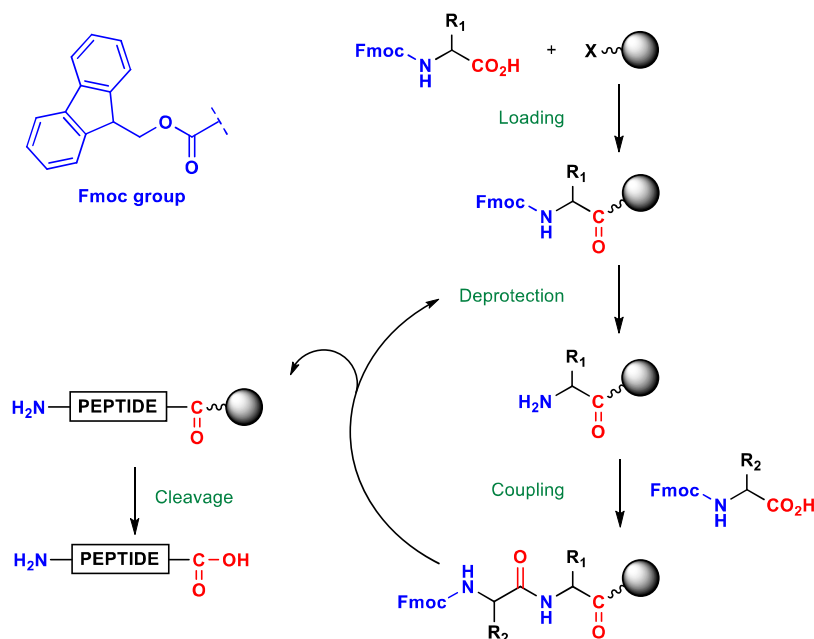
Figure 2.1 Experimental scheme of Fmoc/tBu SPPS[9].

Apart from the use of a solid support as the first PG, to employ protected amino acids is also crucial to avoid side-reactions and the formation of impurities. Depending on the PGs that are used there are two main SPPS strategies: i) *tert*-butoxycarbonyl (Boc) /benzyl (Bzl) strategy reported by Merrifield[38]; and, ii) Fluorenylmethoxycarbonyl (Fmoc) /*tert*-Butyl (*t*Bu) strategy reported by Louis Carpino[42,43] (Figure 2.1). The Fmoc/*t*Bu strategy is based on an orthogonal scheme in which these two PGs are removed by different mechanisms[44]. The Fmoc group is removed from the α-amino group through a β-elimination reaction with a base. The sidechain PGs

---

[1] Thanks to this innovative work, Bruce Merrifield was awarded with the Chemistry Nobel Prize in 1984.

(*e.g.* Trt, *t*Bu, Boc and Pbf[2]) and the peptide resin bond are cleaved in mild acid media, mainly trifluoroacetic acid (TFA). In contrast, the Boc/Bzl strategy requires the use of TFA after each coupling cycle to remove the Boc group and requires strong acids such as hydrofluoric acid to cleave the peptide from the polymeric resin and remove the Bzl groups[45].

As the Fmoc/*t*Bu strategy does not involve the use of hazardous reagents for peptide cleavage, and it minimizes the use of TFA to only one step of the synthesis, this strategy has been established as the preferred chemical approach for SPPS. Despite this, the use of the Fmoc group has some disadvantages: i) its hydrophobicity does not permit to work in an aqueous context; and ii) its aromatic character favors π-π interactions that might lead to the collapse of the resin. As a consequence, the base and the solvent of the Fmoc removal step are very important because deletion peptides might be generated as a result of poor Fmoc removal. Traditionally, solutions of piperidine in *N,N*-dimethylformamide (DMF) have been extensively used.
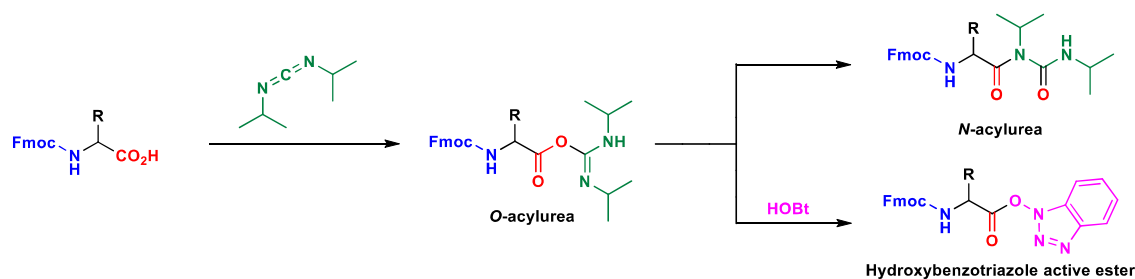
Figure 2.2 Activation scheme of Fmoc-amino acids with DIPCDI/HOBt

Apart from Fmoc removal, the amide bond formation is also a very demanding reaction. Carbodiimides are the most widely used coupling reagents, being diisopropylcarbodiimide (DIPCDI) the standard one for Fmoc/*t*Bu chemistry. In this thesis, EDC [3] a water-soluble carbodiimide will be extensively used. The general reaction of amino acids with carbodiimides generates a highly reactive *O*-acylurea that might form several undesired products such as *N*-acylurea (Figure 2.2). To prevent this, the activation is normally carried out in the presence of *N*-hydroxyl-containing reagents, which render more suitable active esters. Hydroxybenzotriazole (HOBt)[46], hydroxysuccinimide (HOSu)[47] and OxymaPure[48] are clear examples of these reagents, which additionally minimize racemization.

After the linear synthesis is completed following the Fmoc/*t*Bu strategy, the final peptide needs to be cleaved from the solid support. Two main cleavage strategies are performed using TFA as the source of protons: i) global cleavage/deprotection with a high content of TFA in the presence of scavengers, which cleaves the peptide from the resin and removes the sidechain PGs; and

---

[2] Pbf (2,2,4,6,7-pentamethyldihydrobenzofuran-5-sulfonyl).
[3] EDC (1-ethyl-3-(3-dimethylaminopropyl)carbodiimide).

ii) cleavage of protected peptides with organic solutions that contain a low proportion of TFA (normally 1-4% in DCM) for the treatment of acid-labile resins (*e.g.* 2-chlorotrityl chloride (CTC))[49]. In cleavage/deprotection procedures, the peptide crude is filtered and precipitated using cold diethyl ether (DEE)[50]. In cleavage of protected peptides, the resin suspension is filtered and the solvent is eliminated under reduced pressure to obtain the protected peptide for further development (*e.g.* disulfide bond formation).

2.1.2 Greening of Solid-Phase Peptide Synthesis

Green Chemistry is defined as the design of chemical products and processes to reduce or eliminate the use and generation of hazardous substances[10]. Since the publication of this report by Anastas and co-workers in the 1990s, green chemistry is now established to a greater or lesser extent in all the fields of organic chemistry, being SPPS no exception.

Under this perspective, SPPS has already some features associated with green chemistry[51]: i) a single reactor is used for all the reactions, minimizing cleaning and matter transfer processes; ii) simple work-up procedures, avoiding extraction techniques; iii) no purification of the intermediates, increasing the final yield and saving solvent and time; iv) quantitative conversion and high yields; v) high purity crudes with straightforward purification; and vi) possibility of parallelization and automatization[51].

Despite these features, standard SPPS also shows low scores on some green chemistry metrics[51]. The use of PGs has a huge negative impact on the atom economy[4] of the process. For example, only 20% of the mass of Fmoc-Gly-OH is retained in the final product when the Gly residue is introduced[51]. Minimizing or avoiding the use of PGs might help to address this issue. Similarly, excess of reagents and large amounts of solvents used in the amino acid coupling, the Fmoc elimination and washes between steps penalize the E-factor[5] metric.

With all these in mind, a great number of green strategies for SPPS have been reported in the literature. Some of these include aqueous-based strategies, use of organic green solvents and use of unprotected amino acids.

2.1.2.1 Aqueous Peptide Synthesis

Water might be considered as the most optimal green solvent[6], but the disposal or recycling of "chemically contaminated" water is not a straightforward process[51,52]. Due to the lack of solubility of Fmoc-amino acids in water, several strategies to overcome this problem have been

---

[4] Atom economy is defined as how much of the mass present in the starting materials remains in the final product[314].

[5] E-factor is defined as the ratio of total mass of waste to the mass of the isolated product.

developed[51]: i) Water-soluble PGs, ii) Aqueous Nanoparticle Peptide Synthesis; and, iii) Microwave-assisted Aqueous Peptide Synthesis.

As SPPS reactions are diffusion-dependent, the swelling of the polymeric support is one of the most important prerequisites for a successful reaction[53]. Water-based SPPS protocols need polymeric supports with high hydrophilic components. Some examples are polyethylene glycol (PEG)-PS resins (*e.g.* TentaGel® (TG)) or PEG-based resins (*e.g.* ChemMatrix® (CM)) with increased water-swelling properties in comparison to the traditional resins based on Polystyrene (PS). In the industrial synthesis of peptides, PS resins are still the polymeric support of choice due to considerations of price and commercial availability. In contrast, PEG-PS or CM reins are often chosen in the research context for the synthesis of difficult peptides.

2.1.2.1.1 Water-soluble Protecting Groups
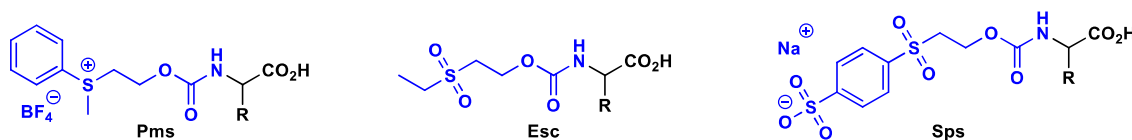
Figure 2.3 Water-soluble N-protecting groups developed by Hojo and co-workers[54–57]

In the 2000s, the first attempts to substitute the Fmoc group by a more water-soluble alternative were performed by Hojo and co-workers[54–57] who introduced the Pms[6], Esc[6] and Sps[6] N-protecting groups (Figure 2.3). The removal of these water-soluble PGs occurred through a β-elimination pathway similar to Fmoc but using a 5% $NaHCO_3$ solution instead of traditional piperidine/DMF mixtures. By using these water-soluble PGs the authors were capable of synthesizing Leu-enkephalin[7], an endogenous opioid peptide neurotransmitter[58] whose sequence is synthetically demanding[59]. The couplings were performed using the previous N-protected amino acids (4 eq), EDC (4 eq) and HONB[8] (4 eq) at RT for 3h in 0.2% Triton X-100 aqueous solution. However, these water-soluble PGs suffered from some drawbacks, such as chemical instability (Pms) or inefficient removal with aqueous solutions (Esc). Because of this, the yields and purities of the model peptide Leu-enkephalin were much lower than those achieved by standard Fmoc/*t*Bu protocols[60].

Recently, Knauer and co-workers[4,61] introduced sulfonates (SO_3^-) as water-solubility enhancing groups, not only into Fmoc but also to sidechain PGs (Figure 2.4). Smoc-amino acid derivatives could be obtained in high yields with only one-step reaction using concentrated sulfuric acid. These new PGs were used to synthesize the hydrophobic H-Val^1-Gly^2-Gly^3-Val^4-Gly^5-OH peptide

---

[6] Pms (2-[phenyl(methyl)sulfonio]-ethoxycarbonyl); Esc (2-ethanesulfonylethoxycarbonyl); and Sps (2-(4-sulfophenylsulfonyl)ethoxycarbonyl).
[7] Leu-enkephalin (H-Tyr^1-Gly^2-Gly^3-Phe^4-Leu^5-OH).
[8] HONB (*N*-hydroxy-5-norbornene-2,3-dicarboxylic acid imide).

using water as the only solvent[4]. The coupling step was performed using the corresponding Smoc-amino acid (3 eq), EDC (5.5 eq), OxymaPure (3 eq) and NaHCO₃ (3 eq) in water for 1h. Removal of the Smoc group was achieved with two washes of either 1M NaOH, 25% aqueous ethanolamine or 5-10% aqueous piperazine.

Figure 2.4 New PGs developed by Knauer and co-workers[4,61]
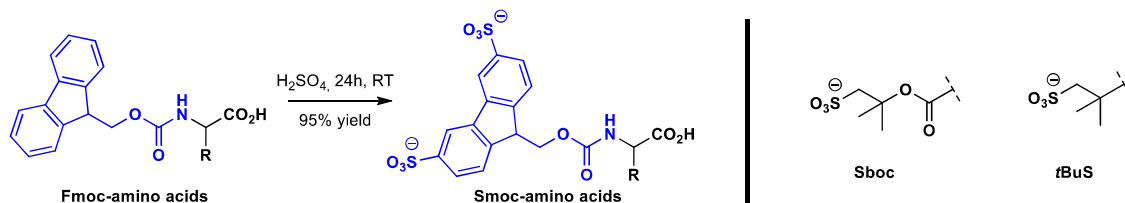
2.1.2.1.2   Aqueous Nanoparticle Peptide Synthesis

Apart from water-soluble *N*-protecting groups, Hojo and co-workers reported as well another innovative approach based on the conversion of either Boc- or Fmoc-amino acids into nanoparticles to enhance their solubility in water[62]. Theoretically, the high surface area of nanoparticles permits their homogeneous mixing with the resin in water, allowing the progression of the coupling reaction. Nanoparticles of Boc- and Fmoc-amino acids[63–67] were prepared using a planetary ball mill in the presence of PEG as a dispersion agent. PEG-based resins compatible with water were also used, as well as Triton X-100 for the washing steps. A variety of activators and additives were employed depending if the coupling reaction was performed at RT[63] or using MW-assistance[64–67]. Fmoc-amino acid nanoparticles (3 eq) were coupled using EDC (3 eq), HONB (3 eq) and DIEA[9] (3 eq) for 1h at RT in water[63]. In contrast, using MW-heating both Boc- or Fmoc-amino acid nanoparticles (5 eq) were coupled using DMTMM[10] (5 eq) and *N*-methylmorpholine (NMM) (5 eq) in 0.2% Triton X-100 at 70ºC for 10 min[65–67]. This water-based protocol permitted the authors to synthesize a variety of demanding peptides such as Leu-enkephalin[63,64,66], acyl carrier protein (ACP$_{65-74}$)[64], oxytocin[65] and rat neuropeptide W-30 (NPW30$_{10-15}$)[67]. These difficult peptides could be obtained in acceptable yields and excellent purities, without racemization.

2.1.2.1.3   MW-aqueous Peptide Synthesis

In organic chemistry, MW-assisted heating has been widely used to overcome low reagent solubilities, as well as to increase reaction rates. In peptide synthesis, MW-assistance has also been used to increase the solubility of Boc- and Fmoc-amino acids in water, as Hojo and co-workers did[65–67]. The main characteristic of MW-heating is that the energy is transferred directly to the reaction mixture rather than first to the reaction vessel and then to the reaction mixture as conventional heating methods[68,69].

---

[9] DIEA (diisopropylethylamine).
[10] DMTMM (4-(4,6-dimethoxy-1,3,5-triazin-2-yl)-4-methylmorpholinium chloride).

Under this perspective, Albericio and co-workers reported a MW-assisted SPPS protocol using water in all the synthetic steps[58]. In this strategy, two MW-cycles composed of Boc-amino acid (5 eq), EDC (5 eq) and HONB (5 eq) in water at 75ºC for 7 min were used in the coupling step. Boc elimination was performed in three MW-cycles using aqueous 1M HCl at 75ºC for 7 min. In addition, 0.5% Triton X-100 was also used to improve the solubility of the amino acid derivatives in water and the swelling of the resin. By applying this protocol, Leu-enkephalin (80% purity) could be synthesized in CM resin[58].

2.1.2.2 Green Organic Solvents

Fmoc/*t*Bu SPPS is the most straightforward way of synthesizing peptides. The use of a solid polymeric PG allows to use excess of reagents to achieve quantitative coupling yields. However, extensive solvent washings have to be performed between the synthetic steps. As water is considered the greenest solvent, it would be desirable to have a robust water-based SPPS methodology. Despite this, aqueous environments are not compatible with conventional PS resins, that are widely used because of their price and commercial availability. In addition, most of the PGs used in standard SPPS (*e.g.* Fmoc, Boc, *t*Bu, Trt, Pbf, etc.) have highly hydrophobic structures that are not soluble in water. Consequently, water is not an option when using PS resins and hydrophobic PGs [51].

DMF, *N*-methylpyrrolidone (NMP) and dichloromethane (DCM), are the organic solvents currently used for couplings and washings in SPPS[70]. All these solvents raise both drastic environmental[71] and health concerns because of their reprotoxicity[72]. Consequently, these solvents are classified as hazardous substances according to several guidelines, and it is desirable to find less harmful substitutes[52].

Before considering a green organic solvent as a good alternative for Fmoc/*t*Bu SPPS various key properties must be assured apart from being non-toxic and sustainable: i) the solubility of protected amino acids and coupling reagents; ii) appropriate swelling of the polymeric support; and iii) acceptable viscosity[6,73]. High viscosities difficult the diffusion of the dissolved reagents inside the resin, impeding them from reaching the reactive sites of the resin beads and decreasing the yields[6]. High viscosity problems might be reduced by increasing the temperature or by using solvent mixtures. In relation to this, resin swelling has to be appropriate (≥ 4 mL·g^{-1}) to allow the dissolved reactants to reach the active sites.

In 2009, acetonitrile (ACN) was the first solvent that could effectively replace DMF in SPPS as reported by Albericio and co-workers[51,74]. The authors designed a protocol in which ACN was used as the major solvent in coupling (OxymaPure/DIPCDI), Fmoc removal and washing steps. By

means of this protocol, model peptides Leu-enkephalin amide[11] and ACP$_{65-74}$[12] could be prepared with purities above 95% using CM resin. Despite this, ACN is not considered as a green solvent[52] because it is not bio-based and cannot be obtained from renewable sources[75]. Nevertheless, ACN can be considered a friendlier alternative to DMF as it is conceived as one of the less problematic dipolar aprotic solvents[71].

In 2013, Watson and co-workers[76] evaluated a panel of green solvents for amide synthesis in substitution of DMF and DCM. A variety of amino acid coupling reactions were examined to conclude that dimethyl carbonate (DMC), 2-methyltetrahydrofuran (2-MeTHF) and ethyl acetate (EtOAc) were suitable alternatives to DMF and DCM[76].

Similarly, Albericio and co-workers[77] demonstrated that 2-MeTHF showed better coupling efficiencies than DMF using DIPCDI/OxymaPure as activators. In addition, 2-MeTHF was used as coupling solvent for the synthesis of Aib-enkephalin amide[13] using both PS and CM resins, obtaining purities of 97% and 82%, respectively. However, DMF was still used in the Fmoc removal and washing steps. To avoid that, Albericio and co-workers[78] reported two complete green SPPS protocols using EtOAc and 2-MeTHF (more details about this protocol in section 9.1.1). By following protocols D and E, Aib-enkephalin amide could be synthesized with purities above 90% in CM resin[78]. On the other hand, moderate purities (~40%) were obtained using protocol E in PS resins, which were only improved when the Fmoc removal step was performed at 40°C (89% purity). In the case of longer peptides such as Aib^{67,68}-ACP$_{65-74}$[14], 87% purity was achieved in CM resin following protocol E but performing the Fmoc removal and coupling steps at 40°C. The authors concluded that the main limitation of these green protocols was the incomplete Fmoc removal, which lowers the purity of the final peptide[78].

Because of the previous problems with Fmoc removal, Albericio and co-workers[79] evaluated the performance of various green solvents confirming the bad performance of 2-MeTHF. Nevertheless, it was found that other green solvents such as *N*-formylmorpholine (NFM) and γ-valerolactone (GVL) were capable of achieving excellent results in CM resin. GVL is considered a green solvent because it is renewable (produced from biomass), has a low melting point (-31°C), a high boiling point (207°C), it is non-toxic and is highly soluble in water[80]. Regarding NFM, it has been reported as a green alternative to hazardous NMP[80].

---

[11] Leu-enkephalin amide (H-Tyr^1-Gly^2-Gly^3-Phe^4-Leu^5-NH$_2$)
[12] ACP$_{65-74}$ (H-Val^1-Gln^2-Ala^3-Ala^4-Ile^5-Asp^6-Tyr^7-Ile^8-Asn^9-Gly^{10}-NH$_2$)
[13] Aib-enkephalin amide (H-Tyr^1-Aib^2-Aib^3-Phe^4-Leu^5-NH$_2$)
[14] Aib^{67,68}-ACP$_{65-74}$ (H-Val^1-Gln^2-Aib^3-Aib^4-Ile^5-Asp^6-Tyr^7-Ile^8-Asn^9-Gly^{10}-NH$_2$)

Following their previous work, Albericio and co-workers[80] reported GVL- and NFM-based SPPS protocols that were evaluated by the demanding synthesis of Aib[67,68]-ACP$_{65-74}$ in PS resins (more details about this protocol in section 9.1.1). Although purities using either GVL or NFM were almost identical (52-54%), they were lower in comparison to protocols that used DMF as the solvent in the Fmoc removal step (89-94%).

Despite the latest results, Albericio and co-workers[81] continued to optimize a protocol using GVL as the single solvent, but this time the authors based their study on the high-efficiency SPPS protocol developed by Collins and co-workers[82]. This protocol involved 165s coupling steps (Fmoc-amino acid/DIPCDI/OxymaPure 5:5:5 eq) and 95s Fmoc removal step (20% piperidine) both at 90ºC using MW-heating and without washes between them (more details about this protocol in section 9.1.1). As a result, only 14 mL of solvent are consumed per amino acid cycle with a duration of 4 min[81,82]. By means of this GVL protocol, a variety of demanding model peptide were synthesized: i) ACP$_{65-74}$ was obtained with a comparable purity profile either with GVL or DMF on PS resin; and, ii) Jung-Redemman[83] decapeptide[15] was obtained on CM resin obtaining better results using GVL than DMF (68% vs 57% purities). As a consequence, Albericio and co-workers[81] proposed GVL as a green alternative for DMF and established its full compatibility with the automation of SPPS in a MW-synthesizer.

North and co-workers[84] reported the use of propylene carbonate (PC) as a green solvent for the synthesis of various model peptides on CM resin. PC is known to be non-toxic, less expensive than DMF and can be prepared by the atom economical reaction between 2-methyloxirane and carbon dioxide (CO_2)[85]. The authors proposed a complete green protocol involving PC in the coupling, Fmoc removal and washing steps (more details about this protocol in section 9.1.1), being capable of synthesizing the model peptide Bradykinin[16] (77% purity). In comparison, this peptide could be obtained with a 79% purity using DMF, demonstrating that PC had no detrimental effect on the synthesis of Bradykinin[84]. In addition, the use of PC as the single solvent enabled the possibility of recycling it as it was not mixed with any other solvent.

Lopez and co-workers[86] performed an extensive study on green solvents that could substitute DMF in SPPS. From the initial 37 green solvents, only tetramethylurea (TMU), 1,3-dimethyl-2-imidazolidinone (DMI), *N*-butylpyrrolidone (NBP) and 1,2-dimethyl-3,4,5,6-tetrahydro-2-

---

[15] Jung-Redemann decapeptide (H-Trp[1]-Phe[2]-Thr[3]-Thr[4]-Leu[5]-Ile[6]-Ser[7]-Thr[8]-Ile[9]-Met[10]-NH$_2$)
[16] Bradykinin (H-Arg[1]-Pro[2]-Pro[3]-Gly[4]-Phe[5]-Ser[6]-Pro[7]-Phe[8]-Arg[9]-OH).

pyrimidinone (DMPU) were selected as reasonable replacements for DMF after carrying out several tests[17].

Using these four green solvents, as well as to dimethylsulfoxide (DMSO) and DMF for comparison reasons, the authors synthesized linear octreotide[18] using an automatic peptide synthesizer. Analysis of the crudes revealed a similar impurity profile, being amino acid deletion sequences the most important impurities. The principal cause of these deletion sequences was assigned to incomplete coupling reactions, which was expected as coupling rates in these solvents are slower in comparison to DMF. Nevertheless, NBP (80%), TMU (78%) and DMI (78%) demonstrated to achieve great peptide purities, though slightly lower than DMF (86%). Consequently, the authors proposed NBP as a promising candidate for green polar aprotic solvents over TMU and DMI, because it is the only one of these that is nontoxic and biodegradable[87]. Despite this, NBP shows a high viscosity that could explain its slightly lower performance in comparison to DMF. To overcome this drawback, North and co-workers proposed to perform the coupling reactions at 40ºC, which is an acceptable temperature even for industrial peptide synthesis[86].

To reduce the viscosity of NBP, Pawlas and co-workers[88] were the first to report the use of binary green solvent mixtures of NBP/EtOAc using different proportions (*e.g.* 1:9 NBP/EtOAc for the washing steps) to reduce the economic impact of NBP (more details about this protocol in section 9.1.1). By doing that, the authors were able to synthesize the melanocortin receptor agonist[19] and perform an on-resin lactamization between the Asp^2-Lys^7 residues of the structure. Although the solvent cost of this NBP/EtOAc protocol is comparable to the use of DMF, the authors propose the recycling of EtOAc from NBP taking advantage of the huge difference on the boiling points of these solvents (77ºC vs 243ºC).

2.1.2.3 Unprotected amino acids in SPPS

The use of PGs lowers both the atom economy and the E-factor of SPPS procedures. As an example, in the introduction of an Arg residue to a peptide chain with Fmoc-Arg(Pbf)-OH, only 24% of the mass of the reagent is still present after the coupling. To minimize the use of PGs and improve the atom economy of SPPS, several strategies have been reported including: i) Acyl benzotriazoles active esters, and ii) *N*-carboxyanhydrides.

---

[17] These tests included: i) Resin swelling; ii) Solubility of reagents and side-products; iii) Coupling reaction using DIPCDI/ OxymaPure; and iv) Fmoc removal.

[18] Linear Octreotide (H-D-Phe^1-Cys^2-Phe^3-D-Trp^4-Lys^5-Thr^6-Cys^7-Throl^8)

[19] Melanocortin receptor agonist (Ac-Nle^1-c[Asp^2-His^3-Phe^4-Arg^5-Trp^6-Lys^7]-NH$_2$)

2.1.2.3.1   Acyl benzotriazoles

Acyl benzotriazoles[89] were used as active esters by Katritzky and co-workers[90–92] to synthesize peptides minimizing the use of PGs in solution phase strategies (Figure 2.5). This methodology consisted in the repetitive coupling of acyl benzotriazoles with unprotected amino acids, growing the peptide from the *N*- to the *C*-terminal (inverse direction). Acyl benzotriazoles might be prepared from Cbz- or Fmoc-amino acids (1 eq) using thionyl chloride (1 eq) and benzotriazole (4 eq) as activators in tetrahydrofuran (THF) at RT. The couplings were carried out in the presence of Et$_3$N in H$_2$O:ACN mixtures. However, this strategy did not work with amino acids that have determined functional groups in their sidechains such as: i) primary amines (*e.g.* Lys) that would react intramolecularly with the α-acyl benzotriazole; or ii) carboxylic acids (*e.g.* Asp, Glu) as the acyl benzotriazole activation is not selective either for the α-carboxylic group or the sidechain[92]. Nevertheless, this strategy permitted to work with amino acids bearing unprotected hydroxyl groups (*e.g.* Ser[90], Tyr[91]), thiols (*e.g.* Cys[91]), secondary amines (*e.g.* Trp[90,91], His[92]) and amides (*e.g.* Asn[92], Gln[91]).
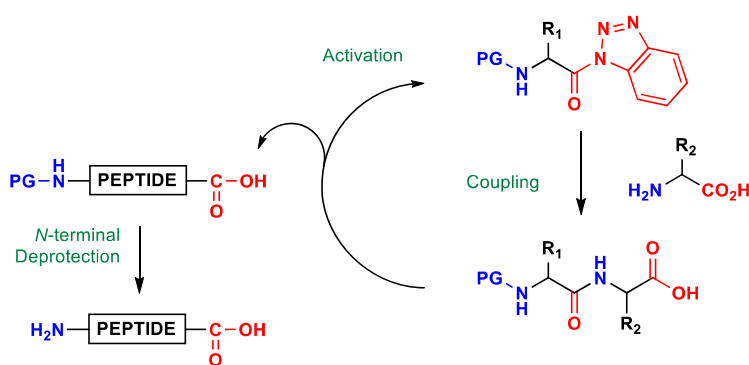
Figure 2.5 Solution phase strategy developed by Katritzky and co-workers[90–92]

2.1.2.3.2   N-carboxyanhydrides

The amino acid coupling is probably the most important step in peptide synthesis as it permits the elongation of the peptide chain. To convert the carboxylic acid into a reactive species is a demanding reaction. The attractiveness of *N*-carboxyanhydrides (NCA) for peptide synthesis resides in their simultaneous α-amino protection and α-carboxylic acid activation[93,94]. As a consequence, the atom economy of NCA condensation is very high as the most part of the NCA mass remains in the newly formed peptide with CO$_{2 (g)}$ as the only byproduct (Figure 2.6). The repeated addition of NCA permits to synthesize the peptide requiring certain degree of control to avoid NCA polymerization[95].
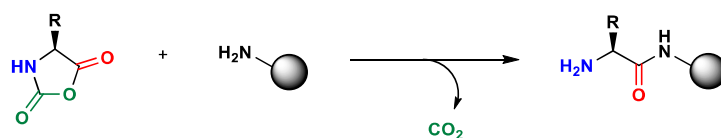
Figure 2.6 Incorporation of NCA with CO₂ (g) as the only byproduct

Lamaty and co-workers[96] have used NCA for the preparation of di- and tripeptides under solvent-free conditions by using ball-milling technology. This methodology permitted to obtain aspartame[20] in only three steps (Figure 2.7). Nevertheless, liquid grinding assistant (1.4 µL of EtOAc per mg of reactants) was needed to increase the reaction rate of the reagents, as well as to scale-up the synthesis to obtain other short peptides[97].
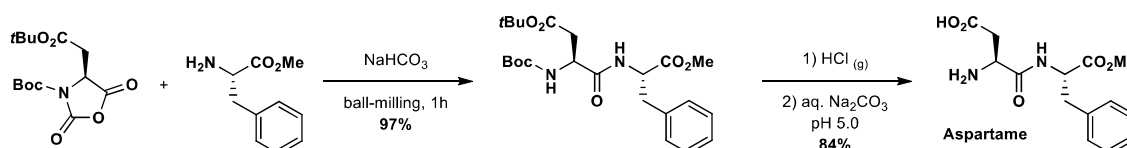
Figure 2.7 Aspartame synthesis in solvent-free conditions using NCA[96]

De Marco and co-workers[95] reported the SPPS of endomorphin-1[98] (EM1)[21] on CM resin using water as the solvent and NCA amino acid derivatives (Figure 2.8). The authors also reported the preparation of these NCA in small scale using triphosgene under solvent-free conditions and MW-heating at 80ºC and used them without any further purification.
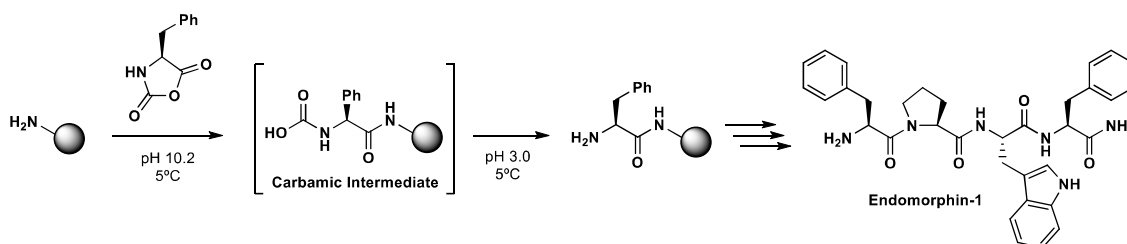
Figure 2.8 Synthesis of Endomorphin-1 by De Marco and co-workers[95]

Regarding peptide synthesis[95], CM resin had to be swollen initially with borate buffer (pH 10.2). Then, the corresponding NCA (3 eq) was added at 5ºC and the suspension was mechanically shaken for 3h. Next, the resin was filtered, washed with citrate buffer (pH 3.0), and finally with borate buffer (pH 10.2). Under these controlled conditions, the authors could effectively avoid NCA polymerization based on the relative stability of the carbamic acid intermediate in an aqueous environment at basic pH. This carbamic acid prevents the formation of the free aminopeptide while the NCA is still present in the reaction mixture, thus avoiding NCA polymerization.

---

[20] Aspartame (H-Asp^1-Phe^2-OMe).
[21] Endomorphin-1 (H-Tyr^1-Pro^2-Trp^3-Phe^4-NH₂)

2.2 Synthetic proposal

Our green SPPS proposal is based on: i) the reduction of hazardous organic solvents using water as the main one; and ii) the minimization of PGs using *N*-α-unprotected amino acids to improve the atom economy of the synthetic process. To do that, we proposed to elongate the peptide chain in the inverse direction[99–102] (from the *N*- to the *C*-terminus). Consequently, we envisaged to perform an activation step previous to the aqueous coupling (Figure 2.9).
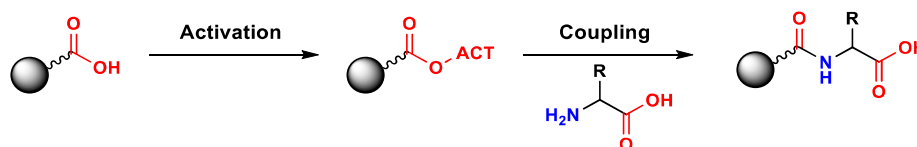
Figure 2.9 Synthetic proposal

2.2.1 *N → C* peptide synthesis

Henkel and co-workers[99] reported the first approach to peptide synthesis in the inverse direction using fluorenylmethyl (Fm) amino acid esters (Figure 2.10). The authors were capable to incorporate the first amino acid ester onto the CTC-TG resin using DIEA. After the elimination of Fm with 20% piperidine, the neutralization of the corresponding piperidinium salt was performed using 1.5% AcOH in DMF. The activation of the *C*-terminus was carried out using DIPCDI (8 eq) and HOBt (3 eq) in DMF for 30 min. Afterwards, the hydroxybenzotriazole salt of the corresponding amino acid ester was coupled in DMF for 20h. By means of this protocol, the model peptide Leu-enkephalin[7] was synthesized in 60% yield, although some by-products were found due to incomplete couplings. In addition, racemization was also observed (8.2% of [D-Phe[4]]-Leu-enkephalin).
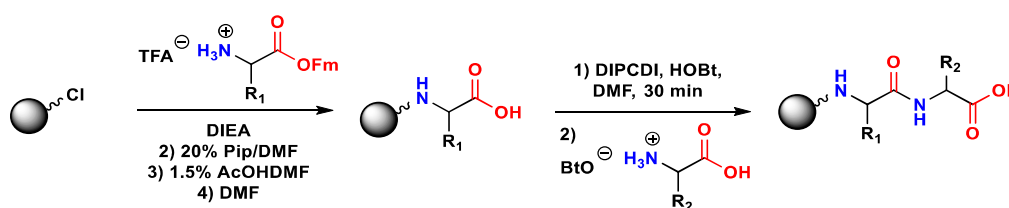
Figure 2.10 N to C peptide synthesis proposed by Henkel and co-workers[99]

Apart from this, Henkel and co-workers[99] also observed two side-reactions that occurred due to the fact that the carboxyl-activated species was anchored to the resin. While the peptide chain is elongated, the activated carboxylic acid may suffer the attack by either: a) the nitrogen of the amine group of the previous amino acid forming the diketopiperazine (DKP) and capping the peptide chain; or b) the oxygen from the carboxyl group of the previous amino acid to form the 5(*4H*)-oxazolone which causes racemization.

2.2.2 Model peptides

Two model peptides were synthesized to perform the experiments related to green SPPS methodologies. In all the cases, the Rink amide linker (RAM) was used as the connector between the resin and the model peptide. The first model peptide (MP1[22], Figure 2.11) was synthesized on three different resins *p*MBHA-PS, CM and TG. The second model peptide (MP2[23], Figure 2.12) was only synthesized in *p*MBHA-PS resin. These tetrapeptides were synthesized following standard Fmoc/*t*Bu SPPS procedures and the succinic linker was coupled after the Thr residue. For more details about these model peptides see section 7.3.1.
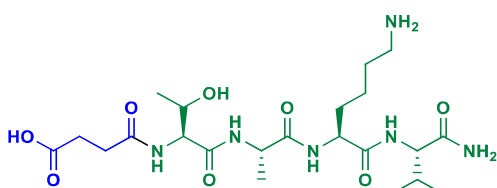
Figure 2.11 MP1 structure
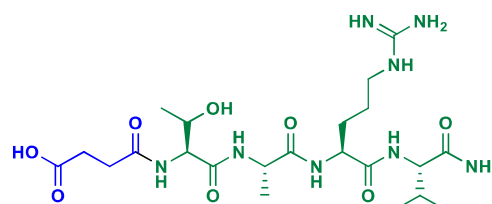
Figure 2.12 MP2 structure

The model tetrapeptides permitted us to analyze the results of each experiment simply by HPLC or HPLC-MS. In addition, the succinic linker was used to provide the first *C*-terminus to perform the activation step. Under a structural point of view, the Lys and Arg residues are the only difference between these two model peptides.

2.2.3 Activation methods

Table 2.1 Active ester methodologies

ACTIVATORS	Active ester	ACTIVATORS	Active ester
HOSu/EDC[103–105]		HOBt/EDC[106]	
PFP/EDC[105,107,108]		OxymaPure/EDC[48,109]	
DAST[110]		DPPA/Et$_3$N[111]	
		DPPA/DIEA[112]	
		NaN$_3$/EDC[113,114]	

An extensive bibliographic search about succinimidyl (-OSu), pentafluorophenyl (-OPFP), benzotriazole (-OBt), Oxyma esters, acid fluorides (-COF) and azides (-N$_3$) activation methods was conducted (Table 2.1). Unless otherwise specified 3 eq of each activator were used per activation

---

[22] MP1 (HO-Suc-Thr-Ala-Lys-Val-NH$_2$)
[23] MP2 (HO-Suc-Thr-Ala-Arg-Val-NH$_2$)

cycle. Although the tables of section 2.3 do not show EDC, this carbodiimide was used in all the activation methods of that section except for DAST or DPPA.

2.2.4 Coupling methods
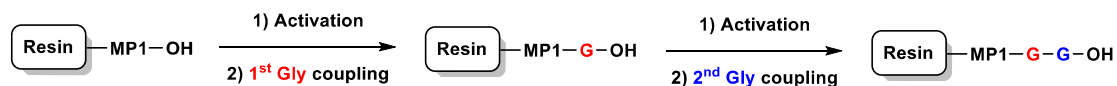
Figure 2.13 Experimental scheme

Our initial goal was to find suitable conditions for both the quantitative activation of the *C*-terminus and the quantitative amino acid coupling. Because of this, Gly was the chosen *N*-α-unprotected amino acid for the initial phase of the project. Therefore, the general scheme of our experiments is represented in Figure 2.13.

Table 2.2 Coupling media

COUPLING	Medium
A	Gly (5 eq), Carbonate buffer pH 9.5-10
B	Gly (5 eq), H_2O + organic/inorganic base (10 eq)
C	Gly (5 eq), Phosphate buffer pH 8.7
D	Gly-OMe (5 eq) + in/organic base (10 eq)
E	L-Val (5 eq), Carbonate buffer pH 9.5-10
F	L-Ala (5 eq), Carbonate buffer pH 9.5-10
G	L-Leu (5 eq), Carbonate buffer pH 9.5-10

The coupling media used in the experiments were coded to facilitate the explanation of the results (Table 2.2). 5 eq of amino acid were used per coupling and 10 eq of organic/inorganic bases were used, unless otherwise specified.

2.3 Results

In general, our green SPPS experiments have been classified in five categories: i) activation experiments; ii) aqueous coupling experiments; iii) hydrolysis studies; iv) one-pot experiments; and v) racemization studies. For more details about the general methodology followed to perform these experiments see section 7.3.3. In addition, the procedure of some key experiments is described in section 7.3.3.2.

2.3.1 Activation experiments

2.3.1.1   Initial experiments

In this initial phase, hazardous solvents such as DCM or DMF were still used to know which activation methods showed better results in terms of yield (Table 2.3). In posterior experiments, we hope to find a suitable green solvent that permits to quantitatively activate the *C*-terminus before the aqueous coupling. Taking this into account, various active esters were prepared using two carbodiimides: EDC and DIPCDI. Due to the poor results offered by DIPCDI[105], EDC[104] was

the carbodiimide that was used in practically all the experiments except for the ones with DAST or DPPA.

Table 2.3 Initial experiments with HOSu, PFP and DAST

EXP	Resin	ACTIVATION	COUPLING	G-G-MP (%)	G-MP (%)	MP (%)
E1-43ii	MP1-PS	HOSu, DCM, 2x2h	A	-	88.5[24]	4.8
				60.4[25]	28.7	-
E1-53ii	MP1-PS	PFP, DCM, 2x2h	B + Et$_3$N	-	70.7	13.4
E1-53iii		DAST, DCM, 2x30min		-	32.5	55.5
E1-56i	MP1-PS	HOSu, DCM, 2x2h	B + Et$_3$N	-	53.4	34.0
E1-56ii		PFP, DCM, 2x2h		-	57.0	16.1

E1-43ii was one of the first successful experiments in which two consecutive Gly residues were coupled to MP1-PS. In addition, we also concluded that: i) active species based on the succinimidyl ester (*e.g.* SuO-MP1) could be detected by HPLC; ii) the Gly coupling did not work at pH < 9.5 because the amino group of Gly was protonated; iii) SuO-G-MP1 species was obtained only if neutralization washes with diluted AcOH solutions were performed; and iv) two activation cycles (2x2h) were needed when using HOSu/EDC method. PFP/EDC[107] activation was quantitative after only one activation even if DMAP was not used (E1-53ii). Pentafluorophenyl ester could be easily followed by HPLC, but its hydrolysis in aqueous Et$_3$N was determined to be around 20%. Therefore, the hydrolysis of the pentafluorophenyl ester was greater than the succinimidyl ester. The formation of the corresponding acid fluoride using DAST[110] did not work owing to the G-MP1 low yield that was obtained (E1-53iii).

When both HOSu and PFP were compared in the same experiment (E1-56), it was observed that the activation with HOSu was not quantitative (75.6% of SuO-MP1) and that the active ester hydrolyzed 20% in the coupling. In contrast, the PFP activation was almost quantitative (94.5% PFPO-MP1), but the hydrolysis was even greater (40%) that what we thought originally. Therefore, similar levels of G-MP1 were obtained in both experiments (~55%).

Due to the conclusions of E1-43ii, we tried to focus on the activation of G-MP1 and the coupling of a second Gly residue. To do that, we had to develop a methodology to obtain G-MP1 in gram-scale. As observed in Table 2.4, excellent results were obtained either with MP1-PS or MP1-CM resins using HOSu/EDC as activators.

---

[24] First coupling of Gly over SuO-MP1.
[25] Second coupling of Gly over SuO-G-MP1.

Table 2.4 Gram-scale experiments with HOSu

EXP	Resin	Reaction Scale (g)	ACTIVATION	COUPLING	G-MP (%)	MP (%)
E1-65i	MP1-PS	2.0			79.6	5.8
E1-72	MP1-PS	4.0			88.6	-
E1-84	MP1-CM	1.0		A	93.1	-
E1-94	MP1-PS	6.0	HOSu, DCM, 2x2h		87.0	5.1
E2-06i	MP1-PS	2.0			90.5	4.9
E2-31	MP1-PS	7.0			91.2	8.8
E2-67	MP1-PS	2.0		A	81.4	4.7
E2-77		2.0			83.0	9.1
E2-88i	MP1-PS	2.0	HOSu, DMF, 2x2h	A	78.3	7.2
E2-88ii		2.0	HOSu, DCM, 2x2h		80.3	4.3

Once gram-scale quantities of G-MP1 were obtained, we focused on the activation of G-MP1 and the coupling of a second Gly residue (Table 2.5). The addition of DIEA during the activation with HOSu did not improve the results either in DCM (E1-67i) or DMF (E1-67iii). The use of MP1-CM permitted to increase the yields of both the first Gly coupling and the second Gly coupling (E1-80), in comparison to the yields obtained in other experiments with PS resin (*e.g.* E1-43). These were reasonable results taking into account the high swelling of PEG resins. Despite this, only promising chemical conditions either for activation or coupling will be tested with CM or TG resins.

Table 2.5 Optimization of G-G-MP

EXP	Resin	ACTIVATION	COUPLING	G-G-MP (%)	G-MP (%)
E1-67i	G-MP1-PS	HOSu + DIEA, DCM, 2x2h	A	18.8	62.2
E1-67iii	(E1-65i)	HOSu + DIEA, DMF, 2x2h		41.3	33.4
E1-80i	MP1-CM	HOSu, DCM, 2x2h	A	83.7	16.3
E1-80ii				84.3	15.7
E2-50ii	G-MP1-PS	HOSu, DMF, 1x2h	A	53.8	27.9
E2-50iii	(E2-31)	HOSu, DMF, 1x1h		59.4	26.2
E2-74i	MP1-PS	HOSu, DMF, 2x2h	A	-	75.3
E2-74ii		HOSu, DMF, 2x2h, 50ºC		-	70.5
E2-76i	G-MP1-PS (E2-67)	HOSu (6 eq), DMF, 2x2h	A	49.0	29.7
E2-87ii	G-MP1-PS (E2-31)	HOSu, DMF, 2x1h	A	73.7	10.2

Some more experiments were performed trying to improve the yields of the second Gly coupling. Temperature (50ºC) did not improve the activation yield of HOSu/EDC method (E2-74ii). Increasing the HOSu equivalents was also not an option, because even worse activation results were obtained. In fact, the use of 6 eq of HOSu worsened the results (E2-76i). The number of activation cycles of G-MP1 using HOSu could not be reduced to only one as worse yields were observed (E2-50). Nevertheless, the time per cycle could be reduced to only 1h, needing less total time to perform the activation (E2-87ii).

2.3.1.2 Alternative activation methods

Apart from HOSu/EDC, other activators were also studied in several experiments to improve the yields obtained by previous methods. PFP was used again in combination with EDC. In addition, other activators such as OxymaPure and hydroxybenzotriazole were also combined with EDC (Table 2.6). Methodologies to form azides were also explored using DPPA or NaN$_3$/EDC.

Table 2.6 Experiments with PFP, HOBt and OxymaPure

EXP	Resin	ACTIVATION	COUPLING	G-G-MP (%)	G-MP (%)
E2-36ii	G-MP1-PS	PFP, DCM, 2x2h	A	69.3	12.7
E2-36iv	(E2-06i)	PFP, DMF, 2x2h		62.5	11.9
E2-56i	G-MP1-PS	PFP, DCM, 2x2h	A	71.4	12.7
E2-56ii	(E2-31)	PFP, DCM, 1x2h		71.6	12.1
E2-78i	MP1-PS	HOBt, DMF 2x2h	A	-	76.9
E2-78ii		HOBt, DMF, 2x1h		-	80.7
E2-92ii	G-MP1 (E2-88i)	HOBt + DIEA, DMF, 2x1h	A	27.6	43.1
E2-93i	G-MP1	HOBt, DMF 2x1h	A	57.5	22.2
E2-93ii	(E2-88ii)	HOSu, DMF 2x1h		73.0	20.1
E3-53i	MP1-PS	OxymaPure, DCM, 1x30min	A	-	40.6
E3-53ii			B + Et$_3$N	-	40.1

PFP activation worked better in DCM than in DMF (E2-36). In fact, PFP/EDC was the only activator that needed only one activation cycle of 2h to be quantitative (E2-56). HOBt activation did not work well with DIPCDI in comparison to EDC, as happened with previous methods. Despite the good results obtained when 2x2h activation cycles were performed, the total activation time could be reduced to 2x1h without affecting the yields obtained (E2-78). The addition of DIEA in the activation with HOBt/EDC worsened the results as it happened with HOSu (E2-92). Direct comparison between HOBt and HOSu confirmed that the latter showed higher yields after the coupling in carbonate buffer (E2-93).

The initial experiments with OxymaPure as activator did not work, because DIPCDI was used as activator. Only when OxymaPure/EDC were combined in DCM for short activation times (2x30min), the activation was nearly quantitative. Nevertheless, the hydrolysis of the active ester was quite high either in carbonate buffer or aqueous Et$_3$N (E3-53).

At that moment, we were interested to directly compare activation methods. Because of this, we began to capture the active esters of small portions of the resin with 5% piperidine in DMSO for 30 minutes to form the Pip-MP species (Table 2.7).

Direct comparison of PFP, HOSu, HOBt and OxymaPure active esters demonstrated that the first was the best method in terms of activation yield (E3-50). Nevertheless, HOSu and OxymaPure methods showed also nearly quantitative activation yields around 90%. HOBt method seemed to

be the least effective method, though it showed also notable yields. DPPA methods worked better with DIEA than with Et_3N (E3-17 vs E3-18). When NaN_3 was directly used with EDC, no azide formation was detected either in DMSO (E3-21) or H_2O (E3-24). In contrast, NaN_3 methods were only effective when HBTU (E3-22) or PyBOP (E3-26) were used as activators.

Table 2.7 Activation experiments using HOSu, PFP, HOBt, Oxymapure and azide methods

EXP	Resin	ACTIVATION	Pip-MP (%)
E3-45	MP2-PS	OxymaPure, DCM, 30 min	89.6
E3-50i		HOSu, DMSO, 2x1h	90.1
E3-50ii	MP1-PS	HOBt, DMSO, 2x1h	86.8
E3-50iii		PFP, DMSO, 1x2h	93.9
E3-17iv	MP2-PS	$DPPA/Et_3N$, DMSO, 2x2h	74.2
E3-18ii	MP2-PS	DPPA/DIEA, DMSO, 2x2h	88.8
E3-21ii	MP2-PS	NaN_3, DMSO, 2x2h	-
E3-22	MP2-PS	NaN_3 + HBTU/DIEA, DMSO, 2x2h	48.0
E3-24i	MP1-CM	NaN_3, H_2O, 2x2h	-
E3-24ii		NaN_3 + Et_3N, H_2O, 2x2h	-
E3-26i	MP2-PS	NaN_3 + PyBOP/DIEA, DMSO, 2x2h	77.4
E3-26ii		NaN_3 + PyBOP/HOBt/DIEA, DMSO, 2x2h	86.8

The major problem of using the azide method was the slow aminolysis between the azide and Gly (E3-23i). After 17h, only ~46% of G-MP2 was obtained, while there was more than 24% of the active azide species still present when the coupling medium was filtered (Table 2.8). In addition, ~10% of hydrolysis was also detected in this first Gly coupling. In the case of the activation of G-MP2 with DPPA, around 60% of Pip-G-MP2 was observed after capturing the azide with 5% piperidine in DMSO. In contrast, after the second Gly coupling only 47% of G-G-MP2 was observed. Similar results were obtained with other activation methods with NaN_3 (E3-27i). Because of these poor results, to increase the aminolysis reaction rates between Gly and azides was established as a priority. Consequently, we tried to use some organic solvents at higher temperature (70ºC). To do that, methyl esters of *N*-unprotected amino acids (*e.g.* Gly-OMe) were employed. Contrarily to what we expected, the organic coupling of Gly-OMe showed worse yields when it was performed at 70ºC than at RT (E3-39). In addition, the same results were obtained when using Gly dissolved in carbonate buffer instead of Gly-OMe dissolved in an organic solvent (E3-40). Therefore, temperature was discarded as an option to increase the coupling rates of azides.

Table 2.8 Experiments using azide methods

EXP	Resin	ACTIVATION	COUPLING	G-G-MP (%)	G-MP (%)	MP (%)
E3-23i	MP2-PS	DPPA/Et₃N, DMSO, 2x2h	A	-	46.1[26]	16.2
				47.0	10.1	-
E3-23iii		DPPA/DIEA, DMSO, 2x2h		-	47.4[26]	3.7
				45.7	11.3	-
E3-27i	MP2-PS	NaN₃ + PyBOP/HOBt/DIEA, DMSO, 2x2h	A	-	40.5	9.4
E3-39iii	MP2-PS	DPPA/Et₃N, DMSO, 2x2h	D, DMSO	-	54.3	31.3
E3-39iv			D, DMSO, 70ºC	-	37.1	19.0
E3-40i	MP2-PS	DPPA/Et₃N, DMSO, 2x2h	A	-	40.3	23.4
E3-40ii			A, 70ºC	-	40.2	37.7

2.3.1.3 Green solvents

After the first experiments with green solvents, we observed that PS resin was not properly swelled during the experiment. Therefore, these experiments were conducted using CM or TG resins (Table 2.9).

Table 2.9 Activation experiments with green solvents

EXP	Resin	ACTIVATION	Pip-MP (%)
E3-11ii	MP1-CM	HOSu, ACN, 2x1h	98.2
E3-11iii		HOSu, GVL, 2x1h	98.3
E3-52ii	MP1-TG	HOSu, ACN, 2x1h	92.2
E3-52iii		HOSu, GVL, 2x1h	76.8
E3-57ii	MP1-TG	HOSu, PC, 2x1h	74.3
E3-57iv		HOSu, NFM, 2x1h	73.7
E3-60i	MP1-TG	PFP, GVL, 1x2h	91.2
E3-60ii		HOBt, GVL, 2x1h	97.9
E3-61ii	MP1-TG	PFP, PC, 1x2h	95.6
E3-61iii		HOBt, PC, 2x1h	91.4
E3-63ii	MP1-TG	HOBt, ACN, 2x1h	93.9
E3-63iii		OxymaPure, ACN, 2x30min	94.5
E3-76ii	MP1-TG	DPPA/DIEA, NBP, 2x2h	67.9

In the case of HOSu/EDC, the best results were obtained in ACN or GVL using CM resin (E3-11). Slightly worse results were obtained using ACN in TG resin. In contrast, the activation yield decreased by 20% when using GVL in the same resin (E3-52). Other green solvents such as PC or NFM also gave moderate activation yields (E3-57). In the case of PFP and HOBt, excellent activation yields were obtained when using GVL (E3-60) or PC (E3-61) in TG resin. EDC/OxymaPure only worked in ACN (E3-63), while it offered only moderate yields in other solvents such as GVL or PC (E3-60 and E3-61, section 9.1.2). Overall, the worst green solvent was NFM which gave the

---

[26] First coupling of Gly over N₃-MP2.

poorest activation yields with all the previous activators (E3-62, section 9.1.2). In the case of DPPA/DIEA method, the only solvent that gave moderate yields was NBP (E3-76).

As expected, when the coupling step was performed after the activation with green solvents, hydrolysis of the active ester was observed again as in previous sections (Table 2.10). In the case of HOSu, notable coupling yields were obtained when either ACN or GVL were used in CM resin (E3-11). In comparison, worse results were obtained when TG resin was used (E3-52).

Table 2.10 Experiments with green solvents

EXP	Resin	ACTIVATION	COUPLING	G-MP (%)	MP (%)
E3-11ii	MP1-CM	HOSu, ACN, 2x1h	A	85.3	4.7
E3-11iii		HOSu, GVL, 2x1h		87.6	3.0
E3-52ii	MP1-TG	HOSu, ACN, 2x1h		78.0	22.0
E3-52iii		HOSu, GVL, 2x1h		55.4	44.6

2.3.2 Aqueous coupling experiments

As explained in previous sections, one of the main problems of this methodology was the hydrolysis of the active ester. To reduce the hydrolysis, several experiments were conducted using a variety of basic buffers, organic bases, and inorganic bases. In addition, some coupling experiments using organic solvents were also performed.

Table 2.11 Basic Buffer experiments

EXP	Resin	ACTIVATION	COUPLING	G-G-MP (%)	G-MP (%)	MP (%)
E1-58ii	MP1-PS	HOSu, DCM, 2x2h	A	61.7	29.7	-
E1-58iii			C	38.2	37.2	-
E2-68i	G-MP1-PS	HOSu, DMF, 2x2h	A	60.6	9.2	-
E2-68ii	(E2-67)		A + recoupling	61.8	8.8	-

The carbonate buffer pH 9.5-10 (A) was one of the preferred coupling media, because of the high coupling yields achieved when this buffer was used (Table 2.11). In contrast, the phosphate buffer pH 8.7 (C) did not work so well, probably because of the protonation of the α-amino group during the coupling (E1-58). To perform a Gly recoupling did not increase the coupling yield of G-G-MP, probably because the succinimidyl ester had already reacted with the second Gly unit or was hydrolyzed before the recoupling was performed.
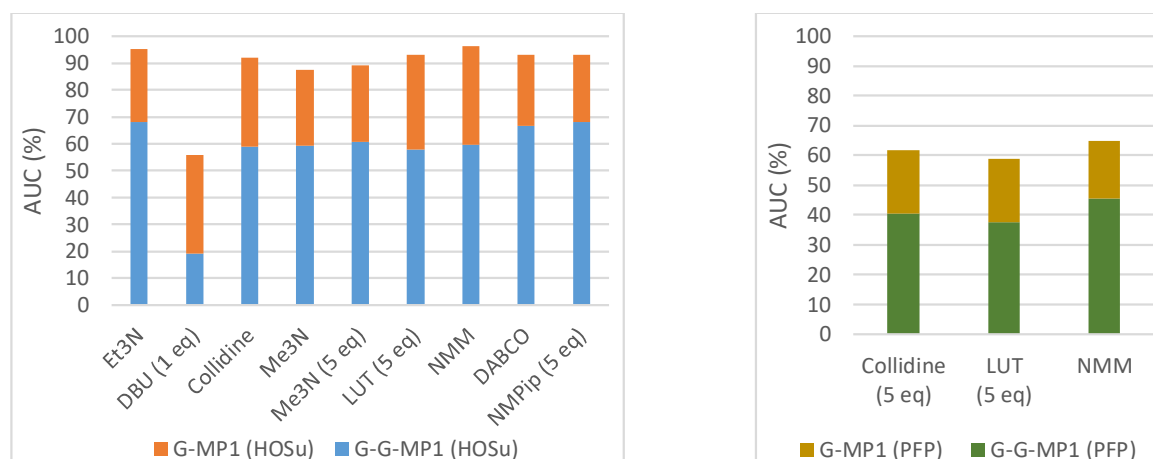
Figure 2.14 Experiments with organic bases: a) HOSu/EDC; b) PFP/EDC

After peforming some experiments with basic buffers, we performed a screening study of tertiary amines to find which of these organic bases caused less hydrolysis of the active ester. To do that, we used both the succinimidyl (Figure 2.14a) and the pentafluorophenyl (Figure 2.14b) esters. In the case of the succinimidyl ester, no organic base showed quantitative coupling yields as the best results were around 70% of G-G-MP1 (Et$_3$N, DABCO and NMPip). The rest of organic bases offered slightly worse results (collidine, Me$_3$N, LUT, NMM). In contrast, DBU failed in the coupling because it formed a stable salt with G-MP1 that could be detected by HPLC-MS (DBU+G-MP1, [M+H]$^+$=726.6 amu). In the case of the pentafluorophenyl ester, the coupling yields were even worse. This was in accordance with previous results (E1-53), in which it was observed that the hydrolysis of the pentafluorphenyl ester was higher in comparison to the succinimidyl ester. For more details about the results of these screening of organic bases see section 9.1.3.
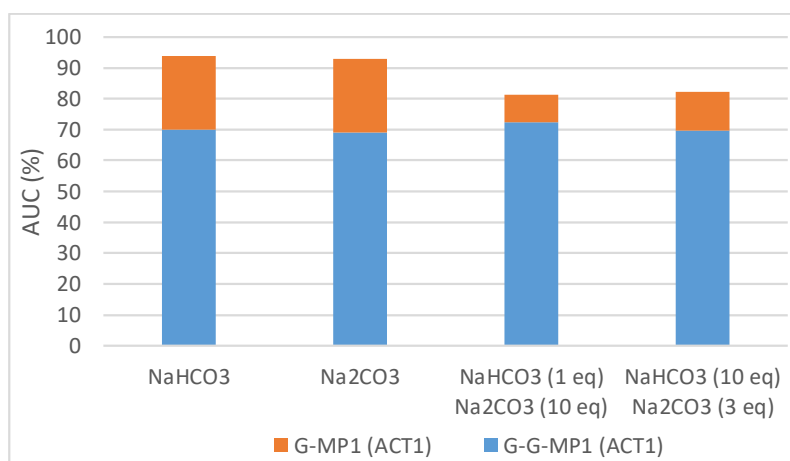
Figure 2.15 Experiments with inorganic bases

Due to the high yields of the carbonate buffer pH 9.5-10 (A), some experiments using different equivalents of NaHCO$_3$ and Na$_2$CO$_3$ were performed (Figure 2.15). Only when 10 eq of base were used, the best results (~69% G-G-MP1) were achieved. In addition, NaHCO$_3$/Na$_2$CO$_3$ mixtures

were also tested, but none of them offered higher yields than the carbonate buffer alone. For more details about the results of these experiments with inorganic bases see section 9.1.3.

Table 2.12 Organic coupling experiments

EXP	Resin	ACTIVATION	COUPLING	MeO-G-MP (%)	MP (%)
E3-38i	MP2-PS	HOSu, DMSO, 2x1h	D + Et$_3$N, DMSO	70.1	12.5
E3-38ii			D + Et$_3$N, DMSO, 70ºC	69.9	14.1
E3-38iii			D + DIEA, DMSO	46.3	10.8
E3-38iv			D + DIEA, DMSO, 70ºC	68.9	18.7

With the objective to reduce the active ester hydrolysis, we thought to use organic solvents such as DMSO to perform the coupling. To do that, glycine methyl ester (Gly-OMe) had to be used instead of Gly due to the insolubility of the latter in organic solvents. After HOSu/EDC activation, we obtained 88% of the succinimidyl ester. Unexpectedly, the coupling was not quantitative using either Et$_3$N or DIEA (E3-38). In addition, temperature (70ºC) was not helpful to improve the coupling yields (Table 2.12).

2.3.3 Hydrolysis experiments
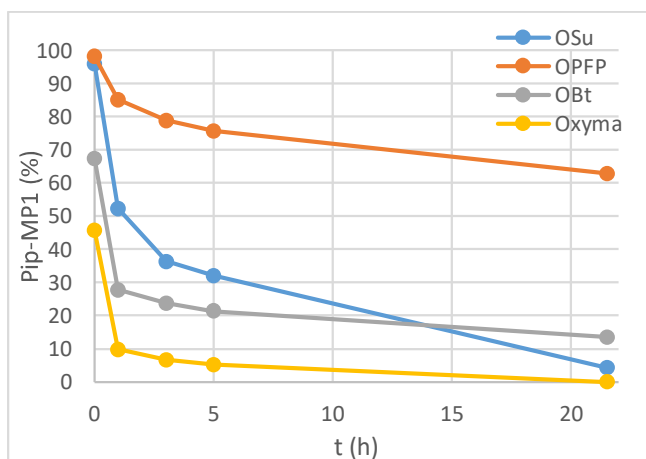
Figure 2.16 Hydrolysis experiments in A
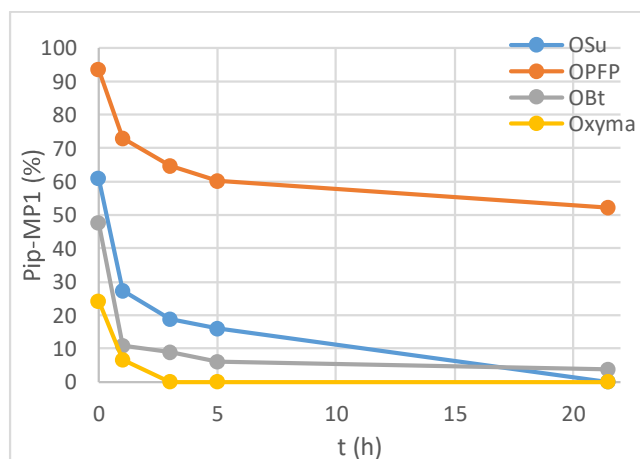
Figure 2.17 Hydrolysis experiments in B+Et$_3$N

Several hydrolysis experiments were conducted to study in detail the behavior of the previous active esters in front of hydrolysis. In this kind of experiments no amino acid was used, so we measured the presence of the active ester at different times after the introduction of the coupling medium (carbonate buffer or aqueous Et$_3$N). To precisely know the quantity of active ester present in each resin sample, we captured the active ester with 5% piperidine in DMSO. For more details on the followed procedure or the complete results obtained in these experiments see sections 7.3.3.2.7 and 9.1.4.

In both carbonate buffer (Figure 2.16) and in aqueous Et$_3$N (Figure 2.17) the active esters behaved similarly. Pentafluorophenyl ester was the most stable active ester being present in more than

50% after 21.5h of experiment. The other three active esters were hydrolyzed below 50% in only 3h on both basic media. In general, the active esters were more stable in the carbonate buffer than in aqueous Et₃N. Nevertheless, they were far from the stability results shown by the pentafluorophenyl ester.
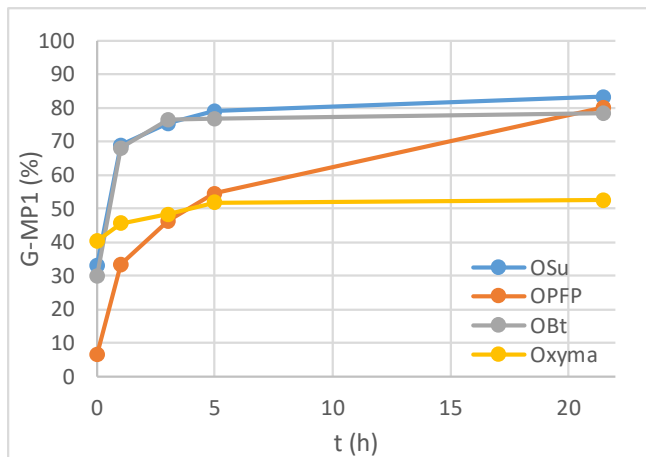
Figure 2.18 Coupling rate experiments in A
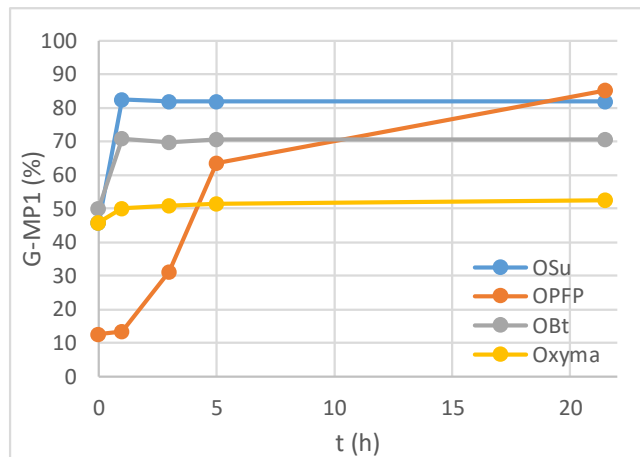
Figure 2.19 Coupling rate experiments in B+Et₃N

In the coupling there are two competitive reactions that must be taken into account: the hydrolysis of the active ester and the aminolysis between the active ester and the amino acid. Once we knew that the pentafluorophenyl ester was the most resistant to hydrolysis, we were interested to know how fast the coupling reaction took place. Under this perspective, some more experiments were conducted in which we measured the presence of G-MP1 at different times after the introduction of the coupling media (carbonate buffer or aqueous Et₃N). In addition, we also measured the presence of the active ester by treating samples of the resin with 5% piperidine in DMSO. For more details on the followed procedure or the complete results obtained in these experiments see sections 7.3.3.2.8 and 9.1.4.

As in previous experiments, the active esters behaved similarly in both carbonate buffer (Figure 2.18) and in aqueous Et₃N (Figure 2.19). In contrast to the hydrolysis experiments, pentafluorophenyl ester was the slowest to react in the coupling reaction with Gly (less than 50% G-MP1 at t_{3h}). In the case of succinimidyl ester, it was the fastest to react with Gly achieving levels of G-MP1 over 69% at t_{1h}. Regarding the coupling medium, the succinimidyl ester presented no significant differences, while the benzotriazole ester achieved worse results in aqueous Et₃N in comparison to carbonate buffer due to increased hydrolysis. Pentafluorophenyl ester achieved similar results at $t_{21.5h}$ in both media, but its aminolysis reaction was faster in aqueous Et₃N. Regarding the Oxyma ester, it showed very poor results probably because of its fast hydrolysis in both media.

2.3.4 One-pot experiments

Table 2.13 One-pot experiments

EXP	Resin	ACTIVATION//COUPLING	G-MP (%)	MP (%)
E3-41iii	MP2-PS	HOSu // D + Et₃N, DMSO, 2h	34.7	41.4
E3-41iv		HOSu // D + Et₃N, DMSO, 2h, 70ºC	69.5	12.0
E3-42ii		HOSu // D + Et₃N, DMSO, 2h, 70ºC + recoupling	52.8	28.0
E3-43ii		HOSu // D + Et₃N, DMSO, 2h, 70ºC + reactivation	55.5	24.4
E3-46ii		HOSu // D + Et₃N, DMSO, 2h + recoupling	60.0	22.6
E3-47ii		HOSu // D + Et₃N, DMSO, 2h + reactivation	51.7	21.6

Similar to previous coupling experiments in which organic solvents were used (*e.g.* DMSO), we also performed one-pot experiments (Table 2.13). This kind of experiments consisted in performing both the activation and coupling steps at the same time. As activators HOSu/EDC were used, while DMSO, Gly-OMe and Et₃N were used for the coupling. In the first experiment, an increase in the G-MP2 yield was observed due to the effect of temperature (70ºC, E3-41). Nevertheless, the yield was far from being quantitative. To improve this yield, we performed various experiments including a recoupling or a reactivation step. Unfortunately, worse results were obtained at 70ºC both performing a recoupling or a reactivation step (E3-42). Despite this, better results were obtained at RT both performing a recoupling (E3-46) or a reactivation (E3-47). Overall, this one-pot experiments were not successful as we expected, because somehow the active ester is not properly formed or it degrades very fast even in organic media. For more details about the procedure followed to perform these one-pot experiments see section 7.3.3.2.4.

2.3.5 Racemization studies

Table 2.14 Racemization studies with HOSu, PFP, HOBt and OxymaPure

EXP	Resin	ACTIVATION	COUPLING	Pip-AA-MP (%)
E3-31ii	MP2-PS	HOSu, DMSO, 2x1h	E	80.9 (rac)
E3-31iii			F	80.4 (rac)
E3-31iv			G	71.9 (rac)
E3-58i	MP1-TG	PFP, DMSO, 1x2h	E	57.8 (rac)
E3-58ii		HOBt, DMSO, 2x1h		71.6 (rac)
E3-59	MP1-TG	OxymaPure, DCM, 2x30min	E	71.8 (rac)

Racemization experiments were performed to know if the previous activation methods were prone to racemization (Table 2.14). To do that, amino acids such as L-Val, L-Ala or L-Leu were coupled to the succinimidyl ester (E3-31). Then, the *C*-terminus was activated once more and the active ester was captured with 5% piperidine in DMSO. For more details about this procedure see section 7.3.3.2.3.

As shown in Figure 2.20, racemization was observed after the activation of V-MP2 with HOSu/EDC (E3-31ii). The same happened in the case of A-MP2 (E3-31iii) and L-MP2 (E3-31iv). The extent of racemization was quite high as the V-MP2 became two clearly identified peaks with the same mass (Pip-V-MP2, $[M+H]^+$=711.5 amu). Other active esters such as pentafluorophenyl or benzotriazole (E3-58), as well as the Oxyma active ester (E3-59) showed equivalent results.
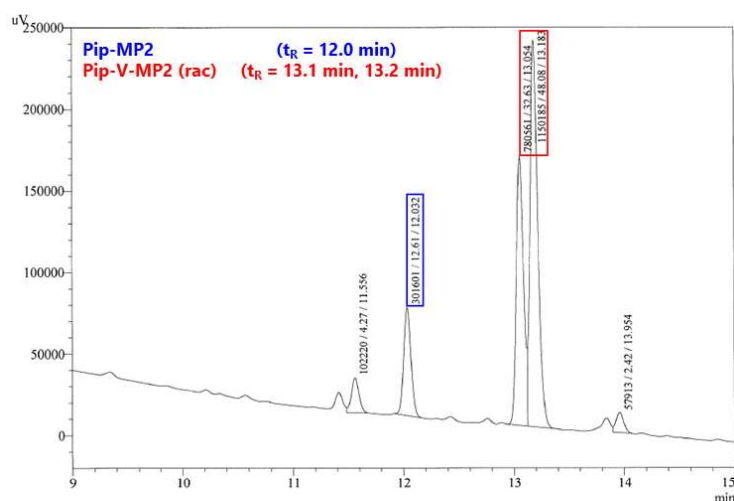
Figure 2.20 Racemic Pip-V-MP2 obtained in E3-31ii

2.4 Discussion and conclusions

The manufacture of peptides via SPPS methods is a multidimensional challenge, in which several key points such as the resin, the linker, the solvents or the coupling reagents are required to assure successful peptide synthesis[115].

To accomplish this first objective of this thesis, a great number of experiments have been performed. In these experiments, various methodologies were explored to reduce the use of hazardous organic solvents (*e.g.* DMF or DCM). In addition, *N-α*-unprotected amino acids such as Gly, Gly-OMe, L-Val or L-Ala were also employed in the coupling step, with the aim to improve the atom economy of the process avoiding the use of Fmoc group.

Active esters such as succinimidyl, pentafluorophenyl, benzotriazole and Oxyma were prepared using EDC in multiple experiments. Only the activation with PFP was quantitative in one activation cycle, while other reagents HOSu, HOBt and Oxyma needed two activation cycles to reach more than 85% of yield. Despite this, some experiments clearly showed how the previous active methodologies caused the racemization of the *C*-terminus on resin (~40%). To perform our synthetic proposal in the inverse direction (from the *N*- to *C*- terminus) might be the most probable cause for this unwanted side reaction to happen. In addition, each activation cycle last for 1 to 2h, providing enough time for *C*-terminus racemization via 5(*4H*)-oxazolone as observed by Henkel and co-workers[99]. A possible solution to this could be to use MW-heating, reducing

the activation time to only few minutes. Nevertheless, it is very difficult to reduce completely 40% of racemization by only applying MW to the activation medium.

To perform one-pot experiments, combining both the activation and the coupling steps, could be another way to improve the reaction rates. The idea behind these one-pot experiments was to rapidly capture the recently formed active ester with Gly-OMe in organic medium. By doing that, we thought that both the racemization and the hydrolysis of the active ester would diminish. However, the results obtained in these one-pot experiments were very disappointing because the maximum yield that was obtained was 70%, very far from being quantitative. In addition, we could not improve these results even when reactivation or recoupling steps were performed.

The relatively quite high hydrolysis of the previous active esters was also another aspect to confront. Overall, aqueous carbonate buffer was the medium in which the best results were obtained despite minimum ~10% of active ester hydrolysis was detected. The capture of the active ester with piperidine made us realize that one of the principal problems of our methodology (apart from racemization) was the yield of the coupling step, as excellent activation results were obtained with various active esters in green solvents (Table 2.10). Under this perspective, the screening of organic bases for the coupling step was not successful as low coupling yields (<70%) were obtained on the succinimidyl and pentafluorophenyl esters. Some hydrolysis experiments on the different active esters either in carbonate buffer or aqueous Et$_3$N revealed that pentafluorophenyl ester was the most resistant to hydrolysis, which was in contradiction to some of our initial experiments with that active ester. In contrast, succinimidyl, benzotriazole or Oxyma esters were hydrolyzed under 50% of the active species in only 3h of experiment in both media. When instead of hydrolysis we studied the coupling rates of the previous active esters, we obtained the complementary results: pentafluorophenyl ester was the slowest to react with Gly in both carbonate buffer and aqueous Et$_3$N, achieving coupling yields of 85%. The other active esters reacted very fast, but they did not achieve better results.

Preparation of azides on resin was also explored, but poor activation yields were obtained in the majority of experiments. Only DPPA/DIEA combination was capable to equal the activation yields (~85%) of previous active esters. Nevertheless, the major problem in the case of azide methods was the extreme slow coupling rates with *N-α*-unprotected amino acids. To improve that, conventional heating and organic media were used with unsatisfactory results. In addition, ~10% of hydrolysis was also detected.

In summary, our synthetic proposal was unsuccessful due to three main drawbacks: i) lack of quantitative formation of a stable active ester on resin; ii) the racemization of the activated amino

acid on resin; and iii) lack of quantitative coupling reaction between the active ester and the *N-α*-unprotected amino acid.

Regarding the future of green SPPS, the major revolution is expected to come from a complete change in the protection scheme as we tried with our synthetic proposal, leading to a reduction or even absence of PGs. From the pharmaceutical industry perspective, the least disruptive short-term scenario for the continued manufacture of therapeutic peptides would be to adjust synthetic protocols to non-hazardous green solvents[116]. Nevertheless, it should be noted that the change of solvent would affect the purity profile and quality aspects associated to the peptide. Therefore, new impurities generated in the manufacturing process will need to be qualified (*e.g.* new toxicology studies), requiring extensive experimental and regulatory paper work[116]. Consequently, it is thought that substantial financial incentives or authority requirements will be mandatory to lead the change of peptide manufacturers towards the use of non-hazardous green solvents.

.

Chapter 3

Green solvent-mediated acidolysis

3 Green solvent-mediated peptide acidolysis

3.1 Introduction
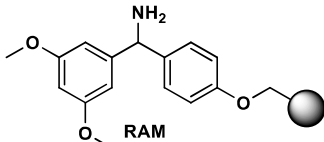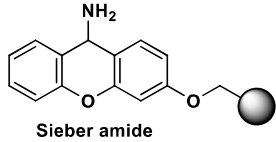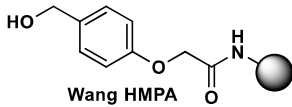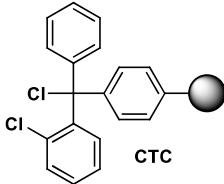
3.1.1 Peptide Acidolysis

Solid-Phase Peptide Synthesis (SPPS) was the strategy reported in 1963 by Bruce Merrifield[38] that consisted in using a polymeric resin as the first permanent protecting group (PG) for the *C*-terminus of the peptide. The use of these solid supports permitted to simplify both the synthetic procedure and the scale-up, which outperformed previous solution-phase strategies. These polymeric resins consisted of small, millimeter-scale solid beads that had to be functionalized with short organic molecules called linkers before their use in SPPS[117].

The proper selection of the polymeric resin is key for successful peptide synthesis, as it should offer mechanical stability in different solvents and temperatures and should be able to swell in different solvents to permit the reagents to easily access the active sites[117]. The first polymeric support used by Merrifield[38] was based on polystyrene (PS), which is still widely used at present for the industrial synthesis of short- to medium-length peptides. In addition, PS resins incorporating polyethylene glycol (PEG) chains (*e.g.* TentaGel® (TG)) or PEG-based resins (*e.g.* ChemMatrix® (CM)) with increased water-swelling properties are also used nowadays for the synthesis of long-peptides or peptides with difficult sequences[117].

3.1.1.1 Linkers and Protecting Groups

Table 3.1 Routine linkers used in standard Fmoc/tBu SPPS

Name	*C*-terminus	Cleavage	Chemical Structure
Rink amide (RAM)	Peptide amides	95% TFA	
Wang HMPA	Peptide acids	95% TFA	
Sieber amide	Protected peptide amides	1-3% TFA	
2-Chlorotrityl chloride (CTC)	Protected peptide acids	1-2% TFA	

Apart from the resin, the linker is extremely important as well because these molecules: i) provide a reversible covalent linkage between the peptide chain and the solid support; and ii) play a protective role against aggregation in the resin beads[117]. In addition, the linker may permit to modify the *C*-terminus of peptides to obtain a peptide amide instead of the carboxylic acid structure. Despite this, linkers are normally categorized depending on their acidic lability in

front of trifluoroacetic acid (TFA) cocktails. Rink amide (RAM), Wang, Sieber or 2-chlorotrityl chloride (CTC) linkers are four of the most used routine linkers in standard Fmoc/*t*Bu SPPS (Table 3.1). The classical RAM linker or other aminomethyl-based linkers are covalently introduced into the resin using standard coupling procedures. In contrast, linkers such as CTC are introduced to the polymer support by direct synthesis[117].

Table 3.2 Sidechain PGs used in standard Fmoc/tBu SPPS[118,119]

Amino acid	PG	Removal conditions	Chemical Structure
Arg	Pbf	90% TFA-scavengers (H_2O and TIS)	
Asn, Gln, Cys, His	Trt	1% TFA in Dichloromethane (DCM)	Pbf Trt
Asp, Glu	*t*Bu (ester)	90% TFA in DCM	
Ser, Thr, Tyr	*t*Bu (ether)		
Lys, Trp	Boc	1) 25-50% TFA in DCM 2) 4M HCl in dioxane	*t*Bu Boc

Overall, Fmoc/*t*Bu SPPS is the most preferred chemical approach for peptide synthesis over solution-phase methods or even other SPPS approaches (*e.g.* Boc/Bzl strategy). The Fmoc/*t*Bu methodology is based on the use of amino acids functionalized with orthogonal PGs: i) a base-labile Fmoc group for the α-amino functional group; and ii) an acid-labile PG for the sidechain functionality. Both PGs are necessary during the amino acid coupling as the Fmoc group prevents amino acid polymerization and the sidechain PG prevents side reactions. Depending on the functional group of the sidechain, various standard PGs such as Pbf, Trt, *t*Bu and Boc are used in routine Fmoc/*t*Bu SPPS[118] (Table 3.2).

3.1.1.2 Standard Acidolysis Strategies
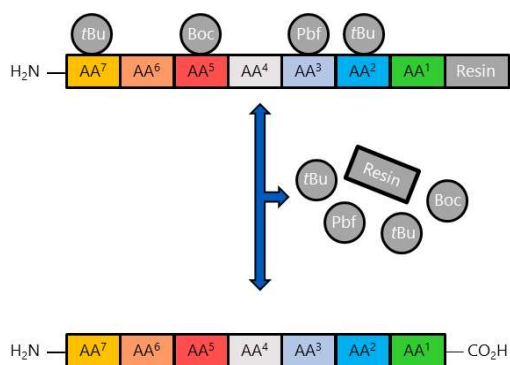
Figure 3.1 Global cleavage/deprotection strategy   Figure 3.2 Cleavage of protected peptides
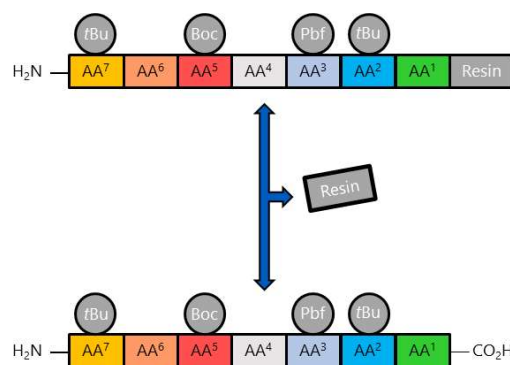
After the coupling of the last amino acid, the linear peptide sequence needs to be cleaved from the polymeric support. In Fmoc/*t*Bu SPPS, two principal acidolysis strategies are performed using

TFA as the source of protons: i) global cleavage/deprotection (Figure 3.1); and ii) cleavage of protected peptides (Figure 3.2).

Global cleavage/deprotection consists in the use of high content TFA cocktails (over 50%) that ensure simultaneously the cleavage of the peptide and the elimination of the sidechain PGs. In this type of cocktails, scavengers are added to trap the stable carbocations produced by the elimination of the sidechain PGs. By doing that, the reaction of carbocations and electron rich sidechains of the peptide is avoided minimizing the formation of impurities[120]. Although water is a common scavenger, other organic substances such as triisopropylsilane (TIS), thioanisole (TAN), anisole or dodecanethiol (DCT) may also be used. After the acidolysis, the peptide is separated from the resin by filtration and precipitated with cold diethyl ether (DEE), which in turn dissolves non-volatile scavengers and any other non-polar byproducts[121]. The resulting suspension is filtered and the product is washed with even more DEE to obtain the corresponding peptide crude. In contrast, cleavage of protected peptides consists in the treatment of the most acid-labile linkers with low content TFA cocktails (less than 10% TFA in DCM)[122]. After the cleavage is completed, the organic solution is separated from the resin by filtration and, in most cases, the cocktail is neutralized and evaporated to obtain the protected peptide for further development (*e.g.* disulfide bond formation)[49]. After the desired chemical transformations on the peptide are performed, the sidechain PGs are eliminated by global deprotection in solution with high content TFA cocktails.

3.1.1.3   **Greening Peptide Acidolysis**

Under an environmental perspective, TFA is an aggressive and extremely corrosive acid capable of inflicting harm to the human body either by inhalation or skin contact leaving hard-to-heal chemical burns[123]. In addition, it is relatively expensive, both for the initial purchase and for the ultimate disposal. Regarding peptide precipitation, DEE is also a high concern substance due to its extreme volatility and flammability. In addition, its proper manipulation is mandatory as DEE/air mixtures are explosive, and it may produce narcotic effects and drowsiness to the operator after some time of exposure. Great quantities of TFA and DEE are needed in standard global cleavage/deprotection: 10 mL of TFA cocktail per gram of peptidyl resin; and, 7 mL of DEE per mL of cocktail[124]. Apart from this, the cleavage of protected peptides represents another concern since 10 mL of diluted TFA in DCM per gram of peptidyl resin are normally used. Under an industrial perspective, the global cleavage/deprotection of 1 kg of peptidyl resin would require 10 L of TFA cocktail and 70 L of DEE for precipitation, while the cleavage would require around 10 L of diluted TFA in DCM. As these solvents are considered as high concern substances, there is an imperative need to find greener substitutes or methodologies that reduce the use of these hazardous solvents.
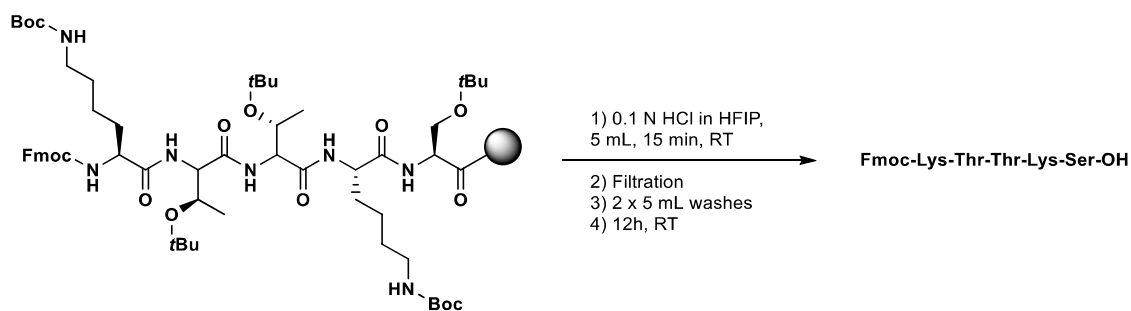
***Figure 3.3 Acidolysis methodology proposed by Stetsenko and co-workers*[11,125]**

In this regard, Stetsenko and co-workers[11,125] investigated the applicability of fluoroalcohols such as hexafluoroisopropanol (HFIP) or trifluoroethanol (TFE) as potential solvents for the cleavage of acid-labile linkers and the elimination of sidechain PGs (Figure 3.3). 0.1N HCl solutions in both HFIP or TFE were capable to eliminate quantitatively Trt and *t*Bu groups from a variety of Fmoc-amino acids in solution. In contrast, 2h treatments with 1N HCl solutions were needed to eliminate Pbf[126], one of the most robust PGs used exclusively for Arg residues. Therefore, peptides with multiple Arg residues would need a prolonged treatment. This methodology was also tested with several acid-labile resin linkers, obtaining excellent results with CTC and Wang linkers in PS, PEG-PS or PEG resins. Finally, the applicability of this methodology was tested with the collagen-stimulating peptide Fmoc-Lys^1-Thr^2-Thr^3-Lys^4-Ser^5-OH[120,127,128], which was prepared on a TentaGel S Trt resin. 0.6 g of the peptidyl resin were cleaved using 0.1N HCl in HFIP for 15 min. After filtration, the resin was washed with more 0.1N HCl in HFIP and the peptide was left stirring at RT for 12h to achieve quantitative deprotection results. Despite these results, this cleavage and deprotection strategy still requires further optimization on the deprotection of multiple Arg residues protected with Pbf, a PG that shows excessive stability in the previous conditions[51]. Nevertheless, as far as we know this is the only successful method in the literature that totally avoids the use of TFA for peptide deprotection.

Concerning peptide precipitation after global deprotection, Albericio and co-workers have recently reported two greener alternatives to DEE: cyclopentyl methyl ether (CPME)[121] and 2-methyltetrahydrofuran (2-MeTHF)[129]. CPME presents favorable environmental, health and safety characteristics such as high boiling point (106ºC), excellent stability under acidic conditions, and a low tendency to form peroxides[121]. To compare the performance of CPME with DEE, the authors synthesized a variety of peptides such as Leu-enkephalin^{27}, ACP$_{65-74}$^{12}, ABRF 1992^{28}, ABC^{29}

---

[27] Leu-enkephalin (H-Tyr^1-Gly^2-Gly^3-Phe^4-Leu^5-OH)
[28] ABRF 1992 (H-Gly^1-Val^2-Arg^3-Gly^4-Asp^5-Lys^6-Gly^7-Asn^8-Pro^9-Gly^{10}-Trp^{11}-Pro^{12}-Gly^{13}-Ala^{14}-Pro^{15}-Tyr^{16}-NH$_2$)
[29] ABC (H-Val^1-Tyr^2-Trp^3-Thr^4-Ser^5-Pro^6-Phe^7-Met^8-Lys^9-Leu^{10}-Ile^{11}-His^{12}-Gly^{13}-Gln^{14}-Cys^{15}-Asn^{16}-Arg^{17}-Ala^{18}-Asp^{19}-Gly^{20}-NH$_2$)

or thymosin[30] by standard Fmoc/*t*Bu SPPS. With the exception of Leu-enkephalin which did not precipitate in CPME, this green ether showed the same results in terms of recovery and purity as DEE, which ensures the use of CPME as a greener alternative for peptide precipitation. In the case of 2-MeTHF, it is considered as a green solvent because it is derived from biomass-renewable resources, has a relatively high boiling point (82ºC) and considerable stability under acidic conditions[129]. As in the previous study, the same peptides were used to investigate the performance of 2-MeTHF in peptide precipitation. As happened before, 2-MeTHF was not able to precipitate Leu-enkephalin but offered comparable results in terms of recovery and purity to DEE in the precipitation of the other model peptides. The conclusion of both studies was that CPME and 2-MeTHF were suitable candidates to replace DEE in peptide precipitation after acidolysis, however, its price limits their industrial use.

Pawlas and co-workers[88] also designed a green protocol for the precipitation of the melanocortin receptor agonist Ac-Nle[1]-*c*[Asp[2]-His[3]-Phe[4]-Arg[5]-Trp[6]-Lys[7]]-NH$_2$. Various greener alternatives to DEE were evaluated being 4-methyltetrahydropyran / *n*-heptane 1:4 mixture the one that showed the best results in terms of yield.

3.1.2 Green solvent

▓▓▓▓▓▓▓▓▓▓▓▓▓▓▓▓▓▓▓▓▓▓▓▓▓▓▓▓▓▓▓▓▓▓▓▓

▓▓▓▓▓▓ ▓▓▓ [130]. ▓▓▓▓▓▓▓▓▓▓▓▓▓▓▓▓▓▓▓▓▓

▓▓▓▓▓▓▓▓▓▓▓▓▓▓▓▓▓▓▓▓▓▓▓ ▓▓▓▓ [131]

Figure 3.4 Phase diagram of ▓

In particular, ▓▓▓▓▓▓▓▓▓▓ (▓▓▓) is one of the most used ▓▓▓ in industrial scale applications due to its advantageous characteristics: low demanding ▓▓▓▓▓▓▓▓▓▓▓▓ ▓▓▓▓, low-cost, non-flammable, non-toxic and green solvent[132–134] (Figure 3.4). In addition,

---

[30] Thymosin (H-Ser[1]-Asp[2]-Ala[3]-Ala[4]-Val[5]-Asp[6]-Thr[7]-Ser[8]-Ser[9]-Glu[10]-Ile[11]-Thr[12]-Thr[13]-Lys[14]-Asp[15]-Leu[16]-Lys[17]-Gly[18]-Lys[19]-Lys[20]-Glu[21]-Val[22]-Val[23]-Gly[24]-Glu[25]-Ala[26]-Glu[27]-Asn[28]-NH$_2$)

properties such as viscosity, density, diffusivity and dielectric constant may be easily tuned by modifying its ███████████████████ conditions[132].

As a consequence of its advantageous characteristics, ████ has found multiple applications as a solvent for a variety of organic chemistry reactions such as olefin metathesis[135,136], asymmetric hydrogenation[137] and Pauson-Khand reactions[138]. In addition, Barstow and co-workers[139] patented a methodology to perform SPPS coupling reactions in█████████████ using Boc-amino acids modified as succinimidyl esters or symmetrical anhydrides (Figure 3.5). By means of this technology, the authors could synthesize the tetrapeptide H-Leu^1-Ala^2-Gly^3-Val^4-OH. Nevertheless, solubility of activated Boc-amino acids in ████ was extremely low (*e.g.* 0.58 mg/mL of Boc-Gly-OSu) and Boc elimination after the coupling reaction had to be performed using standard procedures at atmospheric pressure[139].
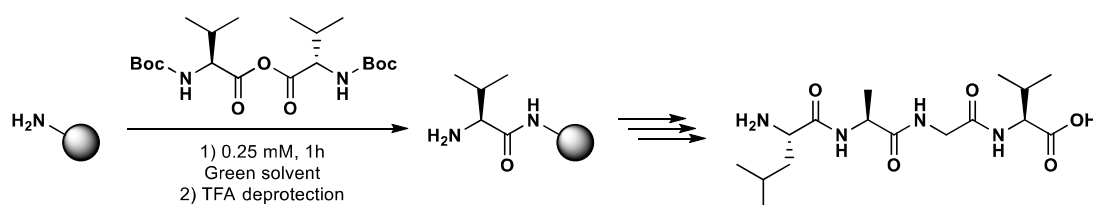
Figure 3.5 Peptide synthesis in ██ developed by Barstow and co-workers[139]

Despite its use in organic chemistry reactions, the most important applications of ████ are in ████████████ chromatography or in extraction processes. Regarding the first one, ████ has already been used as a solvent for the purification of up to 40-mer peptides[140] and small molecules[141]. In general, █████████████ chromatography provides several advantages over traditional HPLC such as speed, practical use of longer columns, normal-phase retention mechanism, and a reduction in the use of organic solvents[142]. For peptide analysis and purification processes, alcohol modifiers (*e.g.* methanol, ethanol, 2-propanol) or additives (*e.g.* TFA, ammonium acetate) are mixed with ████ to perform the chromatographic separation[140,143]. Nevertheless, the heat generated from higher flow rates may decrease resolution and not many studies involving peptides are available at present[8]. Concerning extraction processes, ████ has been principally used for the extraction of a variety of substrates, from which caffeine[144,145] is the most important one. O'Brien and co-workers[146] patented in 1991 a process in which caffeine could be recovered from ████ by the use of two different vessels (Figure 3.6). First, the coffee beans are mixed with ████ in the extraction vessel to dissolve the caffeine. Second, the extracted caffeine is recovered from ████ in the absorption vessel by using a countercurrent flow of water at high pressure.
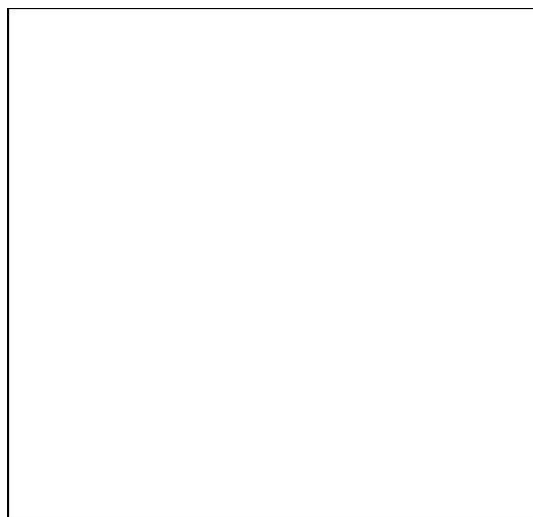
Figure 3.6 Caffeine extraction method

3.2 Acidolysis proposal

Fmoc/*t*Bu SPPS is the preferred method for the preparation of peptides both in the research context and in the pharmaceutical industry[51]. After the synthesis of the linear peptide chain, this strategy conceives the use of high concern substances such as TFA, DEE or DCM to perform either the cleavage of protected peptides or their global cleavage/deprotection. Because of this, our acidolysis proposal is based on the possible use of ▇ in peptide acidolysis procedures.

▇▇ ▇▇▇▇▇▇▇▇▇▇▇▇▇▇▇▇▇▇▇▇▇▇▇▇▇▇▇▇▇▇ This laboratory managed by ▇▇▇▇▇ ▇▇▇▇▇▇▇▇ combines both scientific research with industrial projects using principally ▇▇▇. Consequently, this research group had the necessary equipment, facilities and expertise that permitted us to conduct our acidolysis experiments using ▇▇▇▇▇▇▇▇▇▇▇▇▇ ▇▇▇▇▇▇▇▇▇▇. Specifically, ▇▇▇▇▇▇▇ was the laboratory technician who helped us in the setting up of our experiments throughout the doctoral thesis.

The equipment that was used to conduct the ▇▇ acidolysis experiments comprised four different ▇▇▇▇▇▇ reactors: ▇▇▇▇▇▇▇▇▇▇▇▇▇▇▇▇▇▇▇▇. For more details and information about these ▇▇▇▇▇▇ reactors see section 7.4.1.

3.2.1 Model peptides

A variety of peptides were synthesized to perform the experiments related to this second objective. The first model nonapeptides were synthesized using both CTC and RAM linkers. As a consequence, the *C*-terminus varied depending on the resin used: ACMP1[31] was synthesized on a CTC resin while its amide version ACMP2[32] was synthesized on a *p*-methylbenzhydrylamine

---

[31] ACMP1 (H-Thr^1-Leu^2-Lys^3-Pro^4-Arg^5-Ser^6-Phe^7-Leu^8-Leu^9-OH)
[32] ACMP2 (H-Thr^1-Leu^2-Lys^3-Pro^4-Arg^5-Ser^6-Phe^7-Leu^8-Leu^9-NH$_2$)

(*p*MBHA) resin functionalized with the RAM linker. Both peptides were synthesized following standard Fmoc/*t*Bu SPPS procedures (Figure 3.7).
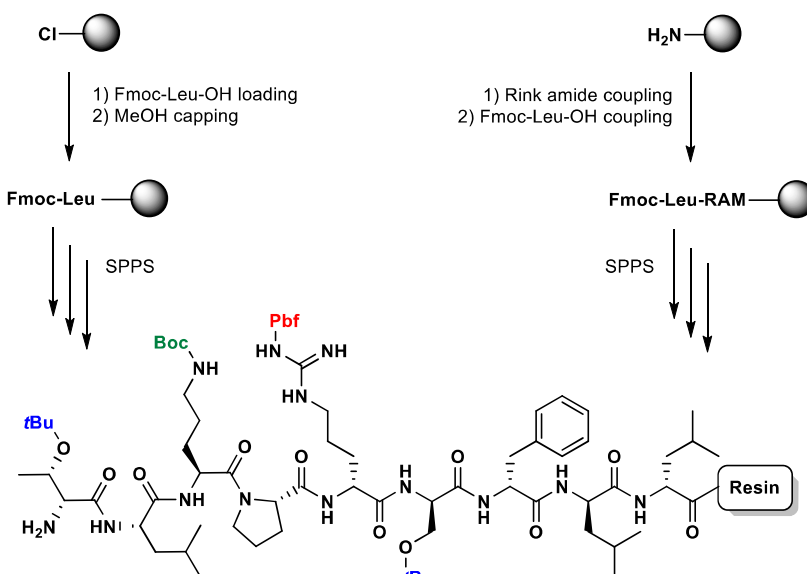
Figure 3.7 Synthesis of ACMP1-CTC and ACMP2-RAM-pMBHA

Interestingly, the amino acid sequence was carefully selected to have different PGs in the peptide structure such as Pbf, *t*Bu or Boc that require different quantities of TFA to be eliminated. Moreover, the use of CTC and Rink amide resins will provide information about what type of linkers can be cleaved with our methodology as these linkers require as well different quantities of TFA to release the peptides. For the final sessions of experiments, two therapeutic peptides were synthesized: somatostatin (SST) and leuprolide (LP). For more details see sections 7.4.2.
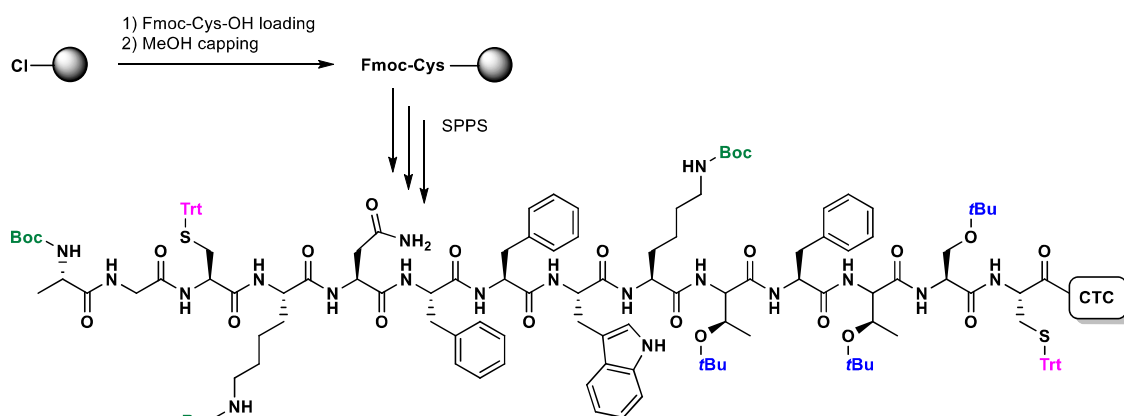
Figure 3.8 Synthesis of SST-CTC

Somatostatin (SST) is a 14-amino acid cyclopeptide hormone that in our body acts as a neuromodulator, a neurotransmitter, and as a potent inhibitor of various secretory processes[13]. SST[33] was synthesized on CTC resin following standard Fmoc/*t*Bu SPPS procedures (Figure 3.8).

---

[33] SST (H-Ala^1-Gly^2-*c*[Cys^3-Lys^4-Asn^5-Phe^6-Phe^7-Trp^8-Lys^9-Thr^{10}-Phe^{11}-Thr^{12}-Ser^{13}-Cys^{14}]-OH)

Leuprolide (LP) is a synthetic nonapeptide that acts as an analog to the luteinizing hormone-releasing hormone displaying receptor agonist activity[151]. When this peptide is given continuously, it inhibits the pituitary gonadotropin secretion and suppresses the testicular steroid genesis, hormone that is involved in prostate cancer. LP[34] was synthesized on CTC resin following standard Fmoc/*t*Bu SPPS procedures (Figure 3.9).
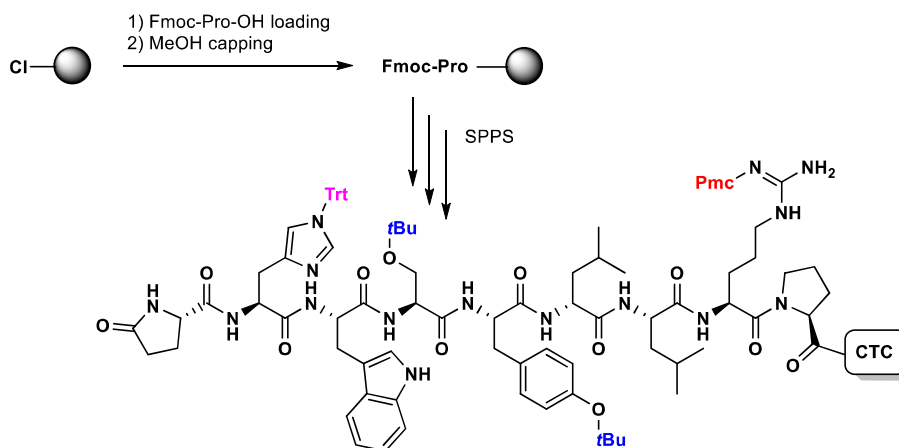
Figure 3.9 Synthesis of LP-CTC

3.3 Results

Once the model peptides were synthesized, some standard mini-acidolysis experiments were conducted using ACMP1-CTC resin and various deprotection cocktails. Afterwards, two types of acidolysis experiments using ▮▮▮ were evaluated: i) global cleavage/deprotection experiments using ▮▮▮▮▮▮▮▮▮▮▮▮ in comparison to standard procedures ▮▮▮▮▮▮▮▮▮; ii) cleavage experiments to obtain protected peptides ▮▮▮▮▮▮▮▮▮▮. The procedure of some key experiments performed throughout the thesis is described in sections 7.4.4 and 7.4.5.

The experiments shown in this section correspond to a research project of BCN Peptides.

3.3.1 Global cleavage/deprotection

3.3.1.1 Standard procedures

Acidolysis experiments using the minimum amount of TFA:H_2O 95:5 cocktail were performed to know if the standard resin/cocktail 1:10 relation could be reduced.

As shown in Table 3.3, it was possible to deprotect the model peptide using a ▮▮▮▮▮▮, though a ▮▮▮▮▮ group remained in ▮▮▮▮▮▮ (entry 3). Nevertheless, our goal was to develop a methodology for the global cleavage/deprotection ▮▮▮▮▮▮ using ▮▮.

---

[34] LP (Pyroglutamic acid^1-His^2-Trp^3-Ser^4-Tyr^5-D-Leu^6-Leu^7-Arg^8-Pro^9-OH)

Table 3.3 Mini-acidolysis experiments using TFA:H₂O 95:5 cocktail

#	Resin (g)	Cocktail	Volume (mL)	Time (h)	ACMP1 (%)		
1	0.5	TFA:H₂O 95:5	1.0	2	37.8		
2	0.5		1.5	2	94.8		
3	0.5		2.0	2	97.9		

Afterwards, some HCl/TFE[11] mixtures were tested in various mini-acidolysis experiments. In general, the results obtained following this methodology were in agreement with the report by Stetsenko and co-workers[11]: i) TFE slowed the elimination of sidechain PGs in comparison to HFIP; ii) higher HCl concentration offered better results; and iii) no quantitative elimination ▬▬▬ was observed even if 2.0M HCl in TFE was used. For more details about these results see section 9.2.1.1.

Table 3.4 Small-scale acidolysis experiments using HCl in ACN mixtures

#	Resin (g)	Cocktail	Volume (mL)	Time (h)	Yield[35] (%)	ACMP1 (%)				
1	0.5	HCl:ACN 1:5	3.0	3	99	21.9				
2	0.5	HCl:ACN 1:4	0.5	3	-	-				
3	0.5		1.0	3	-	0.7				
4	1.0	HCl:ACN 2:1	1.5	3	81	21.5				
5	1.0	HCl:ACN 1:1	2.0	3	96	22.1				
6	1.0	HCl:ACN 1:2	3.0	3	95	11.6				
7	1.0	HCl:ACN 1:3	4.0	3	93	19.5				
8	1.0	HCl:ACN 1:1	2.0	6	93	23.8				
9	1.0		2.0	8	105	32.1				

Apart from HCl (pK$_a$ -6.3), other strong acids such as sulfuric acid (pK$_a$ -3.0), *p*-toluenesulfonic acid (*p*TSA) (pK$_a$ -2.8) and TFA (pK$_a$ 0.2) were tested at various concentrations in TFE. As expected, deprotection results ▬▬▬ either the time or the acid concentration was increased. Despite this, in some experiments with H$_2$SO$_4$ and *p*TSA the HPLC analysis revealed peptide degradation due to acid stress. ▬▬▬▬▬▬▬, being insufficient. For more details about these results see section 9.2.1.1.

Overall, HCl/TFE mixture gave the best results in terms of global cleavage/deprotection of ACMP1-CTC, though with some limitations. Because of this, HCl was used in further small-scale acidolysis experiments using ▬▬▬ (Table 3.4). After the first experiments, HCl:ACN 1:5 in

---

[35] Acidolysis yield calculated from the theoretic mass of peptide expected to be obtained.

3h (entry 1) gave the best results, while water only worsened the deprotection. Increasing the time to 20h using ACN as the co-solvent produced peptide degradation, so more 3h studies trying to lower the cocktail volume and increasing the acid concentration were conducted (entries 2-3). Despite the increase in acid concentration, the decrease of cocktail volume worsened the results. As a consequence, some experiments maintaining the relation ███████████████ and increasing the amounts of ACN were performed (entries 4-7). The use of HCl:ACN 1:1 gave the best results with 22.1% of ACMP1 and 96% yield (entry 5). Extending the time of the acidolysis to 6-8h helped to improve the results without observing any peptide degradation (entries 8-9). In contrast, ███████████ eliminated quantitatively when HCl was used in the acidolysis cocktail.

██

███████████████████

3.3.1.2   Green solvent experiments: first series

The first experiments with █████ were designed on the ████████████████████████ ████████████████████. Ideally, the addition of the cocktail should have been ███████ ███████████, but as we did not have any ██████████████████, in some experiments we had to add the ██████████████████████.

In the 1st session, a glass containing ACMP1-CTC█████ and an eppendorf with█████████ was introduced inside█████ reactor without letting the██████████████ the resin. After introducing ████inside the reactor and achieving ██████████conditions (████████████), it was clearly observed that██████████████████████ into █████. Therefore,████████ seemed to be ██████████ further experiments to know if█████ could████████████.

.

In the 2nd session, two glass vials were used to█████████████████ the peptidyl resin and the ██████████████ reactor (Figure 3.10). To do that, some plastic supports or metallic wires were used to put the small glass vial inside the big one. In addition, magnetic stirrers were introduced inside████████████████████████████. In the first experiment,█████████ ACMP1-CTC and ██████████ were used, as well as ██████████████ In contrast to the previous session, the██████████████ made possible the ████████████ into ████████████████████ ██████████████. After████████████, the reactor was ████████████ bubbling the████ on ████████ solution to████████████. The recovered resin was treated with █████and ████████████████ was analyzed by HPLC detecting████████████ that corresponded to protected ACMP1████████ (Table 3.5, entry 1). A second experiment following this same methodology was performed with the same quantities of ACMP2-RAM-*p*MBHA and████████████████████████ were detected in the HPLC analysis of the samples.
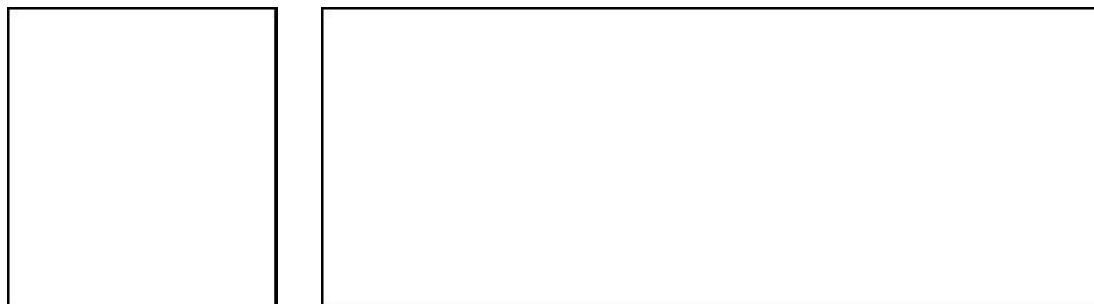
Figure 3.10 Experiment scheme of 2nd session

In the 3rd session the experiment time ███████ and the ███████ was increased while maintaining ███████ relation. To do that, ACMP1-CTC resin ███████ was introduced in a ███-permeable paper bag and ███████ introduced in a glass vial (Figure 3.11). Both the bag and the vial were introduced ███████ reactor to conduct the experiment. After the introduction of ███ (███████), it was clearly observed how the initial ███████ ███████ after some minutes of stirring. The experiment was left ███████ these conditions. Afterwards, the resin inside the paper bag was ███████, and the filtrate was lyophilized to obtain ███████ ACMP1 ███ (Table 3.5, entry 2). In comparison to the previous session, the ███████ was increased to ███ improving the results. Consequently, we tried to increase even more the ███████ but maintaining the ███████ relation.

Table 3.5 Results of sessions 2 and 3

#	Session	Experiment	Resin (g)	Cocktail	Volume (mL)	Time (h)	Yield (%)							
1	2	1	██	██	██	██	▮	▮	▮	██	██			
2	3	1	██	██	██	██	██	▮	██	██	██			
3	3	2	██	████	██	██	██	██	██	██	██			

In this 3rd session, a second experiment was performed using the ███████ ███████ (Figure 3.11). For this experiment, ACMP1-CTC ███████ was introduced inside a ███-permeable paper bag and was treated with ███████. After ███████ introduction, the cocktail dissolved in ███forming a ███████ to observe what was ███████. ███████ the reactor was ███████ and some ███████ was observed, probably due to ███████ mixture.

After washing the ███████████████, the filtrate was lyophilized ████████████
████████████ (Table 3.5, entry 3). Although the results ████████ in comparison to the first experiment, the observed ████████ made us discard ██████████████ for further experiments.
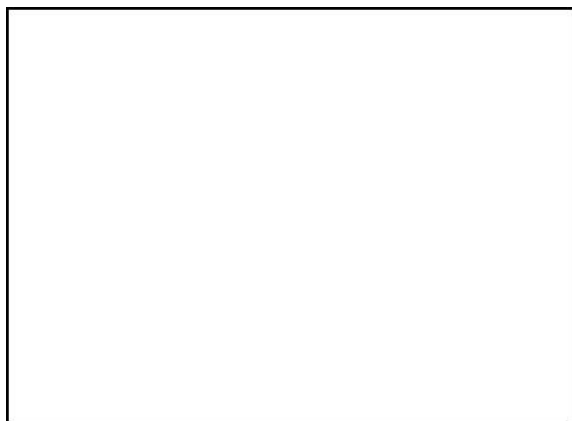
Figure 3.11 Experiment scheme of 3ʳᵈ session
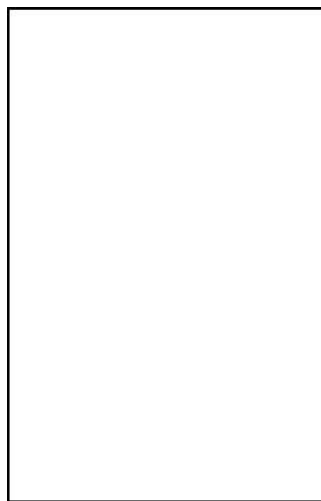
Figure 3.12 Experiment scheme of 4ᵗʰ and 5ᵗʰ sessions

During the experiments of the 3ʳᵈ session, we found that part of the ██████ peptides was collected in the ████████ in which █████████████████████████████ and also in the ██████████████ between experiments, which meant that ███ was ████████████ the █████████████ peptide from ████████. Because of that, in the next sessions we began to ████ ██████████ both reactor and the resin ████████████████████████████ of the reactor during the ████████████████. These fractions were also analyzed by HPLC.

Table 3.6 Results of sessions 4 and 5

#	Session	Experiment	Resin (g)	Cocktail	Volume (mL)	Time (h)	Fraction	Yield (%)	ACMP1 (%)	██	██	██	██	██
1	4	-	██	██	██	██	E	██	██	██	██	██		
2				██			W	██	██	██	██	██		
3	5	-	██	██	██	██	E	██	██	██	██	██		
4				██			W	██	██	██	██	██		

In the 4ᵗʰ session, the ████████ relation was increased while ██████████████████ proportion (Figure 3.12). For this reason, ACMP1-CTC████████ was introduced directly inside the ██████████████████████████████. Then, ████ (████████, 38ºC) was introduced and the experiment was left ██████████████. After that time, the reactor was ████████████████ the exit ████ on ██████████████ . Apart from that, the treated resin was recovered using ████████ ██████████████ . Later, ████████████████ the filtrate ████████████████ were lyophilized to obtain, ████████████████████████████████████ ACMP1 ████████ (Table 3.6, entries 1-2). After

HPLC analysis, both the ██████ and the ████████ were █████████ Nevertheless, elimination was only ██████████ because the █████████ inside the reactor was ███.

The previous experiment was reproduced in the 5th session but treating █████ of ACMP1-CTC with ████████████████ in ████████████ for ██ (Figure 3.12). After the █████████ was collected, █████████ was introduced in the reactor and a second █████████████was performed. After stirring █████████████, this second █████████████was also collected █████ ███ fraction. Afterwards, the resin was █████████ and the reactor was ███████████████████ obtaining the ███████ fraction. Both ████████████████████ were lyophilized to obtain ████████ ████████████████ ACMP1███████ (Table 3.6, entries 3-4). ████████████████, both █████ and ███elimination were █████████, but the results did not ███████ as we expected, probably because the █████████ in████ was █████████████ In addition, it was observed that it was not possible to increase the ████████████████████████ reactor, because of the ███ ████████ achieved in this experiment█████████ . As a consequence, performed some█████████ experiments using the ████████████████.

3.3.1.3 Green solvent experiments: second series

████ does not█████████████ in ████ without ███████ as observed in previous experiments. This probably happens because both ████████████████████████ █████████[36]. Because of that, we speculated that to use████████████████████ acidolysis methodology because at room temperature (RT) it may present a████████ ████████[37] compared to ██████[130].
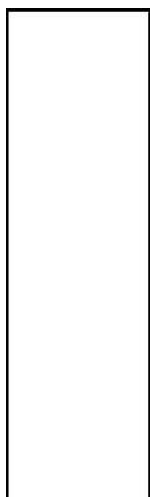
Figure 3.13 Scheme of 6th and 7th sessions   ***Figure 3.14 HPLC analysis of*** ████████ ***fraction (1st experiment, 6th session)***

In the 6th session,██████ of ACMP1-CTC and █████████████████ were introduced directly inside █████████ reactor (Figure 3.13). Then,█████████ (█████████████) was introduced and the experiment

---

[36] ████ has a ████████████████ at 20ºC while ███████████████████████████ and 38ºC.
[37] ████████ at -23.2ºC and ████ ███[315].

was left ▮▮▮ After that time, the exit ▮▮▮▮ was collected on ▮▮▮▮▮ and the resin was recovered using more of this mixture. Both ▮▮▮▮▮▮▮ fractions were lyophilized to obtain ▮▮▮▮▮▮▮▮▮▮▮▮▮ ACMP1 ▮▮▮ (Table 3.7, entries 1-2). Although the ▮▮ content inside the reactor was increased to ▮▮▮ the results obtained were ▮▮▮ than in previous experiments because the ▮▮▮▮▮ could not be eliminated ▮▮▮▮▮ (Figure 3.14). In the second experiment of session 6th, ▮▮▮ ACMP1-CTC were treated with ▮▮▮▮▮▮▮ and ▮▮▮▮▮▮▮▮▮▮ for ▮▮. In these conditions, ▮▮▮▮▮▮▮▮▮▮▮▮ ACMP1 ▮▮▮ (Table 3.7, entries 3-4) were obtained from the ▮▮▮▮▮▮ fractions. Again, the ▮▮ ▮▮▮ could not be ▮▮▮▮ quantitatively, highlighting the ▮▮▮▮▮▮▮▮▮ in the acidolysis process, because even at ▮▮▮▮ concentration ▮▮▮▮▮ could not be ▮▮▮▮ completely.

Table 3.7 Results of sessions 6 and 7

#	Session	Experiment	Resin (g)	Cocktail	Volume (mL)	Time (h)	Fraction	Yield (%)	ACMP1 (%)	▮	▮	▮	▮
1	6	1	▮	▮▮▮	▮	▮	▮	▮	▮	▮	▮	▮	▮
2				▮			▮	▮	▮	▮	▮	▮	▮
3		2	▮	▮▮▮	▮	▮	▮	▮	▮	▮	▮	▮	▮
4				▮			▮	▮	▮	▮	▮	▮	▮
5	7	1	▮	▮▮▮	▮	▮	▮	▮	▮	▮	▮	▮	▮
6				▮			▮	▮	▮	▮	▮	▮	▮
7		2	▮	▮▮▮	▮	▮	▮	▮	▮	▮	▮	▮	▮
8				▮			▮	▮	▮	▮	▮	▮	▮

In the first experiment of 7th session, ▮▮▮ ACMP1-CTC were treated with ▮▮▮▮▮▮ ▮ trying to ▮▮▮▮▮▮▮ of a previous small-scale experiment (Table 3.4 ▮▮▮). After the introduction of ▮▮▮▮▮▮▮▮ the experiment was left ▮▮▮. Then, ▮▮▮▮ ▮▮▮ fractions were collected and lyophilized ▮▮▮▮▮▮▮▮▮▮▮▮ ACMP1 ▮▮▮ (Table 3.7, entries 5-6). In comparison to the standard experiment (Table 3.4 ▮▮▮), the addition of ▮▮▮▮▮▮▮▮▮ probably because of ▮▮▮▮▮ in ▮▮. In the second experiment of 7th session, ▮▮▮ of ACMP1-CTC were treated with ▮▮▮▮▮▮▮ and ▮▮▮▮▮ (▮▮▮▮▮ ▮▮ , reproducing ▮▮▮▮▮▮▮ small-scale experiment (Table 3.3 ▮▮▮). Using ▮▮ volumes of ▮▮▮▮▮▮ permitted to obtain a ▮▮▮▮▮▮▮▮▮ ACMP1 ▮▮▮ in the ▮▮ fraction as well as ▮▮▮▮▮ elimination (Table 3.7, entry 7). Despite this, ▮▮▮▮▮ were only ▮▮▮▮▮▮ because the ▮▮▮▮▮▮▮▮▮▮ content in ▮▮▮▮ As ▮▮▮▮ seemed to be ▮▮▮

parameter in acidolysis procedures, we discarded to ▮▮▮▮ in further experiments in favor of ▮▮ which had a greater ▮▮▮▮▮ and ▮▮▮▮▮▮▮▮ during the experiment.
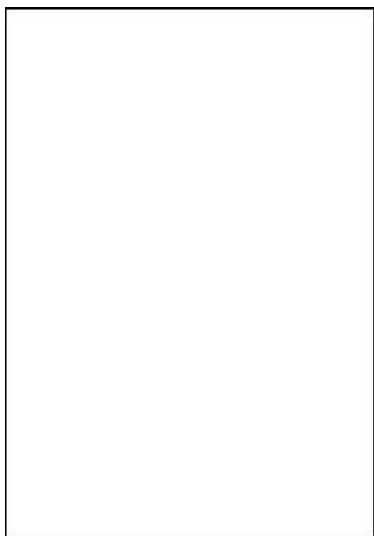
Figure 3.15 Experiment scheme of session 8th
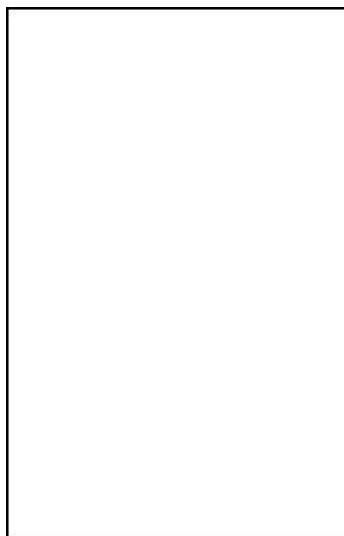
Figure 3.16 Experiment scheme of sessions 9th and 10th

For the experiment of session 8th, ▮▮▮▮ was not equipped ▮▮▮▮▮ at the exit ▮▮▮. Consequently, a ▮▮-permeable bag was used to introduce the ▮▮▮▮ ACMP1-CTC used in the experiment (Figure 3.15). Then, ▮▮▮▮▮▮▮▮▮▮▮▮▮▮▮▮▮▮▮ were introduced and left ▮▮▮▮▮. After this time, the reactor was ▮▮▮▮▮▮▮▮▮▮ and the resin was recovered using more of this ▮▮▮ mixture. Both ▮▮▮▮▮ fractions were lyophilized to obtain ▮▮▮▮▮▮▮▮▮ ACMP1 ▮▮▮ (Table 3.8, entries 1-2). These results confirmed ▮▮▮▮▮▮▮▮▮ acidolysis, because with ▮▮▮▮ ▮▮▮▮▮▮▮ were obtained in comparison to session 6th experiments (Table 3.8, entries 1-4). Despite this, the ▮▮▮ obtained in the 8th session were ▮▮▮▮▮▮ achieved in sessions 4th and 5th with the ▮▮ reactor.

Table 3.8 Results of sessions 8, 9 and 10

#	Session	Resin (g)	Cocktail	Volume (mL)	Time (h)	Fraction	Yield (%)	ACMP1 (%)				
1	8	▮	▮▮	▮	▮	▮	▮	▮	▮	▮	▮	▮
2			▮			▮	▮	▮	▮	▮	▮	▮
3	9	▮	▮▮	▮	▮	▮	▮					
4			▮			▮	▮	▮▮▮▮▮▮▮				
5	10	▮	▮▮	▮	▮	▮	▮	▮	▮	▮	▮	▮
6			▮			▮	▮	▮	▮	▮	▮	▮

In session 9th, one last experiment using ▮▮▮▮ was performed reproducing ▮▮▮▮▮ of a previous small-scale experiment (Table 3.4 ▮▮▮) but incorporating ▮▮▮▮. This time

though, ██████ was added at ███████, which permitted to introduce ████████ directly into the ████ reactor (Figure 3.16). ████████ ACMP1-CTC were treated █████████████████████ ██████████████████████. ████████████████ fractions were lyophilized to obtain ██████████ protected ACMP1████████ (Table 3.8, entries 3-4). Surprisingly, peptide ████████████ was observed in the HPLC analysis ████████ fractions, which was ██████████████ with the results obtained in the ████████████████ experiment using ██████████████████ without ████(Table 3.4, entry 8). In addition, it was observed that both in this and other experiments, the use of ███████████████████████ the acidolysis yields. Therefore, ████████████ discarded for further acidolysis experiments.

In session 10th, the same experiment as in session 8th was reproduced but extending the ████████ and using a ██████████████ (Figure 3.16). ████████ ACMP1-CTC were treated with ███ ██████████████████████████████. ██████████████ fractions were lyophilized to obtain ████████████████ ACMP1 ███████ (Table 3.8, entries 5-6). The results did ██████████ in comparison to session 8th, because the ████████████████████████ the same in both experiments. This meant that ████████████ to the acidolysis process was not ██████████████████ concentration in ████.

3.3.1.4   Green solvent experiments: third series

After ten sessions using either ██████████████, we reviewed the results obtained. Interestingly, it was observed that in the 2nd session, ██████████████████████ of the resin ██████████, once the resin was already ██████████████ (Figure 3.17). In addition, after ██████████████ the resin ██████████ meaning that ██████████ to the inner core ██████████████ during the experiment (Figure 3.18). Due to these observations, we tried to ██████████ this experiment but using ██████████ and ██████████████████████ to the resin.
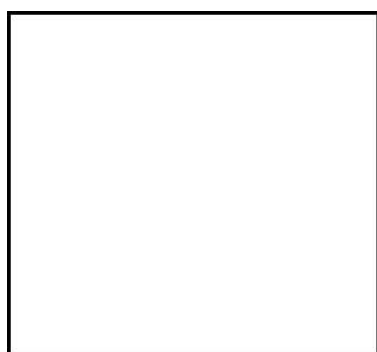
Figure 3.17 Non-swelled resin of 2nd session   *Figure 3.18* ██████████ *resin of 2nd session*

In the first experiment of 11th session, ████████ ACMP1-CTC were introduced ██████████████ vial that was placed ██████████ reactor (Figure 3.19). Then, ████████████████████ was introduced directly into the vial and ████████████████████ was added to the reactor. After ██████████, it was

observed how the ███████████████ began to stir with ████████ volume ████████, which was not possible at ███████████████ (Table 3.3). In these conditions, the experiment was left ██████████. Afterwards, in the ████████████ we observed a great quantity of ████████████ ████████████ at less ████████████. After complete ████████████, the ████████████ mixture was treated with ████████████ and the corresponding filtrate was lyophilized to give ████████████ ACMP1████ (Table 3.9, entry 1).
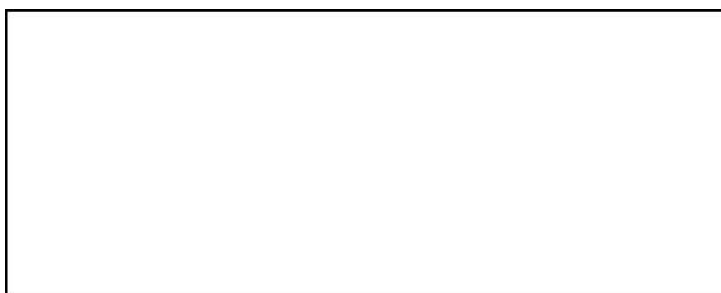
Figure 3.19 Experiment scheme of sessions 11th, 12th and 13th

In this session, a second experiment was performed in which ████████ ACMP1-CTC were treated with █████████████████████████████████████. In this second experiment it was definitively confirmed that ████████ dissolves █████, because the volume of the █████ ████████ experiment (Figure 3.20). The dilution ████████ due to ████████ could also explain how ████████ resin could be stirred ████████████ of the █████ in the first experiment. After treating the resin ████████████, the filtrate was lyophilized to obtain ████████████ ACMP1 ████████ (Table 3.9, entry 2).
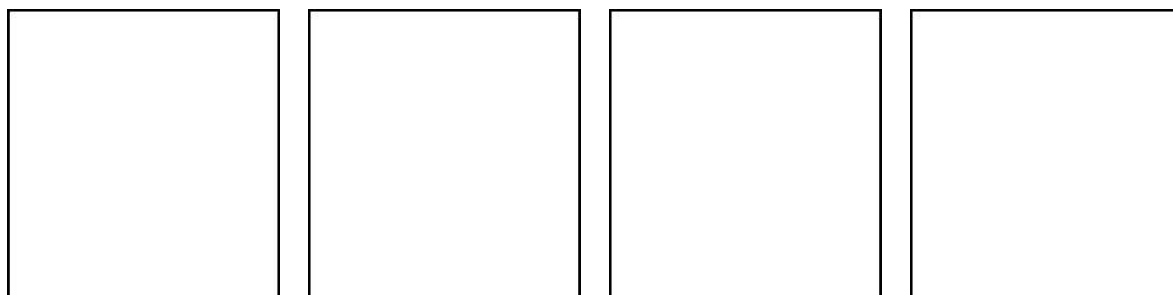
Figure 3.20 Second experiment of 11th session: i) ACMP1-CTC (█████); ii) ████████ introduction (█████);
iii) beginning of the experiment (█████); iv) end of the experiment ████████████

Overall, the goal of 11th session was to use the ████████████ to ████████████ of the resin ████████. Although this effect was slightly seen in the ████████████, we also observed the ███████████████████████████, which permits the ████████████ resin with ██ ████████████ of cocktail but it also ██████ it. Due to ████████████, only quantitative ████████ ████████ elimination were achieved as in other previous sessions.

Table 3.9 Results of sessions 11, 12 and 13

#	Session	Experiment	Resin (g)	Cocktail	Volume (mL)	▮	Time (h)	Yield (%)	ACMP1 (%)	▮	▮	▮	▮
1	11	1	▮	▮	▮	▮	▮	▮	▮	▮	▮	▮	▮
2		2		▮	▮	▮	▮	▮	▮	▮	▮	▮	▮
3	12	1	▮	▮	▮	▮	▮	▮	▮	▮	▮	▮	▮
4		2		▮	▮	▮	▮	▮	▮	▮	▮	▮	▮
5	13	1	▮	▮	▮	▮	▮	▮	▮	▮	▮	▮	▮
6		2		▮	▮	▮	▮	▮	▮	▮	▮	▮	▮

In session 12th, two more experiments were performed in which ▮▮▮ of ▮▮▮ were used trying ▮▮▮ of the cocktail. In the first experiment, ▮▮▮ ACMP1-CTC were treated with ▮▮▮ and ▮▮▮. In the second one, the previous conditions were reproduced but with only ▮▮▮ ▮ ▮▮▮. In both experiments, the resin was treated with ▮▮▮ and the filtrate was lyophilized to give ▮▮▮ ACMP1 ▮▮▮ (Table 3.9, entries 3-4). Although the experiments were conducted at ▮▮▮, their results were ▮▮▮ different. Therefore, ▮▮▮ did not ▮▮▮ these results. Probably, the difference may be attributed to ▮▮▮ of the experiment.
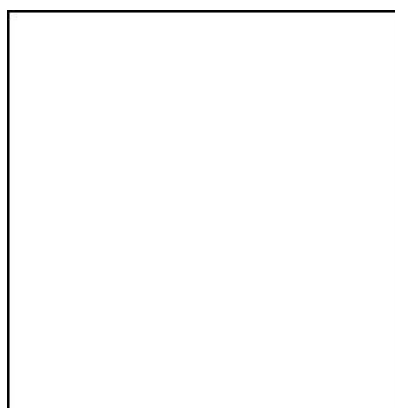
Figure 3.21 Second experiment of session 13th

Considering ▮▮▮, it was thought to perform more experiments with even ▮▮▮ ▮▮▮, but it was not possible as ▮▮▮ did not permit it: at ▮▮▮, the junction that permitted to ▮▮▮.

After knowing this information, two more experiments were performed but using ▮▮▮ ▮▮▮. Consequently, ▮▮▮ of ▮▮▮ would be avoided and we would know if

████████████ with an inert gas such as N₂ ████████████████ process or not. In the first experiment of 13ᵗʰ session, ████████ ACMP1-CTC were treated with ██████████████████████ in N₂ ████████████████████. In this case, using ██████████████████ in N₂, ████████████████████ during the experiment. In addition, no ████████ were observed at the end of the ████████████████, which meant ████████████████ N₂ was not ██████████████. After ████████████████████████████ ████ and lyophilizing the filtrate, ████████████████████ ACMP1 ██████████(Table 3.9, entry 5) were obtained. In the second experiment, the ██████████████████████ reproduced but with a ████████ ████████ of N₂ ████████████████████ (Table 3.9, entry 6). In contrast to the first experiment, we observed how part of ██████████████████████████. This meant that the ██████████████ was not complete using ████████ volume of ████████ in N₂ (Figure 3.21). In agreement with that, the ██████████████ results of these last two experiments with N₂ did ██████████████ the results of previous sessions, because ████████████████████ during the experiment.

3.3.2 Cleavage of protected peptides

███

██ ██ ██ ██ ██ ████████ ████ ██ ██ ██ ██ ██ ██████ ██ ████

███

███

███

███

███

████████

Considering ██████████████, we ██████████████████ the acidolysis strategy to obtain protected peptides from CTC resin ████████████████ in ████. ██████████████████████████████ ██ Acidolysis of protected peptides ██ ████████████████████ quantity of both TFA and DEE, because the resin ████████████████████████ has only to ████████████████ peptide to eliminate the sidechain PGs. ██████████████████████

███

██████████████████████ In addition, ████████████████ totally avoided in this process, which benefited our methodology ██████████████████████ perspective. To perform these cleavage studies, some more experiments were performed using the ██████████████████████.

3.3.2.1   Green solvent experiments: final series
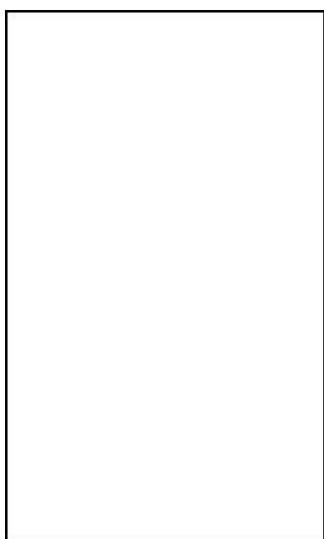
Figure 3.22 ████████████ *tube*
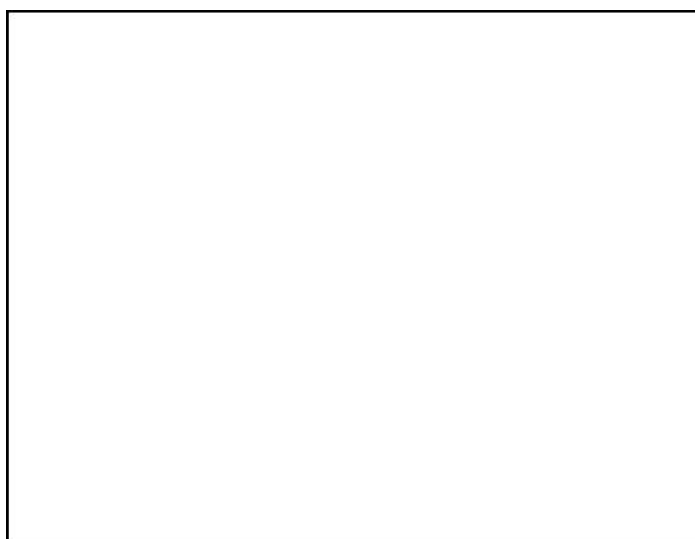
Figure 3.23 Experiment scheme of sessions 14th, 15th

In these new series of experiments, the key was ████████████████ inside the reactor after ████████████████ the resin with ███. In previous sessions, we were ████████████ resin with ████████████████ in the ██ reactor (Figure 3.10). To do this, a ████████ tube with a volume of ████████████████████████ before the entrance ████████████████████ (Figure 3.22 and Figure 3.23). By using this ████████ tube, the ███ reactor with the resin inside could be ████████ with ███. Then, the ████████ tube could be ████████████████████ with ███ using a syringe. After reconnecting ████████████ tube, the ███ could be introduced inside the ████████████████. By doing this, we could avoid ████████████████████████, instead ████████ would enter the ████████████████.

██

██

████████████████████████████

In the first experiment of session 14th, ████ of ACMP1-CTC were introduced directly inside the ████ reactor, which was ████████ with ████████████████ With both entrance ████ closed, the ████████ tube was ████████████████████████ were introduced inside with a syringe. Immediately, the ████████████████████ and ████████ with ███ ████████████████. The entrance ████ were opened and ████████ entered the reactor which was ████████████████. Then, the experiment was left ████████████. Afterwards, the reactor was ████████████████ and the resin was recovered using more of this mixture. Both ████████████ fractions were lyophilized to obtain ████████████████████ ACMP1 ████████ (Table 3.10, entries 1-2).

Table 3.10 Results of sessions 14 and 15

#	Session	Experiment	Resin (g)	Cocktail	Volume (mL)	███	Time (h)	Fraction	Yield (%)	███	███	███
1	14	▪	▪	▬	▪	▪ ▪	▪	▮	▪	▬	▬	▮
2				▪		▬		▪	▪	▬	▬	▬
3		▪	▪	▬	▪	▬ ▪	▪	▮	▮	▮	▮	▮
4				▬		▬		▮	▪	▮	▬	▮
5	15	▪	▪	▬	▪	▬ ▪	▪	▪	▮	▪	▬	▬
6		▪	▪	▪	▪	▬ ▪	▪	▪	▪	▪	▬	▬
7		▪	▪		▪	▬	▪	▪	▪	▮	▬	▬

In the second experiment, the methodology was reproduced with ██████ ACMP1-CTC and ▪
███████████████████████████████████████ was performed with ██████████████
████████████████████████ fractions were lyophilized, but ████████████████ ACMP1
██████ were obtained only from the ██████████████ (Table 3.10, entries 3-4). After the HPLC
analysis of this fraction, we could obtain ████████████████ ACMP1, which was ████████████
████████████████ was to cleave ACMP1 with all ██████████████.

For the experiments of 15th session, both ██████████ and the █████████████████ were ████████ to
try ██████████ the results. In addition, the resin was ██████████ with ███████████████████████
██████████████████████. In the first experiment, ████████ ACMP1-CTC resin were ██████████ with
████████████████████. Then, ████████████████████ were added using the ██████████ tube and
████████████████████, leaving the experiment stirring for ▪. After lyophilization, the ██████████
fraction gave ████████████████ ACMP1 ██████████ (Table 3.10, entry 5). In the second experiment,
██████ of ACMP1-CTC were ██████████ with ██████████████████████ and treated with ██████████
████████████ using ████████████████████████. After ▪ the resin was recovered using ██████████
▪ and the filtrate was lyophilized to obtain ████████████████ ACMP1 ██████ (Table 3.10, entry
6). In the third experiment of the session, the last methodology was reproduced but using only
████████████████████. The ██████████ fraction of this third experiment gave ████████████████
ACMP1 ██████ (Table 3.10, entry 7). Session 15th permitted us to develop a methodology to cleave
██████████ ACMP1 with all ██████████████████████████████████████ (██████████████████) and
██████████ the resin ████████████████████ (Figure 3.24). ████████████████████████████, we
performed more experiments using therapeutic peptides such as somatostatin or leuprolide
instead of the ACMP1 model peptide.
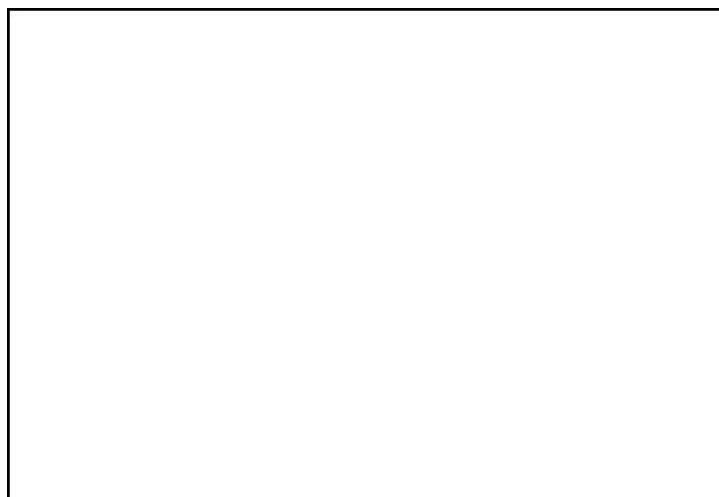
Figure 3.24 HPLC analysis of ▮▮▮▮ fraction (first experiment, 15th session)[38]

3.3.2.2 Cleavage of protected Somatostatin

The previous methodology with the ▮▮▮▮▮ was used to cleave SST-CTC[39] in session 16th (Figure 3.23). In the first experiment, ▮▮▮ of SST-CTC were ▮▮▮▮▮▮▮▮▮▮ ▮▮▮. Then, ▮▮▮▮▮▮▮▮▮▮ were added using the ▮▮▮▮ tube and ▮▮▮▮▮▮▮▮ ▮▮▮, and the experiment was left ▮▮▮▮▮▮. After ▮▮▮▮▮▮▮ no SST in the ▮▮▮▮ fraction was obtained (Table 3.11, entry 1).

▮▮

Table 3.11 SST-CTC results of sessions 16, 17 and 18

#	Session	Experiment	Resin (g)	Cocktail	Volume (mL)	▮	Time (h)	Fraction	Yield (%)	▮	▮
1	16	1	▮		▮	▮	▮	▮	▮	▮	▮
2	17	1	▮	▮	▮	▮ ▮	▮	▮	▮	▮	▮
3	18	3	▮	▮	▮	▮	▮	▮	▮	▮	▮

Despite the results obtained in session 16th, two more experiments with SST-CTC were conducted, this time using more quantity of ▮▮▮▮ for ▮▮. Following the same methodology as in session 16th, ▮▮▮▮ SST-CTC were ▮▮▮▮▮ with ▮▮▮▮ (▮▮▮▮▮) and treated for ▮ with ▮▮▮▮▮▮▮▮▮▮ in ▮▮▮▮▮▮▮▮▮▮▮. The ▮▮▮▮ fraction gave only ▮▮▮ of ▮▮▮▮▮▮▮▮ (Table 3.11, entry 2). This time HPLC-MS analysis revealed ▮▮▮▮▮▮▮

---

[38] ▮▮▮▮▮▮▮▮▮▮▮▮▮▮▮▮▮▮▮▮▮ ▮▮▮▮▮ ▮▮▮ ▮▮▮▮▮▮▮ ▮▮▮▮▮▮▮▮▮▮▮▮▮▮▮▮▮▮▮▮▮▮▮▮▮▮▮▮▮

[39] SST-CTC → **Boc**-Ala[1]-Gly[2]-Cys(**Trt**)[3]-Lys(**Boc**)[4]-Asn[5]-Phe[6]-Phe[7]-Trp[8]-Lys(**Boc**)[9]-Thr(***t*Bu**)[10]-Phe[11]-Thr(***t*Bu**)[12]-Ser(***t*Bu**)[13]-Cys(**Trt**)[14]-CTC resin

████████ SST █████ were recovered from ████████████ of the resin: i) ██████ SST █████ ([M+2H]$^{2+}$=1147.4 amu) corresponding to the loss of ████████ and ████████████; and, ii) ████████ SST █████ ([M+2H]$^{2+}$=1197.7 amu) corresponding to the loss ████████ group and the ████████████████ group. Due to the ████████████████████████████, we speculated that part of the ████████████████████ inside the resin ████████████ of its ████████████. ████████████████████████████████. In addition, standard acidolysis ████████████████ determined that the cleavage with ████████████████ in both sessions 16th and 17th. ████████████████████████████████

██

██████

3.3.2.3   Cleavage of protected Leuprolide

Table 3.12 LP-CTC results of sessions 17 and 18

#	Session	Experiment	Resin (g)	Cocktail	Volume (mL)	██	Time (h)	Fraction	Yield (%)	██	██	██	██	██	██	██
1	17	3	██	██	██	██ ▬	██	██	██	██	██	██	██	██	██	██
2	18	1	██	▬	██	██ ▬	██	██	██	██	██	██	██	██	██	██
3		2	██	██	██	▬	██	██	██	██	██	██	██	██	██	██

The previous methodology ████████████ tube was used to cleave LP-CTC[40] in session 17th (Figure 3.23). In the third experiment of that session, ████ of LP-CTC were ████████ with ████ ████████████. Then, ████████████ were added using ████████████████, and the experiment was left ████████████. After ████████████ , ████████ protected LP ████████ were obtained ████████████████ fraction. After HPLC analysis, protected LP ████████████████ obtained in this experiment (entry 1, Table 3.12).

████████████████████████████████ In addition, a mini-acidolysis experiment of the resin ████████████████████ of the resin was ████████████. With these results in hand, we designed two more experiments ████████ quantity of ██████ to obtain a ████████████████████████ LP in the ████████ fraction.

---

[40] LP-CTC → Pyroglutamic acid^1-His(**Trt**)^2-Trp^3-Ser(***tBu***)^4-Tyr(***tBu***)^5-D-Leu^6-Leu^7-Arg(**Pmc**)^8-Pro^9-CTC resin
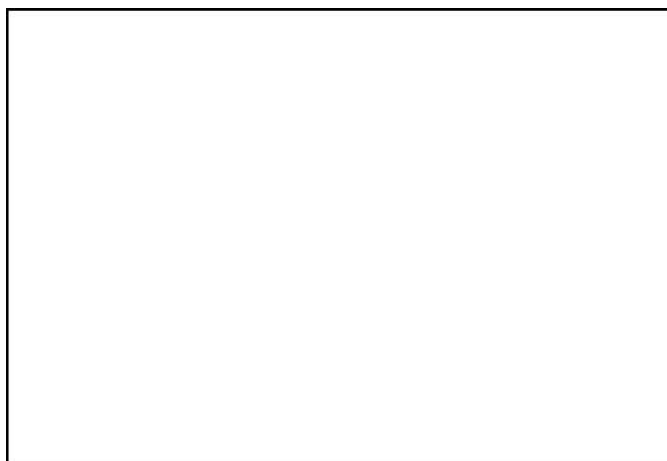
Figure 3.25 HPLC analysis of ▒▒▒▒ fraction (second experiment, 18th session)

In session 18th, the previous methodology was reproduced but using only ▒▒▒▒▒▒▒▒▒▒▒ . After ▒▒ of stirring, the reactor was ▒▒▒▒▒▒▒ on ▒▒▒▒▒▒ and the resin was recovered with ▒▒▒▒▒▒▒▒▒ . The ▒▒▒▒ fraction was lyophilized to obtain ▒▒▒▒▒▒ LP ▒▒▒▒ (Table 3.12, entry 2). After HPLC analysis, ▒▒▒▒▒ LP ▒▒▒▒▒▒▒▒▒▒▒▒ the results of previous experiments. Following the previous methodology, a second experiment was performed using ▒▒▒▒ LP-CTC but maintaining ▒▒▒▒▒▒▒▒▒▒ . In this case, the lyophilized washing fraction gave ▒▒▒▒▒▒▒ LP ▒▒▒▒ (Table 3.12, entry 3). Again, HPLC analysis revealed that ▒▒▒▒▒▒▒▒▒▒▒▒ obtained (Figure 3.25).

3.3.2.4 Leuprolide global deprotection in solution

After obtaining ▒▒▒▒▒▒▒▒▒▒▒▒▒▒▒ in sessions 17th and 18th, a series of mini-acidolysis experiments were designed to study ▒▒▒▒▒▒▒▒▒▒▒▒▒ worked with ▒▒▒▒▒▒▒▒▒ in comparison to standard procedures used in solid-phase (Table 3.13). As a reference, we reproduced the standard acidolysis procedure of LP-CTC treating ▒▒▒▒▒▒▒▒▒▒▒▒▒ (entry 1). Then, 20 mg of protected LP were treated with various volumes of cocktail A in solution (entries 2-5). The HPLC-MS analysis of these samples revealed ▒▒▒▒▒▒▒▒ were obtained when the amount of cocktail A ▒▒▒▒▒▒▒ : 1) LP+▒▒▒ ([M+H]$^+$= 1449.2 amu); and, 2) LP+▒▒▒ ([M+H]$^+$= 1383.3 amu). To reduce the amount of these impurities, cocktail B and C were used in ▒▒▒▒▒▒▒▒ , but the results were even worse than with cocktail A (entries 6-7 vs entry 5). The same happened when the time of the experiments was varied (entries 8-9).

Table 3.13 Mini-acidolysis experiments in solution of protected LP (sessions 17ᵗʰ and 18ᵗʰ)

#	Protected LP (mg)	Cocktail[41]	Volume (µL)	Time (h)	LP (%)		
1	20 (resin)	A	■	■	97.3	■	■
2	20	A	■	■	96.7	■	■
3	20	A	■	■	■	■	■
4	20	A	■	■	■	■	■
5	20	A	■	■	■	■	■
6	20	B	■	■	35.1	■	■
7	20	C	■	■	56.6	■	▮
8	20	A	■	■	65.7	■	■
9	20	A	■	■	80.2	■	■

With the previous results in hand, ███████████ experiments ██████████████ LP were performed (Table 3.14). First, ██████████ LP were treated with ██████ cocktail A (████████) ████████████. After that time, the peptide was precipitated in cold DEE (██████), centrifuged and the supernatant was discarded. The peptide crude was washed with more DEE (████████) and dried under vacuum to obtain █████ of LP (entry 1). The HPLC analysis revealed that ████████████████ was similar to the one obtained in the mini-acidolysis experiment (Figure 3.26).

Table 3.14 ███████ *acidolysis experiments* █████████████ **LP**

#	Protected LP (g)	Cocktail	Volume (mL)	DEE (mL)	Time (h)	Yield (%)	LP (%)		
1	■	■	■	■	■	■	■	■	■
2	■	■	■	■	■	■	■	■	■

A second experiment was performed, in which ██████████████ LP were treated with ███████ of cocktail A █████. After the precipitation in cold DEE (███████) and the washings (████████), the peptide crude was dried overnight under vacuum to obtain ████████ LP (entry 2). Again, the HPLC results showed that █████████████ was similar to previous experiments using this procedure (█████). Finally, this ██████████████ were purified via preparative HPLC to obtain █████████ pure LP (Figure 3.27).

---

[41] **Cocktail A →** ████████████████████████ // **Cocktail B →** ████████████████████████ // **Cocktail C →** ████████████████

Figure 3.26 Acidolysis in solution of 1.9 g of protected LP

Figure 3.27 Purified LP (isocratic)

3.4 Discussion and conclusions

Eighteen sessions of acidolysis experiments using ▮▮ have been performed following two different strategies: global cleavage/deprotection (sessions 1-13) and cleavage of protected peptides (sessions 14-18).

Under the first strategy, ▮▮▮▮▮▮▮▮▮▮▮▮▮▮ was used to develop a global cleavage/deprotection methodology ▮▮▮▮▮▮▮▮. ▮▮▮▮▮

▮▮▮▮▮▮▮▮▮▮▮▮▮▮▮▮▮▮▮▮▮▮▮▮▮▮▮▮

▮▮▮▮▮▮▮▮▮▮▮▮▮▮ ▮ ▮▮▮▮▮▮▮▮▮▮▮▮▮

▮▮▮▮▮▮▮▮▮▮▮▮▮▮▮▮▮▮▮▮▮▮▮▮▮▮▮▮

▮▮▮▮▮▮ ▮ ▮▮▮ ▮▮▮▮ ▮ ▮▮▮▮ ▮ ▮▮▮▮ ▮ ▮▮▮ ▮▮▮ ▮▮▮▮

▮▮▮▮▮▮▮▮▮▮▮▮▮▮▮▮▮▮▮▮▮▮▮▮▮▮▮▮

▮▮▮▮▮▮▮▮▮▮▮▮▮▮▮▮▮▮▮▮▮▮▮▮

▮▮ is not as a greener alternative ▮▮▮▮▮▮▮▮ on the cell walls of ▮ reactor (3rd session) caused by ▮▮▮▮▮ mixtures. Using ▮▮▮ the co-solvent for ▮▮ did not improve the results as it lowered the acidolysis ▮▮▮ ▮ caused peptide ▮▮▮▮. Unexpectedly, we also found that ▮▮▮▮▮▮▮▮▮▮▮, increasing its volume and ▮▮▮▮. As a consequence, it was possible to ▮▮▮▮▮▮▮▮▮▮▮▮, but again only ▮▮▮▮▮▮ elimination were obtained. Initially, we hypothesized that the ▮▮▮▮▮▮▮▮ the resin with ▮▮▮▮ the elimination of ▮▮▮▮▮, but our experiment with N_2 ▮▮▮▮▮▮▮▮▮ (session 13th).

▮▮▮▮▮▮▮▮▮▮▮▮▮▮▮▮▮▮▮▮▮▮▮▮▮▮▮▮

▮▮▮▮▮▮▮▮▮▮▮▮▮▮ With this in mind, we developed a methodology to cleave ▮▮▮▮ ACMP1 in the ▮▮ reactor without the need ▮▮▮▮▮ (sessions 14-15). After some optimization experiments, we put this ▮▮▮▮▮▮▮ with

two therapeutic peptides such as SST and LP. In the case of SST, the methodology ██████ ████████████████████████ protected SST: i) ████████████████████████████ from the resin beads; and, ii) its cleavage ███████████████ (17th session).

███

██████ ███

███

███

███

██████████████████████████████████████

Table 3.15 Comparison between our green solvent-cleavage strategy and standard procedures

METHOD COMPARISON		Green solvent-cleavage strategy		Standard procedure
		18th session	Estimation	
Resin (LP-CTC)		██	██	80.0 g
Green solvent cleavage	██████	██	██	-
	██████	██	██	-
	██████	██	██	-
	███████	██	██	-
	██████	██	██	-
	██████	██	██	-
Global Deprotection	**Cocktail**[43]	██	██	0.8 L
	DEE	██ ██	██ ██	14.6 L[44c]

███

██ ██ ███ Table 3.15

███

███

███

███

███

███

███

██████████████████████████████████████

In comparison to our green solvent-mediated cleavage strategy for LP-CTC, the standard acidolysis procedure would require ██████████████████████████████████

---

[42] Cleavage cocktail → ████████████████

[43] Cocktail A →████████████████████████

[44] ██████████████████████████ ███████████████████████████████ █████████████████████████████████ ██.

████████. For example, for 80.0 g of LP-CTC, 0.8 L of cocktail A and 14.6 L of cold DEE would be needed (Table 3.15). ██

██

██

██

██

██ ████████████

██

██

██

██

██

██

██

██

██

████████████████████████████████████

Chapter 4

Synthesis of Somatostatin Analogs

4 Synthesis of Somatostatin Analogs

4.1 Introduction

4.1.1 Somatostatin

Somatostatin (SST14)[45] is an endogenous peptide hormone composed by 14 amino acids, that was first isolated in 1973 from ovine hypothalamus based on its ability to inhibit the release of growth hormone (GH) from the anterior pituitary[12,153] (Figure 4.1). Some years later, SST14 was found to act as a neuromodulator and a neurotransmitter in the human body[13,154]. Currently, SST14 is in the market for the treatment of acromegaly and neuroendocrine tumor therapy. Apart from the natural peptide, other approved synthetic somatostatin analogs (SSAs) are octreotide, lanreotide, vapreotide and pasireotide.
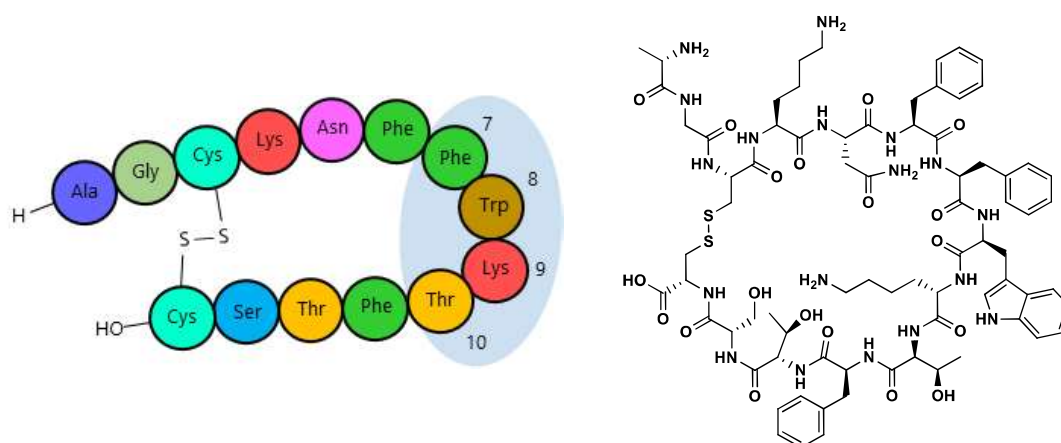
Figure 4.1 SST14: H-Ala^1-Gly^2-c(Cys^3-Lys^4-Asn^5-Phe^6-Phe^7-Trp^8-Lys^9-Thr^{10}-Phe^{11}-Thr^{12}-Ser^{13}-Cys^{14})-OH

4.1.2 Somatostatin receptors

SST14 induces its biological effects through direct binding to somatostatin receptors (SSTRs). In humans, five different somatostatin receptors (SSTR1-5) were cloned and characterized in the early 1990s[154,155], being named chronologically according to their respective publication dates[153,154]. From a structural point of view, SSTR1-5 possess seven transmembrane domains (TMDs) that provide the characteristic architecture of G-protein-coupled receptors (GPCRs)[153]. In our body, SSTRs have been found expressed in the pituitary, pancreas, gastrointestinal (GI) tract, brain and in a variety of tumor cells. At present, the X-ray crystal structures of SSTRs are not available.

An extremely important characteristic of SSTRs is that upon ligand binding the whole ligand-receptor complex is internalized inside the cells, which is critical for receptor downregulation,

---

[45] Also known as Somatotropin Release-Inhibiting Factor (SRIF).

resensitization and signaling[156]. This so-called SSTR-mediated internalization is also the principal base for the use of SSAs as peptide conjugates for the delivery of cytotoxic drugs or radiometals either for cancer treatment or diagnosis. After the internalization of the ligand-receptor complex, this interaction with the ligand is disrupted and the receptor might be either recycled back to the cellular membrane or degraded.

Differences in the cell trafficking and internalization capabilities of the different receptor subtypes have to be considered[157]. Several studies have shown that SSTR2, SSTR3 and SSTR5 are internalized to a much higher extent than SSTR1 (very slow[158,159]) and SSTR4 (absent[160]) after ligand stimulation[161,162]. Related to this, some other studies suggest that SSTR2 is efficiently recycled to the cell membrane (60-90 min) and does not enter to any degradative pathway[153,161]. SSTR3-ligand complex is internalized after 30 min[161], but this subtype shows a rapid downregulation (50%) upon prolonged ligand exposure (6 to 12h) when transfected to cells[161,163–165]. Regarding SSTR4, low levels of internalized human SSTR4 in transfected cells were detected upon SST14 treatment[166]. The proportion of SSTR5 internalized after 30 minutes of SST14 exposure is considerably lower than SSTR2 receptor (30-40% vs 80-90%, respectively)[167,168]. The SSTR5 dynamics regarding internalization and trafficking are ligand- and context-dependent.

Because of the variety of physiological functions and the capability to internalize inside the cells, SST14 may play a role in the treatment of various human diseases. Despite this, the clinical use of this natural peptide has been impeded by its short plasma half-life ($t_{1/2}$ < 3 min)[13,169], which makes continuous parenteral infusion necessary and restricts its use to hospital level[33]. Because of these reasons, researchers were specifically interested on the minimum structural requirements for biological activity to design and develop somatostatin analogs (SSAs), either with selective or multireceptor affinities.

4.1.3 Development of Somatostatin analogs

Since the discovery of SST14, it has not been possible to obtain X-ray crystal structures of any of the SSTR-subtypes. Therefore, the great research efforts carried out since the 1970s to find more stable therapeutic SSAs have followed ligand-based drug design strategies.

The initial work on the development of SSAs was performed by Vale et al[155,170,171], whose approach was to synthesize different series of peptide ligands structurally-related to the parent SST14. The most important series of this study were: i) progressive shortening of the peptide; ii) replacement of each amino acid with alanine; iii) replacement of each residue with the corresponding D-amino acid; iv) replacement of single residues with other amino acids; and v) deletion and/or modification of multiple residues[155].

In the D-amino acid series, D-Trp[8] substitution increased the inhibition potency by 6-8 times of GH release *in vitro* and glucagon and insulin release *in vivo*[34], being **(D-Trp[8])-SST** the first analog to be reported with significant higher potency than SST14. The increase of pharmacological activity might be related either to the stabilization of a biologically active conformation or a higher resistance to degradation[155]. The alanine scan series was particularly useful for interpreting the roles of each amino acid sidechains[170,171]. Alanine substitution of Gly[3], Lys[4], Asn[5], Thr[10], Thr[12] and Ser[13] did not reduce the GH-inhibition activity, indicating that the functional groups of their sidechains were not crucial for SSTR-binding. In contrast, alanine replacement of Phe[6], Phe[7], Trp[8], Lys[9] and Phe[11] decreased enormously the GH-inhibiting potency to less than 4%. Related to this, Trp[8] was considered to be the crucial amino acid for binding to SSTRs due to the presence of the indole NH group that permits hydrogen-bonding with the receptor, as well as interaction with Lys[9] to favor the biological active conformation of the molecule[172].

The single and multiple amino acid deletion series permitted to discover the smallest peptide derived from SST14 that could inhibit GH secretion[46]. Based on these pioneering findings, the fragment Phe[7]-Trp[8]-Lys[9]-Thr[10] was proposed as the pharmacophore of the SST14 structure[155]. Therefore, these four amino acids were considered to be very important for the binding interaction with SSTRs, being Trp[8]-Lys[9] the most critical ones[172].
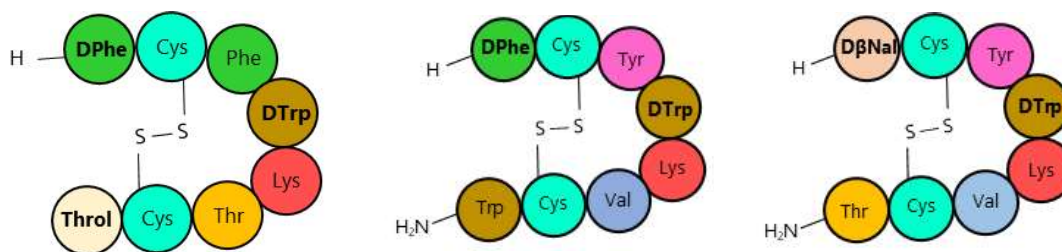
Figure 4.2 Structure of octreotide (left), vapreotide (middle) and lanreotide (right)

Using the previous hexapeptide as a starting point, Bauer et al.[18] decided to prepare a series of analogs incorporating additional residues at both ends to find a more stable peptide. To mimic Phe[6] of the parent SST14, D-Phe residue was added to the *N*-terminal. This proved to be advantageous for biological activity, because the aromatic sidechain may occupy the available conformational space of Phe[6] in SST14, as well as protect the disulfide bond against enzymatic degradation. At the *C*-terminus, the addition of threoninol (Throl) further increased the activity by protecting the pharmacophore fragment against enzymatic degradation. The resulting octapeptide named octreotide[47] (Figure 4.2) displayed greater potency, increased metabolic stability ($t_{1/2} \sim 117$ min) and selectivity for GH inhibition over insulin and glucagon, in comparison

---

[46] H-*c*(Cys[1]-Phe[2]-D-Trp[3]-Lys[4]-Thr[5]-Cys[6])-OH.
[47] Octreotide (H-D-Phe[1]-*c*(Cys[2]-Phe[3]-D-Trp[4]-Lys[5]-Thr[6]-Cys[7])-Throl[8]).

to SST14. These characteristics made octreotide (Sandostatin®, SMS201-995) the first commercial SSA approved for clinical use[153,173]. The previous findings encouraged researchers to use this octapeptide scaffold as a starting point for further development of new SSAs. In the following years, vapreotide[48] (Sanvar®, RC-160)[19,174] and lanreotide[49] (Somatuline®, BIM-23014)[20,175] became the next commercial SSAs (Figure 4.2 and Table 4.1).

Table 4.1 Binding affinities of octreotide, vapreotide, lanreotide and pasireotide

Compound	SSTR1 K_i (nm)	SSTR2 K_i (nm)	SSTR3 K_i (nm)	SSTR4 K_i (nm)	SSTR5 K_i (nm)	Bibliography
SST14	**1.1**	**1.3**	**1.6**	**0.53**	**0.9**	Patel et al.[176]
Octreotide	> 1000	**2.1**	**4.4**	> 1000	**5.6**	
Vapreotide	> 1000	**5.4**	31	> 1000	**0.7**	
Lanreotide	> 1000	**1.8**	43	66	**0.62**	
Pasireotide	9.3	**1.0**	**1.5**	> 100	**0.16**	Bruns et al.[21]

As octreotide, the initial biological function of these analogs was to inhibit GH secretion. This anti-secretory effect happens because all three octapeptides bind with high affinity to SSTR2, which is the responsible of GH-inhibition. In the case of octreotide, affinity to a lesser extent with SSTR5 and SSTR3 was also demonstrated, displaying no affinity for SSTR1 and SSTR4[176]. Regarding lanreotide and vapreotide, both presenting the Tyr[3]-D-Trp[4]-Lys[5]-Val[6] fragment, they were capable of binding to SSTR5 with even higher affinity than SSTR2 at the expense of losing some part of their affinity to SSTR3[176]. As in the case of octreotide, both vapreotide and lanreotide showed no binding with SSTR1 and SSTR4.
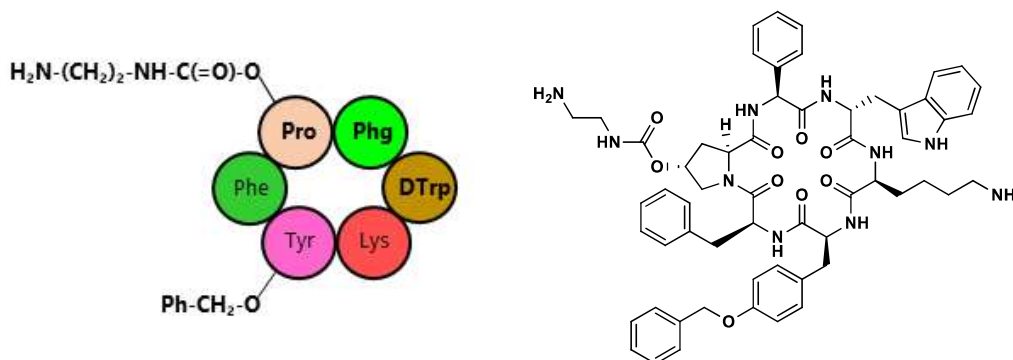
Figure 4.3 Structure of pasireotide

Until the 2000s, this first generation of SSAs were the only ones approved and commercialized for treating SSTR-related diseases. The specific binding profile of these analogs left room for the search of a second generation of multireceptor SSAs with affinity for all SSTR subtypes and high stability. The search of a multireceptor ligand led to the discovery of pasireotide (Signifor®, Figure 4.3), a cyclic hexapeptide with affinity for SSTR5 > SSTR2 > SSTR3 > SSTR1[21,177]. Although this

---

[48] Vapreotide (H-D-Phe[1]-*c*(Cys[2]-Tyr[3]-D-Trp[4]-Lys[5]-Val[6]-Cys[7])-Trp[8]-OH).
[49] Lanreotide (H-D-β-Nal[1]-*c*(Cys[2]-Tyr[3]-D-Trp[4]-Lys[5]-Val[6]-Cys[7])-Thr[8]-OH).

peptide does not show any affinity for SSTR4, it is the only commercialized analog with affinity for SSTR1[178]. Because of its binding to four out of five SSTRs, it is considered to be a multireceptor analog with a half-life *in vivo* of nearly 23h in rats[21].

4.1.4 Biological applications

4.1.4.1 SST14 in the human body

The first biological activity of SST14 and related analogs was to inhibit GH-secretion[12] via SSTR2 and SSTR5. In the following years, other anti-secretory and regulatory activities of SST14 on many other hormones were reported: inhibition of glucagon secretion via SSTR2 and insulin secretion via SSTR5[179]. Prolactic thyroid-stimulating hormone, gastrin and ghrelin are other examples. As a consequence, SST14 is not only present in the hypothalamus as originally thought, but also in the anterior pituitary gland, the GI tract and the pancreas among other parts of our body[153,155,180,181].

Apart from regulation of hormone secretion, anti-proliferative effects are the second main role of SST14 in our body and the rationale to use SSAs to treat SSTR-positive tumors. In fact, SST14 was found to stimulate apoptotic mechanisms through SSTR3, and to a lesser extent SSTR2, which contribute to its anti-proliferative mechanisms[182–184]. This explains why SST14 and related analogs inhibit tumor growth in various cultured cell lines and animal tumor models[185,186].

4.1.4.2 SSTRs incidence in cancer

The expression of SSTRs in various human tumors, made researchers focus on the applicability of SSAs in oncology. The main clinical implications in human tumors are: i) long-term therapy; ii) cancer diagnosis; and iii) cancer treatment.

SSTR-*in vitro* evaluation is extremely important to identify tumor types suitable to be targeted using SSAs. To predict with certainty the *in vivo* SSTRs status of a tumor, it is vital to analyze the receptors of the primary tumor and its metastases. To analyze tissue from a tumor biopsy is still the best way to determine the SSTRs status of a tumor[187]. Having identified receptors in human tumor cell lines or in human tumors grown in animals is not enough, as great differences may occur in receptor expression[188,189]. It is also important to investigate the presence of SSTR proteins rather than *m*RNA, because in human tumors *m*RNA and protein levels may differ[190]. Receptor binding methodologies (binding assays or receptor autoradiography) and receptor immunochemistry are valuable techniques as they provide information about receptor protein expression. Nevertheless, SSTR *m*RNA abundance might also be significant when the previous methods are unable to give valuable information[187].

High expression and density of SSTRs has been found in neuroendocrine tumors (NETs)[50], GH-secreting pituitary adenomas, gastroenteropancreatic (GEP) tumors, pheochromocytomas, neuroblastomas, and to a lesser extent in medullary thyroid cancers and small-cell lung cancers. Other non-neuroendocrine tumors including brain tumors, breast carcinomas, lymphomas, renal cell cancers, prostatic, ovarian, gastric and hepatocellular carcinomas have also shown to express SSTRs[187]. The distribution of SSTRs in these tumors is very important because more homogeneity of receptor expression is normally translated to a more effective targeting either for cancer diagnosis or treatment[187]. As an example, gastroenteropancreatic neuroendocrine tumors (GEP-NETs) display normally the most homogeneous SSTRs distribution. In contrast, other tumors such as breast carcinomas are characterized by a high heterogeneous distribution of SSTRs, with regions of high density of receptors next to regions lacking these receptors[187].

SSTR2 is the most abundant receptor subtype expressed in the majority of human tumors[191], such as somatotroph and thyrotroph pituitary adenomas (>80%), as well as in pheochromocytomas and paragangliomas (>70%)[191–194]. In brain tumors, SSTR2 is present in most meningiomas[191,195], medulloblastomas[196–198] and neuroblastomas[199]. In GEP-NETs, SSTR2 represents the most expressed receptor subtype, being identified in >70% of cases at a high expression intensity[191,192,200–205]. 32-56% of bronchopulmonary NETs, as well as NETs of other origins including thymus, breast, cervix, or prostate express also SSTR2[206,207]. Depending on tumor grade and location, SSTR2 was observed in 45-100% of colorectal carcinomas[184,208] and in 41-67% of hepatocellular carcinomas[209–211]. SSTR2 was found in 20-79% of breast cancers[191,192,212–215], in 57% of cervical carcinomas, in 39% of endometrial cancers[216] and in 30% of ovarian carcinomas[216,217]. Moderate to strong SSTR2 expression was observed in 50% of prostate cancers with neuroendocrine differentiation (NED)[218,219].

SSTR1 is the most abundant receptor subtype in prostate carcinomas, sarcomas[220–222] and bronchopulmonary NETs[223]. In addition, its presence was also confirmed in pituitary somatotroph adenomas, pancreatic adenocarcinoma, stomach cancer, urinary bladder cancer, pheochromocytoma, GI NETs, breast carcinoma, cervix carcinoma, and ovarian tumors[224].

SSTR3 is also present in different human tumors, especially in pituitary adenomas. Gonadotropic and non-functioning pituitary adenomas express high levels of SSTR3, whereas expression of SSTR2 and SSTR5 is very low or absent[225–227]. SSTR3 is expressed in about 30-50% of

---

[50] Neuroendocrine tumors (NETs) originate in the neuroendocrine system cells, which have traits of both hormone-producing endocrine cells and nerve cells, and help to control many functions of our body. All NETs are considered malignant tumors and may begin to grow in any part of the body, including the lung (30%), GI tract (43%) and pancreas (7%). NETs can also begin in other organs.

pheochromocytomas and paragangliomas[194]. Although SSTR2 is clearly the most abundant receptor in GEP-NETs, SSTR3 was also detected in 52-90% of cases[204,225,228]. However, strong SSTR3 expression was only noted in 5-29% of cases[204,228,229]. Low SSTR3 expression levels occur also in bronchopulmonary NETs[230]. In about 50% of tumors with NED derived from breast, cervix, or prostate, weak to moderate SSTR3 expression was observed[207]. SSTR3 was also detected in 56% of GI stromal tumors[231].

The cellular expression of human SSTR4 is in general less characterized[153]. Despite this, SSTR4 has been found in cells of the bronchial glands, the exocrine pancreas, in the GI tract (stomach and duodenum), in kidney tubules, and in the parathyroid gland[232]. In contrast to other SSTRs, lack of SSTR4 binding sites and immunoreactivity in pituitary tissue suggests that this receptor does not play a major role in the control of the human anterior pituitary[220,233]. According to receptor autoradiography, SSTR4 cannot be frequently found in human tumors[220].

SSTR5 is expressed with high intensity in all somatotroph and most of corticotroph adenomas, whereas it is low expressed in gonadotroph and non-functioning pituitary adenomas[192,226,227]. SSTR5 was detected in 38-57% of medullary and in most of papillary and follicular thyroid carcinomas (>75%)[234–237]. SSTR5 was also identified in pheochromocytomas, paragangliomas[192,194], and lymphomas[238,239]. Regarding GEP-NETs in general, SSTR5 is the second most abundant subtype after SSTR2, being detected in 62-93% of GEP-NETs[192,204,205,228,229]. SSTR5 was observed in 31-45% of bronchopulmonary NETs[230,240] and occasionally also in other tumors with NED[207]. SSTR5 was detected in 39-70% of colorectal cancers, being its expression higher in well differentiated tumors as compared to poorly differentiated ones[184,208]. SSTR5 was also detected in most breast, cervical, ovarian, and prostate carcinomas[192], as well as in 45% of Merkell cell tumors[241].

Overall, the positive SSTR-expression in different types of cancer and the development of stable analogs have made possible the clinical application of SSAs to treat cancer, principally NETs[187].

4.1.4.3 Long-term cancer therapy

The first successful clinical application of SSAs was the symptomatic treatment of hormone-secreting tumors. Thanks to hormone-inhibiting effects, treatment with SSAs usually results in a significant improvement of life quality of patients, basically because of normalization of hormone levels[187]. Related to this, the introduction of long-acting release (LAR) formulations of octreotide, lanreotide and pasireotide facilitated enormously long-term therapies and improved also the life quality of patients by reducing the number of needed administration doses[242,243]. Acromegaly

and Cushing's Disease (CD) are the principal diseases in which long-term SSA therapy is applied, as well as in patients with NETs.

Acromegaly is a slowly progressive disease resulting from the increased release of GH and insulin-like growth factor 1, which in the majority of cases is induced by a pituitary tumor[244]. Octreotide and lanreotide have proven to be safe and effective for long-term acromegaly management. Because of this reason, they are always recommended as first-line therapy in patients who are not suitable for surgery or who are unlikely to be cured by surgery[244]. The second-generation analog pasireotide has also been used successfully in acromegaly patients resistant to octreotide or lanreotide treatment, achieving GH-control in 15-20% of subjects[245]. Despite this, the high affinity of pasireotide for SSTR5, increases significantly the percentage of patients that develop hyperglycemia secondary effects which may limit its use in patients with uncontrolled diabetes mellitus[244–246].

CD is caused by a tumor originating from the corticotroph cells of the pituitary gland. This tumor chronically stimulates the hypersecretion of adrenocorticotropic hormone (ACTH) that leads to adrenal cortisol overproduction[247–249]. High levels of circulating cortisol in patients with untreated CD exert suppressive effects on SSTR2 and SSTR5 expression, but as the latter is less sensitive than SSTR2 to these suppressive cortisol effects[250], SSTR5 is considered the target for medical treatment in patients with untreated CD[249]. With the introduction of pasireotide with high affinity for SSTR5, this analog was evaluated for its efficacy in inhibiting ACTH and cortisol production in patients with CD[249]. After *in vitro* demonstration that pasireotide was effective in reducing ACTH secretion, several clinical trials testing its efficacy in CD patients were initiated. A double-blind, randomized phase III trial with 162 patients treated with pasireotide showed that median urinary-free cortisol (UFC) levels were suppressed by 50%, whereas 24% exhibited normalized UFC levels after 6 months.

GEP-NETs are the type of tumors with the highest homogeneity and abundance of SSTR2-expression[251]. In addition, they exhibit significant morbidity and mortality, and after diagnosis fewer than 50% are surgically resectable[252]. Since the introduction of SSAs, survival in NET patients has improved three-times[253,254]. In the PROMID clinical trial (85 patients with metastatic midgut NET), octreotide LAR demonstrated to increase the median time to tumor progression from 6 to 14.3 months[255], as well as stabilization in two-thirds of patients. In addition, in the 96-week CLARINET trial, lanreotide autogel demonstrated prolonged disease-free survival on 204 patients that were randomized to receive either this treatment or placebo[256].

Due to all these reasons, both the FDA (US) and the EMA (EU) gave approval for the commercialization of these SSAs for long-term somatostatin therapy. Octreotide LAR (Sandostatin LAR®, Novartis) has been authorized in the EU since the 1990s for treating acromegaly, GEP-NETs, and bleeding gastroesophageal varices. The FDA approved octreotide LAR in 1998 as a long-term treatment of patients with acromegaly, carcinoid tumors or vasoactive intestinal peptide tumors (VIPomas). Lanreotide (Somatuline® Depot, Biomeasure[51]) was approved in 2007 by the FDA as a long-term treatment of acromegaly in patients who have had an inadequate response to surgery and/or radiotherapy. In 2014, the FDA also approved lanreotide (Somatuline® Depot, Ipsen Biopharmaceuticals) for the treatment of patients with unresectable, well- or moderately-differentiated locally advanced or metastatic GEP-NETs to improve progression-free survival. Finally, in 2017 the FDA approved lanreotide for the treatment of carcinoid syndrome[52].

In 2014, the FDA approved pasireotide LAR (Signifor® LAR, Novartis) for the treatment of patients with acromegaly who have had an inadequate response to surgery and/or whom surgery is not an option. This long-acting formulation was also approved by the FDA in 2018 for the treatment of patients with CD for whom pituitary surgery was not an option or had not been curative. In the EU, pasireotide was approved by the EMA in 2014 for the treatment of patients with acromegaly, and two years before in 2012 it had been approved for patients with CD.

4.1.4.4   Tumor diagnosis and treatment with radiolabeled analogs

In 1989, Krenning et al.[257] reported [^{123}I]-(Tyr^3)-octreotide ([^{123}I]-TOC[53]), which was the first reported radioligand based on octreotide. The Tyr^3 modification permitted to label this compound with [^{123}I] for successful non-invasive single-photon emission computed tomography (SPECT) imaging of SSTR-positive tumors in 10 patients. This initial report was considered as a pioneering study in the field of SSTR-imaging, a proof-of-concept for peptide receptor imaging (PRI) and a starting point for development of radiolabeled peptide ligands.

Nevertheless, with the objective to overcome the biodistribution problems of [^{123}I]-TOC, Bakker et al.[258–260] reported in 1991 the conjugation of a chelator to the *N*-terminus of octreotide, which permitted the radiolabeling with a γ-emitter, resulting in [^{111}In]-DTPA-octreotide[54] (also known as [^{111}In]-pentetreotide, Figure 4.4). This radioligand demonstrated to be superior due to ease of preparation, appropriate half-life and absence of accumulation in the upper abdominal

---

[51] Affiliated within the Ipsen Group.
[52] Neurochemical imbalance in the body caused by a cancerous tumor which can result in diarrhea and skin flushing.
[53] TOC is the abbreviation of (Tyr^3)-Octreotide.
[54] DTPA (diethylenetriaminepentaacetic acid).

region[261]. In addition, the use of chelators (*e.g.* DTPA[54]) conjugated to the *N*-terminus of the peptide facilitated the fast and simple complexation procedures[153].
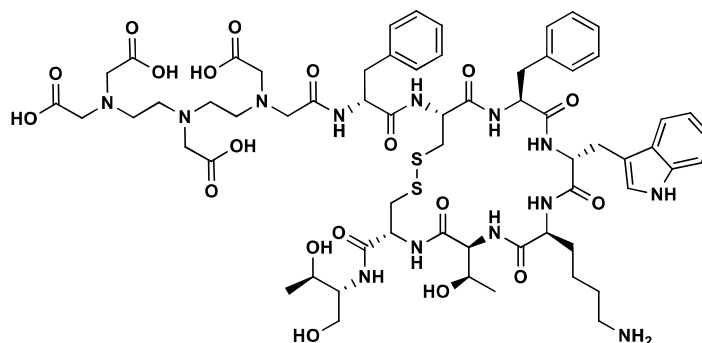
Figure 4.4 Structure of DTPA-octreotide (pentetreotide)

Because of its higher SPECT sensitivity and specificity in patients with GEP-NETs compared to classic imaging techniques, [^{111}In]-pentetreotide (Octreoscan®, Curium) was approved in 1994 by the FDA as the first peptide-based imaging radiopharmaceutical grounded on the results in 250 patients[153]. This established the way to design and synthesize radiolabeled-SSAs consisting in three major elements crucial for the diagnosis or treatment of SSTR-positive cancers: i) the <u>radiometal</u> may be used either for diagnostic (*e.g.* [^{68}Ga]) or treatment (*e.g.* [^{177}Lu]) of the tumor; ii) the <u>peptide ligand</u> (in this case SSAs) permits the internalization of the entire radioligand and the accumulation of the radiometal inside the tumoral cells[262]; and iii) the <u>chelator</u> is a molecule that is conjugated normally at the *N*-terminus of the ligand and allows the radiometal labelling.

After the introduction of [^{111}In]-pentetreotide, the development of a treatment using radiolabeled-SSAs was the next step. In 1998, Stolz et al.[263] reported the first radiolabeled-SSA for tumor treatment, [^{90}Y]-DOTA-(Tyr[3])-octreotide ([^{90}Y]-DOTATOC)[55], which provided the proof-of-principle for peptide-receptor radiotherapy (PRRT)[263]. Nevertheless, one of its main limitations was the radiation-induced destruction of surrounding and/or distant SSTR-positive normal tissue, in particular radiosensitive tissues such as those of the immune system, kidney or liver. To overcome this problem, [^{177}Lu] instead of [^{90}Y] was used as β-emitter with shorter penetration depth and co-emission of low energy photons, allowing therapy monitoring by means of SPECT. [^{177}Lu]-radioligands such as [^{177}Lu]-DOTA-(Tyr[3])-octreotate ([^{177}Lu]-DOTATATE) became the PRRT agents of choice[153].

---

[55] DOTA (1,4,7,10-tetraazacyclododecane-1,4,7,10-tetraacetic acid). The introduction of the DOTA chelator became a key aspect as this molecule improves thermodynamic and kinetic stability, as well as suitability for all the commonly used radiometals.

Nowadays, DOTATOC and DOTATATE (Figure 4.5) have become the most often clinically used SSAs for radiolabeling, being the [^{68}Ga]- and [^{177}Lu]-radiolabeled ligands the preferred ones for diagnosis and treatment[264,265].

A kit preparation of [^{68}Ga]-DOTATATE (NetSpot®, Advanced Accelerator Applications[56]) was approved by the FDA in 2016 for positron emission tomography (PET) diagnosis of NETs. In the same year, the preparation kit of [^{68}Ga]-DOTATOC (SomaKIT TOC, Advanced Accelerator Applications) was also approved by the EMA. Three years later, in 2019 the FDA approved as well [^{68}Ga]-DOTATOC (University of Iowa Hospital & Clinics) as a diagnostic agent for NETs. Related to this, in 2014 the phase III clinical trial NETTER-1 evaluated for the first time the efficacy, survival and toxicity of [^{177}Lu]-DOTATATE as a therapy for GEP-NETs[266,267]. This study demonstrated that [^{177}Lu]-DOTATATE significantly improved progression-free survival in patients with advanced midgut NETs in comparison to octreotide LAR. As a consequence, EMA approved [^{177}Lu]-DOTATATE (Lutathera®, Advanced Accelerator Applications[56]) in 2017 for the treatment of GEP-NETs, followed by the FDA in 2018.

R = -CH$_2$OH   (DOTATOC)
R = -CO$_2$H   (DOTATATE)
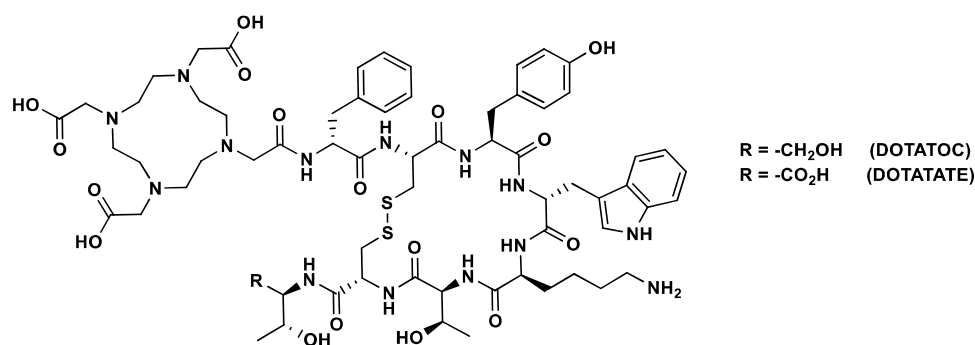
Figure 4.5 Structures of DOTATOC and DOTATATE

Radiolabeled-SSAs with high affinity to all five SSTR-subtypes are expected to expand the clinical indications of the currently SSTR2-targeted radioligands, as well as improving tumor targeting, imaging sensitivity and therapeutic efficacy by cross-reactivity to co-expressed SSTR1, SSTR3, SSTR4 and SSTR5[153]. However, not all SSTRs are able to internalize to a similar degree (SSTR3 > SSTR2 >> SSTR1)[157], which has to be taken into account for the development of such radioligands[187]. Under this point of view, pasireotide-based radioligands would be interesting, as these compounds would theoretically bind to SSTR1, SSTR2, SSTR3 and SSTR5. As far as we know, only few publications on pasireotide-based radioligands have been reported. In 2005, Lewis et al.[268] reported DOTA-pasireotide (Figure 4.6) with excellent affinities for SSTR2, SSTR3 and SSTR5. In 2007, Zlatopolskiy et al.[269] prepared five DOTA-pasireotide analogs and labeled them with [^{68}Ga] and [^{111}In]. In 2012, Fani et al.[270] performed binding and internalization studies comparing

---

[56] Acquired by Novartis in 2018.

[^{68}Ga]-DOTA-pasireotide with pasireotide, which showed similar comparable profiles. In addition, this radiolabeled analog permitted to clearly detect SSTR2- and SSTR5-tumor xenografts *in vivo* by PET imaging.
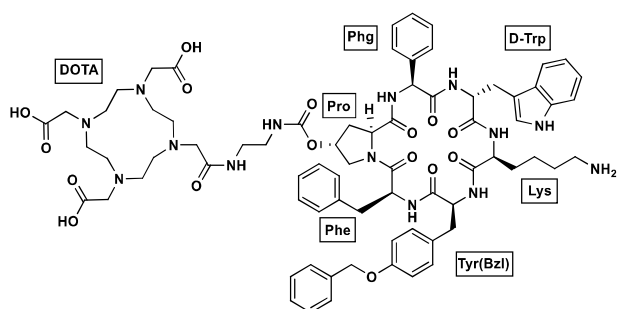
Figure 4.6 DOTA-pasireotide by Lewis et al.[268]   *Figure 4.7 DOTA(Lys)-PA by Liu et al.*[271]
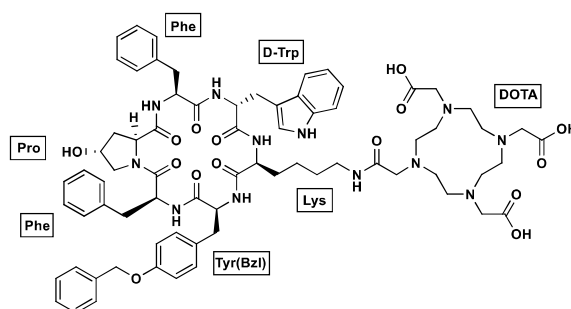
Apart from these, other three reports by Liu et al.[271–273] were published between 2016-2020. In 2018 Liu et al.[271] reported [^{68}Ga]-DOTA(Lys)-PA1 (Figure 4.7) which showed higher tumor uptake compared to [^{68}Ga]-DOTATATE in preclinical mice models with A549 tumors[57]. Nevertheless, this radioligand displayed high accumulation in the liver, being a challenge for further clinical applications because of plausible interferences with imaging quality.

In 2012, Tatsi et al.[274] developed [^{111}In]-DOTA-(D-Trp[8])-SST14 that showed high affinity to all SSTRs and localized in experimental tumors with expression of SSTR2, SSTR3 and SSTR5. Taking into account that high *in vivo* stability of a peptide radioligand is extremely important for successful tumor imaging and treatment, the re-evaluation of native or slightly modified SST14 needs to be considered in the context of peptidase activity *in vivo* (responsible for rapid breakdown of intravenous administered SST14)[153].

4.2 Research background

SST14 has generated great interest because of its biological and pharmacological properties. BCN Peptides patented a synthetic strategy for the production of octreotide in 1999[275]. Concurrently, Riera Lab (IRB Barcelona) specialized in the asymmetric synthesis and development of bioactive compounds such as unnatural amino acids. To gain knowledge of the SST14 structure and to synthesize new SSAs, a collaboration between BCN Peptides and Riera Lab was established. In contrast to most of the research efforts to find more stable and shorter analogs, the main objective of this collaboration was to study the effect of introducing diverse aromatic unnatural amino acids maintaining the 14-amino acid structure. The introduction of these amino acids modulates the analog conformation, which in turn has an effect on the biological activity and

---

[57] A549 is a human lung adenocarcinoma cell line that expresses SSTR5 > SSTR1, SSTR3 > SSTR2 according to Western Blot results of Liu et al.[271]

binding profile. In addition, the reduction of the original 12-amino acid cycle to a 6-amino acid cycle restricts the flexibility of the original molecule by limiting interaction with other SSTRs than SSTR2[33].

Table 4.2 Binding affinities of the most important SSAs developed by Dr. M. Gómez

Analog	ID	SSTR1 K_i (nm)	SSTR2 K_i (nm)	SSTR3 K_i (nm)	SSTR4 K_i (nm)	SSTR5 K_i (nm)	Serum[58] $t_{1/2}$ (h)
SST14	**-**	**0.65**	**0.0016**	**0.8**	**0.91**	**0.37**	*2.7*
Octreotide	**-**	> 1000	**0.0815**	15.2	> 1000	11.7	200
(Msa^6)-SST	**A13**	8.52	1.49	**1.36**	3.62	**0.91**	*2.4*
(Msa^7)-SST	**A14**	4.17	**0.019**	> 1000	28.7	> 1000	*5.2*
(Msa^{11})-SST	**A15**	20.0	**0.024**	2.8	6.45	2.1	*1.7*
(Msa^6,D-Trp^8)-SST	**A45**	2.58	4.55	**0.78**	3.78	**0.36**	*26.2*
(Msa^7,D-Trp^8)-SST	**A46**	**0.27**	**0.0024**	7.49	> 1000	26.3	*24.6*
(Msa^{11},D-Trp^8)-SST	**A47**	2.81	**0.14**	**1.31**	> 1000	**0.73**	*41.0*

By following this strategy, a great number of SSAs have been synthesized, analyzed and characterized in detail throughout different doctoral theses[22–26], publications[27–32] and two patents[33,276]. At present, BCN Peptides is conducting veterinary clinical trials with one of these analogs, **A64**.
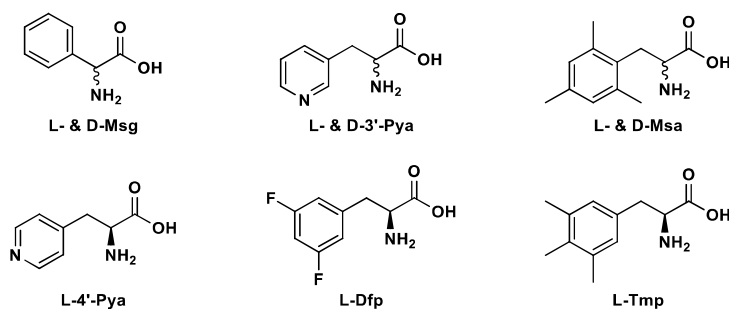
Figure 4.8 Unnatural aromatic amino acids used in the synthesis of SSAs

The first doctoral thesis exclusively dedicated to the synthesis and development of SSA was performed by Dr. Marc Gómez at BCN Peptides[23] (Table 4.2). In this work, a series of SSAs were synthesized: i) modifications on the aromatic residues of SST14 (Phe^6, Phe^7, Trp^8 and Phe^{11}) with L- and D-mesitylglycine (L- & D-Msg), D-3'-pyridilalanine (D-3'-Pya) and L- and D-mesitylalanine (L- & D-Msa) (Figure 4.8); ii) synthesis of Lys^4 analogs (addition of various functional groups or fatty acid conjugation at the *N*-terminus); iii) design of new analogs from the hits of the first series (L-Msa combinations); and iv) conjugated analogs with radiometals (*e.g.* [^{68}Ga]) or with fluorescent molecules (*e.g.* carboxyfluorescein). The first serum stability and metabolites studies were also

---

[58] These serum stability studies did not take into account the loss of the [Ala^1-Gly^2] exocyclic fragment of the structure.

performed, as well as various proposals for the use of some of the synthesized analogs (Table 4.2) to treat various SSTR-related diseases.

Table 4.3 Binding affinities of the most important SSAs developed by Dr. Á. Rol

Analog	ID	SSTR1 K_i (nm)	SSTR2 K_i (nm)	SSTR3 K_i (nm)	SSTR4 K_i (nm)	SSTR5 K_i (nM)
SST14	**-**	**1.88**	**0.016**	**0.25**	**1.55**	**0.76**
Octreotide	**-**	480	**0.77**	13.0	> 1000	21.0
(Dfp⁶,D-Trp⁸)-SST	**-**	21	0.35	**0.38**	16.0	**5.0**
(Dfp⁷,D-Trp⁸)-SST	**A58**	14	**0.36**	1.1	12	2.1
(Dfp¹¹,D-Trp⁸)-SST	**-**	14	**0.066**	3.81	11	5
(3'-Pya⁷,D-Trp⁸)-SST	**-**	8.1	0.29	**0.7**	4.5	**2.4**
(3'-Pya¹¹,D-Trp⁸)-SST	**-**	**6.4**	**0.14**	1.65	11.5	2.8
(4'-Pya⁷,D-Trp⁸)-SST	**-**	42	**0.051**	3.83	43	**13.4**
(4'-Pya¹¹,D-Trp⁸)-SST	**-**	7.1	**0.062**	0.42	10.3	**2.7**

NMR characterization and *in silico* conformational studies of the SSAs developed by Dr. Marc Gómez were performed by Dr. Pablo Martín-Gago at Riera Lab[24]. These studies expanded our knowledge on SSAs as it was observed that complete loss of structuration implied loss of SSTRs-binding, while structural rigidity increased SSTR2-affinity. In addition, it was also demonstrated that SSTR1- and SSTR3-binding required increased flexibility[28–30,33].

Table 4.4 Binding affinities of the most important SSAs developed by Dr. Anna Escolà

Analog	ID	SSTR1 K_i (nm)	SSTR2 K_i (nm)	SSTR3 K_i (nm)	SSTR4 K_i (nm)	SSTR5 K_i (nM)	Serum $t_{1/2}$ (h)
SST14	**-**	**3.07**	**0.036**	**0.53**	**3.75**	**2.50**	0.25
(Msa⁷,D-Trp⁸)-SST⁵⁹	**A46**	**2.36**	**0.054**	7.47	> 1000	> 1000	0.45
(Msa⁷,D-Trp⁸,D-Cys¹⁴)-SST	**-**	43.8	**0.015**	63.3	68.8	45.1	0.5
(D-Ala¹,Msa⁷,D-Trp⁸, D-Cys¹⁴)-SST	**-**	44.5	**0.014**	52.8	84.4	44.2	0.65
(D-Cys³,¹⁴,Msa⁷, D-Trp⁸)-SST	**-**	22.5	**0.023**	49.4	150.1	43.7	1.08
(D-Ala¹,D-Cys³,¹⁴,Msa⁷, D-Trp⁸)-SST	**A74**	10.69	**0.034**	6.9	26.0	14.0	40.0

Following the previous work, Dr. Álvaro Rol at Riera Lab and Macias Lab completed some series of the previous analogs using additional unnatural aromatic amino acids such as the L-3'-Pya, L-4'-Pya, L-difluorophenylalanine (L-Dfp) and L-trimethylphenylalanine (L-Tmp) (Table 4.3). The conclusions of Dr. Álvaro Rol were that the incorporation of electron-poor aromatic residues in substitution of Phe⁷ favored the binding with SSTR3, while incorporation of Msa⁷ reduced the binding affinity for SSTR4 and SSTR5 and increased the binding affinity for SSTR2. In addition, it was also concluded that apart from the orientation of the AA⁶-AA¹¹ aromatic complex and the

---

[59] Originally synthesized by Dr. Marc Gómez and Dr. Pablo Martín-Gago.

structural rigidity of the analog, the relative position of the complex AA[6]-AA[11] to AA[7] and the D-Trp[8]-Lys[9] pair orientation influence as well SSTR2-affinity.

Dr. Anna Escolà at Riera Lab picked up the thread of this research project and continued to develop new SSAs using different combinations of unnatural amino acids such as L-(2',4')-dimethylphenylalanine (L-Dmp) and both 3'-Pya and 4'-Pya at position 7 in combination to Msa[6] [26] (Table 4.4). Apart from modifying the aromatic residues of SST14, an extensive study on the design of more stable analogs using D-amino acids was performed in collaboration with Lead Molecular Design S.L.
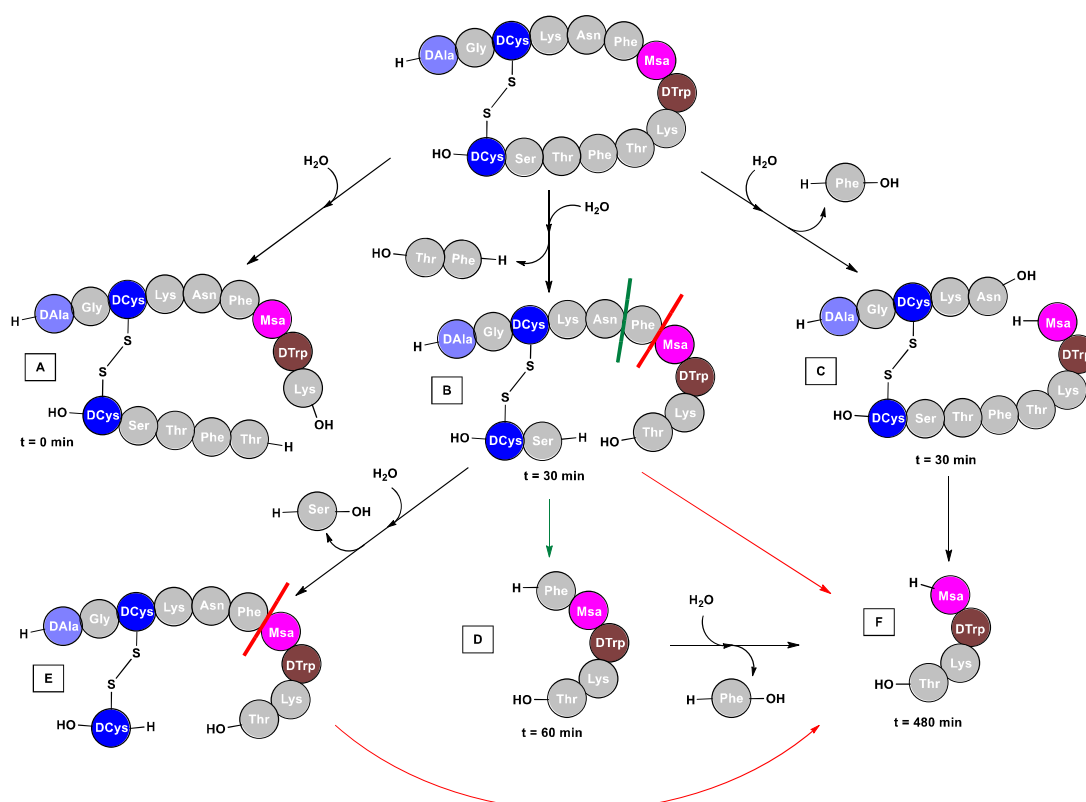
Figure 4.9 Degradation pathway of A74. Adapted from the thesis of Dr. Anna Escolà[26]

(Msa[7],D-Trp[8])-SST (**A46**) (Table 4.2) synthesized by Dr. Marc Gómez and characterized by Dr. Pablo Martín-Gago[23,24,28] was one of the most stable and SSTR2-selective analogs that maintained the 14-residue structure. Its human serum half-life ($t_{1/2}$ = *24.6*h) was outstanding as determined by HPLC. However, when the serum stability studies of **A46** were performed, the loss of the exocyclic [Ala[1]-Gly[2]] fragment was not considered for the half-life calculation, because the peaks of **A46** and **des[Ala¹,Gly²]-A46** co-eluted. As a consequence, the half-life of **A46** was overestimated. In the thesis of Dr. Anna Escolà, the use of UPLC-MS/MS permitted to take into account **des[Ala¹,Gly²]-A46**. Therefore, the real serum half-life of **A46** was found to be 27 min (0.45 h).

To synthesize more stable analogs, selected residues in the exocyclic part of the tetradecapeptide scaffold were substituted for their D-enantiomers. This strategy was applied to protect the cyclic

structure and the disulfide bond from degradation by serum peptidases, similarly as Bauer et al.[18] did for the design of octreotide.

The use of D-enantiomers in the exocyclic region increased gradually the stability of each analog. Surprisingly, **A74**[60] displayed a serum half-life of 40h, being the 14-amino acid SSA with the highest half-life to the best of our knowledge. The proposed metabolites of **A74** in human serum are represented in Figure 4.9. The use of D-amino acids both at the *N-* and *C-*terminus (D-Ala[1], D-Cys[3,14]) greatly increased the stability of the analog. Furthermore, as observed in **A46,** the introduction of Msa[7] made the analog more rigid with high SSTR2-binding affinity. In addition, the use of these D-amino acids increased SSTR4 and SSTR5 binding, but decreased the affinity for SSTR1 leaving the SSTR3 binding unaffected.

4.3 Results

4.3.1 Design of new analogs

The design of multireceptor SSAs was based on our research background on 14-amino acid SSAs, concretely in the results found by Dr. Anna Escolà[26]. In the present thesis, two series of analogs were designed: i) analogs with one Msa residue in their structure (Msa series); and ii) analogs with three or more D-amino acids in critical positions (D-amino acid series).

4.3.1.1 Msa series (A75 & A82)
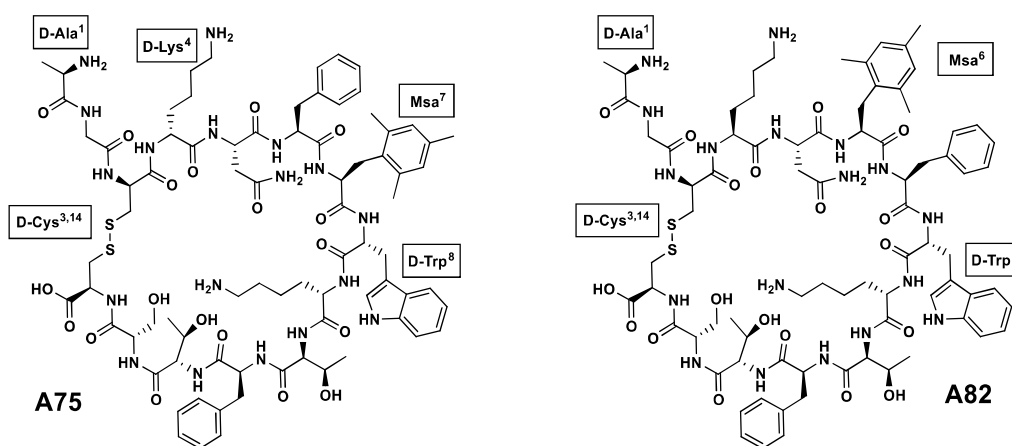
Figure 4.10 Msa series: A75 (left) and A82 (right)

A75[61] (Figure 4.10) was designed as a more stable version of **A74** incorporating D-Lys[4]. By means of this, our goal was to improve the 40h half-life in serum of **A74** without affecting the SSTR2 binding. Therefore, D-Lys[4] was introduced because this residue was considered as non-critical for the binding.

---

[60] **A74:** (D-Ala[1],D-Cys[3,14],Msa[7],D-Trp[8])-SST
[61] **A75:** (D-Ala[1],D-Cys[3,14],D-Lys[4],Msa[7],D-Trp[8])-SST

A82[62] (Figure 4.10) was designed as a more stable version of **A45**, which is an analog developed by Dr. Marc Gómez[23] and Dr. Martín-Gago[24]. As happened with **A46**, the original serum half-life of **A45** (*26.2*h) was also overestimated as the peaks of **A45** and **des[Ala¹,Gly²]-A45** co-eluted. Interestingly, **A45** is an analog with high binding affinities for SSTR3 and SSTR5 (Table 4.2). Therefore, we considered to incorporate D-amino acids (D-Ala¹ and D-Cys³,¹⁴) in the exocyclic region of the structure to protect the disulfide bond from degradation by serum peptidases. Therefore, we expected to increase the half-life of **A82** in comparison to **A45**.

4.3.1.2   D-amino acids series (A76-A81)

The D-amino acids series comprises six analogs (**A76**-**A81**) that were designed considering the degradation pathway of **A74**. D-amino acids were introduced at various key positions of the structure to protect the pharmacophore and to try to delay the appearance of metabolites A, B or C detected in the degradation study of **A74** (Figure 4.9). The goal of this second series of SSAs was to determine which D-amino acids were the most critical ones to improve the serum half-life of these SSAs without adding any other unnatural amino acids (Figure 4.11).

A76: (D-Ala¹,D-Cys³,¹⁴)-SST

A77: (D-Ala¹,D-Cys³,¹⁴,D-Trp⁸)-SST

A78: (D-Ala¹,D-Cys³,¹⁴,D-Phe⁶,¹¹)-SST

A79: (D-Ala¹,D-Cys³,¹⁴, D-Phe⁶,¹¹,D-Trp⁸)-SST

A80: (D-Ala¹,D-Cys³,¹⁴,D-Thr¹⁰)-SST

A81: (D-Ala¹,D-Cys³,¹⁴,D-Trp⁸,D-Thr¹⁰)-SST
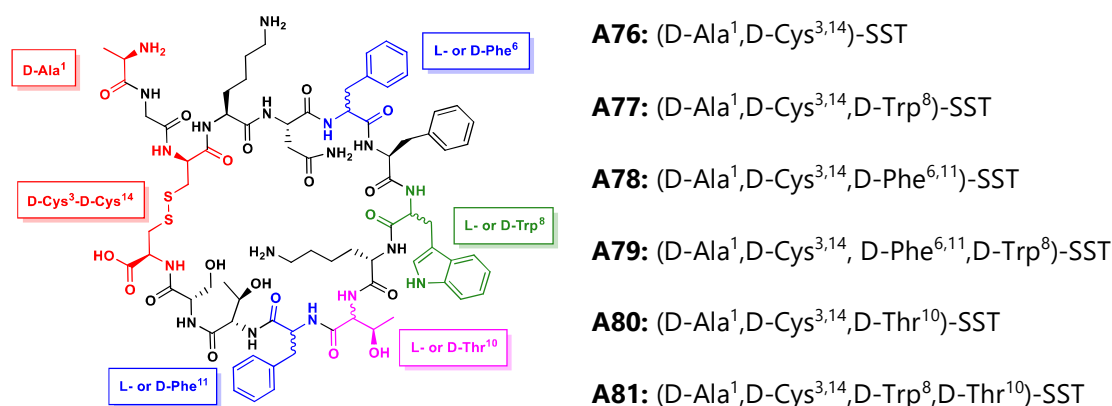
Figure 4.11 D-amino acids series: A76-A81

A76 included only D-amino acids in the exocyclic part of the structure to know how much these modifications would increase the serum half-life of the analog in comparison to SST14. **A77** had the same modifications as **A76** but adding D-Trp⁸ to protect even more the pharmacophore. **A78** was designed to protect the pharmacophore region by adding D-Phe⁶,¹¹ to delay the formation of metabolites B and C (Figure 4.9). As the π-π aromatic interactions between AA⁶ and AA¹¹ are so important for the biological function of SST14 and its analogs, we discarded to substitute only one of these residues, because the aromatic interaction would be disrupted. **A79** presented the same modifications as **A78**, but with D-Trp⁸ in the pharmacophore region. **A80** incorporated

---

[62] **A82:** (D-Ala¹,D-Cys³,¹⁴,Msa⁶,D-Trp⁸)-SST

D-Thr^{10} in its structure to protect the critical residues Trp^8-Lys^9 and to delay the formation of metabolite A (Figure 4.9). **A81** had the same modifications as **A80**, but D-Trp^8 was also included.

4.3.2 Development of Somatostatin analogs

A74-A82 analogs were synthesized by manual Fmoc/*t*Bu Solid-Phase Peptide Synthesis (SPPS) on 2-chlorotrityl (CTC) resin (Figure 4.12). **A74** was also synthesized to perform extended stability studies.
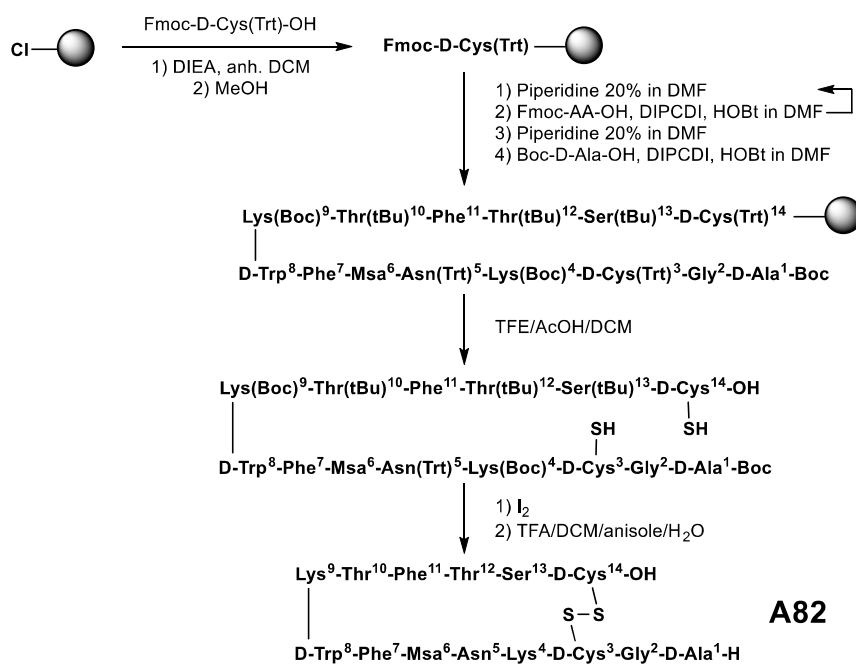
Figure 4.12 Synthetic development of A82 ([D-Ala^1,D-Cys^{3,14},Msa^6,D-Trp^8]-SST)

The first amino acid (Fmoc-D-Cys(Trt)-OH) was incorporated to the resin using DIEA as the base and DCM as the solvent. Once incorporated, the unreacted positions of CTC resin were capped using MeOH and the Fmoc group was eliminated with 20% piperidine solution in DMF. The coupling of the rest of amino acids was performed using DIPCDI and HOBt as coupling reagents and controlled via ninhydrin test. After the incorporation of the las amino acid (Boc-D-Ala-OH), the resin was dried under vacuum. For more details see sections 7.5.1 and 9.3.1.

The cleavage of the protected peptide was performed using a mixture of DCM/TFE/AcOH 70:20:10 (v/v). This cocktail was able to cleave the linear peptide from the CTC resin and eliminate the Trt protecting groups (PGs) which permitted the formation of the disulfide bond in solution using I$_2$ as the oxidant (Figure 4.12). The oxidized peptide was treated with TFA/DCM/anisole/H$_2$O 55:30:10:5 (v/v) to eliminate the remaining sidechain PGs. For more details see sections 7.5.1.2, 7.5.1.3 and 9.3.1.

Once the peptide crudes were obtained, **A74**-**A82** were purified by Preparative LC using eluents A and B (A: H$_2$O+0.02%TFA; B: ACN) (Table 4.5). **A80**-**A81** were the most difficult analogs to purify

as they seemed to precipitate in the head of the column requiring more quantity of eluent B to make them elute. Because of this, **A80**-**A81** were the only analogs that needed to be purified using gradient methods. After obtaining the peptides above 95% purity, the ion exchange (Table 4.5) from trifluoroacetate (TFA⁻) to acetate (AcO⁻) was performed using Dowex resin. For more details see sections 7.5.1.4, 7.5.1.5 and 9.3.1.

Table 4.5 Purification and ion exchange of A74-A82

ID	PURIFICATION			ION EXCHANGE	
	Pure peptide (g)	Purity (%)	Recovery (%)	Acetate peptide (g)	Recovery (%)
A74	0.73	98.6	23	0.66	91
A75	2.77	98.5	32	2.29	84
A76	0.80	99.3	14	0.69	86
A77	1.63	99.3	31	1.43	88
A78	0.81	96.9	17	0.70	87
A79	2.03	97.7	42	1.78	88
A80	0.84	97.9	15	0.73	87
A81	0.85	98.2	17	0.68	81
A82	0.81	99.5	21	0.71	87

4.3.3 Serum stability and metabolic studies

Serum stability studies were performed on each of the SSAs synthesized previously (**A74-A82**). In this thesis, the HPLC analysis of the stability samples was performed using isocratic methods to separate any possible metabolites from the principal peak. Taking this into account, **A45**, **A46** and **A74** were re-evaluated. An extended study of **A74** was performed to know if this analog was more stable that what was thought originally[26]. In contrast, **A45** and **A46** were also re-evaluated because in their original stability studies the loss of [Ala^1-Gly^2] fragment was not considered due to gradient HPLC methods.

To perform the serum stability studies a stock solution of the peptide was prepared (solution A). Then, a 1:10 dilution of solution A in human serum was also prepared (solution B). Taking into account the time points of the study (t_i), aliquots of solution B were prepared in various eppendorfs that were incubated at 37°C. Serum proteases were precipitated using cold ACN, centrifuged to the bottom of the eppendorf and the supernatant was filtered for posterior HPLC analysis. Standards of the peptide, serum and solvent were also prepared. The stability samples were analyzed by HPLC using the isocratic method of each analog. The serum half-life of each peptide was calculated from the HPLC degradation data using the linear regression of the natural logarithm of the peak percentage (Ln (A_i/A_0·100)) with respect to time (t_i). The determination of the slope, corresponding to the experimental constant (-K_e) allowed the calculation of the half-life ($t_{1/2}$). For more details about the methodology and the half-life calculations see section 7.5.3.1.

Metabolite studies were performed on each of the SSAs synthesized previously (**A74-A82**) except for **A75** and **A78**. To perform these studies, the stability samples were re-analyzed by HPLC but using a gradient method[63] instead of the isocratic one. Therefore, the metabolite peaks could be differentiated from the principal peak. Afterwards, HPLC-MS permitted to assign each peak a determined mass that corresponded to the structure of the metabolite. For more details about the metabolites studies see section 7.5.3.2.

In the following sections, a summary of all the performed stability studies and the most important metabolites of each peptide will be shown. See sections 9.3.2 and 9.3.3 for more details about all the performed stability studies and the complete list of metabolites derived from our analogs.

4.3.3.1 A46, A74 and A75

Table 4.6 Stability studies of A46, A74 and A75

ID	Study	Half-life (h)	Mean (h)
A46	**I**	0.87	
	II	1.11	1.0
	III	1.08	
A74	**I**	56.1	-
	IIA	43.6	
	IIB	55.5	53.8
	IIC	62.4	
A75	**I**	202.0	-
	IIA	242.0	
	IIB	241.2	252.1
	IIC	273.2	

Initial stability studies of **A46** ([Msa[7],D-Trp[8]]-SST) performed by Dr. Marc Gómez did not consider the loss of the [Ala[1],Gly[2]] exocyclic fragment as the samples of the study were analyzed by HPLC gradient method (20-80%B in 30 min). Consequently, the peaks of **A46** and **des[Ala[1],Gly[2]]-A46** co-eluted and the serum half-life of the analog was overestimated (*24.6*h). In the thesis of Dr. Anna Escolà, the use of UPLC-MS/MS permitted to differentiate the principal peak from the metabolite peak. Therefore, the experimental value obtained (27 min, 0.45h) was conceived as the real serum half-life of **A46**. In contrast, in this thesis we analyzed our stability samples by HPLC isocratic methods. Three stability studies in different experimentation days (study I, II and III) of **A46** were performed with the objective to reproduce the half-life value obtained by Dr. Anna Escolà[26].

The results obtained for **A46** doubled the half-life value obtained by Dr. Anna Escolà, but as expected the use of an isocratic method still gave a more realistic result than the one obtained by gradient methods (Table 4.6). Nevertheless, a sample of study III was analyzed by HPLC-MS to

---

[63] Generally, 5-70%B in 45 min (A: H_2O+0.1%TFA; B: ACN+0.07%TFA), except for **A77** (5-40%B in 45 min).

find that even though an isocratic method was used, the peaks of **A46** ($[M+2H]^{2+}$=840.8 amu) and **des[Ala^1]-A46** ($[M+2H]^{2+}$=805.2 amu) still co-eluted, which meant that the serum half-life of **A46** ($t_{1/2}$ = 1.0h) was still overestimated. Despite this, the other analogs were analyzed by isocratic methods but checking by HPLC-MS if any metabolite peaks co-eluted with the principal peak of the chromatogram. No metabolic study of **A46** was performed.

As concluded in the thesis of Dr. Anna Escolà[26], **A74** ([D-Ala^1,D-Cys^{3,14},Msa^7,D-Trp^8]-SST) was to date the most stable SSA based on the 14-amino acid structure ($t_{1/2}$ = 40.0h). With the objective to validate our methodology, we performed extended stability studies of **A74**. The initial study I ($t_{1/2}$ = 56.1h) confirmed that **A74** was even more stable than what we thought originally. This result was confirmed by study II ($t_{1/2}$ = 53.8h) (Table 4.6).
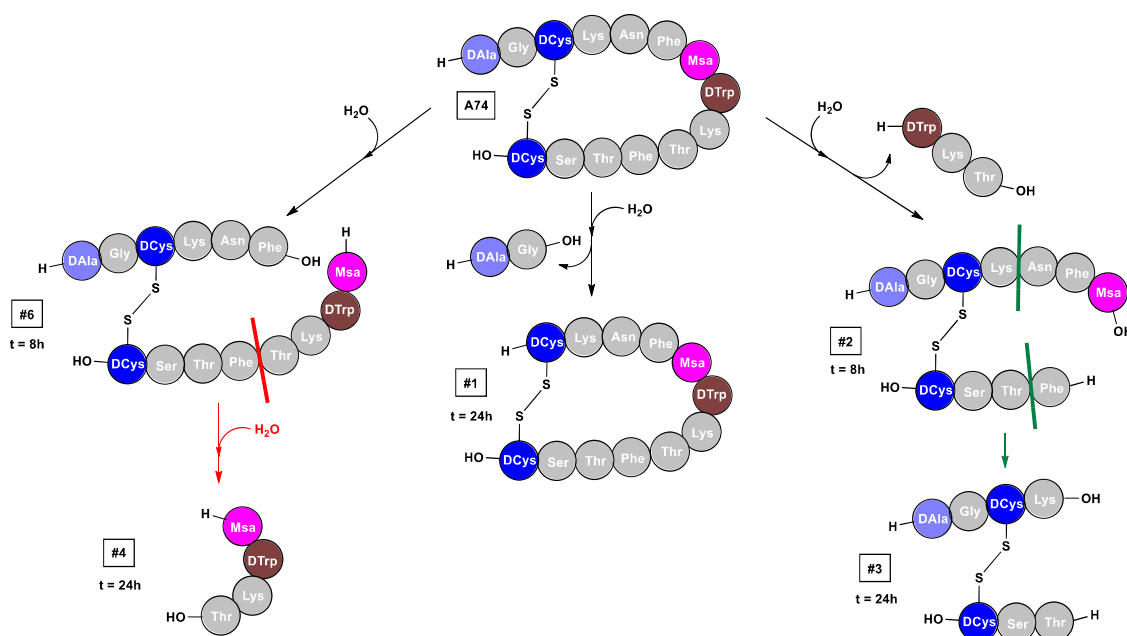
Figure 4.13 Metabolites of A74

In the metabolic study of **A74**, we found seven peaks in total corresponding to different metabolites (Figure 4.13). In comparison to the degradation study performed by Dr. Anna Escolà, the only common fragment was Msa^7-D-Trp^8-Lys^9-Thr^{10} (peak #4), which probably appeared after the opening of the cyclic structure between Phe^6-Msa^7 (peak #6). The loss of [D-Trp^8-Lys^9-Thr^{10}] (peak #2) was also observed, as well as the loss of the exocyclic [D-Ala^1-Gly^2] fragment (peak #1).

A75 ([D-Ala^1,D-Cys^{3,14},D-Lys^4,Msa^7,D-Trp^8]-SST) was designed as an even more stable version of **A74** including D-Lys^4 in its structure. Despite this, the stability studies of **A75** were complicated to perform as it showed some solubility issues that difficulted its recovery from solution B aliquots. When ACN was added to solution B, both **A75** and the serum peptidases precipitated, so the analog was barely detectable by HPLC. To overcome this, an extensive recovery study was performed (Table 4.7). Both MeOH and EtOH worsened the results obtained by using ACN (entries

1-3). Consequently, various solutions of TFA in ACN were tested (entries 4-6). The presence of only 1% of TFA in ACN improved 8-times the recovery of **A75** in comparison to ACN alone (entry 1 vs 4). In addition, when 5% TFA in ACN was used, the recovery was 10-times greater (entry 1 vs 5). From that point, the addition of TFA did not improve the recovery results (entry 6). As a result, we decided to use 5% TFA in ACN as it permitted to precipitate the serum peptidases and recover **A75** for HPLC analysis.

Table 4.7 Recovery studies of A75

Entry	Precipitating Agent	AUC[64]	Recovery[65]
1	ACN	558,962	1.0
2	MeOH	43,899	0.1
3	EtOH	276,726	0.5
4	1% TFA in ACN	4,709,115	8.4
5	5% TFA in ACN	5,882,960	10.5
6	10% TFA in ACN	5,923,536	10.6

The use of 5% TFA in ACN permitted to perform the stability studies of **A75** ($t_{1/2}$ = 252.1h), which confirmed that **A75** was more stable than **A74** due to the presence of the D-Lys^4 residue (Table 4.6). Despite that **A75** was one of the first analogs that was designed and synthesized, its stability studies were the last that were performed owing to its recovery problems. Therefore, no metabolic study of **A75** was performed due to lack of time.

4.3.3.2 A76 and A77

Table 4.8 Stability studies of A76 and A77

ID	Study	Half-life (h)	Mean (h)
A76	**I**	2.6	-
	IIA	1.0	
	IIB	1.1	1.1
	IIC	1.2	
A77	**I**	52.4	-
	IIA	46.1	
	IIB	49.9	48.1
	IIC	48.3	

Both stability studies performed on **A76** ([D-Ala^1,D-Cys^{3,14}]-SST) confirmed that it was the least stable of the synthesized analogs ($t_{1/2}$ = 1.1h) (Table 4.8). This was an expected result as **A76** was the analog with the less D-amino acid modifications in its structure. Despite this, the addition of

---

[64] Mean of the areas of two consecutive injections of the sample.
[65] Calculated from the area of **A75** observed in the HPLC analysis after precipitating with ACN.

D-amino acids in the exocyclic part of the structure increased 4-times the stability of this analog in comparison to SST14 ($t_{1/2}$ = 0.25h)[66].

In total, ten peaks corresponding to metabolites of **A76** were identified (Figure 4.14). The loss of [D-Ala[1]] (peak #2) was detected at the beginning of the experiment, which derived in the loss of the exocyclic fragment [D-Ala[1],Gly[2]] (peak #1). The loss of the pharmacophore [Phe[6]-Phe[7]-Trp[8]-Lys[9]] (peak #3) and the loss of [Lys[4]-Asn[5]] (peak #5) were also detected. The absence of any D-amino acids in the pharmacophore region permitted the rapid metabolization of the analog by serum proteases. Because of this reason, the majority of the metabolites were related to the loss of pharmacophore residues.
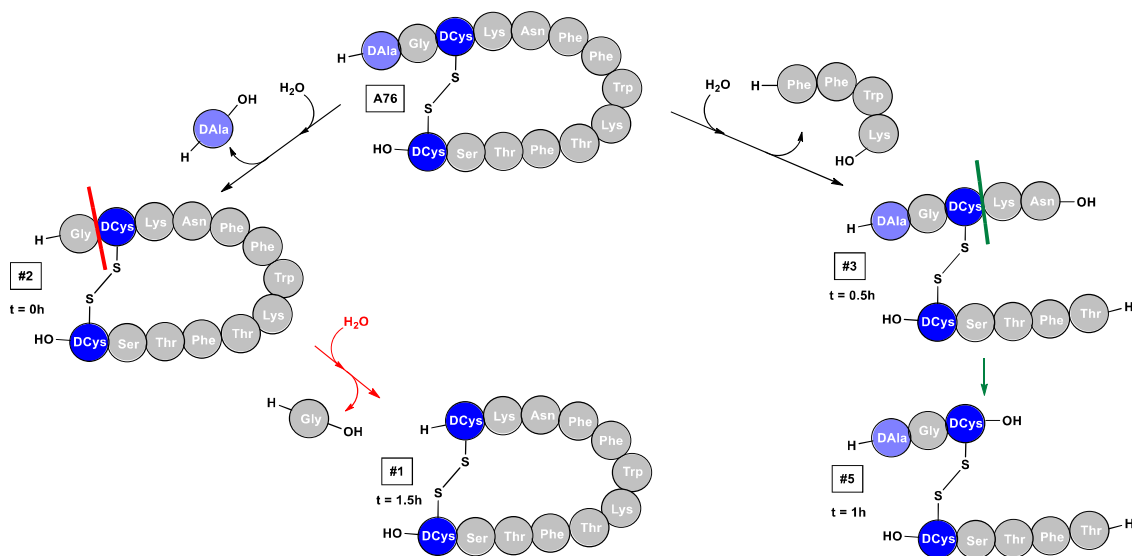
Figure 4.14 Metabolites of A76

Regarding **A77** ([D-Ala[1],D-Cys[3,14],D-Trp[8]]-SST), the introduction of D-Trp[8] improved the half-life of this analog 43-times in comparison to **A76** (48.1h vs 1.1h) (Table 4.8). Therefore, it is important to have a balance of D-amino acid modifications both at the exocyclic part of the structure (D-Ala[1],D-Cys[3,14]) but also in the pharmacophore region (D-Trp[8]).

Several peaks corresponding to metabolites of **A77** were identified (Figure 4.15). The loss of [Phe[7]-D-Trp[8]-Lys[9]] fragment (peak #3a) was observed, which also lost the [Thr[10]-Phe[11]-Thr[12]] fragment (peak #5). Similarly to previous analogs, the loss of the pharmacophore [Phe[7]-D-Trp[8]-Lys[9]-Thr[10]] (peak #8) was also detected. Finally, fragment [Phe[7]-D-Trp[8]-Lys[9]-Thr[10]] was observed at t_{8h}, derived from a parent metabolite (peak #2).

---

[66] Evaluated by Dr. Anna Escolà[26].
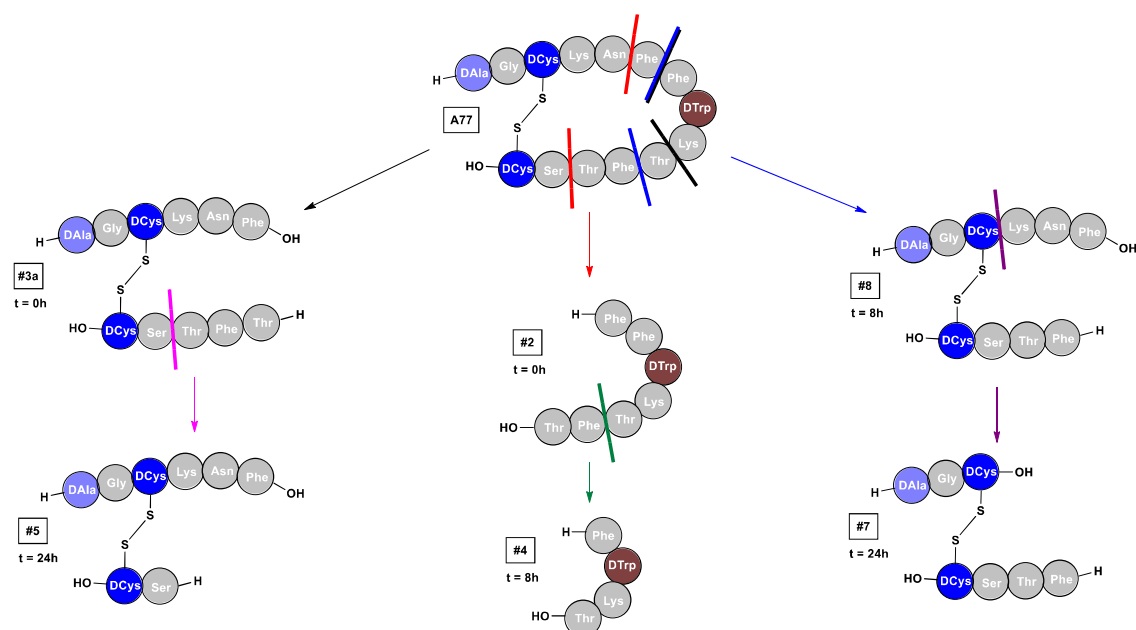
Figure 4.15 Metabolites of A77

4.3.3.3 A78 and A79

The stability studies of **A78** ([D-Ala[1],D-Cys[3,14],D-Phe[6,11]]-SST) were contradictory as study I ($t_{1/2}$ = 140.6h) showed a greater half-life than study II ($t_{1/2}$ = 36.7h) (Table 4.9). Some parameters between studies I and II were checked to understand this result: the area of the peptide standards, the variation coefficient of each sample, etc. All of them were verified as normal with no aberrant values observed. Due to lack of time, we could not perform any more stability study of **A78**. Therefore, we still do not have an explanation about the deviation between both results. Due to this contradictory studies, no metabolic studies of **A78** were performed.

Table 4.9 Stability studies of A78 and A79

ID	Study	Half-life (h)	Mean (h)
A78	I	140.6	-
	IIA	38.9	36.7
	IIB	35.4	
	IIC	35.8	
A79	I	331.6	-
	IIA	520.4	410.9
	IIB	353.7	
	IIC	358.6	

In contrast, the half-life stability values of **A79** ([D-Ala[1],D-Cys[3,14],D-Phe[6,11],D-Trp[8]]-SST) were in accordance between each other (Table 4.9). As observed for **A77**, the introduction of D-Trp[8] improved the half-life of the analog as it protects the pharmacophore from the serum peptidases. Considering all the analogs of the D-amino acid series, **A79** is the analog with the highest number of D-amino acids (six in total). Consequently, **A79** was expected to be the most stable analog of this series ($t_{1/2}$ = 410.9h).
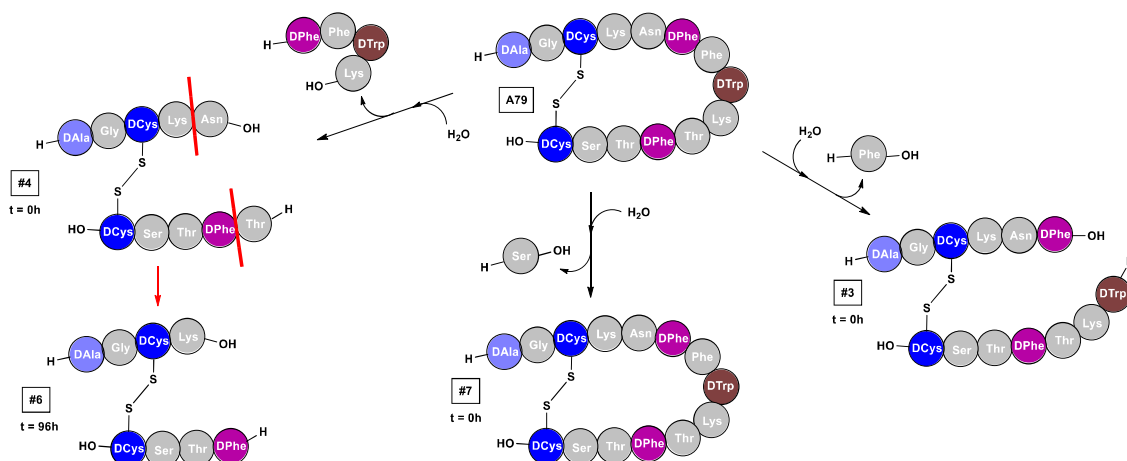
Figure 4.16 Metabolites of A79

The loss of single amino acids such as [Phe[7]] (peak #3) and [Ser[13]] (peak #7) were detected at the beginning of the experiment at t_{0h} (Figure 4.16). The loss of the pharmacophore [D-Phe[6]-Phe[7]-D-Trp[8]-Lys[9]] (peak #4) was also observed. This last metabolite derived to des-[Asn[5]-D-Phe[6]-Phe[7]-D-Trp[8]-Lys[9]-Thr[10]]-**A79** (peak #6) as it also lost the [Asn[5]] and [Thr[10]] residues. The loss of [D-Ala[1]-Gly[2]] fragment was also observed at t_{168h}.

4.3.3.4   A80 and A81

Table 4.10 Stability studies of A80 and A81

ID	Study	Half-life (h)	Mean (h)
A80	I	42.0	-
	IIA	58.2	56.7
	IIB	55.7	
	IIC	56.2	
A81	I	104.2	-
	IIA	164.5	174.9
	IIB	197.8	
	IIC	162.4	

Both studies performed on **A80** ([D-Ala[1],D-Cys[3,14],D-Thr[10]]-SST) showed that only with the introduction of D-Thr[10] the half-life of **A80** was more than 50-times higher in comparison to **A76** (56.7h vs 1.1h) (Table 4.10). Therefore, it seems as a critical position to protect the pharmacophore of the analog.

The loss of single residues such as [D-Ala[1]] (peak #2) and [Phe[6]] (peak #3) was observed at the beginning of the experiment (Figure 4.17). The loss of the pharmacophore fragment [Phe[6]-Phe[7]-Trp[8]-Lys[9]] (peak #9) was also observed. This metabolite also lost the [Lys[4]-Asn[5]] residues to give des-[Lys[4]-Asn[5]-Phe[6]-Phe[7]-Trp[8]-Lys[9]]-**A80** (peak #5). Fragment [Phe[7]-Trp[8]-Lys[9]-D-Thr[10]-Phe[11]-Thr[12]] (peak #6) was also detected at t_{24h}, which probably came from metabolite #11 detected at the beginning of the experiment.
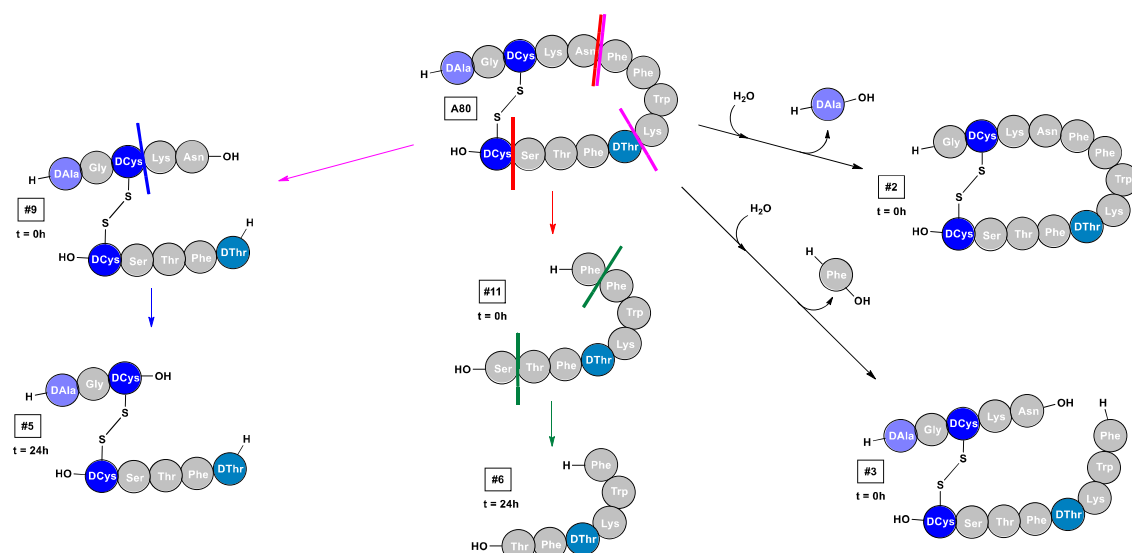
Figure 4.17 Metabolites of A80

Regarding **A81** ([D-Ala[1],D-Cys[3,14],D-Trp[8],D-Thr[10]]-SST), the incorporation of D-Trp[8] increased 3-times the serum half-life in comparison to **A80** (174.9h vs 56.7h) (Table 4.10). In fact, **A81** was the second most stable analog of the D-amino acid series behind **A79**.
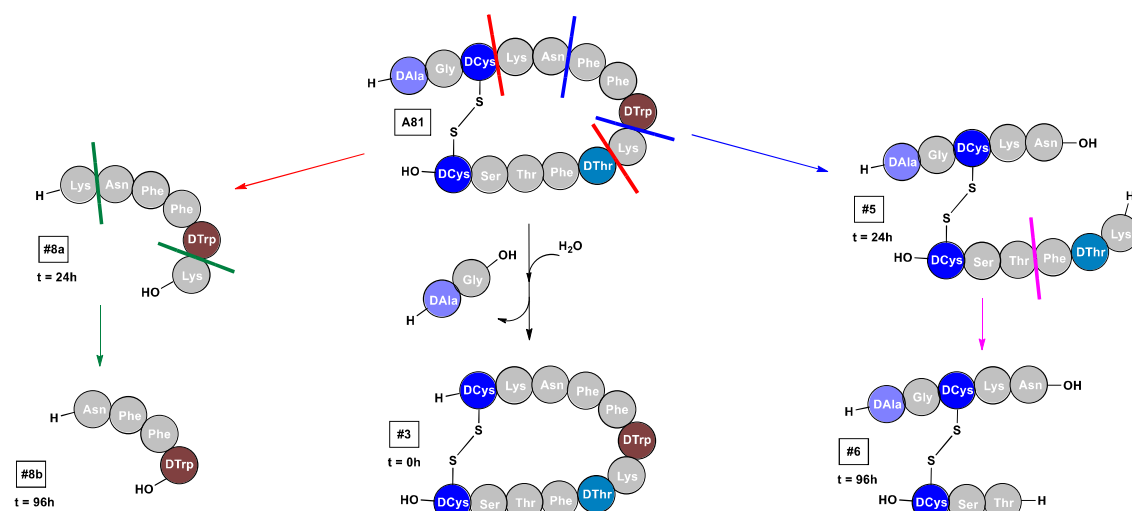
Figure 4.18 Metabolites of A81

As happened in other metabolic studies, the loss of the exocyclic [D-Ala[1]-Gly[2]] fragment (peak #3) was observed at t$_{0h}$ (Figure 4.18). Fragment [Asn[5]-Phe[6]-Phe[7]-D-Trp[8]] (peak #8b) was also observed, which probably came from a longer metabolite (peak #8a). The loss of [Phe[6]-Phe[7]-D-Trp[8]] fragment (peak #5) was also detected. This last species was even more degraded to give metabolite #6.

4.3.3.5 A45 and A82

Initial stability studies performed on **A45** ([Msa[6],D-Trp[8]]-SST) did not consider the loss of the [Ala[1]-Gly[2]] exocyclic fragment, because the samples were analyzed by HPLC gradient methods (20-80% in 30 min). Therefore, the peaks of **A45** and **des[Ala[1],Gly[2]]-A45** co-eluted and the serum

half-life of the analog was overestimated (*26.2*h). The HPLC isocratic method used to analyze the stability samples was able to separate the peaks of **A45** ([M+2H]$^{2+}$=840.8 amu) and **des[Ala^1,Gly^2]-A45** ([M+2H]$^{2+}$=777.0 amu). However, we observed through HPLC-MS that **des[Ala^1]-A45** ([M+2H]$^{2+}$=805.2 amu) still co-eluted with the principal peak. Therefore, the half-life of **A45** (t$_{1/2}$ = 1.5h) was still overestimated (Table 4.11). Nevertheless, we assumed that the value obtained was much closer to the real stability of **A45** than the previous results using the HPLC gradient method. No metabolic study of **A45** was performed.

Table 4.11 Stability studies of A45 and A82

ID	Study	Half-life (h)	Mean (h)
A45	**I**	1.5	-
A82	**I**	75.0	-
	IIA	112.3	95.2
	IIB	86.9	
	IIC	86.5	

In comparison to **A45**, the incorporation of exocyclic D-amino acids greatly improved the half-life of **A82** ([D-Ala^1,D-Cys^{3,14},Msa^6,D-Trp^8]-SST), which was 63-times higher in comparison to **A45** (95.2h vs 1.5h) (Table 4.11). This was very similar to what was observed in the case of **A46** and **A74**. In addition, the half-life of **A82** was even better than **A74**, which only differs by the position of the Msa residue.
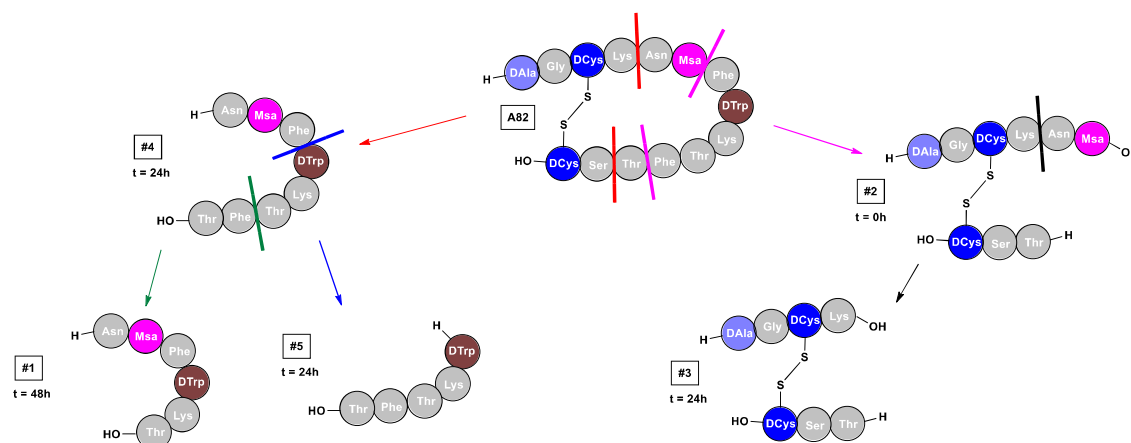
Figure 4.19 Metabolites of A82

Regarding the metabolites of **A82**, the loss of [Phe^7-D-Trp^8-Lys^9-Thr^{10}-Phe^{11}] (peak #2) was detected at the beginning of the experiment (Figure 4.19). This last species also lost the [Asn^5-Msa^6] fragment (peak #3) after 24h. Fragment [Asn^5-Msa^6-Phe^7-D-Trp^8-Lys^9-Thr^{10}-Phe^{11}-Thr^{12}] (peak #4) was also detected at t$_{24h}$. From this structure, two more metabolites were observed: fragment [D-Trp^8-Lys^9-Thr^{10}-Phe^{11}-Thr^{12}] (peak #5) and fragment [Asn^5-Msa^6-Phe^7-D-Trp^8-Lys^9-Thr^{10}] (peak #1). In addition, we also detected the loss of a Phe residue (peak #6), but due to lack of time we could not collect the peak to determine to which residue corresponded. Despite this,

due to the presence of Msa[6] and D-Trp[8], we would expect that **des[Phe^{11}]-A82** corresponded to metabolite #6

4.3.4 Biological experiments

Once the stability studies of **A74-A82** were performed, BCN Peptides established a collaboration with the research group of Prof. Justo Castaño and Prof. Raúl Luque in the *Instituto Maimónides de Investigación Biomédica de Córdoba* (IMBIC). Prof. Justo Castaño is the responsible of the Department Cell Biology, Physiology and Immunology of the *Universidad de Córdoba* (UCO) and the principal investigator of the Hormones and Cancer Research Group of IMBIC[277–281].

Our goal with this collaboration was to send various of our analogs to evaluate their *in vitro* efficacy in cellular models of:

- Neuroendocrine Tumors (NETs): SSTR2 overexpression[191,192,200–205].
- Pancreatic adenocarcinoma: SSTR2 and SSTR3 overexpression[282].
- Bladder cancer: shows presence of SSTR1[224] and overexpression of SSTR5[283,284].
- Prostate cancer: overexpression of SSTR1[280,285,286].
- Hepatocellular carcinoma (HCC): overexpression of SSTR5[287]. HuH-7 (HCC cell line) expresses SSTR1, SSTR2 and SSTR5[288].
- Glioblastoma: SSTR3 and SSTR5 overexpression

In addition, the research group of Prof. Castaño is also capable of combining the *in vitro* evaluation with *in vivo* experiments (transgenic models, xenografts)[289–291].

On July 2021, **A74**, **A75** and **A82** among other previously synthesized analogs were selected for their *in vitro* evaluation because of different reasons:

- **A74** ($t_{1/2}$ = 53.8h), **A75** ($t_{1/2}$ = 252.1h) and **A82** ($t_{1/2}$ = 95.2h) show serum half-lives above 50h. This is a great improvement in comparison to the parent peptide SST14 ($t_{1/2}$ = 0.25h)[66], while maintaining the 14-amino acid structure. The increase of stability is caused by the presence of both D-amino acids in key positions of the structure, as well as unnatural aromatic amino acids such as Msa.
- **A74** presents an excellent binding affinity for SSTR2, while it also shows affinity for SSTR3 to a lesser extent. Although the binding of **A75** has not been characterized yet, this analog is expected to present similar binding affinities to **A74**. This is extremely probable as the only structural difference between each peptide is the presence of D-Lys[4] that is non-critical for binding and does not modify the flexibility of the analog.

- Although the binding of **A82** has not been characterized yet, this analog is also expected to present a similar binding than **A45** because their structural differences reside in the exocyclic D-Ala^1 and D-Cys^{3,14}. As these exocyclic residues are non-critical for the binding, it is also very probable that **A82** presents excellent binding affinities for SSTR3 and SSTR5, as well as moderate affinities for SSTR1 and SSTR2 (Table 4.12).
- **A74**-**A75**-**A82** are already intellectually protected by BCN Peptides as their structure is included in the Markush formula of patent WO2010128098A1[33] that refers to somatostatin analogs that contain at least one unnatural aromatic amino acid in their structure (*e.g.* Msa in substitution of one of the natural Phe^6, Phe^7 or Phe^{11} residues).

The shipment of **A74**-**A75**-**A82** was performed while this chapter was being written (July 2021). Therefore, we would be delighted to show at least preliminary results of the *in vitro* experiments in the thesis defense. If the *in vitro* results are positive, we would evaluate these compounds *in vivo* thanks to the research group of Prof. Castaño. In addition, SSTR-binding assays would be externalized to Eurofins Scientific[292] to know the real binding affinities of **A75** and **A82**. The structure of these peptides would be also characterized by NMR (^{1}H-^{1}H TOCSY and ^{1}H-^{1}H NOESY spectra) in collaboration with Macias Lab at the IRB Barcelona[23–26].

4.4 Discussion and conclusions

Table 4.12 Summary of the stabilities of the characterized analogs

Analog	ID	SSTR1 K_i (nm)	SSTR2 K_i (nm)	SSTR3 K_i (nm)	SSTR4 K_i (nm)	SSTR5 K_i (nM)	Serum $t_{1/2}$ (h)
SST14	-	**3.07**	**0.036**	**0.53**	**3.75**	**2.50**	0.25^{66}
(Msa^6,D-Trp^8)-SST	A45	2.58	4.55	**0.78**	3.78	**0.36**	1.5
(Msa^7,D-Trp^8)-SST	A46	**2.36**	**0.054**	7.47	> 1000	> 1000	1.0
(D-Ala^1,D-Cys^{3,14},Msa^7, D-Trp^8)-SST	A74	10.69	**0.034**	6.9	26.0	14.0	53.8
(D-Ala^1,D-Cys^{3,14},D-Lys^4,Msa^7,D-Trp^8)-SST	A75	-	-	-	-	-	252.1
(D-Ala^1,D-Cys^{3,14})-SST	A76	-	-	-	-	-	1.1
(D-Ala^1,D-Cys^{3,14},D-Trp^8)-SST	A77	-	-	-	-	-	48.1
(D-Ala^1,D-Cys^{3,14},D-Phe^{6,11})-SST	A78	-	-	-	-	-	36.7
(D-Ala^1,D-Cys^{3,14}, D-Phe^{6,11},D-Trp^8)-SST	A79	-	-	-	-	-	410.9
(D-Ala^1,D-Cys^{3,14},D-Thr^{10})-SST	A80	-	-	-	-	-	56.7
(D-Ala^1,D-Cys^{3,14},D-Trp^8,D-Thr^{10})-SST	A81	-	-	-	-	-	174.9
(D-Ala^1,D-Cys^{3,14},Msa^6,D-Trp^8)-SST	A82	-	-	-	-	-	95.2

A74-**A82** were synthesized using Fmoc/*t*Bu SPPS standard methodologies on CTC resin. Once the linear peptide structure was synthesized, the protected analogs were cleaved from the resin and were oxidized in solution to form the characteristic disulfide bond of the SST scaffold. Peptide crudes were obtained after the complete removal of the sidechain PGs using high content TFA cocktails in solution. Afterwards, the crudes were purified using preparative LC to obtain the peptides with purities above 95%. Stability studies in human serum using isocratic HPLC methods

were conducted to characterize the synthesized analogs (Table 4.12). Finally, the stability samples were re-analyzed by HPLC-MS to study the degradation metabolites of the majority of the analogs.

In the case of **A74**, originally designed by Dr. Anna Escolà, extended stability studies demonstrated that this analog was more stable than originally thought (53.8h vs 40.0h[66]). The stabilities of **A45** and **A46**, both designed by Dr. Marc Gómez, were re-evaluated using isocratic HPLC methods instead of the originally used gradient methods. Nevertheless, the half-life of both **A45** ($t_{1/2}$ = 1.5h) and **A46** ($t_{1/2}$ = 1.0h) was still overestimated even with the isocratic methods, because some metabolites such as **des[Ala^1]-A45** or **des[Ala^1]-A46** still co-eluted with the principal peak. Despite this, the stability values were considered to be closer to the real half-lives of **A45** and **A46** than the ones obtained in previous studies with gradient methods. The stability studies of **A75** were difficult to perform as this analog presented recovery problems from solution B. After some recovery studies, 5% TFA in ACN was found to be the proper solution to use as the precipitating agent. Finally, the half-life of **A75** ($t_{1/2}$ = 252.1h) could be calculated.

Prolonged half-life of 14-amino acid analogs can be obtained by preventing or delaying their degradation by blood/serum peptidases. The use of unnatural and D-amino acids slows down the action of these degradation enzymes increasing the stability of peptides. The series of analogs designed in the present thesis are based in the use of D-amino acids alone (**A76**-**A81**) or in combination with unnatural amino acids (**A75** and **A82**). The stability results of both series of analogs confirmed that the introduction of exocyclic D-Ala^1 and D-Cys^{3,14} increased their stability as the pharmacophore of the structure was more protected from serum peptidases. Examples of this are the comparison between **A45** and **A82** (1.5h vs 95.2h) or between **SST14** and **A76** (0.25h vs 1.1h) (Table 4.12).

In addition to these exocyclic D-amino acids, the introduction of D-Trp^8 alone increased also the stability of some analogs of the D-amino acids series as the pharmacophore was even more protected. Therefore, there has to be an equilibrium of D-amino acids in all the regions of the structure. For example, **A76** ($t_{1/2}$ = 1.1h) has only exocyclic D-amino acids in its structure, which clearly are not enough to protect the pharmacophore. On the other hand, **(D-Trp^8)-SST** would probably present a similar stability as the D-Trp^8 modification does not provide enough protection to the pharmacophore. Despite this, the combination of exocyclic D-amino acids and D-Trp^8 establishes a synergy that has a huge impact on the stability of the analog as happens with **A77** that has a serum half-life 43-times higher in comparison to **A76** (48.1h vs 1.1h).

Regarding other analogs of the D-amino acids series, the stability results of **A79** showed that this is the 14-amino acid analog with the highest serum half-life (410.9h) that has been synthesized to the best of our knowledge. As **A79** is the analog with the major number of D-amino acids in its structure, this was an expected result. About **A80**, D-Thr[10] may be considered as a critical residue because in comparison with **A76** the serum half-life increased 51-times (56.7h vs 1.1h). In relation to this, **A81** was the second analog with the highest half-life ($t_{1/2}$ = 174.9h) behind **A79**.

The main difference when using either unnatural or D-amino acids to increase the serum stability of somatostatin analogs is how these residues affect the flexibility of the molecule. Consequently, the use of D-amino acids in residues that are non-critical for binding should not affect the flexibility of the analogs (*e.g.* D-Ala[1] and D-Cys[3,14]). In contrast, the use of unnatural amino acids (*e.g.* Msa) at certain positions of the structure increases its rigidity favoring the binding to SSTR2. For example, analogs **A46** and **A74** that only differ by the exocyclic D-amino acids, have a similar binding profile with high SSTR2 affinity and moderate affinity for SSTR1 and SSTR3 (Table 4.12). In fact, the presence of Msa[7] is the responsible of the flexibility restriction of these analogs, which increases their affinity for SSTR2. The same thing should happen between **A45** and **A82**, which only differ in the exocyclic D-amino acids. Consequently, **A82** is expected to have a similar binding profile to **A45**: excellent affinities for SSTR3 and SSTR5 and moderate ones for SSTR1 and SSTR2. In the case of **A78** and **A79** that contain D-Phe[6,11], their binding is totally unpredictable. The same happens with **A80** and **A81** that contain D-Thr[10].

With the recent approval of DOTATOC and DOTATATE either for diagnosis [^{68}Ga] or treatment [^{177}Lu] of SSTR2-positive tumors, there is a medical need of finding multireceptor SSAs with affinity for SSTR1, SSTR3 and/or SSTR5 to use them for the diagnosis or treatment of human tumors that overexpress these types of receptors. Under this point of view, an aspect to consider is the SSTR-mediated internalization that permits the radiolabeled analog to enter the tumor cell. Several studies have shown that SSTR2, SSTR3 and SSTR5 are internalized to a much higher extent than SSTR1 (very slow[158,159]) or SSTR4 (absent[160]) after ligand stimulation[161,162]. As pasireotide[293] is the only commercial analog that binds with excellent affinities for SSTR1, SSTR2, SSTR3 and SSTR5, the development of radiolabeled-pasireotide analogs seemed to be the logical step to fulfil this medical need. Despite this, the few publications that reported radiolabeled DOTA-pasireotide analogs did not succeed. Therefore, there is still a medical need to develop analogs that bind preferentially to SSTR3 and SSTR5, and that can be conjugated with DOTA to enable their radiolabeling.

Prior to the results of biologic and binding experiments, considerable expectations are put on **A82** being a stable analog ($t_{1/2}$ = 95.2h) that probably binds with high affinity for SSTR3 and SSTR5.

Depending on the results of the biologic experiments, the real binding affinities of **A82** will be evaluated to know its potential to be used as a radiolabeled analog for diagnosis and treatment of tumors that overexpress SSTR3 and/or SSTR5.

Chapter 5

Synthesis of (*S*)-Bicalutamide

5 Synthesis of (*S*)-Bicalutamide

5.1 Introduction

5.1.1 Bicalutamide

Bicalutamide is an oral non-steroidal anti-androgen used in the treatment of prostate cancer and hirsutism. It was first administered in 1995 in combination with chemical or surgical castration for the treatment of advanced prostate cancer and some years later was also administered as monotherapy for the treatment of earlier stages of this disease[35].
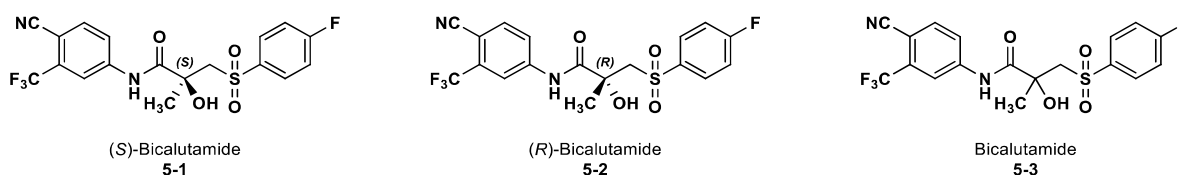
Figure 5.1 Chemical structure of (S)-bicalutamide (5-1), (R)-bicalutamide (5-2) and racemic bicalutamide (5-3)

Bicalutamide acts as a pure anti-androgen that competes with testosterone and dihydrotestosterone for binding sites on the androgen receptor. Since all stages of adenocarcinoma of the prostate are driven by a transcriptionally active androgen receptor, preventing its activation[36] and accelerating its degradation[35] halts the tumor growth.

Bicalutamide is administered clinically in its racemic form, though the anti-androgenic activity is exclusively found in the (*R*)-enantiomer, being the (*S*)-enantiomer inactive (Figure 5.1). (*R*)-Bicalutamide is absorbed slowly, is not affected by food intake, and shows a half-life in plasma of one week. On the other hand, (*S*)-bicalutamide is absorbed faster and displays a shorter plasma half-life[35]. Although both enantiomers are metabolized in the liver[36], the concentrations of (*R*)-bicalutamide in plasma at the steady state become 100 times higher than those of (*S*)-enantiomer. While (*S*)-bicalutamide is known to be inactive as an anti-androgen, it is co-administered with the (*R*)-enantiomer due to its low toxicity.

5.1.2 Lysosomal Storage Diseases

Lysosomal Storage Diseases (LSDs) are genetic disorders that involve the accumulation of macromolecules inside the cells, specifically in the lysosomes[35]. These cellular organelles are responsible for the metabolism and recycling of macromolecules (*e.g.* carbohydrates, lipids, nucleic acids and proteins), the control of nutrient sensing, amino acid and ion homeostasis and calcium signaling[37,294–296].

This abnormal storage of macromolecules is caused normally by the deficiency or malfunction of a particular lysosomal hydrolytic enzyme involved in the degradation of a specific substrate[37]. In

general, LSDs are a group of 70 monogenic disorders of lysosomal metabolism that are inherited in an autosomal recessive manner, though few of them are X-linked[35,37].

Normally, LSDs are caused by mutations in genes encoding lysosomal proteins such as glycosidases, proteases, integral membrane proteins, transporters, enzyme modifiers or activators. Consequently, these mutations affect the function of these encoded proteins, that result in lysosome general abnormal function and the gradual accumulation of the substrate inside the lysosome[37]. This accumulation of macromolecules might initiate a cascade of secondary effects (*e.g.* altered calcium homeostasis, signaling pathways, trafficking, inflammation and oxidative stress), ultimately leading to irreversible cellular damage, organ dysfunction or degeneration and even death[37].

Table 5.1 Lysosomal Storage Diseases[297]

Metabolism	Disorder	Enzyme deficiency/malfunction
Mucopolysaccharides	MPS I (Hurler, Scheie syndrome)	Alpha-*L*-iduronidase
	MPS II (Hunter syndrome)	Iduronate-2-sulfatase
	MPS IIIA (Sanfilippo syndrome)	Heparan-*N*-sulfatase
	MPS IIIB (Sanfilippo syndrome)	*N*-acetylglucosaminidase
	MPS IIIC (Sanfilippo syndrome)	Acetyl CoA glucosamine *N*-acetyltransferase
	MPS IIID (Sanfilippo syndrome)	*N*-acetylglucosamine-6-sulfatase
	MPS IVA (Morquio syndrome)	*N*-acetylgalactosamine-6-sulfate sulfatase
	MPS IVB (Morquio syndrome)	*β*-galactosidase
	MPS VI (Maroteaux-Lamy syndrome)	Arylsulfatase B
	MPS VII (Sly syndrome)	*β*-glucuronidase
Glycogen	Pompe disease	*α*-alglucosidase
Sphingolipids	Gaucher disease (types I, II, III)	Glucocerebrosidase
	Fabry disease (X-linked)	*α*-galactosidase
	Krabbe disease	Galactocerebrosidase
	Metachromatic leukodystrophy	Arylsulfatase A
Lipid trafficking and cholesterol	Niemman-Pick disease type C	Cholesterol transporters

LSDs are historically classified depending on: i) the basis of their storage product (mucopolysaccharides, glycogen, sphingolipids and other macromolecules); or ii) the nature of their molecular abnormality (defect in post-translational processing of lysosomal enzymes, lysosomal membrane and transport defects, neuronal lipofuscinoses and defect in lysosome-related organelle biogenesis)[35]. Table 5.1 shows a list of the most important LSDs and their related enzyme deficiency/malfunction[297].

The global incidence of LSDs is approximately 1 in 5,000 live births[35]. The most common are Fabry disease (2.5 cases per 100,000 males), metachromatic leukodystrophy (2.5 cases per 100,000

individuals), Pompe disease (2.5 cases per 100,000 individuals) and Gaucher disease (2 cases per 100,000 individuals)[37].

The biochemical type of the stored macromolecules affects differentially the lysosome function as macromolecules have diverse roles in specific cellular processes, which underlies the variable clinical pathology of LSDs[37]. In addition, these genetically and clinically heterogeneous disorders normally appear as pediatric neurodegenerative diseases that are often related to visceromegaly (enlargement of abdominal organs such as the liver and spleen)[37,298].

Diagnosis of LSDs is based on clinical symptoms and confirmation of increased storage or genetic alterations using several diagnostic tests such as enzymatic analysis and single gene sequencing[37,298].

5.1.2.1 Available Therapies

The ultimate cause of LSDs is the lack of activity of an enzyme responsible of the degradation of a determined substrate, eventually leading to its toxic accumulation. However, residual enzymatic activity depends generally on the enzyme mutation and in most cases the severity of the disease correlates with the degree of enzymatic deficiency. It is considered that a residual enzymatic activity of only 10-20% of normal values may be enough for function recovery resulting in wild type phenotype[35].

For many years, the treatment of patients suffering from LSDs mainly consisted of supportive care. In the 1990s, new therapeutic strategies emerged: Haematopoietic stem cell transplantation, Enzyme replacement therapy, and Substrate reduction therapy were the most important ones[35].

Haematopoietic stem cell transplantation (HSCT) rationale consists in providing the patient with compatible stem cells with normal enzyme levels, which would donate enzyme to compensate the deficient cells of the patient[37]. The success of this therapy resides on the possibility of encountering a compatible donor of bone marrow, or alternatively umbilical cord[35,37]. Consequently, HSCT might be associated to high rates of morbidity and mortality due to rejection, toxicity or infections caused by the transplantation of exogenous stem cells[35]. This therapy was the first treatment for LSDs that showed any success and was continued to be used despite the previous risks. Nowadays, HSCT is currently the standard of care for children with Hurler disease and has shown prominent results with metachromatic leukodystrophy and Krabbe disease, which are LSDs for which no other treatment is available[35,37].

Enzyme replacement therapy (ERT) is normally applied when an enzymatic deficiency exists, and its basis is established on the ability of cells to endocytose macromolecules (such as the deficient enzyme). After endocytosis, the fusion between endosomes and lysosomes would take

place restoring the enzyme levels inside the lysosome. Consequently, ERT is only possible with enzymes that are soluble or easily solubilized, so it does not work for example with lipophile membrane-bound enzymes[37]. Another limitation of ERT is that not all organs are accessible to the exogenously administered enzyme, being orthopedic, cardiovascular, neurological and ocular symptoms especially difficult to treat[37]. In addition, the blood-brain barrier prevents the entry of exogeneous enzymes into brain parenchyma. As a result, the enzyme requires either modification to take advantage of existing transport systems or direct administration into the brain or spinal canal. Despite these limitations, ERT is a well-tolerated therapy with low toxicity and moderate side effects. However, its therapeutic effect is temporary needing to be administered weekly, biweekly or monthly, which represents a high cost for the patient. Until now, ERT has been developed and approved for the treatment of Gaucher disease, Fabry disease, Pompe disease, lysosomal acid lipase deficiency and mucopolysaccharidoses types I, II, IV, VI and VII.
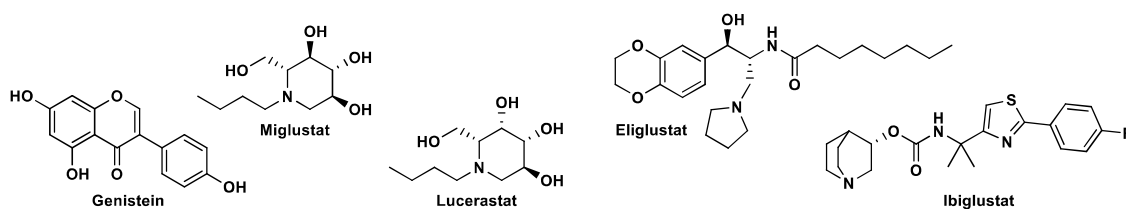
Figure 5.2 Chemical structures of Miglustat, Eliglustat, Genistein, Ibiglustat and Lucerastat

Substrate reduction therapy (SRT) uses small molecules to inhibit the formation of a determined macromolecule in the lysosome to prevent its toxic accumulation[299,300]. This includes a variety of drugs that inhibit the biosynthesis of storage metabolites[37] (Figure 5.2). This treatment is only currently available for Gaucher and Niemann-Pick type C diseases, treated with miglustat and eliglustat, respectively. The mechanism of action of both drugs consists in blocking GlcCer synthase, which inhibits the first step of glycosphingolipids biosynthesis[301,302]. Other advantages of SRT drugs are that they are orally administered and are stable at ambient temperatures, making it easier for the patient. Despite this, these drugs may have adverse effects or complications related to drug metabolism inside the body. In addition, they are relatively expensive and limited to affluent health-care systems. In principle, SRT drugs may be developed for all LSDs, but currently are restricted to glycosphingolipidoses because, to date, only biosynthetic inhibitors specific to this pathway have been identified and developed. Several other SRT drugs are currently being evaluated in clinical trials: i) genistein that indirectly reduces proteoglycan biosynthesis for MPS III; ii) ibiglustat for Gaucher disease and Fabry disease; and iii) lucerastat for Fabry disease.

5.1.2.2   The potential of (*S*)-Bicalutamide

In general, the previous therapies offer limited benefits because of incompatible donors, possible graft failure and inability to cross the blood-brain barrier. In addition, these therapies are not

100% efficient and, in most cases, only partial improvement of symptoms is observed. Consequently, there is a medical need to develop more effective and universal therapies because many LSDs have at present no real treatment.

Farrera and co-workers[35] at BCN Peptides demonstrated the potential use of (S)-bicalutamide, a molecule without any anti-androgenic activity, as an exocytosis activating compound that is capable of decreasing the toxic accumulation of substrates inside the lysosomes. Related to this, the importance of the stereochemistry of the chiral center of bicalutamide was verified, demonstrating that (S)-bicalutamide favored exocytosis in a more effective way than the (R)-enantiomer. In addition, as (S)-bicalutamide was effective *in vitro* in all the diseases tested, it proved to be a potential universal treatment for prevention of the damaging clinical symptoms of LSDs. This may also represent an advantage for the treatment of LSDs in children, since the treatment with racemic bicalutamide would delay their sexual development. Furthermore, the lack of anti-androgen activity of (S)-bicalutamide would prevent the damaging side effects observed in chronic treatments of prostate cancer with bicalutamide, which are derived from the anti-androgen activity of the (R)-enantiomer.

In vitro experiments with fibroblasts of patients suffering from various LSDs were performed by Farrera and co-workers[35] to demonstrate the exocytosis effect of (S)-bicalutamide. First, the authors observed that bicalutamide was able to increase the *in vitro* enzymatic activity of β-hexosaminidase between 23 to 100% in fibroblasts of a patient affected by Sanfilippo B disease, indicating an enhancement in lysosomal exocytosis. In addition, it was confirmed that bicalutamide was able to decrease the glycosaminoglycans (GAGs) accumulation in fibroblasts of three patients affected by Sanfilippo B disease: i) 17-54% in the first patient; ii) 16-20% in the second patient; and iii) 13-53% in the third patient. Consequently, bicalutamide treatment of the fibroblasts of patients affected with Sanfilippo B reduced the levels of accumulated GAGs, thus increasing their exocytosis.

Regarding the stereochemistry, (S)-bicalutamide demonstrated to be non-toxic for fibroblasts of thirteen patients affected by various LSDs such as Sanfilippo A and San Filippo B among others. In contrast, cell viability assays evidenced the higher toxicity of the (R)-enantiomer against the same panel of fibroblasts. Additionally, (S)-bicalutamide was able to significantly increase lysosomal exocytosis in ten of the thirteen cellular cultures of fibroblasts from Sanfilippo A and Sanfilippo B patients, while (R)-bicalutamide was only able to increase the lysosomal exocytosis in one of the tested cultures. Consequently, the treatment with (S)-bicalutamide appeared to be more effective and universal than the (R)-enantiomer. Finally, (S)-bicalutamide showed a significant and dose-dependent decreasing effect on GAGs accumulation, reaching the same

levels as in healthy fibroblasts. On the contrary, the (*R*)-enantiomer also showed a decrease of GAG levels but only in few cases and with lower intensity.

Overall, the administration of the single enantiomer (*S*)-bicalutamide could represent an effective and universal detoxification therapy for patients suffering from LSDs that have no real treatment. (*S*)-bicalutamide, a non-toxic compound without any anti-androgenic activity, is already administered together with the (*R*)-enantiomer to treat prostate cancer and hirsutism, though only the latter is the responsible for the anti-androgenic activity. Despite these promising results, the effectiveness of (*S*)-bicalutamide was only tested *in vitro*. Therefore, the potential of this treatment has to be confirmed *in vivo* through preclinical and clinical studies.

5.2 Research Background

5.2.1 Bicalutamide synthesis

The original synthesis of racemic bicalutamide (**5-3**) consisted in four linear steps and was patented in 1984 by Tucker and co-workers[303] (Figure 5.3). The first step of the synthesis consisted in the amidation reaction of 4-cyano-3-(trifluoromethyl)aniline (**5-4**) with methacryoyl chloride. Next, the corresponding methacrylamide (**5-5**) was transformed into epoxide (**5-6**) using a strong oxidant such as *m*-chloroperoxybenzoic acid (*m*CPBA). Afterwards, the epoxide (**5-6**) was opened through the nucleophilic attack of 4-fluorobenzenthiol (**5-7**) using sodium hydride. Finally, the resulting thiol precursor (**5-8**) was oxidized to obtain bicalutamide (**5-3**) using *m*CPBA.
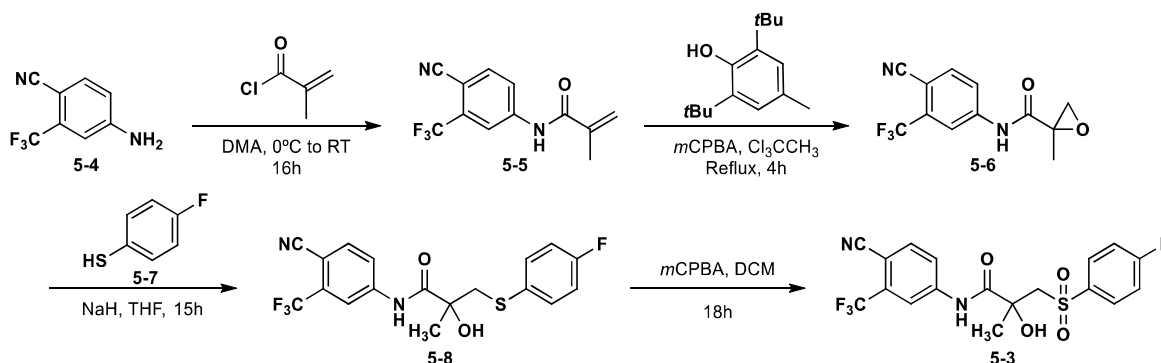
Figure 5.3 Original synthesis of racemic bicalutamide (5-3)[303]

Some years later, Thijs and co-workers[304] also patented the synthesis of racemic bicalutamide (**5-3**) in only three steps (Figure 5.4). In contrast to the original synthesis, the epoxide (**5-6**) was opened through the nucleophilic attack of sodium 4-fluorobenzenesulfinate (**5-9**) instead of the thiol derivative (**5-7**). By doing this, bicalutamide (**5-3**) could be directly obtained avoiding the last oxidation step[303].
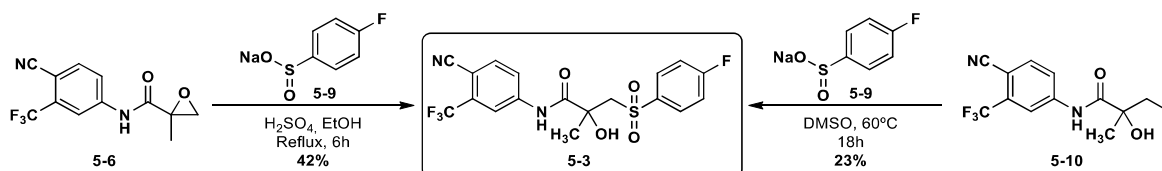
Figure 5.4 Synthesis of bicalutamide (5-3) from epoxide (5-6) or iodoamide (5-10)[304]

Interestingly, Thijs and co-workers[304] demonstrated as well that the nucleophilic attack of 4-fluorobenzenesulfinate (**5-9**) worked not only with epoxides (**5-6**) but also with halogen derivatives such as the iodoamide precursor (**5-10**) (Figure 5.4).

5.2.2 (*S*)-Bicalutamide synthesis
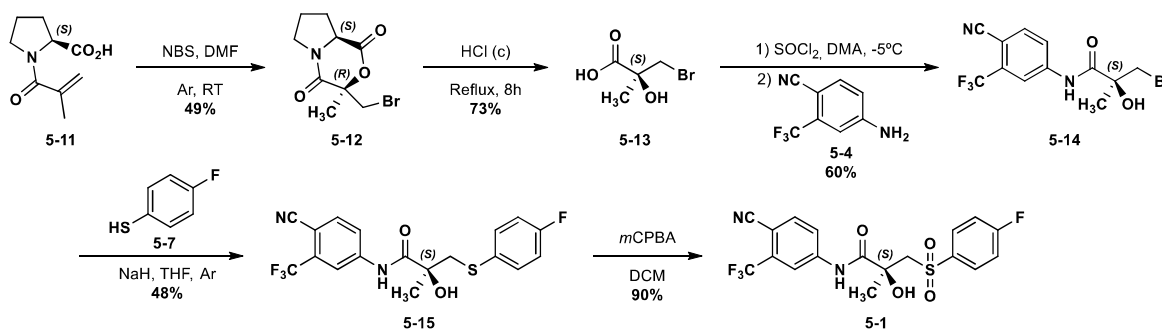
Figure 5.5 Synthesis of (S)-bicalutamide (5-1) reported by Tucker and co-workers[305]

Tucker and co-workers[305] were also the first to report the synthesis of (*S*)-bicalutamide (**5-1**) (Figure 5.5)[303]. Their strategy was based on the bromolactonization of the *N*-methacrylamide of *L*-proline, which was originally reported by Terashima and co-workers[306,307], so *L*-proline was the starting enantiopure material from which (*S*)-bicalutamide (**5-1**) could be obtained. Reaction of the *N*-methylacrylamide of *L*-proline (**5-11**) with *N*-bromosuccinimide (NBS) in DMF produced bromolactone (**5-12**) in 49% yield. Importantly, bromolactone (**5-12**) was shown to be a single diastereomer by ^{1}H- and ^{13}C-NMR, according to the authors. Next, acid hydrolysis under reflux conditions delivered the bromoacid (**5-13**) in 73% yield. Then, the bromoacid (**5-13**) was transformed to the corresponding acid chloride using thionyl chloride and was coupled to aniline (**5-4**) in 60% yield. Next, the nucleophilic substitution of 4-fluorobenzenthiol (**5-7**) on bromoamide (**5-14**) was performed using sodium hydride in THF giving the corresponding thiol precursor (**5-15**) in 48% yield. Finally, the thiol precursor (**5-15**) was oxidized using *m*CPBA in DCM to obtain (*S*)-bicalutamide (**5-1**) in 90% yield. The synthesis proposed by Tucker and co-workers[305] comprised five linear steps that permitted to obtain enantiopure (*S*)-bicalutamide (**5-1**) in 9% overall yield using the natural amino acid *L*-proline as the starting material. In addition, this strategy may be easily adapted to the use of *D*-proline to obtain (*R*)-bicalutamide (**5-2**)[308].
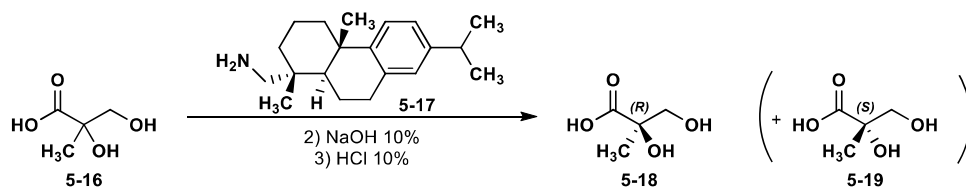
Figure 5.6 Chiral resolution: 2,3-dihydroxy-2-methylpropionic acid (5-16) with (+)-dehydroabiethylamine (5-17)

Another methodology to prepare (*S*)-bicalutamide (**5-1**) was patented in 2001 by Sörös and co-workers[309]. These authors based their strategy on the synthesis of racemic 2,3-dihydroxy-2-methyl-propionic acid (**5-16**) and its chiral resolution using (+)-dehydroabiethylamine (**5-17**) to crystallize the enantiopure (*R*)-2,3-dihydroxy-2-methylpropionic acid (**5-18**) (Figure 5.6).
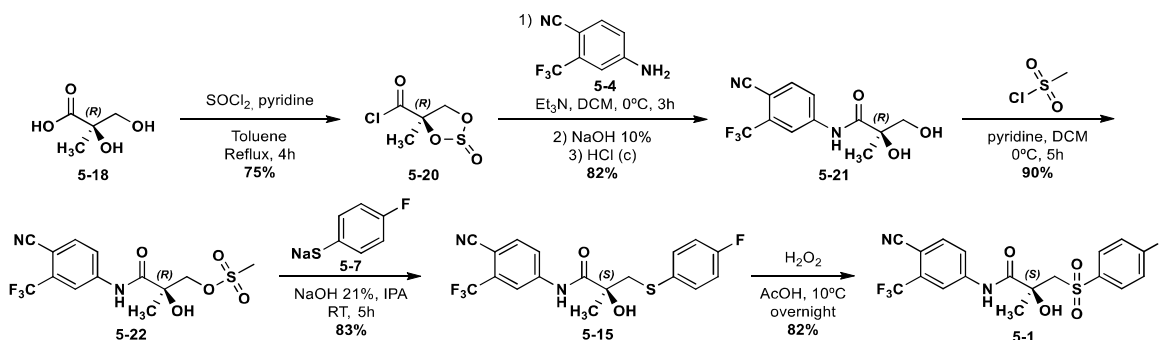
Figure 5.7 Synthesis of (S)-bicalutamide (5-1) reported by Sörös and co-workers[309]

Once the chiral resolution was performed, (*R*)-2,3-dihydroxy-2-methylpropionic acid (**5-18**) was transformed to intermediate (**5-20**) using thionyl chloride and pyridine under reflux conditions in 75% yield (Figure 5.7). Next, aniline (**5-4**) was coupled to compound (**5-20**) at 0ºC. Immadiately after, basic and acid hydrolysis eliminated the dioxathiolane moiety giving the desired dihydroxyamide (**5-21**) in 82% yield. Afterwards, methanesulfonyl chloride and pyridine were used to obtain the corresponding methylsulfonate intermediate (**5-22**) in 90% yield. Then, the nucleophilic substitution using 4-fluorobenzenthiol (**5-7**) was performed to give the thiol precursor (**5-15**) in 83% yield. Finally, the thiol precursor (**5-15**) was oxidized using hydrogen peroxide in AcOH to obtain (*S*)-bicalutamide (**5-1**) in 82% yield. The synthesis proposed by Sörös and co-workers[309] consisted of five linear steps that permitted to obtain enantiopure (*S*)-bicalutamide (**5-1**) in 37% overall yield using (*S*)-2,3-dihydroxy-2-methylpropionic acid (**5-19**) as the starting material. In addition, the authors could prepare (*R*)-bicalutamide (**5-2**) using the same methodology.

5.3 Results

The development of a synthetic procedure to obtain (*S*)-bicalutamide (**5-1**) was performed in two phases: i) development of an initial batch and characterization of the principal impurities; and ii) optimization of the reactions to obtain the target product (**5-1**) and its precursors to minimize the impurities of the final batch. After all, the final aim was to obtain (*S*)-bicalutamide (**5-1**) with

high purity, accomplishing the specifications described for bicalutamide (**5-3**) in the Pharmacopeia.

5.3.1 Initial synthesis of (*S*)-Bicalutamide (1ˢᵗ phase)

The synthesis of (*S*)-bicalutamide (**5-1**) was designed from the (*S*)-3-bromo-2-hydroxy-2-methylpropanoic acid ((*S*)-bromoacid (**5-13**)), which is commercial in both pure enantiomeric configurations (Figure 5.8). The corresponding (*S*)-bromoamide (**5-14**) intermediate was synthesized starting from (*S*)-bromoacid (**5-13**) using 4-cyano-3-trifluoromethylaniline (**5-4**). The other precursor, sodium 4-fluorobenzenesulfinate (**5-9**) was obtained from 4-fluorobenzenesulfonyl chloride (**5-23**).
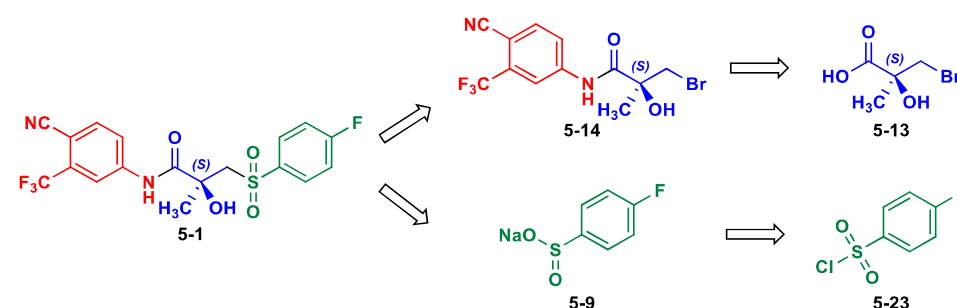
Figure 5.8 Retrosynthesis of (S)-bicalutamide (5-1)

After various failed attempts of synthesizing (*S*)-bicalutamide (**5-1**) from the corresponding epoxide intermediate (**5-6**) (Figure 5.4), we decided to use an halogen atom as the leaving group for the attack of 4-fluorobenzenesulfinate (**5-9**) as reported by Thijs and co-workers[304]. As a difference, the bromine atom was preferred over the iodine atom, because as previously said (*S*)-bromoacid (**5-13**) was already commercial.
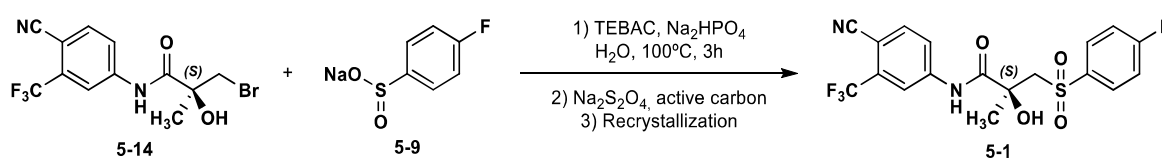
Figure 5.9 Initial synthesis of (S)-bicalutamide (5-1)

In the initial synthesis, (*S*)-bicalutamide (**5-1**) was obtained from the reaction between (*S*)-bromoamide (**5-14**) and sulfinate (**5-9**) precursors in H_2O without the presence of any organic solvent and using triethylbenzylammonium chloride (TEBAC) as the phase transfer agent (Figure 5.9). Afterwards, the crude was purified by recrystallization using IPA/H_2O and following a similar procedure to the one reported by Dolitzky and co-workers[310].
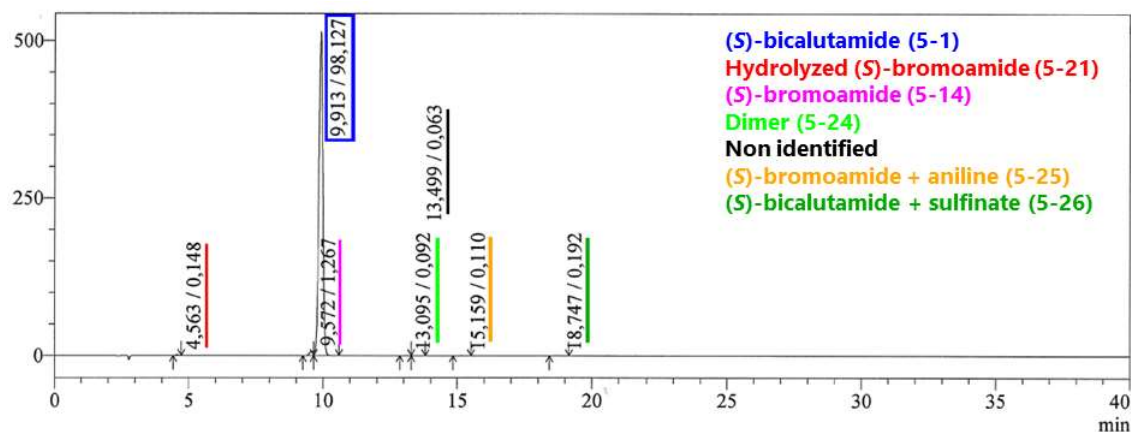
Figure 5.10 HPLC analysis of the initial batch of (S)-bicalutamide (5-1) (53%B in 40 min)

The principal impurities obtained in this initial batch of (*S*)-bicalutamide (**5-1**) were identified by HPLC-MS[67] (Figure 5.10) and summarized in Table 5.2.

Table 5.2 Principal impurities of the initial batch of (S)-bicalutamide (5-1) (53%B in 40 min)

Entry	HPLC RRT[68]	AUC (%)	M_{obs} (m/z)	M_{imp}-M_{BCL} (m/z)	ID	Structure
1	1.00	98.13	429.9	-	(*S*)-bicalutamide (**5-1**)	MW 430.4
2	0.46	0.15	287.9	-142.0	Hydrolyzed (*S*)-bromoamide precursor (**5-21**)	MW 288.2
3	0.97	1.27	351.9	-78.0	(*S*)-bromoamide (**5-14**)	MW 351.1
4	1.31	0.09	558.1	+128.2	Dimer (**5-24**)	MW 558.4
5	1.36	0.06	-	-	-	Non-identified
6	1.53	0.11	456.0	+26.1	(*S*)-bromoamide + aniline (**5-25**)	MW 456.3
7	1.89	0.19	572.1	+142.2	(*S*)-bicalutamide + sulfinate (**5-26**)	MW 572.5

Apart from the previous impurities, there was one that could not be detected with the previous analytical method[67], whereas it was detected using the Pharmacopeia analytical method for

---

[67] (*S*)-bicalutamide (**5-1**) HPLC-MS (1st method): 53%B in 40 min (A: H_2O+0.1%TFA; B: ACN+0.07%TFA).
[68] Relative Retention Time (RRT) with respect to (*S*)-bicalutamide (**5-1**) (t_R = 9.9 min).

racemic bicalutamide. The previous HPLC-MS method was slightly modified[69] separating the previous impurity from the principal peak. As the mass of the impurity was the same as (*S*)-bicalutamide (**5-1**), we postulated that this compound could be impurity B (**5-27**) which was described in the European Pharmacopeia (Figure 5.11 and Table 5.3).
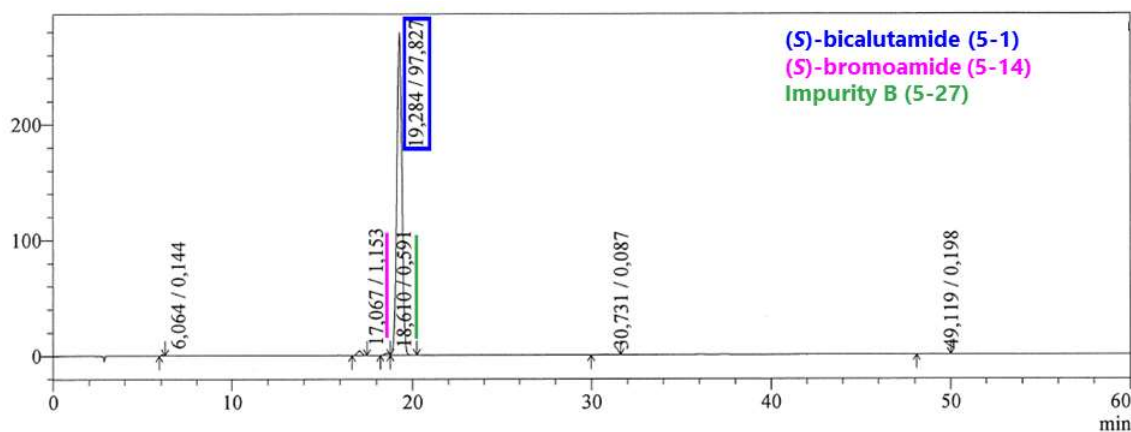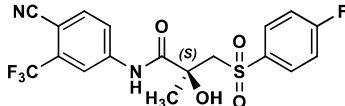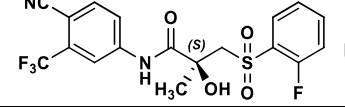
Figure 5.11 HPLC analysis of the initial batch of (S)-bicalutamide (5-1) (45%B in 60 min)

To demonstrate that, we synthesized a batch of impurity B (**5-27**) to perform a co-injection with one of our (*S*)-bicalutamide batches (section 5.3.2.4).

Table 5.3 Impurity B of the initial batch of (S)-bicalutamide (5-1) (45%B in 60 min)

HPLC RRT [70]	AUC (%)	M_{obs} (m/z)	M_{imp}-M_{BCL} (m/z)	ID	Structure
1.00	97.83	429.9	-	(*S*)-bicalutamide (**5-1**)	
0.97	0.59	430.0	0.1	Impurity B (**5-27**)	

The specifications required by the European Pharmacopeia were extremely demanding: i) minimum purity of 99.5%, ii) known impurities ≤ 0.15%; iii) unknown impurities ≤ 0.1%; and iv) impurities over 0.05% should be integrated in the HPLC analysis. The initial batch of (*S*)-bicalutamide (**5-1**) did not fulfill the previous requirements because of various impurities detected in the HPLC analysis. Despite this, the initial (*S*)-bicalutamide batch was analyzed by ^{1}H-NMR and chiral HPLC[71] showing a 99% of ee. Therefore, the chirality did not change during the different steps of the synthetic route.

---

[69] (*S*)-bicalutamide (**5-1**) HPLC-MS (2nd method): 45%B in 60 min (A: H_2O+0.1%TFA; B: ACN+0.07% TFA).

[70] Relative Retention Time (RRT) with respect to (*S*)-bicalutamide (**5-1**) (t_R = 19.3 min).

[71] (*S*)-bicalutamide (**5-1**) chiral HPLC: 100%A in 30 min (A: Heptane/EtOH (60:40)); t_R = 6.3 min

5.3.2 Optimization of the synthetic route (2nd phase)

In the second phase both the synthesis of (S)-bicalutamide (**5-1**) and the synthesis of its precursors ((S)-bromoamide (**5-14**) and sulfinate (**5-9**)) were optimized to minimize the impurities present on the final product to comply the specifications required by the European Pharmacopeia. In addition, the scale of the reactions was gradually increased from 1 g to 50 – 250 g.
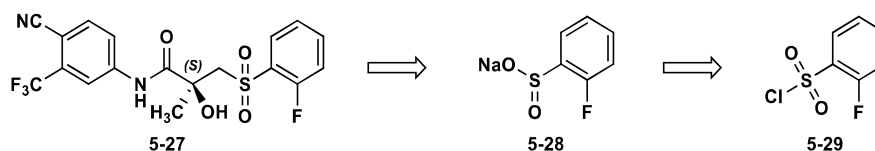
Figure 5.12 Retrosynthesis of impurity B (5-27)

To begin with the optimization, the impurities of all the starting materials ((S)-bromoacid (**5-13**), aniline (**5-4**) and sulfonyl (**5-23**)) and the precursors ((S)-bromoamide (**5-14**) and sulfinate (**5-9**)) were extensively examined. Those starting materials that permitted us to synthesize the corresponding precursors in the purest form were the ones selected to avoid possible impurities or isomers in the final product. The most critical starting material was sulfonyl (**5-23**), which could contain the impurity 2-fluorobenzenesulfonyl chloride (**5-29**) that in turn would produce impurity B (**5-27**) (Figure 5.12). As impurity B (**5-27**) is an isomer of (S)-bicalutamide (**5-1**), the 4-fluorobenzenesulfonyl (**5-23**) of various commercial suppliers was carefully analyzed by HPLC[72] to investigate which one contained the least quantity of the *ortho*-impurity (**5-29**) (Table 5.4). The starting material from Fluorochem was the purest and the only one that did not contain the *ortho*-impurity (**5-29**). Therefore, it was selected to synthesize the final batch.

Table 5.4 Levels of ortho-fluoro sulfonyl (5-29) impurity from various commercial houses

Distributor	Sulfonyl (5-23) (%)	*Ortho*-fluoro sulfonyl (5-29) (%)
Sigma-Aldrich	99.03	0.96
T&W Group	98.71	0.51
AlfaAesar	99.40	0.32
Fluorochem	99.46	Not detected

Regarding the precursors, the initial synthetic methodology was modified to obtain them in its chemically and optically purest forms, avoiding all the steps or procedures during their syntheses that could lower their purity, which in turn would affect the purity of the final product. The optimization of these syntheses is described in the following sections.

---

[72] Sulfonyl (**5-23**) HPLC: 20-100%B in 20 min (A: H_2O+0.1%TFA; B: ACN+0.07%TFA); t_R = 17.4 min

5.3.2.1 (S)-Bromoamide optimization
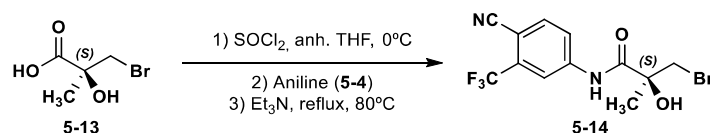
Figure 5.13 Synthesis of (S)-bromoamide (5-14)

(S)-bromoamide (**5-14**) precursor was prepared in two simple synthetic steps (Figure 5.13) similarly as the methodology patented by Dalton and co-workers[308], who performed the same type of reactions but using the (R)-enantiomer. These synthetic steps were: i) the activation of (S)-bromoacid (**5-13**) using thionyl chloride in anh. THF; and ii) the amide formation by introduction of aniline (**5-4**) in basic conditions. Some key steps in this reaction were to heat the reaction mixture overnight (t ≥ 12h) after the introduction of the aniline and recrystallize the product in toluene. In these conditions, a brown solid (7.9 g, 84% yield, 98.95% purity) was obtained. At that point, the product was recrystallized and discolored with active carbon using IPA/H_2O mixtures, but the white solid (5.1 g, 64% yield, 95.76% purity) that was obtained was not purer than the crude. On the contrary, the HPLC-MS analysis of the first and second batches of (S)-bromoamide (**5-14**) (E6-116 and E6-130) revealed that the IPA/H_2O recrystallization formed two principal impurities (Figure 5.14): i) hydrolyzed impurity (**5-21**) formed from the hydrolysis of (S)-bromoamide (**5-14**); and, ii) isopropyl impurity (**5-30**) that corresponded to the ether formed by IPA and (S)-bromoamide (**5-14**).
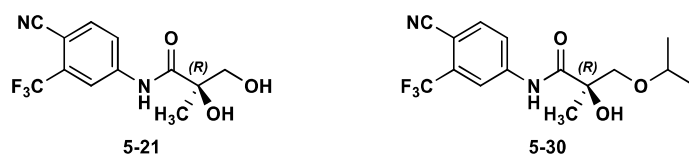
Figure 5.14 Hydrolyzed (5-21) and Isopropyl (5-30) impurities of (S)-bromoamide (5-14)

As hydrolyzed impurity (**5-21**) was already found in the initial batch of (S)-bicalutamide (**5-1**) in the 1st phase, we decided to avoid the IPA/H_2O recrystallization. In contrast, we observed that the recrystallization with toluene was much more effective. In the next experiment (E6-160), we even tried to perform two recrystallization/discoloration procedures with toluene, but this required the filtration in hot (~65ºC) of the active carbon. As a consequence, it was decided to perform the discoloration directly on the EtOAc organic phase of the work-up. By doing this, the active carbon could be filtered at RT. Then, the toluene recrystallization could be performed without any complications. Thanks to these changes, the purity of (S)-bromoamide (**5-14**) was improved with only one toluene recrystallization (99.20% purity, E6-168). For more details see sections 7.6.2 and 9.4.1.

5.3.2.2   4-fluorobenzenesulfinate optimization

The sulfinate (**5-9**) precursor was prepared by the reduction of 4-fluorobenzenesulfonyl chloride (**5-23**) with sodium sulfite in aqueous basic medium as reported by various research groups[311–313] (Figure 5.15). The critical step of this reaction was to select the proper commercial house to provide the 4-fluorosulfonyl (**5-23**) starting material to avoid the formation of 4-fluorobenzene sulfinate (Table 5.4) that in turn would form impurity B. Once the starting material (**5-23**) was selected, only little changes were performed on the initial procedure (E6-124) to synthesize 4-fluoro sulfinate (**5-9**) (18.3 g, 98% yield, 97.70% purity). Some of these changes were: i) to establish the equivalents of Na_2SO_3 and Na_2CO_3 to 1.2; and ii) to reduce to ½ the H_2O volumes (from 9 to 4.5 vol) to reduce the evaporation time of the solvent after the reaction.

5-23   **5-9**
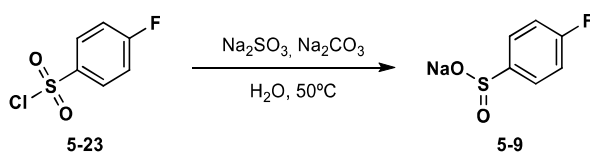
Figure 5.15 Synthesis of 4-fluorobenzenesulfinate (5-9)

After the evaporation of H_2O, the 4-fluoro sulfinate (**5-9**) had to be dissolved in EtOH, filtered and the solvent was removed under reduced pressure. We tried to reduce the amount of EtOH used by refluxing it in less quantity but it did not work. On the contrary, when the scale of the reaction was increased, we had to increase proportionally the volume of EtOH used in the work-up to increase the yield of the reaction. In addition, the time needed to dissolve the product in EtOH was also increased to improve the yields (E6-190). The final wash with ACN served us to eliminate possible impurities from the sulfinate (**5-9**), such as the sulfonyl (**5-23**) as starting material. For more details see sections 7.6.3 and 9.4.2.

5.3.2.3   (*S*)-Bicalutamide optimization

The nucleophilic attack of 4-fluorobenzensulfinate (**5-9**) over the bromine atom of (*S*)-bromoamide (**5-14**) worked producing the target product (*S*)-bicalutamide (**5-1**) (Figure 5.9), as explained in section 5.3.1. Nevertheless, various impurities were detected in the initial batch by HPLC-MS (Table 5.2). With the objective to minimize those impurities, some changes were applied to the synthetic procedure.

To diminish the formation of the disulfinate impurity (**5-26**), the initial equivalents of 4-fluoro sulfinate (**5-9**) were reduced to 3 (E6-156). As there was no impact neither positive or negative after applying this change, we continued to use only 3 eq of 4-fluoro sulfinate (**5-9**) in the following reactions.

To diminish the hydrolyzed (*S*)-bromoamide (**5-21**), the H_2O volumes were reduced from 5 to 4, and the temperature of the reaction was established at 100ºC. In addition, the heating time was fixed at 1h as the reaction had already finished by that time. To diminish the temperature was not an option as more than 15h were necessary for the reaction to finish at 80ºC. To add the (*S*)-bromoamide (**5-14**) after heating the rest of the reagents reduced a little bit the hydrolyzed impurity (**5-21**), but the improvement was so minimal that we decided to introduce it with the other reagents as it was done in previous reactions. At that moment, we assumed that some part of the (*S*)-bromoamide (**5-14**) would hydrolyze inevitably. Therefore, we focused on developing a robust and reproducible recrystallization procedure that could eliminate this and other impurities present in the crude. Other modifications applied to the procedure were: i) to use high purified Milli-Q H_2O; and, ii) to use an inert atmosphere (N_2) during the reaction to avoid the oxidation of sulfinate (**5-9**) to the corresponding sulfonate which would terminate the reaction.
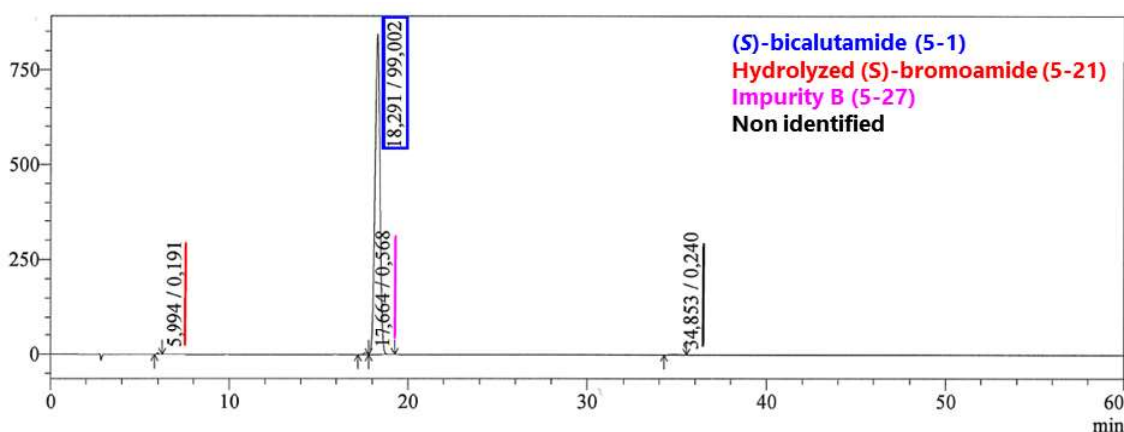
Figure 5.16 HPLC analysis of E6-156 (45%B in 60 min)

Regarding the discoloration/recrystallization step (**procedure A**) used in the initial synthesis of (*S*)-Bicalutamide (**5-1**), the use of IPA/H_2O in the initial synthesis of (*S*)-bicalutamide was not optimal for various reasons: i) after filtering the active carbon, H_2O was added to have a relation IPA/H_2O 1:3 that made the product precipitate but with some time it became an impurified oil, so it was not reproducible; and, ii) the filtration of active carbon at 65ºC could present complications in bigger-scale procedures. Because of these reasons, we decided to change the recrystallization methodology. **Procedure B** consisted in dissolving the (*S*)-bicalutamide (**5-1**) crude in IPA/H_2O 1:1 at high temperature (110-120ºC) to have a more vigorous reflux. In these conditions, H_2O was slowly added (even dropwise) until some permanent turbidity was observed. Afterwards, some pure (*S*)-bicalutamide (**5-1**) crystal seeds were added to help the recrystallization process. At that moment, the heat was turned off and the product was left to cool to RT without taking out the flask from the hot oil bath. After achieving RT conditions, the flask was cooled using an ice bath for 15 min and the product was filtered. It was also very important to wash the filtered crystals

with the same IPA/H₂O proportion in which the permanent turbidity was observed. By means of this method, we were able to improve the purity of E6-156 batch from 81.53% to 99.00% (Figure 5.16), which demonstrated that **procedure B** was a robust and reproducible purification method to obtain (*S*)-bicalutamide (**5-1**) in its pure form.

Due to the previous results, **procedure B** was the chosen methodology to recrystallize (*S*)-bicalutamide (**5-1**) in further experiments. This implied that the discoloration of the product had to be performed before the recrystallization. To do that, (*S*)-Bicalutamide (**5-1**) was extracted from the reaction medium with EtOAc and the discoloration was performed directly in this organic phase, which permitted to obtain a white solid after only one recrystallization (E6-193). For more details see sections 7.6.4 and 9.4.3.

5.3.2.4 Impurity B synthesis
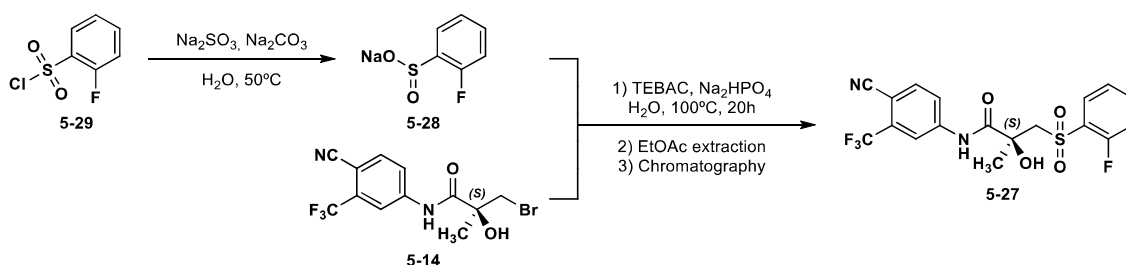
Figure 5.17 Synthesis of ortho-fluorobenzenesulfinate (5-28) and impurity B (5-27)

An isomer of (*S*)-bicalutamide (**5-1**) was detected in the 1ˢᵗ phase of the development (Figure 5.11). This isomer was thought to be impurity B (**5-27**) as described by the European Pharmacopeia. To demonstrate that, we synthesized a small-scale batch of impurity B (**5-27**) (Figure 5.17) to perform various co-injections with one of our (*S*)-bicalutamide (**5-1**) batches. First, the synthesis of *ortho*-fluoro sulfinate (**5-28**) (3.9 g, 93% yield, 99.69% purity) was performed following the procedure described in 5.3.2.2. Afterwards, impurity B (**5-27**) (0.8 g, 57% yield, 96.94% purity[73]) was synthesized following the procedure described in section 7.6.4 and using (*S*)-bromoamide (**5-14**) and *ortho*-fluoro sulfinate (**5-28**) as starting materials. For more details about the formation of impurity B see section 9.4.4.

Finally, a 95:5 co-injection between (*S*)-bicalutamide (**5-1**) (E6-156, 99.00% purity) and impurity B (**5-27**) (E6-164, 96.94% purity) was performed. Because of the co-injection, the peak corresponding to impurity B (**5-27**) increased from 0.57% (Figure 5.16) to 3.27% (Figure 5.18). This demonstrated that the isomeric impurity detected in the 1ˢᵗ phase was undoubtedly impurity B (**5-27**).

---

[73] Impurity B (**5-27**) HPLC: 45%B in 60 min (A: H₂O+0.1%TFA; B: ACN+0.07%TFA); t_R = 18.2 min
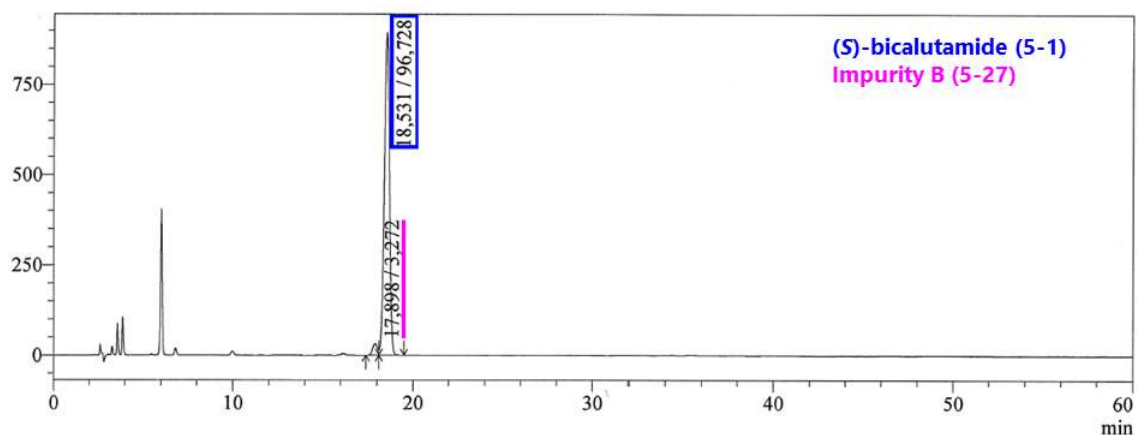
Figure 5.18 Co-injection of E6-156 and E6-164 (95:5) (45%B in 60 min)

5.3.3 Pilot batch synthesis

After the optimization of the 2nd phase, we synthesized a pilot batch of (S)-bromoamide (**5-14**) (E6-168, 79.8 g, 77% yield, 99.20% purity) and 4-fluorobenzenesulfinate (**5-9**) (E6-190, 185.4 g, 99% yield, 98.97% purity)[74]. Once these batches were obtained, we synthesized a pilot batch of (S)-bicalutamide (**5-1**) (E6-195, 51.3 g, 69% yield, 98.94% purity)[75]. Nevertheless, this last batch of (S)-bicalutamide (**5-1**) did not conform the high-demanding specifications of the European Pharmacopeia. As a consequence, we decided to perform a recrystallization process of all the (S)-bicalutamide (**5-1**) batches that we had in our hands at that moment[76] using also the pilot batch (E6-198).
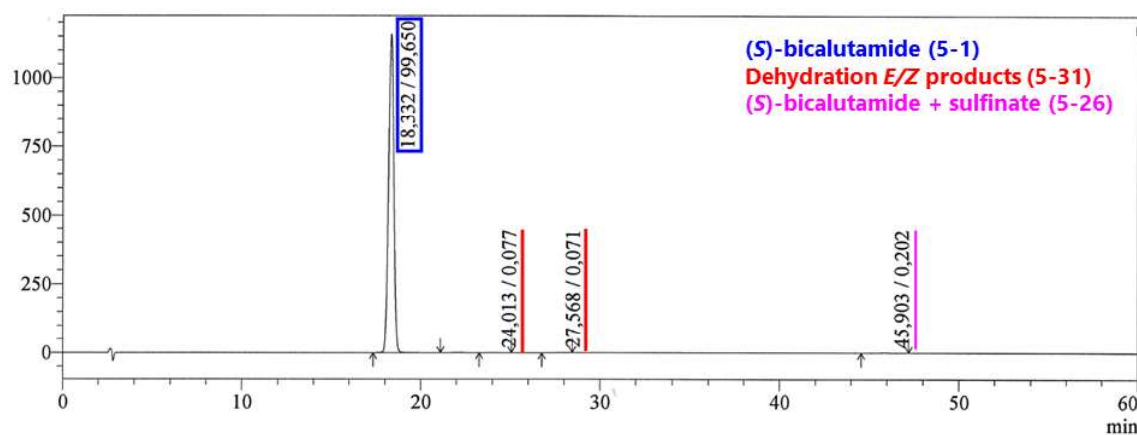
Figure 5.19 HPLC analysis of E6-198 (45%B in 60 min)

This first recrystallization (E6-198) helped to increase the purity of (S)-bicalutamide (**5-1**) to 99.65%, which was higher than the purity of the pilot batch (E6-195, 98.94%), but was not enough to comply the desired specifications. In the HPLC-MS analysis, we could identify two peaks corresponding to the E/Z dehydration products (**5-31**) ([M-H+TFA]⁻=525.1 amu) formed from the

---

[74] The procedures to obtain (S)-bromoamide (**5-14**) (E6-168) and 4-fluorobenzenesulfinate (**5-9**) are described in sections 7.6.2 and 7.6.3.

[75] The procedure to obtain (S)-bicalutamide (**5-1**) (E6-195) is described in section 7.6.4.

[76] (S)-bicalutamide (**5-1**) batches: E6-140, E6-178, E6-186, E6-193 and E6-195.

dehydration of (*S*)-bicalutamide (**5-1**) (Figure 5.20). In addition, we detected the (*S*)-bicalutamide + sulfinate (**5-26**) impurity, which was previously identified in the 1st phase of the development (Table 5.2).
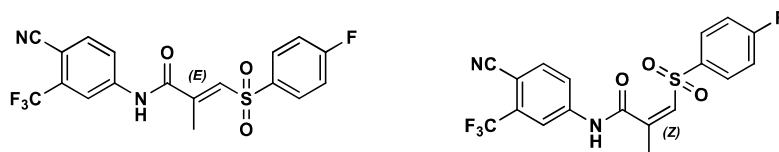
Figure 5.20 Dehydration E/Z products (5-31)

Because of the presence of these impurities, we decided to perform a second recrystallization (E7-058) of the previous batch. This second purification permitted to obtain (*S*)-bicalutamide (**5-1**) with a 99.79% purity (Figure 5.21). In addition, the previous impurities were both reduced. For more details see sections 7.6.4 and 9.4.5.
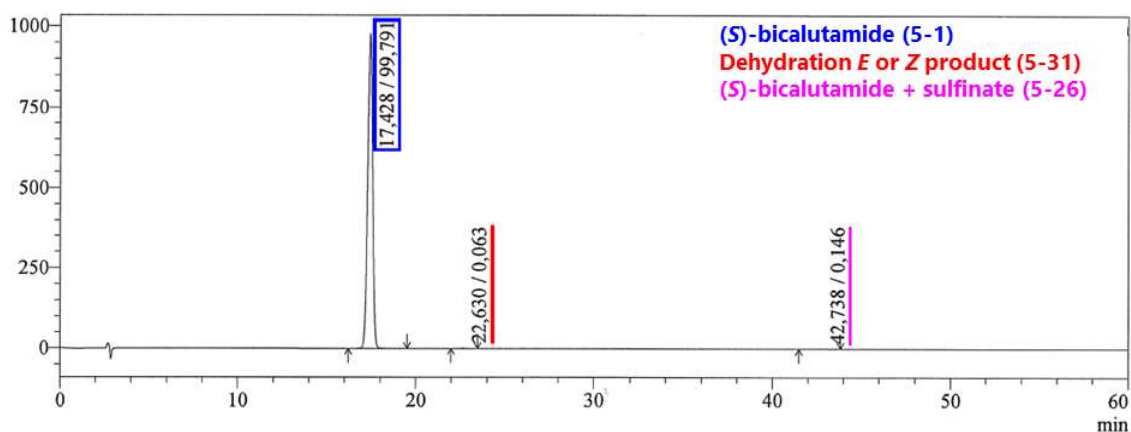
Figure 5.21 HPLC analysis of E7-058 (45%B in 60 min)

5.4 Discussion and conclusions

The development of a synthetic procedure to obtain a batch of (*S*)-bicalutamide (**5-1**) that conforms the specifications of the European Pharmacopeia[77] was accomplished in two phases: i) synthesis of an initial batch of (*S*)-bicalutamide (**5-1**) and characterization of its principal impurities; and ii) optimization of the reactions to obtain (*S*)-bicalutamide (**5-1**) and its precursors in the purest form.

In the 1st phase, HPLC-MS analysis permitted us to identify various impurities present in the initial batch of (*S*)-bicalutamide (**5-1**) (Table 5.2), from which the most critical was impurity B (**5-27**) an isomer with the fluor atom at *ortho*-position instead of *para*-position. To reduce this impurity, we decided to examine the starting material 4-fluorobenzenesulfonyl (**5-23**) from various commercial

---

[77] Specifications: i) minimum purity of 99.5%, ii) known impurities ≤ 0.15%; iii) unknown impurities ≤ 0.1%; and iv) impurities over 0.05% should be integrated in the HPLC analysis.

houses to know which one could provide this reagent with the less amount of the *ortho*-fluorobenzenesulfonyl (**5-29**) impurity.

In the 2nd phase, each of the reactions to obtain (*S*)-bicalutamide (**5-1**) and its precursors (**5-9** and **5-14**) were carefully examined and modified to obtain these compounds in the purest form. In comparison to the initial procedure, the discoloration of (*S*)-bromoamide (**5-14**) was performed directly on the EtOAc organic phase after the work-up of the reaction. In addition, IPA/H_2O mixtures in favor of toluene were used to perform the recrystallization of this precursor to avoid the formation of the dihydroxy (**5-21**) and isopropyl (**5-30**) impurities. Regarding 4-fluorobenzenesulfinate (**5-9**), H_2O volumes in the synthesis were reduced to 4 to diminish the amount of time needed to evaporate the solvent once the reaction had finished. On the contrary, it was not possible to reduce EtOH volumes used in the work-up without significantly affecting the yield of the reaction. Concerning (*S*)-bicalutamide (**5-1**), H_2O volumes could be reduced to 4 to minimize the formation of the dihydroxy (**5-21**) impurity. In addition, the heating time was established to 1h at 100ºC and the discoloration was performed directly on the organic phase after EtOAc extraction. Furthermore, the recrystallization procedure was slightly modified in comparison to the initial methodology of the 1st phase: instead of precipitating the product adding water to have a final IPA/H_2O 1:3 proportion, water was slowly added at 110-120ºC until some permanent turbidity was observed. In these conditions, the heat was turned off to slowly crystallize the product improving its purity. As it did not happen with the initial method, this last recrystallization technique (**procedure B**) was extremely robust and reproducible, but most importantly it improved the purity of (*S*)-bicalutamide (**5-1**) obtaining also excellent recoveries. After two or three recrystallizations, we could finally obtain a pilot (*S*)-bicalutamide (**5-1**) batch (E7-058, 63.4 g, 99.79% purity) that conformed the specifications of the European Pharmacopeia.

Our convergent route permitted to obtain (*S*)-bicalutamide (**5-1**) starting from the (*S*)-bromoacid (**5-13**) in two steps with a 53% overall yield, which greatly improved the linear routes described in section 5.2.2: i) the original synthesis of (*S*)-bicalutamide (**5-1**) with a 26% overall yield starting also from the (*S*)-bromoacid (**5-13**) (Figure 5.5)[305]; and ii) another linear synthesis of (*S*)-bicalutamide (**5-1**) with a 38% overall yield starting from the dihydroxybromoacid (**5-18**) (Figure 5.7)[309]. The use of 4-fluorobenzenesulfinate (**5-9**) as one of the precursors instead of 4-fluorobenzenethiol (**5-7**) permitted to avoid the last oxidation step with *m*CPBA or H_2O_2, which increased the overall yield.

Once the synthetic development of (*S*)-bicalutamide (**5-1**) was finished, all the optimization was properly reported and summarized. This document permitted to prepare production guides to obtain (*S*)-bicalutamide (**5-1**) following *Good Manufacturing Practices* (GMP). With all the acquired

knowledge during the development of the route, quality specifications for the starting materials and synthetic intermediates could be established to obtain the final product (**5-1**) in the required quality. Finally, the Production Department of BCN Peptides could synthesize the first GMP batch of (*S*)-bicalutamide (**5-1**) (SBIC1801, 263.1 g, 99.60%) to evaluate this compound in *in vivo* preclinical studies.

Chapter 6

Global conclusions

6 Global conclusions

Several methodologies were explored to reduce the use of both hazardous organic solvents (*e.g.* DMF) and protecting groups (*e.g.* Fmoc). Our synthetic proposal was based on the synthesis of peptides in the inverse direction (*N*- to *C*-terminus) in two steps: i) activation with active esters in green solvents; and ii) aqueous coupling of *N*-α-unprotected amino acids. Unsuccessful results were obtained because of three main drawbacks: lack of quantitative activation, on resin racemization and lack of quantitative coupling.

Green solvent-mediated acidolysis methods were developed under two strategies: i) global cleavage/deprotection and ii) cleavage of protected peptides. ████████████████

████ █ █ █ █ ██ █ █ █ █ █ █ █ █ ██ █ █ █ █ █ █

████████████████████████████████████

████████████████████████████████████

████████████████████████████████████

████████████████████████████████████

████████████████████████████████████

████████████████████████████████████

████████████████████████████████████

████████████████████████████

The synthesis of eight new tetradecapeptide somatostatin analogues (**A75**-**A82**) containing unnatural and D-amino acids was performed. The serum stability and the degradation metabolites of the new peptides were also characterized. The introduction of both unnatural (*e.g.* Msa) and D-amino acids (*e.g.* D-Ala[1], D-Cys[3,14] and D-Trp[8]) permitted to obtain very stable analogs such as **A75** ($t_{1/2}$=252h), **A79** ($t_{1/2}$=410h), **A81** ($t_{1/2}$=174h) and **A82** ($t_{1/2}$=95h). To the best of our knowledge, these are the most stable somatostatin analogs based on the 14-amino acid scaffold. Prior to the results of biologic and binding experiments, considerable expectations are put on **A82**, which is an stable analog with probable high affinity for SSTR3 and SSTR5.

The synthesis of (*S*)-bicalutamide (**5-1**) and its precursors was accomplished in two phases: i) characterization of the impurity profile of an initial batch of product; and ii) optimization of the synthetic route to obtain (*S*)-bicalutamide (**5-1**), as well as its precursors (*S*)-bromoacid (**5-13**) and 4-fluorobenzenesulfinate (**5-9**). Apart from reaction optimization, to find a robust crystallization method was critical for the purification of the final product. A pilot batch of (*S*)-bicalutamide (**5-1**) (63.4 g, 99.79% purity) that conformed the quality standards required by the European Pharmacopeia was synthesized. The report document with all the development of the synthetic

route helped to prepare the production guides of (*S*)-bicalutamide (**5-1**) and its precursors, which in turn permitted BCN Peptides to synthesize a first GMP batch of (*S*)-bicalutamide (**5-1**) (SBIC1801, 263.1 g, 99.60%) for its evaluation in *in vivo* preclinical studies.

Chapter 7

Experimental section

7 Experimental section

7.1 General Information & instruments

Anh. THF was purchased from Sigma Aldrich. Anh. DCM and DMF were obtained using molecular sieves. Non-anhydrous solvents were obtained from Panreac, Sigma Aldrich, Carlo Erba or Scharlab. Aqueous reactions were performed using Milli-Q water. Commercially available reagents were purchased from Sigma Aldrich, Alfa Aesar, Fluorochem, T&W Group, Iris-Biotech GmbH

Depending on the temperature needed in the experiment, different options were considered:

- T = 15-25ºC: room temperature (RT) was supposed.
- T > 25ºC: different options were used: i) laboratory stove; ii) laboratory dry bath; or iii) oil bath in combination with a hot plate magnetic stirrer.
- T < 5ºC: different options were used: i) an ice/water bath (0-5ºC); or ii) a dry ice/acetone bath (<-70ºC).

Nuclear Magnetic Resonance (NMR) spectra were acquired at RT on a Varian Mercury 400. ^{1}H and ^{13}C spectra were referenced by its solvent residual peaks. ^{1}H and ^{13}C monodimensional spectra were acquired to assign the signals of the ^{13}C NMR, as well as bidimensional homonuclear COSY and HSQC. Chemical shifts were reported in parts per million (ppm) and coupling constants (*J*) in Hz. Peak multiplicities were assigned as follows: s (singlet), d (doublet), dd (double doublet), t (triplet), q (quartet), m (multiplet) and brs (broad signal).

High Resolution Mass Spectrum (HRMS) experiments were carried out in the Institute for Research in Biomedicine (IRB). The samples were introduced by automatic nano-electrospray into an LTQ-FT Ultra mass spectrometer. Conditions: spray voltage 1.7 kV, capillary voltage 40 V, capillary temperature 200ºC, 120 V tube lense, m/z range 200 – 2000 amu and positive ionization. The software used for the data acquisition was Xcalibur (ThermoScientific).

Reverse-Phase High Performance Liquid Chromatography (HPLC) was used for analysis and characterization of compounds and experiment monitoring. Chromatograms were acquired in a Shimadzu HPLC composed by two LC-20AT pumps, an SIL-20A HT automatic injector, an SPD-20A UV-vis detector, a CBM-20A system controller and a CTO-10AS VP oven. Kromasil C8 columns with particle size 5 μm and dimensions 25x4.6 mm were used. Solvent flux was 1 mL/min, detection wavelength 220 nm and two eluents were employed (eluent A: H_2O+0.1%TFA and eluent B: ACN+0.07%TFA). HPLC quality acetonitrile and Milli-Q water were used to prepare the eluents.

Preparative Liquid Chromatography (LC) was performed to purify peptide crudes. HPLC Shimadzu composed by two LC-8A pumps, an SIL-8A automatic injector, an SPD-6A UV-vis detector, an SCL-8A system controller and a C-R6A Chromatopac integrator recorder. Detection wavelength was 220 nm and two eluents were employed (eluent A: H_2O+0.02% TFA and eluent B: ACN). Dissolved crude samples were always filtered with 0.45 μm PVDF filters before injection. Two different columns were used:

-   Merck NW50 (MK9) column filled with Kromasil C8 particle size 10 μm and solvent flux 55 mL/min. Column diameter 5 cm.
-   Novasep preparative column (NS17) filled with Kromasil C8 particle size 10 μm and solvent flux 110 mL/min. Column diameter 10 cm.

High Performance Liquid Chromatography-Mass Spectrometry (HPLC-MS) was used to verify the molecular weight of the synthesized peptides and to identify their impurities. Shimadzu HPLC-MS composed by two LC-20AT pumps, an SIL-20A HT automatic injector, an SPD-20A UV-vis detector, a CBM-20A system controller, a CTO-10AS VP oven, and an electrospray LCMS 2020 detector or LCMS 8040 triple quadrupole. Kromasil C8 columns with particle size 5 μm and dimensions 25x4.6 mm were used. Solvent flux was 1 mL/min, detection wavelength 220 nm and two eluents were used (eluent A: H_2O+0.1%TFA and eluent B: ACN+0.07%TFA). HPLC quality acetonitrile and Milli-Q water were used to prepare the eluents. In general, ESI positive or negative methods were used depending on the analyzed molecule: for peptides, ESI positive method was used; for small molecules, ESI negative method was used.

pHmeter SevenMulti (Mettler Toledo) equipped with two modules (pH or conductivity) was used to determine the pH of some buffer solutions.

Thin-layer Chromatography (TLC) with silica gel TLC-aluminum sheets (Merck 60 F$_{254}$) was used to monitor the evolution of specified reactions. UV 254 nm and 365 nm were used to observe the stains of the starting materials and products.

Lyoalfa 6 Telstar (-80ºC) equipped with a manifold with eight valves was used either to lyophilize H_2O/ACN solutions that contained peptide products or to dry peptidyl resins.

Liberty automated peptide synthesizer (CEM Corporation, model Liberty 908505) was used occasionally for the preparation of some model peptides when specified.

Interchim PuriFLASH® 430 was used as an automated column chromatography system for the purification of non-peptidic crudes by normal-phase column chromatography upon silica using Hexane/Ethyl acetate (EtOAc) mixtures.

7.2 Standard Solid-Phase Peptide Synthesis

All the peptides obtained by standard Fmoc/*t*Bu SPPS were synthesized manually using a reaction vessel with a pore filter plate, both connected to a vacuum pump. Reagents and solvents were introduced inside the reaction vessel, which contained the resin. After the reaction was completed, the solvent, excess of reagents and reaction byproducts were eliminated by filtration.

7.2.1 Ninhydrin test

Ninhydrin test was used to determine qualitatively the presence of primary amines in the peptidyl resin, which was used to control the coupling steps during standard peptide synthesis. To perform the test, a small portion of resin (circa 0.5-2 mg) was introduced in a small test tube and was washed five times with DMF. Then, three drops of Reagent A and one drop of Reagent B were introduced in the tube. The resulting mixture was heat at 110ºC for 2 minutes. Afterwards, the color of the resin and the solution were observed. Yellow color indicated the negative presence of primary amine groups, while blue color indicated the contrary.

Reagent A was prepared by melting 40 g of phenol using a water bath at 40ºC. Then, 10 mL of ethanol were added. At the same time, 6.5 mg of KCN were dissolved in 10 mL of water and 2 mL of the resulting solution were diluted to 100 mL with pyridine free of primary amines. Both solutions were stirred separately with 4 g of Amberlite MB-2 resin, filtered and mixed, obtaining a single solution. Reagent B was prepared by dissolving 2.5 g of ninhydrin in 50 mL of ethanol, which was conserved in a closed bottle protected from light.

In the case the ninhydrin test was positive after the initial coupling, a reactivation step was performed. Even if after the reactivation step the ninhydrin test was positive, a recoupling step was performed. Even if after the first recoupling step the ninhydrin test was still positive, the recoupling was left overnight. Reactivation step: additional quantities of DIPCDI and HOBt were directly added to the reaction vessel. After minimum 30 min, another ninhydrin test was performed. Recoupling step: additional quantities of Fmoc-amino acid, DIPCDI and HOBt dissolved in DMF were added to the reaction vessel after filtration. After minimum 30 min, another ninhydrin test was performed.

7.2.2 Synthesis on *p*MBHA resin

Based on the initial functionalization of *p*MBHA resin Fmoc-Rink amide (1.5 eq) and HOBt (1.5 eq) were dissolved in the minimum amount of DMF. DIPCDI (1.5 eq) was added and the resulting mixture was stirred for 30 seconds. Next, this solution was introduced in the reaction vessel with the resin and the reaction was left for minimum 1h. The ninhydrin test was performed to monitor the amino acid coupling. When the ninhydrin test was negative, DMF washes (3x1min) were

performed and the Fmoc group was eliminated with 20% piperidine in DMF (2x5min). Afterwards, DMF washes (5x1min) were carried out.

The next amino acids were incorporated using the corresponding Fmoc-amino acid (2.5 eq), DIPCDI (2.5 eq) and HOBt (2.5 eq) in DMF. After introducing the last amino acid residue, the resin was washed with DMF (5x1min), DCM (3x1min) and DEE (3x1min). The peptidyl resin was transferred to a container and was dried under vacuum for minimum 12h. The dry peptidyl resin was weighed to know the final resin mass. The peptide mmols were calculated using the initial functionalization of *p*MBHA resin. The final resin functionalization was calculated dividing the peptide mmols by the final resin weight (Equation 7.1).

$$f\,(mmol/g) = \frac{Peptide\ mmols}{Final\ resin\ weight}$$

Equation 7.1 Resin functionalization

7.2.3 **Synthesis on CTC resin**

2-chlorotrytil resin (CTC, f_i = 1.6 mmol/g) was used to obtain peptides with carboxylic acid as its *C*-terminal. The first Fmoc-amino acid (1 eq) was suspended in anh. DCM adding the minimum quantity of anh. DMF for complete dissolution and DIEA (2 eq). The resulting solution was added to the resin and the mixture was stirred for 5 minutes. Afterwards, more DIEA (2 eq) was added diluted with the same volume of anh. DCM. The resulting mixture was gently stirred during 40 min. After this time, MeOH (0.8 mL/g) was added and the mixture was stirred for 10 min. The mixture was transferred to the corresponding reaction vessel, the resin was filtered and washed with anh. DCM (3x1min) and DMF (5x1min). The Fmoc group was eliminated upon treatment with 5% piperidine in DCM/DMF 1:1 (1x10min) and 20% piperidine in DMF (1x15min). DMF washes were performed after Fmoc elimination (5x1min).

The rest of Fmoc-amino acids were incorporated to the peptide chain using DIPCDI and HOBt as coupling reagents at RT. To do that, Fmoc-amino acid (2.5 eq) and HOBt (2.5 eq) were dissolved in the minimum amount of DMF and were cooled using a dry ice/acetone bath. DIPCDI (2.5 eq) was added and the resulting mixture was stirred for 30 seconds. The preactivated amino acid was introduced in the reaction vessel with the resin and the reaction was left for minimum 1h. The ninhydrin test was performed to monitor the amino acid coupling.

When the ninhydrin test was negative, DMF washes (3x1min) were performed. Next, the Fmoc group was eliminated after treatment with 20% piperidine in DMF (2x5min). Afterwards, DMF washes (5x1min) were carried out and the next Fmoc-amino acid was incorporated. Boc-amino acids were used as the *N*-terminal amino acid.

After the complete incorporation of the Boc-amino acid, the resin was washed with DMF (3x1min), MeOH (4x1min) and DEE (4x1min). The peptidyl resin was transferred to a container and was dried under vacuum for minimum 12h. The dry peptidyl resin was weighed to calculate the increase of resin mass (ΔMass). Knowing this parameter, the total mmols of the synthesized peptide were calculated (Equation 7.2), as well as the resin functionalization (f) (Equation 7.3).

$$Peptide\ mmols = \frac{\Delta Mass\ (g) \cdot 1000}{Peptide\ MW\ (g/mol)}$$

Equation 7.2. Peptide mmols

$$f\ (mmol/g) = \frac{Peptide\ mmols}{Final\ resin\ weight}$$

Equation 7.3. Resin functionalization

7.2.4 Mini-acidolysis experiments

Mini-acidolysis experiment were performed generally by treating 20 mg of dry peptidyl resin with 200 μL of a deprotection cocktail (TFA/DCT/TAN/TIS/H$_2$O, 85:6:3:3:3) for 2h. After this amount of time, the supernatant was added to DEE (3 mL) to precipitate the peptide. The resulting suspension was centrifuged at 5,000 rpm for 1 min (Hettich EBA 12) and the supernatant was discarded. Three more DEE washes were performed by repeating this procedure before drying the peptide. Afterwards, 1 mg of the dried peptide was weighed and dissolved in 1 mL of ACN/H$_2$O 1:1 +1% TFA solution for posterior analysis by HPLC with a linear gradient 5-85%B in 20 min (A: H$_2$O+0.1%TFA; B: ACN+0.07%TFA).

7.3 Green Solid-Phase Peptide Synthesis

7.3.1 Synthesis of model peptides

Two different model peptides (MP1 and MP2) were synthesized from different polymeric supports using in all the cases Rink amide linker to obtain peptide amides. In all the model peptides, succinic acid was incorporated after the introduction of the Thr residue. To do that, succinic anhydride (2.5 eq) was dissolved in DMF and DIEA (5 eq) was added. The resulting mixture was added to the peptidyl resin and the reaction was left for minimum 1h. When the ninhydrin test was negative, we proceeded with the DMF washes (5x1 min) as in the general procedure (section 7.2.2).

7.3.1.1 Model peptide 1 (MP1)
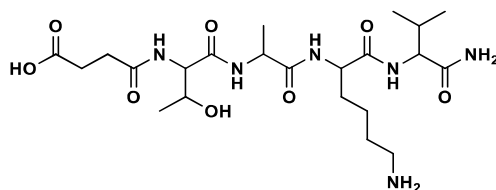
Figure 7.1 MP1 cleaved from the resin

HO-Succinic-Thr-Ala-Lys-Val-NH$_2$ (MP1) (Figure 7.1) was synthesized from three different resins: i) *p*-Methylbenzhydrylamine (*p*MBHA) resin (f = 1.2 mmol/g) based on PS; ii) ChemMatrix

(CM) resin (f = 1.0 mmol/g) based on PEG; and iii) TentaGel (TG) resin (f = 0.49 mmol/g) based on PS-PEG.

- **MP1-PS** was synthesized following the general synthesis procedure using 20.0 g of *p*MBHA resin (f_i = 1.2 mmol/g), Rink amide as the linker and Fmoc-Val-OH as the first amino acid. Final functionalization: 0.54 mmol/g. **HPLC:** 5-85%B in 20 min, t_R = 9.57 min. **MS:** calculated for $C_{22}H_{40}O_8N_6$: 516.6; found: 517.4 [M+H]$^+$.

- **MP1-CM** was synthesized following the general synthesis procedure using 5.0 g of CM resin (f_i = 1.0 mmol/g), Rink amide as the linker and Fmoc-Val-OH as the first amino acid. Final functionalization: 0.61 mmol/g. **HPLC:** 5-85%B in 20 min, t_R = 9.64 min. **MS:** calculated for $C_{22}H_{40}O_8N_6$: 516.6; found: 517.4 [M+H]$^+$.

- **MP1-TG** was synthesized following the general synthesis procedure using 5.0 of TG resin (f_i = 0.49 mmol/g), Rink amide as the linker and Fmoc-Val-OH as the first amino acid. Final functionalization: 0.34 mmol/g. **HPLC:** 5-85%B in 20 min, t_R = 9.63 min. **MS:** calculated for $C_{22}H_{40}O_8N_6$: 516.6; found: 517.4 [M+H]$^+$.

7.3.1.2 Model peptide 2 (MP2)
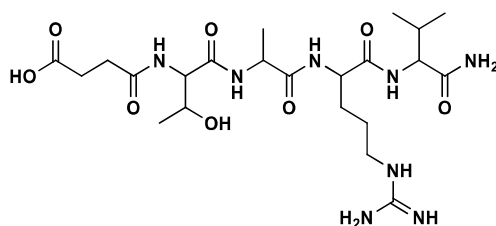
Figure 7.2 MP2 cleaved from the resin

HO-Succinic-Thr-Ala-Arg-Val-NH₂ (MP2) (Figure 7.2). **MP2-PS** was synthesized using 15.0 g of *p*MBHA resin (f_i = 1.1 mmol/g), Rink amide as the linker and Fmoc-Val-OH as the first amino acid. Final functionalization: 0.43 mmol/g. **HPLC:** 5-85%B in 20 min, t_R = 10.67 min. **MS:** calculated for $C_{22}H_{40}O_8N_8$: 544.6; found: 545.2 [M+H]$^+$.

7.3.2 Buffer preparation

Na₂CO₃/NaHCO₃ pH 9.7 (carbonate buffer): sodium carbonate (53.0 g) was weighed and dissolved in Milli-Q water (200 mL, 2.5M). Sodium bicarbonate (16.8 g) was weighed and dissolved in Milli-Q water (200 mL, 1M). The buffer was prepared by mixing Na₂CO₃ 2.5M (24 mL), NaHCO₃ 1.0M (80 mL) and Milli-Q water (96 mL). The pH of the buffer was 9.7 as measured with the pH-meter.

NaH₂PO₄/Na₂HPO₄ pH 8.7 (phosphate buffer): sodium dihydrogen phosphate monohydrate (31.0 g) was weighed and dissolved in Milli-Q water (150 mL, 1.5M). Disodium hydrogen phosphate (40.0 g) was weighed and dissolved in Milli-Q water (150 mL, 1.5M). The buffer was

prepared by mixing NaH_2PO_4 1.5M (5 mL), Na2HPO4 1.5M (50 mL) and Milli-Q water (45 mL). The pH of the buffer was 8.7 as measured with the pH-meter.

7.3.3 Green SPPS Experiments

All the experiments related to Green Solid-Phase Peptide Synthesis (G-SPPS) in the present doctoral thesis were performed using polypropylene syringes with a polyethylene filter connected to a vacuum pump. Reagents and solvents were introduced inside the syringe or the reaction vessel, which contained the resin. After the appropriate amount of time, the solvent, excess of reagents and reaction byproducts were eliminated by filtration. Each experiment will be presented with this code "EX-YYi": "X" and "YY" refer to the lab book and the page where the experiment was noted being "i" the number of the experiment. Example: E1-65ii refers to the second experiment noted in the page 65 of the 1st lab book.

7.3.3.1 Mini-acidolysis and HPLC analysis
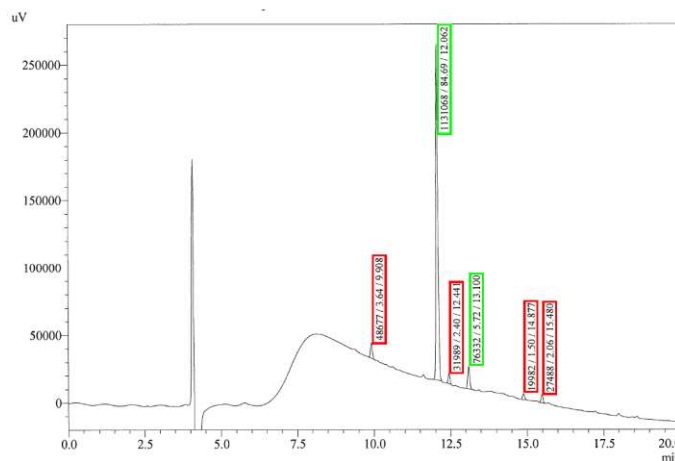
Figure 7.3 E3-34iii activation: accepted peaks (in green) and rejected peaks (in red)

After each experiment, reaction controls were performed doing mini-acidolysis experiments as described in section 7.2.4. Apart from the general deprotection cocktail (TFA/DCT/TAN/TIS/H$_2$O 85:6:3:3:3), other simpler cocktails such as TFA:TIS:H$_2$O 95:2.5:2.5 were also used. Afterwards, 1 mg of the dried peptide was weighed and dissolved in 1 mL ACN/ H$_2$O 1:1 +1% TFA solution for posterior analysis by HPLC.

Peptide samples were analyzed by the linear gradient 5-85% in 20 min (A: H$_2$O+0.1%TFA; B: ACN+0.07%TFA). General integration procedure: i) all the peaks of the chromatogram were integrated; ii) the 5% of the area of the principal peak was calculated (*e.g.* 5% of 1,131,068 is 56,553); iii) all the peaks with an area below the previous 5% were rejected (*e.g.* rejected peaks t$_R$ = 9.9, 12.4, 14.9, 15.5 min); iv) the new percentage values of the peaks left were calculated (*e.g.* t$_R$ = 12.1 min (93.7%), t$_R$ = 13.1 min (6.3%)) (Figure 7.3).

7.3.3.2 Experimental procedures
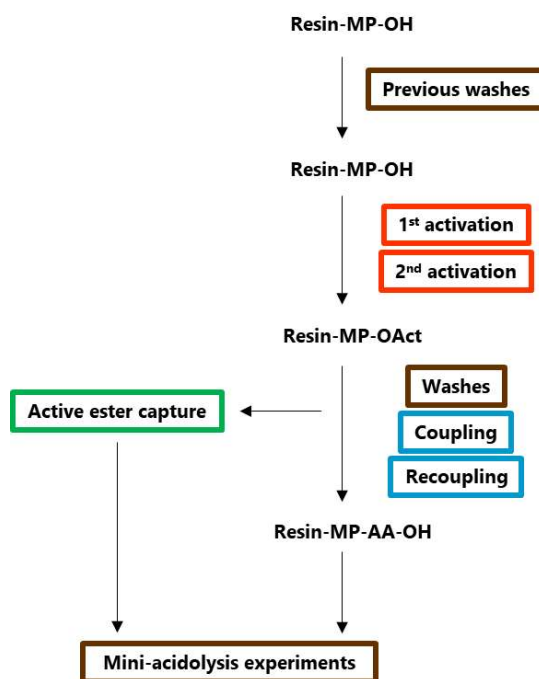
Figure 7.4 General experimental procedure

General experimental procedure (Figure 7.4). The peptidyl resin was weighed in the corresponding polypropylene syringe. Although 0.2 g of peptidyl resin was the standard quantity used in most of the experiments, some of them were performed in gram-scale using 1.0 or 2.0 g. The resin was swelled with the solvent that will be used in the activation (usually 5x1min + 1x10min). The activation was performed by adding the reagents dissolved in the proper solvent. Depending on the activators, one or two activation cycles were performed. Once the *C*-terminus is activated, the resin is washed with the solvent used in the activation (5x1min). Then, in some of the experiments a small portion of the peptidyl resin was taken out to capture the active ester with piperidine. The resin was washed again to condition it for the aqueous coupling: depending on the miscibility of the activation solvent in H_2O, some transition washes were performed. For example, if the activation solvent was DCM, apart from this solvent, the resin was washed with DMF or DMSO that are water-miscible solvents. After the H_2O washes, the coupling was performed by adding the reagents dissolved in the proper aqueous conditions. Normally, the coupling reactions were performed overnight (14-24h). After the coupling, the resin was washed with H_2O (5x1min), DMF or DMSO (5x1min), DCM (5x1min), DEE (5x1min), and the resin was dried under vacuum. Finally, mini-acidolysis experiments were conducted following the general procedure (section 7.2.4) to analyze the results by HPLC or HPLC-MS.

Active ester capture with piperidine. A small portion of peptidyl resin was treated with a 5% solution of piperidine in the appropriate solvent for minimum 30 min. Afterwards, the peptidyl resin was washed with the same solvent (5x1min), DCM (5x1min), DEE (5x1min) and the resin was

dried under vacuum. Mini-acidolysis experiment was conducted to analyze the activation results by HPLC or HPLC-MS.

7.3.3.2.1   Experimental procedure of E3-10i
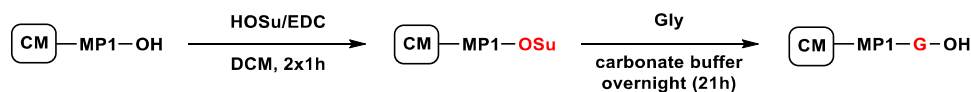
Figure 7.5 General scheme of E3-10i

MP1-CM (0.2g, f = 0.61 mmol/g) was weighed in a polypropylene syringe and was washed with DCM (5x1min) and swelled in the same solvent (1x10min). HOSu (3.0 eq, 0.37 mmol, 43 mg) and EDC (3.0 eq, 0.37 mmol, 71 mg) were weighed and dissolved in DCM (2 mL). The resulting solution was introduced in the syringe and was left for 1h. This activation procedure was repeated once more. The resin was washed with DCM (5x1min) and DMSO (5x1min). A small portion of the resin was taken out and treated with 5% piperidine in DMSO (1x30min) to capture the active ester. The rest of the peptidyl resin was washed with H_2O (5x1min). Gly (5.0 eq, 0.61 mmol, 47 mg) was weighed and dissolved in carbonate buffer (2 mL). This solution was introduced inside the syringe and the reaction was left overnight (21h). After that amount of time, the resin was washed with H_2O (5x1min), DMSO (5x1min), 5% piperidine in DMSO (1x30min). Finally, the resin was washed with DMSO (5x1min), DCM (5x1min), DEE (5x1min) and was dried under vacuum for 15 min. Mini-acidolysis experiments of the resin was performed, as well as the previous active ester sample.

7.3.3.2.2   Experimental procedure of E3-27ii
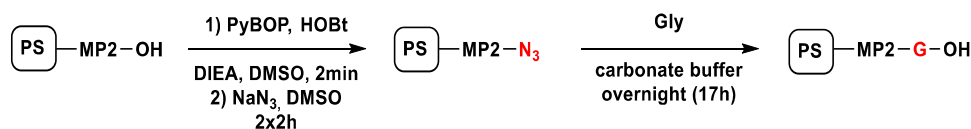
Figure 7.6 General scheme of E3-27ii

MP2-PS (0.2 g, f = 0.43 mmol/g) was weighed in a syringe and was washed with DMSO (5x1 min) and swelled in the same solvent (1x20min). NaN_3 (6.0 eq, 0.52 mmol, 34 mg)) was weighed separately from PyBOP (3.0 eq, 0.26 mmol 14 mg) and HOBt (6.0 eq, 0.52 mmol, 80 mg), and were dissolved in DMSO (2 mL and 1 mL). PyBOP/HOBt solution was added to the syringe and DIEA (6.0 eq, 0.52 mmol, 91 µL) was also added. The preactivation was left for 2 min. Then, the NaN_3 solution was added and the reaction was left for 2h. This activation procedure was repeated once more. The resin was washed with DMSO (5x1min). A small portion of the resin was taken out and was treated with 5% piperidine in DMSO (1x30min) to capture the azide. The rest of the peptidyl resin was washed with H_2O (5x1min). Gly (5.0 eq, 0.43 mmol, 33 mg) was dissolved in carbonate buffer (1.5 mL) and was introduced inside the syringe. The reaction was left overnight (17h). After that amount of time, the resin was washed with H_2O (5x1min), DMSO (5x1min), 5% piperidine in DMSO (1x30min). Finally, the resin was washed with DMSO (5x1min), DCM (5x1min),

DEE (5x1min) and was dried under vacuum for 15 min. Mini-acidolysis experiments of the resin was performed, as well as the previous active ester sample.

7.3.3.2.3 Experimental procedure of E3-31ii
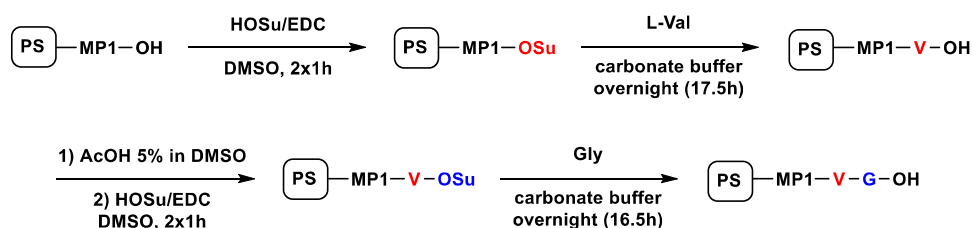
Figure 7.7 General scheme of E3-31ii

MP1-PS (0.4 g, f = 0.43 mmol/g) was weighed in a syringe and was washed with DMSO (5x1min) and swelled in the same solvent (1x20 min). HOSu (3.0 eq, 0.52 mmol, 60 mg) and EDC (3.0 eq, 0.52 mmol, 100 mg) were dissolved in DMSO (1.5 mL) and were added to the syringe. The reaction was left for 1h and this activation procedure was repeated once more. The peptidyl resin was washed with DMSO (5x1min). A small portion of the resin was taken out and was treated with 5% piperidine in DMSO (1x30min) to capture the active ester. The rest of the resin was washed with H_2O (5x1min). L-Val (5.0 eq, 0.87 mmol, 101 mg) was dissolved in carbonate buffer (3 mL) and was introduced inside the syringe. The reaction was left overnight (17.5h) and a recoupling was performed using the same amounts of L-Val and carbonate buffer. The reaction was left for 4.5h. The resin was washed with H_2O (5x1min) and DMSO (5x1min). A small portion of the resin was taken out and was treated with 5% piperidine in DMSO (1x30min). The rest of the peptidyl resin was washed with 5% AcOH in DMSO (5x1min) and DMSO (5x1min). HOSu (3.0 eq, 0.52 mmol, 60 mg) and EDC (3.0 eq, 0.52 mmol, 100 mg) were dissolved in DMSO (1.5 mL) and were introduced in the syringe. The reaction was left for 1h and this activation procedure was repeated once more. The peptidyl resin was washed with DMSO (5x1min). A small portion of the resin was taken out and was treated with 5% piperidine in DMSO (1x30min) to capture the active ester. The rest of the peptidyl resin was washed with H_2O (5x1min). Gly (5.0 eq, 0.87 mmol, 66 mg) was dissolved in carbonate buffer (2 mL) and was introduced inside the syringe. The reaction was left overnight (16.5h). The resin was washed with H_2O (5x1min), DMSO (5x1min), 5% piperidine in DMSO (1x30min), DMSO (5x1min), DCM (5x1min), DEE (5x1min) and was dried under vacuum for 15 min. Mini-acidolysis experiments of the resin, activation and coupling samples were performed.

7.3.3.2.4 Experimental procedure of E3-41iv
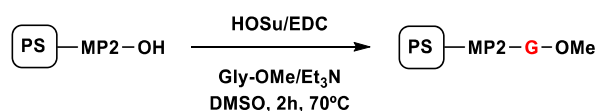
Figure 7.8 General scheme of E3-41iv

MP2-PS (0.2 g, f = 0.43 mmol/g) was weighed in a syringe and was washed with DMSO (5x1min) and swelled in the same solvent (1x20min). After that amount of time, the peptidyl resin was transferred to an amino acid hydrolysis glass tube. HOSu (3.0 eq, 0.26 mmol, 30 mg), EDC (3.0 eq, 0.26, 50 mg) and Gly-OMe (5.0 eq, 0.43 mmol, 39 mg) were dissolved in DMSO (1.5 mL) and added to the syringe. Et₃N (10.0 eq, 0.87 mmol, 120 µL) was introduced and the resulting mixture was manually stirred for some seconds. The glass tube was closed and was heat at 70ºC on a block heater. The reaction was left for 2h. Afterwards, the resin was transferred back to a syringe and washed with DMSO (5x1min), 5% piperidine in DMSO (1x30min), DMSO (5x1min), DCM (5x1min), DEE (5x1min) and was dried under vacuum for 15 min. Mini-acidolysis experiments of the resin was performed.

7.3.3.2.5 Experimental procedure of E3-60ii
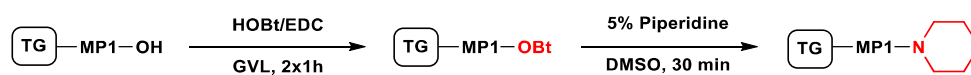
Figure 7.9 General scheme of E3-60ii

MP1-TG (0.1 g, f = 0.34 mmol/g) was weighed in a syringe and was washed with GVL (5x1min) and swelled in the same solvent (1x30 min). HOBt (3.0 eq, 0.10 mmol, 16 mg) and EDC (3.0 eq, 0.10 mmol, 19 mg) were dissolved in GVL (1 mL). The resulting solution was introduced in the syringe and was left for 1h. This activation procedure was repeated once more. The resin was washed with GVL (5x1min), DMSO (5x1min) and 5% piperidine in DMSO (1x30min). Finally, the resin was washed with DMSO (5x1min), DCM (5x1min), DEE (5x1min) and was dried under vacuum for 15 min. Mini-acidolysis experiments of the resin was performed.

7.3.3.2.6 Experimental procedure of E3-65iv
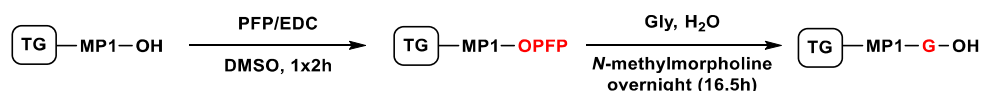
Figure 7.10 General scheme of E3-65iv

MP1-TG (0.1 g, f = 0.34 mmol/g) was weighed in a syringe, was washed with DMSO (5x1min) and swelled in the same solvent (1x30 min). PFP (3.0 eq, 0.10 mmol, 19 mg) and EDC (3.0 eq, 0.10 mmol, 19 mg) were dissolved in DMSO (1 mL). The resulting solution was introduced in the syringe and was left for 2h. The resin was washed with DMSO (5x1min) and H₂O (5x1min). Gly (5.0 eq, 0.17 mmol, 13 mg) was weighed and dissolved in H₂O (0.75 mL). NMM (10.0 eq, 0.34 mmol, 37 µL) was added and the resulting solution was introduced in the syringe. The reaction

was left overnight (16.5h). After that amount of time, the resin was washed with H_2O (5x1min), DMSO (5x1min), 5% piperidine in DMSO (1x30min). Finally, the resin was washed with DMSO (5x1min), DCM (5x1min), DEE (5x1min) and was dried under vacuum for 15 min. Mini-acidolysis experiments of the resin was performed.

7.3.3.2.7   Experimental procedure of E3-69ii
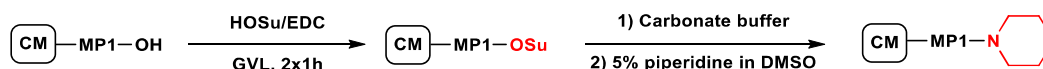
Figure 7.11 General scheme of E3-69ii

MP1-CM (0.30 g, f = 0.62 mmol/g) was weighed in a syringe and was washed with GVL (5x1min) and swelled in the same solvent (1x30min). HOSu (3.0 eq, 0.55 mmol, 64 mg) and EDC (3.0 eq, 0.55 mmol, 106 mg) were dissolved in GVL (2 mL). The resulting solution was introduced in the syringe and was left for 1h. This activation procedure was repeated once more. The resin was washed with GVL (5x1min) and H_2O (5x1min). Carbonate buffer pH 9.5-10 was introduced in the syringe. Immediately after, a small portion of the resin (t_{0h}) was taken out, was washed with H_2O (5x1min) and DMSO (5x1min) and was treated with 5% piperidine in DMSO (1x30min). Small portions of the resin were taken at 1h (t_{1h}), 3h (t_{3h}), 5h (t_{5h}) and 21.5h ($t_{21.5h}$) and were treated as the t_{0h} sample. After the piperidine treatment, the samples were washed with DMSO (5x1min), DCM (5x1min), DEE (5x1min) and were dried under vacuum for 15 min. Mini-acidolysis experiments of the samples were performed.

7.3.3.2.8   Experimental procedure of E3-80i
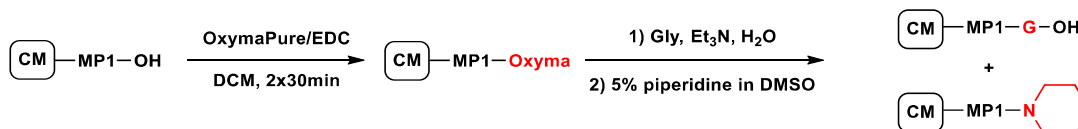
Figure 7.12 General scheme of E3-80i

MP1-CM (0.25 g, f = 0.62 mmol/g) was weighed in a syringe and was washed with DCM (5x1min) and swelled in the same solvent (1x30min). OxymaPure (3.0 eq, 0.46 mmol, 66 mg) and EDC (3.0 eq, 0.46 mmol, 89 mg) were dissolved in DCM (2 mL). The resulting solution was introduced in the syringe and was left for 30 min. This activation procedure was repeated once more. The resin was washed with DCM (5x1min) and DMSO (5x1min). A small portion of the resin was taken out and treated with 5% piperidine in DMSO (1x30min). The rest of the resin was washed with H_2O (5x1min). Gly (5.0 eq, 0.92 mmol, 70 mg) was weighed and dissolved in H_2O (3 mL). This solution was introduced inside the syringe and Et_3N (10.0 eq, 1.84 mmol, 258 μL) was added. Immediately after, a small portion of the resin (t_{0h}) was washed with H_2O (5x1min), DMSO (5x1min) and was treated with 5% piperidine in DMSO (1x30 min). Small portions of the resin were taken at 1h (t_{1h}), 3h (t_{3h}), 5h (t_{5h}) and 21.5h ($t_{21.5h}$) and were treated as the t_{0h} sample. After the piperidine

treatment, the samples were washed with DMSO (5x1min), DCM (5x1min), DEE (5x1min) and were dried under vacuum for 15 min. Mini-acidolysis experiments of the samples were performed.

7.4 Green solvent-mediated Peptide Acidolysis

██

██

████████████████████████████████████

7.4.1 Green solvent reactors
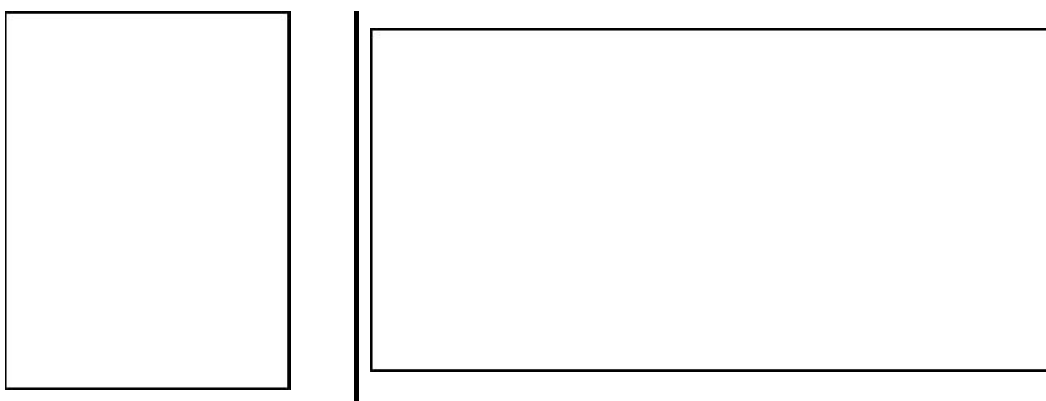
Figure 7.13 ██ *reactor (left) and schematic representation (right)*

All the reactors used to perform green solvent acidolysis experiments are ████████████████

██

██ .
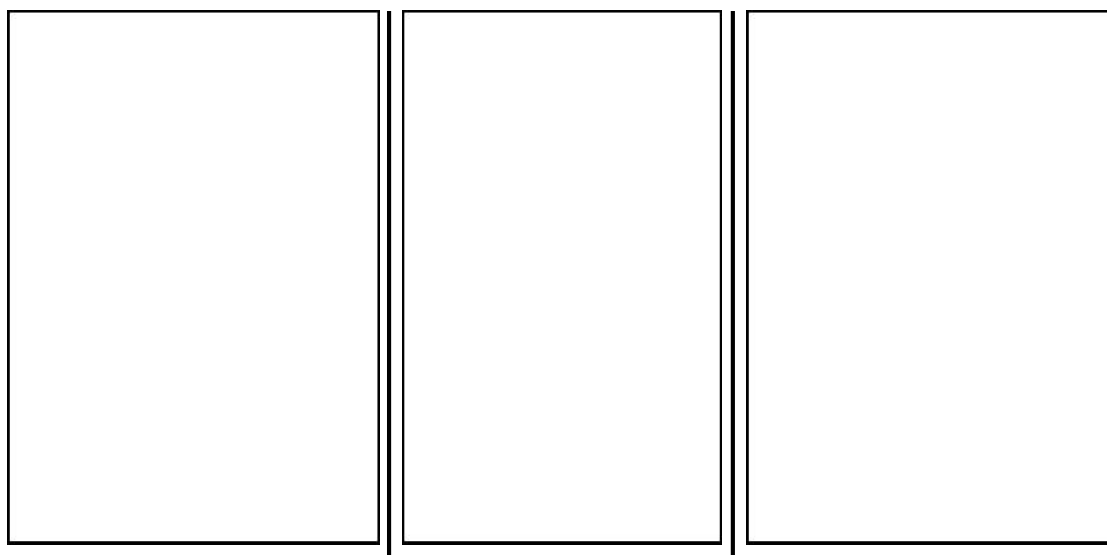
Figure 7.14 ██████ *(left),* ██████ *(right) and schematic representation of both reactors (middle)*

██████████ was the only reactor which permitted to observe what was happening inside of it while the experiment was being carried out thanks to a spy-hole made of sapphire (Figure 7.13).

██

██
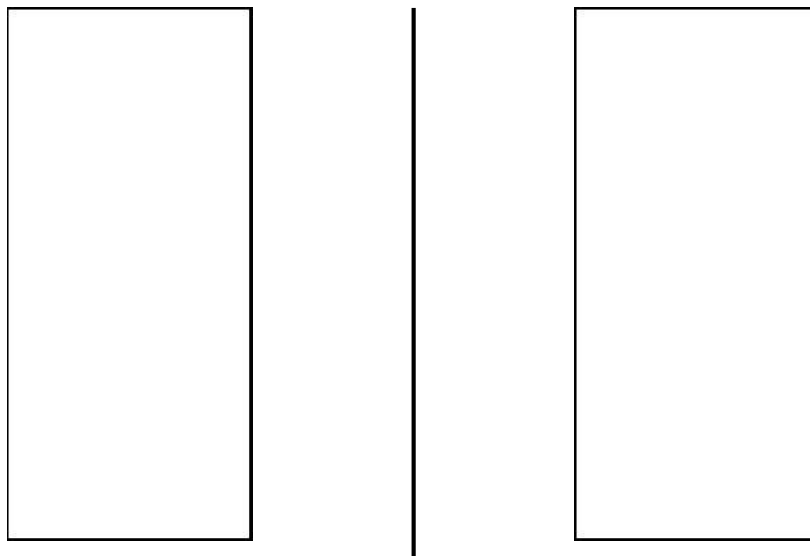
Figure 7.15 ██ *(left) and schematic representation (right)*

████████████████████████████████████ reactors were very similar between each other and consisted in cells of different volume that can be opened ██████████████████████████ for the experiment. ██ ████████████████████████████████████. ████████████████ have to entrances for ██ and N_2, as well as one exit to ████████████ the reactor. ████████████████████ ████████████████████████████████████. Due to the similarities between them, both reactors were represented with the same scheme (Figure 7.14).

██████████████ was the only homemade reactor ████████████████████████. Due to its small volume, it was not possible to have any controlled systems ██████████████████████████. ████ had only one entrance for ██ and the corresponding exit to ████████████ the reactor. The addition of ████████████████████████████████ to achieve a final volume of (Figure 7.15).

7.4.2 Synthesis of model peptides

7.4.2.1 ACMP1-CTC

ACMP1-CTC (Figure 7.16) was synthesized using 10.0 g of CTC resin (f = 1.6 mmol/g) and Fmoc-Leu-OH as the first amino acid. Final functionalization: 0.46 mmol/g. **HPLC:** 20-100%B in 20 min, t_R = 10.2 min. **MS:** calculated for $C_{51}H_{87}O_{12}N_{13}$: 1074.3; found: 1074.9 $[M+H]^+$.
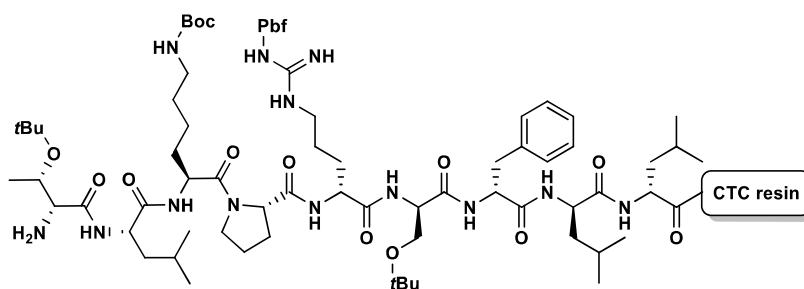
Figure 7.16 ACMP1-CTC model peptide

7.4.2.2 ACMP2-*p*MBHA

ACMP2-RAM-*p*MBHA (Figure 7.17) was synthesized using 1.0 g of *p*MBHA resin (f = 1.2 mmol/g) that was washed with DCM (3x10min) and DMF (3x1min) inside a 20 mL polypropylene syringe equipped with a polyethylene filter and connected to a vacuum pump. Then, Fmoc-Rink amide (1.5 eq) and HOBt (2.0 eq) were dissolved in the minimum amount of DMF. DIPCDI (2.0 eq) was added and the resulting mixture was stirred for 30 seconds. Next, this solution was introduced in the reaction vessel with the resin and the reaction was left for 2h. The ninhydrin test was performed to monitor the amino acid coupling. When the ninhydrin test was negative, DMF washes (5x1 min) were performed and the resin was transferred to the reaction vessel of a Liberty CEM peptide synthesizer that was used to finish the synthesis. Fmoc deprotection was carried out using 20% piperidine in DMF (2x10 min) at RT. Fmoc-amino acids (3.0 eq) were coupled in DMF using DIPCDI (3.0 eq) and HOBt (3.0 eq) as the activating system (2x1h) at RT. Final functionalization: 0.35 mmol/g.
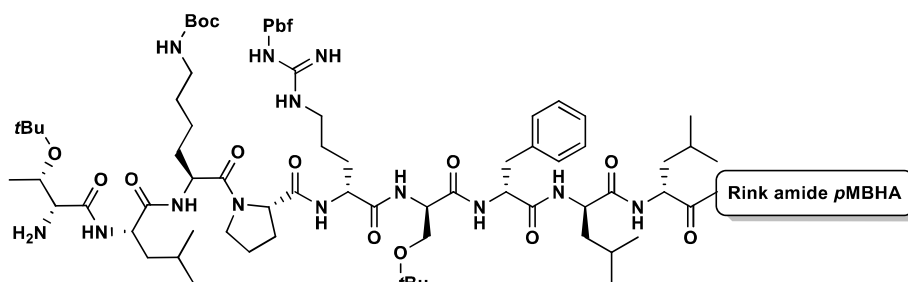
Figure 7.17 ACMP2-pMBHA model peptide

7.4.2.3 Somatostatin-CTC

SST-CTC (15.0 g) was kindly provided by the Production department of BCN Peptides from a GMP batch of SST which are routinely synthesized by the company (Figure 7.18). This batch of SST-CTC was synthesized using CTC resin (f_i = 1.6 mmol/g) and Fmoc-Cys(Trt)-OH as the first amino acid. Final functionalization: 0.31 mmol/g. **HPLC:** 5-85%B in 20 min, t_R = 14.4 min. **MS:** calculated for $C_{76}H_{104}O_{19}N_{18}S_2$: 1639.9; found: 820.8 $[M+2H]^{2+}$.
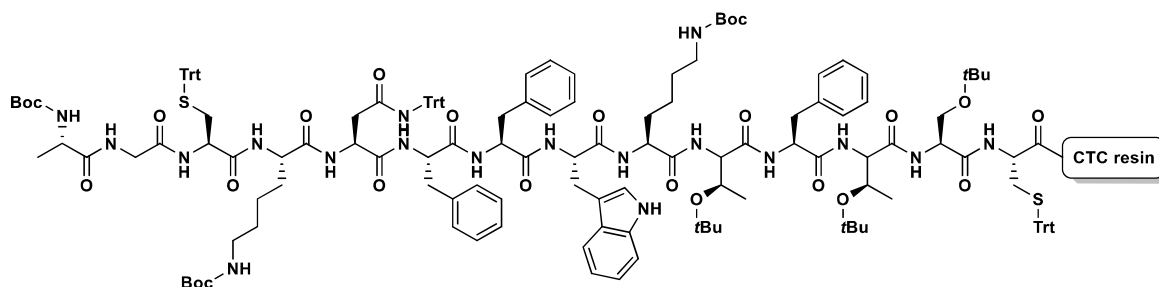
Figure 7.18 Somatostatin-CTC

7.4.2.4 Leuprolide-CTC

LP-CTC was synthesized using 8.0 g of CTC resin (f = 1.6 mmol/g) and Fmoc-Pro-OH as the first amino acid (Figure 7.19). Final functionalization: 0.38 mmol/g. **HPLC:** 20-100%B in 20 min, t_R = 10.6 min. **MS:** calculated for $C_{57}H_{79}O_{13}N_{15}$: 1182.4; found: 1182.8 [M+H]$^+$.
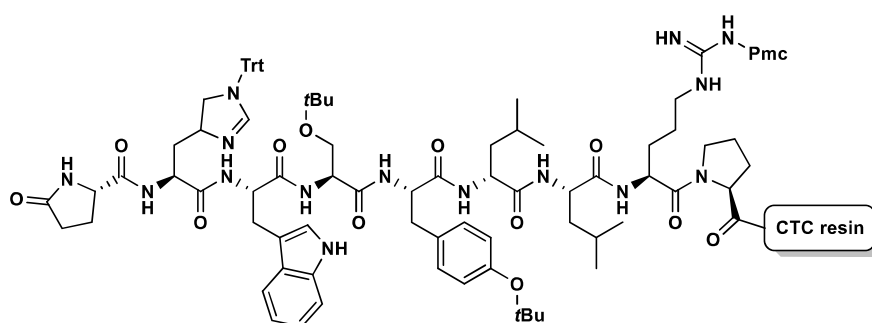
Figure 7.19 Leuprolide-CTC

7.4.3 Treatment of peptide fractions

After each experiment, ▮▮

▮▮▮▮▮▮▮▮▮▮. Both the filtrate ▮▮▮▮▮▮▮▮▮▮▮▮▮▮▮▮▮▮▮▮▮▮▮ fraction were frozen with a dry ice/acetone bath and lyophilized for minimum 12h. The treated peptidyl resin was also dried under vacuum for minimum 12h. ▮▮▮▮▮▮▮▮▮▮▮▮▮▮▮▮▮▮▮▮▮▮▮▮▮▮▮▮▮▮▮▮

▮▮

▮▮

▮▮▮▮▮▮▮▮▮▮▮▮▮▮▮▮▮▮▮▮▮▮▮▮▮▮▮. 1 mg of each peptide fraction was weighed, dissolved in ▮▮▮▮▮▮▮▮ and was analyzed by HPLC or HPLC-MS using the gradient method 20-100%B in 20 min (A: H_2O+0.1%TFA; B: ACN+0.07%TFA). Occasionally the gradient method 40-100%B in 20 min was also used to analyze protected peptides. ▮▮▮▮▮▮▮▮▮▮▮▮▮▮

▮▮

7.4.4 Global cleavage/deprotection

7.4.4.1 Standard procedures

Small-scale experiments (██████████████████) were performed by treating the appropriate amount of dry peptidyl resin with the corresponding quantity████████████████ for the proper amount of time while stirring.

- In the case the deprotection cocktail was ███████████, the supernatant was added to DEE (████████████████████████████████) and the resulting suspension was centrifuged at 5,000 rpm for 1 min (Hettich EBA 12). ██████████████████ ████████████████████████████████ █████. Finally, 1 mg of the dried peptide was weighed and dissolved in 1 mL ACN/ H_2O 1:1 +5% AcOH solution for posterior analysis by HPLC.
- In the case the deprotection cocktail was based ████████ the resin suspension was filtered and the filtrate was frozen in a dry ice/ acetone bath before lyophilization. Finally, 1 mg of the dried peptide was weighed and dissolved in 1 mL ACN/ H_2O 1:1 +5% AcOH solution for posterior analysis by HPLC.

Mini-acidolysis experiments were performed as described in section 7.2.4. 1 mg of the dried peptide was weighed and dissolved in 1 mL ACN/ H_2O 1:1 +5% AcOH solution for posterior analysis by HPLC.

7.4.4.2 Green solvent procedures: first and second series

In this section, a sample of the most relevant experiments carried out with ██████████ and ████ ████ in various reactors will be described in detail.

5th session, Experiment 1. ████ was opened and ████████ ACMP1-CTC were introduced, ████ ████████████████████ (Figure 7.20). Immediately, the reactor was closed and █████████ was introduced into the reactor ████████████████████. After the reactor was totally filled (██████████) the entrance ████ was closed and it was ██████████████████████ ████. When it was sure that the █████████████████████, we began to stir the contents of the reactor. Due to the solubilization ████████████, the █████████ fell rapidly. Therefore, more ████ was introduced in the reactor by opening the entrance ████. The final ████ conditions were █████████████. The experiment was left ███████████. Then, the exit tube of the reactor was submerged in a 1L bottle containing ███████████████. In addition, the exit tube was heat with an ██ ████████████████████████████████. Under these conditions, the reactor was slowly █████████ by opening the exit ████. The ███████████ of the reactor was completed

████. Without opening the reactor, more ████████ was added through another entrance. After closing it again, more ████ was introduced in the reactor, to stir it for ██████. After that amount of time, the reactor was ████████ again under the same conditions as before. The previous ██████ mixture was considered as ████████. Finally, the reactor was opened and the treated peptidyl resin was recovered ████████████████████ ██████████.
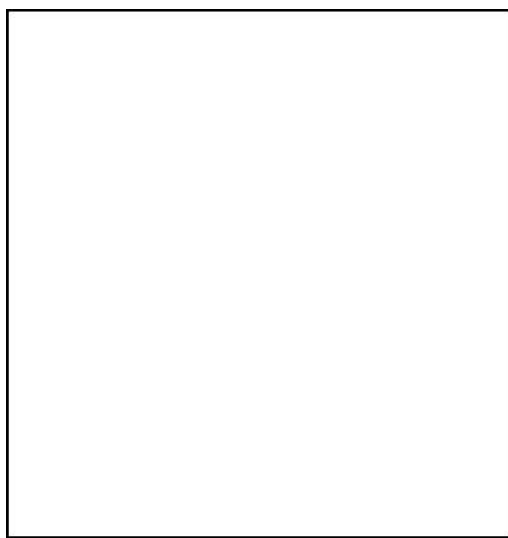
Figure 7.20 Scheme of 5th session, Experiment 1
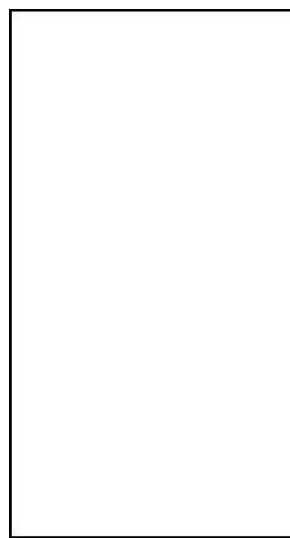
Figure 7.21 Scheme of 6th session, Experiment 1

6th session, Experiment 1. ████ was opened and ████ of ACMP1-CTC were introduced, as well as ████████████ (Figure 7.21). Immediately, the reactor was closed and ████████ was introduced into the reactor by opening the entrance ████ . After the reactor was totally filled (████████), the experiment was left for ██. Then, the ██ tube of the reactor was submerged in a 0.5 L bottle containing ████████████. In addition, the ██ tube was heat with an electrical resistance and ██████████ were used to avoid the formation of any peptide blockages in the exit tube due to the expansion of ███. Under these conditions, the reactor was slowly ██████████ by opening the exit ████. The ████████████ was completed in ████. Afterwards, more ████████ was introduced into the reactor. The reactor was ████████ again to obtain the ██fraction. Finally, the reactor was opened and the treated peptidyl resin was recovered using ████████ which was collected as the████████ fraction.

7.4.4.3 Green solvent procedures: third series

12th session, Experiment 1. ████ was opened and ████████ ACMP1-CTC inside a glass vial were introduced (Figure 7.22). A magnetic stirrer and ████████████ were also introduced inside the glass vial. Immediately, the reactor was closed and ██████████ was introduced into the reactor by opening the entrance ████. After the reactor was totally filled (████████), the stirring was turned on but the magnetic stirrer could not move the ████████████████ mixture. After 5 min,

████████ dissolved ██████ permitting the stirring of the ████████████ mixture. The stirring was set at ████████ and the experiment was left for ██. After that amount of time, the reactor was slowly ████████████. ██████████, some ████████████ coming out the ████████████ were observed. ████████, the ████████████████████████ to half of the glass vial. After the ████████████ was completed, the reactor was opened and the glass vial that contained the ████████████ solid mixture was introduced inside ████████████████████. The peptidyl resin ████████████ ████████████ was considered as the ████████ fraction[78].
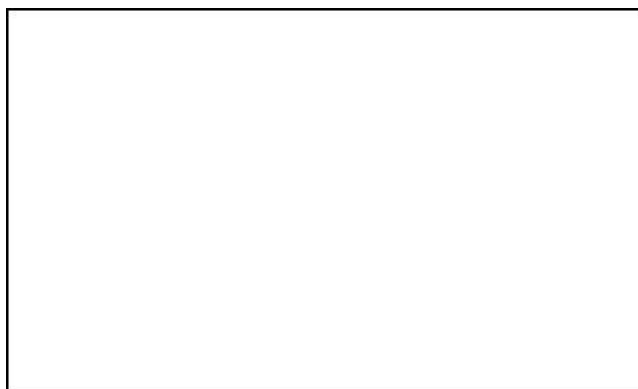
Figure 7.22 Scheme of 12th session, Experiment 1

7.4.5 Cleavage of protected peptides

7.4.5.1 Green solvent procedures: final series

18th session, Experiment 1. ██████ was opened and ████████ LP-CTC was introduced (Figure 7.23). The reactor was closed and ██████████ was introduced into the reactor ████████████████████ ████████████ (Figure 7.23). After the reactor was filled (████████████), ████████████████████ were closed. Then, ████████████████████████████████████ ██████ was introduced inside the ████████ tube using a syringe and a needle. Immediately after the joint was closed again and ████████████████████████████. The ████████ tube was ████████████ with ████████ (████████████) and ████████████████████ were opened consecutively to introduce the cocktail into the reactor. Once the reactor was filled, both entrance ██████ were closed and the experiment was left ██████. Then, ██████ tube of the reactor was submerged in a 0.5 L bottle containing ████████████████████. The reactor was ████████████ by opening the exit ██████. The ████████████ of the reactor was completed in ████████. ████████████ solution was considered as the exit fraction. Finally, the reactor was opened and the treated peptidyl resin was recovered using ████████████████ which was collected ████████████ fraction.

---

[78] In this experiment, ████████████ was obtained.
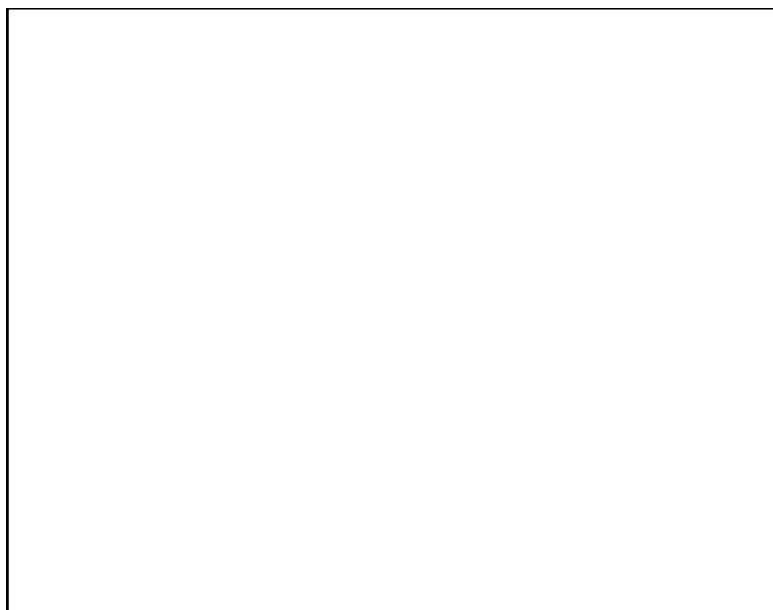
Figure 7.23 Scheme of 18th session, Experiment 1

7.4.6 LP global deprotection in solution and purification

The elimination of the sidechain protecting groups was performed through the acidolysis in solution between the ████████████████████████ ██ ██ ██ ████████████████████ (███████ in total) and a ██████████ (██████████████████████████████████) for ██ at RT. After this time, the acidic solution was poured over ████████████████████████ previously cooled to -10ºC using a dry ice/acetone bath and contained in two 50 mL falcons. Both falcons were centrifuged at 5,000 rpm for 1 min (Hettich EBA 12) and ██████████████████ ████████. After this first wash, ████████████ used to transfer all the peptide crude to only one of the falcons. Then, the resulting suspension was centrifuged once more and ██████████████ ████████████. Afterwards, ████████████ washes were performed. After the last wash, the wet solid obtained was dried under vacuum for minimum 12h. ████████████████████

████████████████████████████

The crude of leuprolide was purified using preparative LC (A: H_2O+0.02%TFA; B: ACN) to obtain the desired purity grade (>99.5%). To do that, the crude was weighed and dissolved in aqueous AcOH 20% (60 mL). Then, the crude solution was filtered with 0.45 μm PVDF filter and injected to the column (MK9, flux 55 mL/min, 20 mL per injection) for its purification using 25%B in 30 min. Column fractions were collected in various crystal tubes and were analyzed by HPLC through 20 μL co-injections of various of the column fractions. When the desired combination of fractions was obtained (purity of the principal peak had to be >99.5%), the selected tubes were joined in a

---

[79] **HPLC:** 20-100%B in 20 min +100%B in 10 min, t_R = 10.6 min; 28%B in 30 min, t_R = 14.6 min (A: H_2O+0.1%TFA; B: ACN+0.07%TFA)

2L round-bottomed flask. Finally, the pure peptide solution was frozen with a dry ice/acetone bath and was lyophilized to obtain pure LP (Figure 7.24).
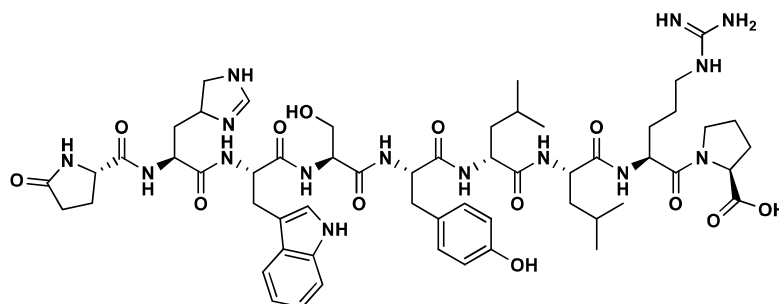
Figure 7.24 Leuprolide structure

LP (H-Pyr[1]-His[2]-Trp[3]-Ser[4]-Tyr[5]-D-Leu[6]-Leu[7]-Arg[8]-Pro[9]-NH2). Protected LP was obtained initially from ▮▮▮▮▮▮▮▮▮▮ ▮▮ ▮▮ ▮▮▮▮▮ . The acidolysis of protected LP was carried out using only▮▮▮▮▮▮▮▮▮▮▮▮ ▮▮▮▮▮▮▮▮ . Peptide crude was purified by preparative LC obtaining ▮▮▮▮ ▮▮▮ ▮▮ . **HPLC:** 5-85%B in 20 min, t_R = 14.3 min; 20-100%B in 20 min, t_R = 10.6 min; 28%B in 30 min, t_R = 14.5 min (A: H_2O+0.1%TFA; B: ACN+0.07%TFA). **HRMS:** calculated for $C_{57}H_{79}O_{13}N_{15}$: 1181.5982; found: 1182.6055 $[M+H]^+$.

7.5 Synthesis of Somatostatin Analogs

All somatostatin analogs (SSAs) in the doctoral thesis were synthesized by manual Fmoc/*t*Bu SPPS. Peptide syntheses were performed by using a reaction vessel with a pore filter plate, both connected to a vacuum pump. Reagents and solvents were introduced inside the reaction vessel, which contained the resin. After the reaction was completed, the solvent, excess of reagents and reaction byproducts were eliminated by filtration.

Ninhydrin test was used to determine qualitatively the presence of primary amines in the peptidyl resin, which was used to control the coupling steps throughout the peptide synthesis.

Fmoc-Msa-OH was previously synthesized in the Riera Lab by Dr. Anna Escolà.

7.5.1 Development of Somatostatin Analogs

7.5.1.1 Solid-Phase peptide synthesis

Analogs **A74-A82** were synthesized following standard Fmoc/*t*Bu SPPS procedures as described in section 7.2.3. Resin functionalization should be between 0.9 and 1.4 mmol/g.

H₂N — Lys(Boc)^9-Thr(tBu)^{10}-Phe^{11}-Thr(tBu)^{12}-Ser(tBu)^{13}-D-Cys(Trt)^{14}

Fmoc-Trp-OH coupling   Fmoc-D-Trp-OH coupling

Fmoc-Trp^8-Lys(Boc)^9-Thr(tBu)^{10}-Phe^{11}-Thr(tBu)^{12}-Ser(tBu)^{13}-D-Cys(Trt)^{14}

Fmoc-D-Trp^8-Lys(Boc)^9-Thr(tBu)^{10}-Phe^{11}-Thr(tBu)^{12}-Ser(tBu)^{13}-D-Cys(Trt)^{14}

A76

Lys(Boc)^9-Thr(tBu)^{10}-Phe^{11}-Thr(tBu)^{12}-Ser(tBu)^{13}-D-Cys(Trt)^{14}

Trp^8-Phe^7-Phe^6-Asn(Trt)^5-Lys(Boc)^4-D-Cys(Trt)^3-Gly^2-D-Ala^1-Boc

A77

Lys(Boc)^9-Thr(tBu)^{10}-Phe^{11}-Thr(tBu)^{12}-Ser(tBu)^{13}-D-Cys(Trt)^{14}

D-Trp^8-Phe^7-Phe^6-Asn(Trt)^5-Lys(Boc)^4-D-Cys(Trt)^3-Gly^2-D-Ala^1-Boc

Figure 7.25 Parallel synthesis of A76 and A77

To take advantage of their structural similarity, each pair of peptides **A76**-**A77**, **A78**-**A79** and **A80**-**A81** were synthesized in parallel. As an example, **A76** and **A77** were synthesized from an initial quantity of 5.0 g of CTC resin (f_i=1.6 mmol/g). After the coupling of Fmoc-Lys(Boc)-OH, the peptidyl resin was divided in two parts by weight and both peptides were continued to be synthesized in parallel (Figure 7.25). In the **A76** peptidyl resin, Fmoc-Trp-OH was coupled, while in the **A77** peptidyl resin Fmoc-D-Trp-OH was incorporated.

7.5.1.2 Oxidative cleavage

The release of the fully protected peptide was achieved by treating the peptidyl resin with solution A (DCM/TFE/AcOH, 70:20:10 v/v, 8.3 vol) for 2h under magnetic stirring. Afterwards, the suspension was filtered either in a reaction vessel keeping the filtrate. The resin was washed three times with more solution A (2.2 vol per wash).

The disulfide bond formation between Cys^{3,14} residues was carried out using I$_2$ as the oxidant. To do that, I$_2$ (10 eq) was dissolved in solution A (3.3 vol) under magnetic stirring. The cleavage filtrate was added to the iodine solution and was stirred for 15 min at RT. Iodine excess was quenched with a 1M aqueous solution of N$_2$S$_2$O$_3$·5H$_2$O (22 eq) until complete discoloration of the oxidation solution. After phase separation, the aqueous layer was washed three times with DCM (2.2 vol per wash). The combined organic phases were washed with 5% aqueous solution of Citric Acid/NaCl 1:1 (5.7 vol), washing the resulting aqueous phase three times with DCM (2.2 vol per wash). The solvent of the combined organic phases was eliminated under reduced pressure until a wet solid was obtained. This solid was dried under vacuum for minimum 1h. The solid was transferred to a filtering plate and was washed with water six times. The resulting solid was dried under vacuum for minimum 12h. Once the oxidation crude was completely dry, it was weighed and the yield was calculated. Yield should be between 100-170%.

7.5.1.3   Global deprotection in solution

The elimination of the sidechain protecting groups was performed through global deprotection in solution using a mixture of TFA/DCM/Anisole/H_2O (55:30:10:5 v/v) at RT for 4h.

As the first step, the deprotection cocktail (15.3 vol) was prepared to treat the oxidation crude for 4h at RT. After this time, the acidic solution was washed once with heptane (16.2 vol) in a separation funnel. The lower phase was poured slowly over DEE (32.5 vol) previously cooled to -10ºC using a dry ice/acetone bath. The temperature of the mixture was controlled to never reach 10ºC. The resulting suspension was left to rest between 15 to 30 min. Afterwards, the suspension was filtered and the resulting solid was washed six times with DEE discarding all the filtrates. The wet solid obtained was dried under vacuum for minimum 12h. The peptide crude was weighed and the global yield was calculated. Yield should be between 100-150%.

7.5.1.4   Purification

The synthesized SSAs were purified using preparative LC (A: H_2O+0.02%TFA; B: ACN) to obtain the desired purity grade (>95%). To do that, SSAs were weighed and dissolved either with aqueous AcOH 20%, 30% or 40% solutions depending on their solubility. Next, the crude solutions were filtered with 0.45 µm PVDF filters and the filtrate was injected to the column for its purification.

Generally, SSAs were purified using an isocratic method of more or less 30 min depending on the analog. **A74**-**A79** and **A82** were purified using isocratic methods between 23 to 27%B in 30 min. In contrast, **A80**-**A81** had to be purified using gradient methods as shown in section 4.3.2. **A74**-**A75** were purified with preparative column MK9 (55 mL/min, 20 mL per injection), while **A76**-**A82** were purified with preparative column NS17 (110 mL/min, 40 mL per injection).

Column fractions were collected in various crystal tubes and were analyzed by HPLC through 20 µL co-injections of various of these fractions. When the desired combination of tubes was obtained (purity of the principal peak had to be >95%), the selected tubes were joined in one or several 2L round-bottomed flasks. Finally, the pure peptide solution was frozen with a dry ice/acetone bath and was lyophilized to obtain the pure SSA. The peptide purity should be above 95.0% by HPLC and purification recovery should be above 15%.

7.5.1.5   Ion exchange (Dowex)

After peptide purification, the ion-exchange from trifluoroacetate (TFA⁻) to acetate (AcO⁻) was performed using Dowex resin. To do that, the purified SSA was dissolved in 0.1M AcOH aqueous solution (30 mg/mL). Dowex resin was weighed and conditioned with three washes of 0.1M AcOH, and incorporated to the peptide solution. The resulting mixture was stirred for 15 min and the peptide was recovered by filtration. This procedure was repeated once more. The peptide solution

was frozen using a dry ice/acetone bath and lyophilized to obtain the peptide in its acetate form. Dowex recovery should be between 80-100%.

Purity determination and characterization of the synthesized SSAs was performed by HPLC using Kromasil C8 at 1 mL/min. Linear gradient 5-85%B in 20 min and isocratic method in 30 min were used to characterize each analog. HPLC-MS and HRMS were used as well to determine the presence of the desired peptide and its molecular weight.

7.5.2 List of Somatostatin Analogs

A74: (D-Ala^1,D-Cys^{3,14},Msa^7,D-Trp^8)-SST

A75: (D-Ala^1,D-Cys^{3,14},D-Lys^4,Msa^7,D-Trp^8)-SST
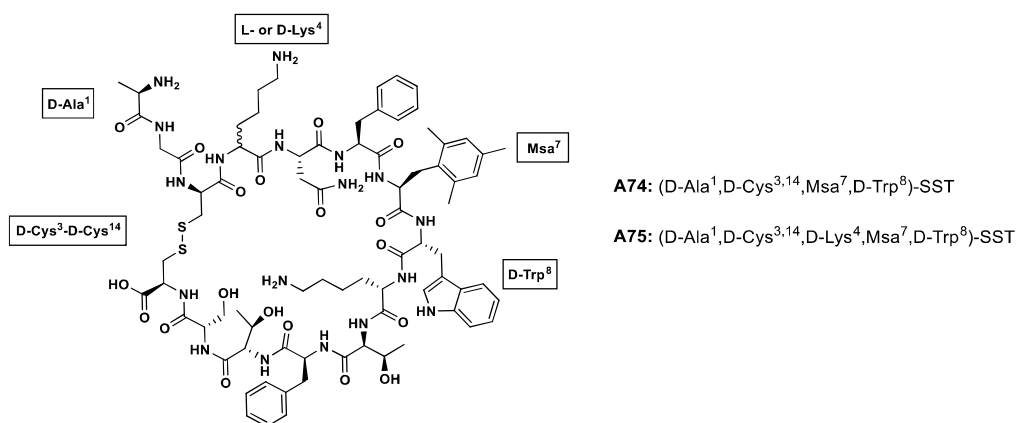
Figure 7.26 Structures of A74 and A75

(D-Ala^1,D-Cys^{3,14},Msa^7,D-Trp^8)-SST (A74): analog A74 (H-D-Ala^1-Gly^2-*c*[D-Cys^3-Lys^4-Asn^5-Phe^6-Msa^7-D-Trp^8-Lys^9-Thr^{10}-Phe^{11}-Thr^{12}-Ser^{13}-D-Cys^{14}]-OH) was synthesized following the general synthesis protocol using 2.0 g of CTC resin (f = 1.6 mmol/g), Fmoc-D-Cys(Trt)-OH as the *C*-terminal amino acid and Boc-D-Ala-OH as the *N*-terminal amino acid. Fmoc-Msa-OH was incorporated at position 7. Peptide crude was purified by preparative LC obtaining 0.73 g with a 98.6% purity. **HPLC:** 5-85%B in 20 min, t$_R$ = 14.6 min; 32%B in 30 min, t$_R$ = 11.3 min (A: H$_2$O+0.1%TFA; B: ACN+0.07%TFA). **HRMS:** calculated for C$_{79}$H$_{110}$O$_{19}$N$_{18}$S$_2$: 1679.9760; found: 840.3875 [M+2H]$^{2+}$ and 1680.7810 [M+H]$^+$. Analog A74 was previously designed by Dr. Anna Escolà.

(D-Ala^1,D-Cys^{3,14},D-Lys^4,Msa^7,D-Trp^8)-SST (A75): analog A75 (H-D-Ala^1-Gly^2-*c*[D-Cys^3-D-Lys^4-Asn^5-Phe^6-Msa^7-D-Trp^8-Lys^9-Thr^{10}-Phe^{11}-Thr^{12}-Ser^{13}-D-Cys^{14}]-OH) was synthesized following the general synthesis protocol using 5.0 g of CTC resin (f = 1.6 mmol/g), Fmoc-D-Cys(Trt)-OH as the *C*-terminal amino acid and Boc-D-Ala-OH as the *N*-terminal amino acid. Fmoc-Msa-OH was incorporated at position 7. Peptide crude was purified by preparative LC obtaining 2.77 g with a 98.5% purity. **HPLC:** 5-85%B in 20 min, t$_R$ = 14.8 min; 32%B in 30 min, t$_R$ = 13.9 min (A: H$_2$O+0.1%TFA; B: ACN+0.07%TFA). **HRMS:** calculated for C$_{79}$H$_{110}$O$_{19}$N$_{18}$S$_2$: 1679.9760; found: 840.3913 [M+2H]$^{2+}$ and 1680.7980 [M+H]$^+$.

(D-Ala^1,D-Cys^{3,14})-SST (A76): analog A76 (H-D-Ala^1-Gly^2-*c*[D-Cys^3-Lys^4-Asn^5-Phe^6-Phe^7-Trp^8-Lys^9-Thr^{10}-Phe^{11}-Thr^{12}-Ser^{13}-D-Cys^{14}]-OH) was synthesized following the general synthesis protocol using 2.5 g of CTC resin (f = 1.6 mmol/g), Fmoc-D-Cys(Trt)-OH as the *C*-terminal amino acid and Boc-D-Ala-OH as the *N*-terminal amino acid. Peptide crude was purified by preparative LC obtaining 0.80 g with a 99.3% purity. **HPLC:** 5-85%B in 20 min, t_R = 14.5 min; 29.5%B in 30 min, t_R = 15.2 min (A: H$_2$O+0.1%TFA; B: ACN+0.07%TFA). **HRMS:** calculated for C$_{76}$H$_{104}$O$_{19}$N$_{18}$S$_2$: 1637.8950; found: 819.3565 [M+2H]$^{2+}$ and 1638.7052 [M+H]$^+$.

A76: (D-Ala^1,D-Cys^{3,14})-SST

A77: (D-Ala^1,D-Cys^{3,14},D-Trp^8)-SST

A78: (D-Ala^1,D-Cys^{3,14},D-Phe^{6,11})-SST

A79: (D-Ala^1,D-Cys^{3,14},D-Phe^{6,11},D-Trp^8)-SST

A80: (D-Ala^1,D-Cys^{3,14},D-Thr^{10})-SST

A81: (D-Ala^1,D-Cys^{3,14},D-Trp^8,D-Thr^{10}))-SST
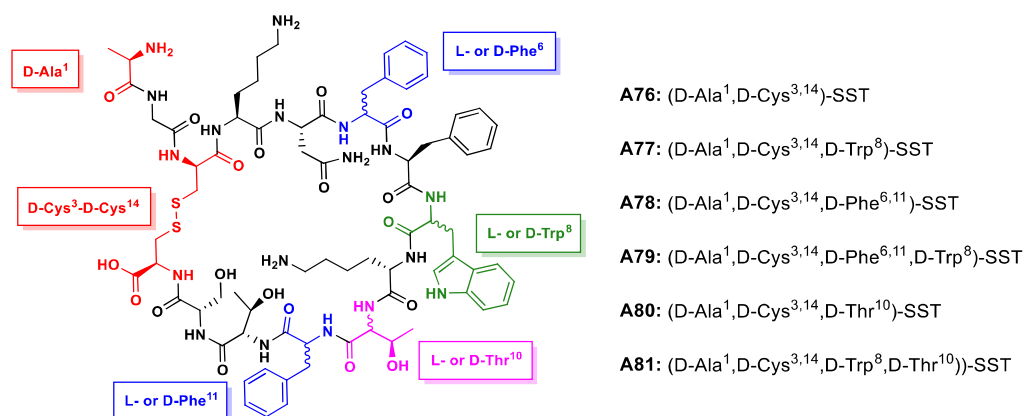
Figure 7.27 Structures of A76-A81

(D-Ala^1,D-Cys^{3,14},D-Trp^8)-SST (A77): analog A77 (H-D-Ala^1-Gly^2-*c*[D-Cys^3-Lys^4-Asn^5-Phe^6-Phe^7-D-Trp^8-Lys^9-Thr^{10}-Phe^{11}-Thr^{12}-Ser^{13}-D-Cys^{14}]-OH) was synthesized following the general synthesis protocol using 2.5 g of CTC resin (f = 1.6 mmol/g), Fmoc-D-Cys(Trt)-OH as the *C*-terminal amino acid and Boc-D-Ala-OH as the *N*-terminal amino acid. Peptide crude was purified by preparative LC obtaining 1.63 g with a 99.3% purity. **HPLC:** 5-85%B in 20 min, t_R = 14.0 min; 27.5%B in 30 min, t_R = 14.7 min (A: H$_2$O+0.1%TFA; B: ACN+0.07%TFA). **HRMS:** calculated for C$_{76}$H$_{104}$O$_{19}$N$_{18}$S$_2$: 1637.8950; found: 819.3566 [M+2H]$^{2+}$ and 1638.7052 [M+H]$^+$.

(D-Ala^1,D-Cys^{3,14},D-Phe^{6,11})-SST (A78): analog A78 (H-D-Ala^1-Gly^2-*c*[D-Cys^3-Lys^4-Asn^5-D-Phe^6-Phe^7-Trp^8-Lys^9-Thr^{10}-D-Phe^{11}-Thr^{12}-Ser^{13}-D-Cys^{14}]-OH) was synthesized following the general synthesis protocol using 2.5 g of CTC resin (f = 1.6 mmol/g), Fmoc-D-Cys(Trt)-OH as the *C*-terminal amino acid and Boc-D-Ala-OH as the *N*-terminal amino acid. Peptide crude was purified by preparative LC obtaining 0.81 g with a 96.9% purity. **HPLC:** 5-85%B in 20 min, t_R = 14.6 min; 30%B in 30 min, t_R = 14.4 min (A: H$_2$O+0.1%TFA; B: ACN+0.07%TFA). **HRMS:** calculated for C$_{76}$H$_{104}$O$_{19}$N$_{18}$S$_2$: 1637.8950; found: 819.3571 [M+2H]$^{2+}$ and 1638.7064 [M+H]$^+$.

(D-Ala^1,D-Cys^{3,14},D-Phe^{6,11},D-Trp^8)-SST (A79): analog A79 (H-D-Ala^1-Gly^2-*c*[D-Cys^3-Lys^4-Asn^5-D-Phe^6-Phe^7-D-Trp^8-Lys^9-Thr^{10}-D-Phe^{11}-Thr^{12}-Ser^{13}-D-Cys^{14}]-OH) was synthesized following the general synthesis protocol using 2.5 g of CTC resin (f = 1.6 mmol/g), Fmoc-D-Cys(Trt)-OH as the *C*-terminal amino acid and Boc-D-Ala-OH as the *N*-terminal amino acid. Peptide crude was

purified by preparative LC obtaining 2.03 g with a 97.7% purity. **HPLC:** 5-85%B in 20 min, t_R = 14.6 min; 30.5%B in 30 min, t_R = 14.5 min (A: H_2O+0.1%TFA; B: ACN+0.07%TFA). **HRMS:** calculated for $C_{76}H_{104}O_{19}N_{18}S_2$: 1637.8950; found: 819.3571 $[M+2H]^{2+}$ and 1638.7064 $[M+H]^+$.

(D-Ala^1,D-Cys^{3,14},D-Thr^{10})-SST (A80): analog A80 (H-D-Ala^1-Gly^2-c[D-Cys^3-Lys^4-Asn^5-Phe^6-Phe^7-Trp^8-Lys^9-D-Thr^{10}-Phe^{11}-Thr^{12}-Ser^{13}-D-Cys^{14}]-OH) was synthesized following the general synthesis protocol using 2.5 g of CTC resin (f = 1.6 mmol/g), Fmoc-D-Cys(Trt)-OH as the *C*-terminal amino acid and Boc-D-Ala-OH as the *N*-terminal amino acid. Peptide crude was purified by preparative LC obtaining 0.84 g with a 96.1% purity. **HPLC:** 5-85%B in 20 min, t_R = 14.1 min; 28%B in 30 min, t_R = 14.3 min (A: H_2O+0.1%TFA; B: ACN+0.07%TFA). **HRMS:** calculated for $C_{76}H_{104}O_{19}N_{18}S_2$: 1637.8950; found: 819.3572 $[M+2H]^{2+}$ and 1638.7064 $[M+H]^+$.

(D-Ala^1,D-Cys^{3,14},D-Trp^8,D-Thr^{10})-SST (A81): analog A81 (H-D-Ala^1-Gly^2-c[D-Cys^3-Lys^4-Asn^5-Phe^6-Phe^7-D-Trp^8-Lys^9-D-Thr^{10}-Phe^{11}-Thr^{12}-Ser^{13}-D-Cys^{14}]-OH) was synthesized following the general synthesis protocol using 2.5 g of CTC resin (f = 1.6 mmol/g), Fmoc-D-Cys(Trt)-OH as the *C*-terminal amino acid and Boc-D-Ala-OH as the *N*-terminal amino acid. Peptide crude was purified by preparative LC obtaining 0.85 g with a 98.7% purity. **HPLC:** 5-85%B in 20 min, t_R = 14.0 min; 29.5%B in 30 min, t_R = 14.7 min (A: H_2O+0.1%TFA; B: ACN+0.07%TFA). **HRMS:** calculated for $C_{76}H_{104}O_{19}N_{18}S_2$: 1637.8950; found: 819.3570 $[M+2H]^{2+}$ and 1638.7061 $[M+H]^+$.

A82: (D-Ala^1,D-Cys^{3,14},Msa^6,D-Trp^8)-SST
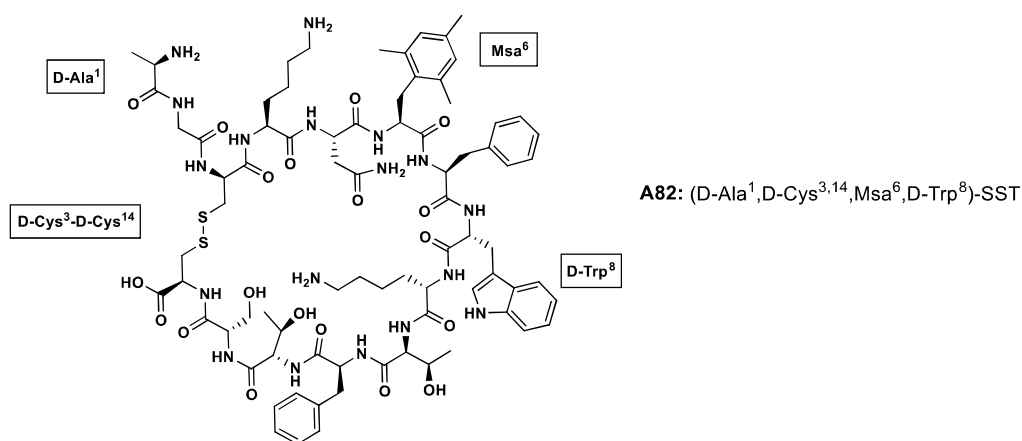
Figure 7.28 Structure of A82

(D-Ala^1,D-Cys^{3,14},Msa^6,D-Trp^8)-SST (A82): analog A82 (H-D-Ala^1-Gly^2-c[D-Cys^3-Lys^4-Asn^5-Msa^6-Phe^7-D-Trp^8-Lys^9-Thr^{10}-Phe^{11}-Thr^{12}-Ser^{13}-D-Cys^{14}]-OH) was synthesized following the general synthesis protocol using 2.0 g of CTC resin (f = 1.6 mmol/g), Fmoc-D-Cys(Trt)-OH as the *C*-terminal amino acid and Boc-D-Ala-OH as the *N*-terminal amino acid. Fmoc-Msa-OH was incorporated at position 6. Peptide crude was purified by preparative LC obtaining 0.81 g with a 99.5% purity. **HPLC:** 5-85%B in 20 min, t_R = 15.0 min; 31%B in 30 min, t_R = 13.9 min

(A: $H_2O+0.1\%TFA$; B: $ACN+0.07\%TFA$). **HRMS:** calculated for $C_{79}H_{110}O_{19}N_{18}S_2$: 1678.7636; found: 840.3900 $[M+2H]^{2+}$ and 1679.7706 $[M+H]^+$.

7.5.3 Characterization of Somatostatin Analogs

7.5.3.1 Serum stability studies
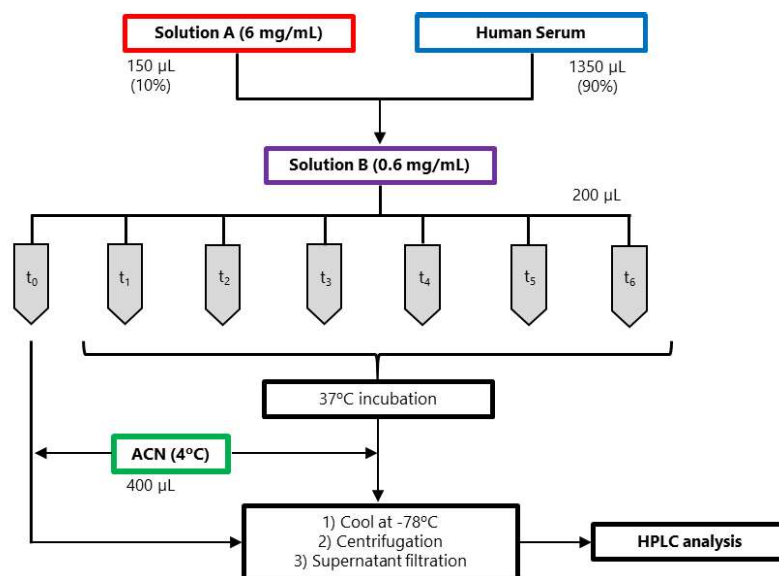
Figure 7.29 Serum stability studies

Human serum (Sigma, H4522) was incubated at 37ºC for minimum 15 min. Meanwhile, peptide stock solution in Milli-Q water (6 mg/mL, solution A) was prepared in a 5 mL plastic tube (Figure 7.29). A 1:10 dilution of solution A was prepared in human serum: *i.e.* 150 µL of solution A and 1350 µL of human serum (0.6 mg/mL, solution B). Immediately after, 200 µL aliquots of solution B were prepared in eppendorfs that were incubated at 37ºC. At specified times (t_i), the aliquots were treated with 400 µL of cold ACN[80] to precipitate the serum proteases (final concentration 0.2 mg/mL, 66% of ACN). In the case of t_0, the sample was directly precipitated with cold ACN without any incubation time. The precipitated samples were cooled for some seconds in a dry ice/acetone bath and were centrifuged at 10,000 rpm for 5 min and 4ºC (Eppendorf 5415 R). The supernatant was filtered with a 0.45 µm PVDF filter and was introduced in a new eppendorf. At this point, the samples were analyzed directly by HPLC or kept in the freezer (T = -20ºC) for posterior analysis. The stability study standards were prepared as follows:

- Peptide standard: 20 µL of solution A + 180 µL of Milli-Q water + 400 µL of ACN.
- Serum standard: 20 µL of solution A + 180 µL of human serum + 400 µL of ACN. After precipitation, this standard was treated following the previous procedure.

---

[80] In general, ACN was used to precipitate serum proteases in all the stability studies performed, except for A75 in which 5% TFA solution in ACN was used due to peptide recovery issues.

- ACN standard: 200 µL of Milli-Q water + 400 µL of ACN.

Immediately before HPLC analysis, both the samples and the standards were diluted to ⅓ of the initial concentration with Milli-Q water (*e.g.* 50 µL of sample + 100 µL of Milli-Q water). This step permitted to decrease the initial 66% ACN of the samples avoiding quick elution from the analytical column. After this dilution step, stability samples (60 µL per injection) were analyzed by HPLC using the corresponding isocratic method for each peptide (A: H_2O+0.1%TFA; B: ACN+0.07%TFA). The serum half-life ($t_{1/2}$) of each peptide was calculated from the HPLC degradation data using the linear regression of the natural logarithm of the peak percentage (Ln ($A_i/A_0 \cdot 100$)) with respect to time (t_i). The determination of the slope that corresponded to the experimental constant (-K_e) allowed the calculation of the half-life of the peptide (Figure 7.30).

Generally, an initial stability study (t_i = 0h, 1h, 4h, 8h, 24h, 48h, 72h) was performed on each peptide to obtain a first orientated result (study I). Afterwards, three stability studies were performed in parallel (studies IIA, IIB and IIC). The time points selected for these replicates were determined taking into account the results of study I. The mean of the half-life values obtained in the replicates of study II was considered as the real half-life of the peptide. For more details about the results obtained see section 9.3.2.

A75 recovery tests were prepared by mixing 20 µL of solution A and 180 µL of serum in an eppendorf. Then, the serum proteases were precipitated by adding 400 µL of a variety of organic solvents and solutions. Finally, the supernatant was filtered, diluted to ⅓ with Milli-Q water and analyzed by HPLC performing two injections of each sample.

t_i (h)	A_i (uA)	(A_i / A_0) · 100	Ln [(A_i / A_0) · 100]
t_0	A_0	$A_0 / A_0 \cdot 100$	Ln [$A_0 / A_0 \cdot 100$]
t_1	A_1	$A_1 / A_0 \cdot 100$	Ln [$A_1 / A_0 \cdot 100$]
t_2	A_2	$A_2 / A_0 \cdot 100$	Ln [$A_2 / A_0 \cdot 100$]
(...)	(...)	(...)	(...)
t_n	A_n	$A_n / A_0 \cdot 100$	Ln [$A_n / A_0 \cdot 100$]

$$t_{1/2} = \frac{ln\,(2)}{K_e} \rightarrow t_{1/2} = \frac{ln\,(2)}{0.6724} = 1.03\,h$$

Serum stability A76 (study IIA)

$y = -0,6724x + 4,8454$
$R^2 = 0,9887$
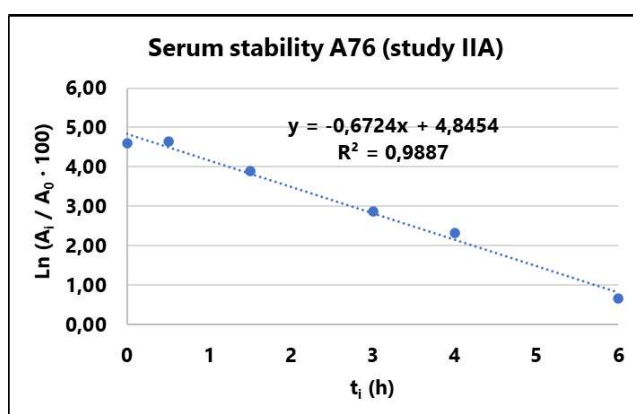
Figure 7.30 Half-life calculation and example

7.5.3.2 Metabolite studies

Serum stability samples of each peptide were re-analyzed by HPLC using the linear gradient 5-70%B in 45 min (A: H_2O+0.1%TFA; B: ACN+0.07%TFA)[81]. The analysis and comparison of these

---

[81] The metabolites of **A77** were analyzed by the linear gradient 5-40%B in 45 min.

data permitted to identify various growing peaks that corresponded to different peptide metabolites. After the identification of the metabolite peaks, one of the serum stability samples of each peptide was analyzed by HPLC-MS using the previous gradient method. Analysis of the obtained data permitted to assign each metabolite peak to a determined mass. When the mass of a peak corresponded to two different structures (*e.g.* Des[Lys[4]]-A78 or Des[Lys[9]]-A78, MW 1527.7350), the corresponding metabolite peak was collected through HPLC analysis. The collected peak was treated with 20 μL of a 1,4-dithiothreitol (DTT) aqueous solution (1 mg/mL) for 1h at RT. This treatment permitted to eliminate the disulfide bond between Cys[3,14] and to analyze the corresponding fragments directly by MS. The identification of these fragments after DTT treatment, permitted to distinguish between the two metabolites.

7.5.3.3 Biologic assays

In July 2021, **A74**, **A75** and **A82** were sent to the research group of Prof. Justo Castaño at IMBIC (Córdoba). These analogs will be evaluated *in vitro* against various cellular models of tumors that overexpress SSTRs. These tumors are shown in section 4.3.4.

7.6 Synthesis of (*S*)-Bicalutamide

7.6.1 Initial synthesis of (*S*)-Bicalutamide

(*S*)-bromoamide (**5-14**) (1.0 eq, 6.3 mmol, 2.2 g), TEBAC (1.1 eq, 6.9 mmol, 1.6 g), Na_2HPO_4 (3.0 eq, 18.8 mmol, 2.7 g) and sulfinate (**5-9**) (3.0 eq, 18.8 mmol, 3.4 g) were introduced in a 50 mL round-bottomed flask. Then, H_2O (5 vol, 10 mL) was added, and the mixture was heat at 100ºC for 3h. Thin-layer chromatography (TLC) (Hexane/EtOAc 1:1) was used to monitor the reaction. The crude was left to cool to 65ºC and sodium dithionite ($Na_2S_2O_7$ 7.1 g), IPA (10 mL) and active carbon (0.2 g) were added. The resulting mixture was heat at 100ºC for 2h. After this amount of time, the crude was filtered at 60ºC using a Büchner funnel with three filters and IPA (10 mL) to wash the carbon cake. H_2O (50 mL) was added slowly to the filtrate to obtain a final IPA/H_2O relation of 1:3. In these conditions, the resulting mixture was left to cool for 12-18h and was filtered to obtain a light-brown solid (2.8 g). A second discoloration of the crude product was performed dissolving it in IPA (1 vol, 3 mL) at 100ºC. Then, an aqueous dithionite solution (0.24 g in 3 mL) and active carbon (0.15 g) were added. The resulting mixture was stirred for 2h at 100ºC. After this amount of time, the mixture was filtered at 65ºC using a Büchner funnel equipped with three filters. The carbon cake was washed with more IPA (3 mL) and H_2O (15 mL) was added to the filtrate. The mixture was left to cool slowly for 12-18h. The crystallized light-brown solid was filtered and dried in a desiccator until constant weight (2.5 g, 90% yield).

7.6.2 Synthesis of (*S*)-Bromoamide (E6-168)
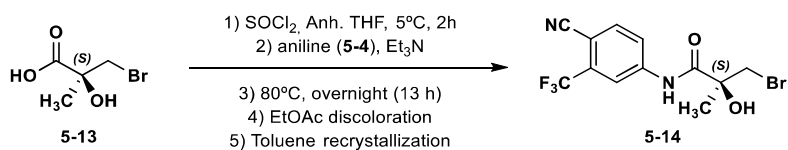
Figure 7.31 Synthesis of (S)-bromoamide (5-14)

(*S*)-Bromoacid (**5-13**) (1.2 eq, 0.354 mol, 64.8 g) was introduced inside a 1L Schlenk flask with a magnetic stir bar. Three vacuum/N_2 cycles were applied. Anh. THF (4.7 vol, 260 mL) was introduced via cannula and the (*S*)-bromoacid (**5-13**) was dissolved by magnetic stirring. The flask was cooled at 5°C with an ice/water bath and thionyl chloride (1.5 eq, 0.44 mol, 32 mL) was added with a syringe. The reagents were allowed to react for 2h to obtain the corresponding acid chloride.

4-cyano-3-trifluoromethylaniline (**5-4**) (1.0 eq, 0.30 mol, 54.9 g) was introduced inside a 0.5L Schlenk flask with a magnetic stir bar. Three vacuum/N_2 cycles were applied to the flask. Anh. THF (2.2 vol, 120 mL) was introduced via cannula and the aniline was dissolved via stirring and sonication. The aniline (**5-4**) solution was transferred via cannula to the acid chloride flask, washing the flask with more anh. THF (0.4 vol, 20 mL). The resulting mixture was allowed to react for 30 min. Anh. Et_3N (1.5 eq, 0.44 mol, 62 mL) was introduced via syringe and the resulting mixture was allowed to react for 30 min more. Using a N_2 flow, a reflux condenser was attached to the 1L Schlenk flask maintaining the anhydrous conditions. The reaction mixture was heat at 80°C overnight (minimum 13h). TLC (Hexane:EtOAc 1:1) was used to monitor the reaction.

The reaction crude was allowed to cool until RT was achieved. Afterwards, the solvent was eliminated under reduced pressure. Then, it was dissolved in EtOAc (350 mL) and washed with aqueous 5% HCl (75 mL) in a 2L separation funnel. After phase separation, the aqueous phase was washed with more EtOAc (75 mL). The resulting organic phase was washed with saturated $NaHCO_3$ solution (3x75mL) and H_2O (3x75 mL). The organic phase was dried over anh. $MgSO_4$ and filtered to a 1L round-bottomed flask.

Active carbon (3.2 g) was added to the crude product dissolved in EtOAc and the resulting mixture was heat at 85°C during minimum 2h for complete discoloration. After this time, the solution was allowed to cool until RT was achieved. Then, active carbon was filtered over a Büchner funnel equipped with three filters. The filtrate was evaporated under reduced pressure to obtain a brown oil. Toluene (100 mL) was used to completely eliminate any rests of EtOAc by evaporation under reduced pressure. This step was performed once more to finally obtain a brown solid (approximately 134 g).

The crude was recrystallized from toluene (0.52 vol, 70 mL) at 120ºC. When the product was completely dissolved heat was turned off and the solution was allowed to cool until RT while stirring. The flask was cooled with an ice/water bath for minimum 10 min. The resulting suspension was filtered and the solid was washed with cold hexane (50 mL). The product was dried under vacuum until constant weight (79.8 g, 77% yield, 99.2% purity by HPLC-MS).

^{1}H-NMR (400 MHz, CDCl$_3$) δ (ppm): 8.98 (brs, 1H), 8.08 (d, J = 2.2 Hz, 1H), 7.99-7.91 (m, 1H), 7.81 (d, J = 8.5 Hz, 1H), 4.02 (d, J = 10.6 Hz, 1H), 3.60 (d, J = 10.5 Hz, 1H), 2.98 (s, 1H), 1.64 (s, 3H).

^{13}C-NMR (101 MHz, CDCl$_3$) δ (ppm): 171.48, 141.10, 135.88, 121.87, 117.36, 117.31, 115.35, 104.97, 75.54, 41.04, 24.80.

HPLC: 45%B in 30 min, t_R = 16.3 min (A: H$_2$O+0.1%TFA; B: ACN+0.07%TFA). **MS:** calculated for C$_{12}$H$_{10}$O$_2$N$_2$BrF$_3$: 351.1; found 464.9 [M-1H+TFA]$^-$.

7.6.3 Synthesis of sodium 4-fluorobenzenesulfinate (E6-190)
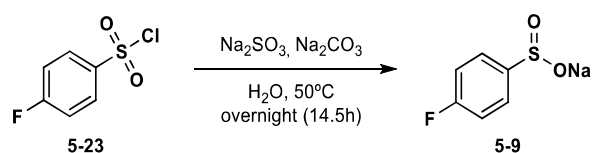
Figure 7.32 Synthesis of sodium 4-fluorobenzenesulfinate (5-9)

Na$_2$SO$_3$ (1.2 eq, 1.26 mol, 159 g) was introduced in a 2L round-bottomed flask and was dissolved in H$_2$O (4.5 vol, 922 mL) by magnetic stirring. Na$_2$CO$_3$ (1.2 eq, 1.26 mol, 133.6 g) was introduced in the flask and was also dissolved. The resulting solution was heat at 50ºC and 4-fluorobenzenesulfonyl chloride (**5-23**) (1.0 eq, 1.05 mol, 205 g) was added in three portions every 10 min. The resulting mixture was heat at 50ºC overnight (minimum 14.5h).

Water was eliminated under reduced pressure to approximately 10% of the initial volume (~ 100 mL). The resulting suspension was filtered and the solid was washed with the minimum amount of EtOH. The filtrate was evaporated under reduced pressure and the two solids were put together in a 5L glass reactor. EtOH (4L) was added and the suspension was left stirring at RT overnight (maximum 14 h). The suspension was filtered over a Büchner funnel equipped with three filters. EtOH (1L) was used to completely clean the reactor and the filtered solid. The filtrate was evaporated under reduced pressure to approximately 10% of the initial volume (~0.5 L). The resulting suspension was filtered and the solid was washed with the minimum amount of ACN. The filtrate was evaporated under reduced pressure and the two solids were put together in a 2L round-bottomed flask. ACN (0.8L) was added and the suspension was left stirring at RT for 30 min and was filtered. The solid was washed with more ACN (0.4L) and the product was dried in a vacuum desiccator until constant weight (185.4 g, 99% yield, 98.9% purity by HPLC-MS).

^{1}H-NMR (400 MHz, DMSO-d$_6$) δ (ppm): 7.50-7.46 (m, 2H), 7.12-7.07 (m, 2H).

HPLC: 8%B in 30 min, t_R = 17.3 min (A: H$_2$O+0.1%TFA; B: ACN+0.07%TFA). **MS**[82]**:** calculated for C$_6$H$_4$O$_2$SFNa: 182.1; found 174.9 [M-1H]$^-$.

7.6.4 Synthesis (E6-195) and recrystallization (E7-058) of (*S*)-Bicalutamide
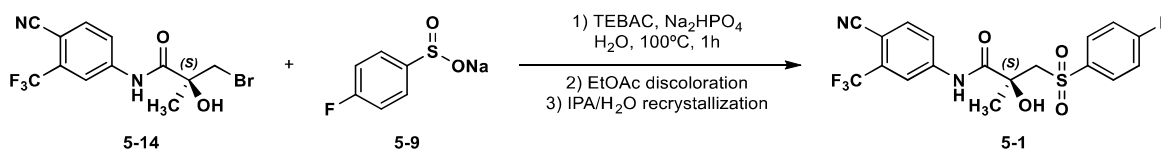
Figure 7.33 Synthesis of (S)-bicalutamide (5-1)

(*S*)-bromoamide (**5-14**) (1.0 eq, 0.17 mol, 60.8 g), sodium 4-fluorobenzenesulfinate (**5-23**) (3.0 eq, 0.52 mol, 94.5 g), triethylbenzylammonium chloride (TEBAC) (1.1 eq, 0.19 mol, 43.3 g) and Na$_2$HPO$_4$ (3.0 eq, 0.52 mol, 73.7 g) were weighed inside a two-neck 1L round-bottomed flask. A reflux condenser was attached and the whole system was purged with N$_2$ for 20 min. Milli-Q water (4 vol, 245 mL) was introduced in a 0.5L Schlenk flask and was degasified with N$_2$ for 20 min.

Degasified Milli-Q water was transferred to the two-neck flask via cannula and the resulting mixture was heat at 100°C for 1h. TCL (Hexane:ETOAc 1:1) was used to monitor the reaction.

The reaction crude was allowed to cool until RT was achieved. Then, it was transferred to a 1L separation funnel and more water (250 mL) was added. The product was extracted with EtOAc (2x200 mL). The organic phase was dried over anh. MgSO$_4$ and filtered to a 1L round-bottomed flask. Active carbon (6.1 g) was added and the mixture was heat at 90°C for 2h for complete discoloration. Afterwards, it was allowed to cool until RT was achieved and was filtered over a Büchner funnel equipped with three filters. The filtrate was transferred to a previously weighed two-neck 1L flask and the solvent was eliminated under reduced pressure to obtain an orange oil (92.5 g, 74.5% purity by HPLC-MS).

Recrystallization (Procedure B): an IPA/H$_2$O 1:1 mixture (184 mL, 2 vol in relation to the previous crude) was added to the two-neck round-bottomed flask. A reflux condenser was attached and the mixture was heat at 120°C. After the product was completely dissolved, H$_2$O (60 mL) was slowly added until a permanent turbidity was observed inside the flask. The heat was stopped and the mixture was allowed to cool until RT was achieved. The product was filtered over a filter plate and

---

[82] The mass found in the HPLC-MS analysis for 4-fluorobenzenesulfinate (**5-23**) did not correspond to this precursor. Despite this, the ^{1}H-NMR peaks of the aromatic protons of sulfinate (**5-9**) were clearly different from the signals of 4-fluorobenzenesulfonyl chloride (**5-23**). We think that the mass observed (174.9 m/z) in the HPLC-MS analysis of sulfinate (**5-23**) corresponds to: i) the oxidized product (sodium 4-fluorobenzenesulfonate (MW 198.1)); or, ii) an adduct with water. Nevertheless, we are sure to obtain sulfinate (**5-23**) because the reaction to prepare (*S*)-bicalutamide (**5-1**) works very well. **MS**: calculated for C$_6$H$_4$O$_3$SFNa: 198.1; found 174.9 [M-1H-Na]$^-$.

was washed with an IPA/H_2O 1:1.65 mixture (50 mL). The product was dried in a vacuum desiccator until constant weight (51.3 g, 69% yield, 98.9% purity by HPLC-MS).

The product was recrystallized twice following the previous procedure to finally obtain pure (*S*)-bicalutamide (47.7 g, 93% recrystallization recovery, 99.8% purity by HPLC-MS).

^{1}H-NMR (400 MHz, CDCl$_3$) δ (ppm): 9.01 (brs, 1H), 7.91 (m, 1H), 7.84-7.81 (m, 2H), 7.73-7.72 (m, 2H), 7.13-7.09 (m, 2H), 4.97 (s, 1H), 3.90 (d, *J* = 14.4 Hz, 1H), 3.43 (d, *J* = 14.4 Hz, 1H), 1.55 (s, 3H).

^{13}C-NMR (101 MHz, CDCl$_3$) δ (ppm): 171.42, 167.51, 164.94, 141.00, 135.80, 135.06, 134.27, 133.94, 130.93, 130.84, 121.81, 117.27, 116.97, 116.74, 115.29, 74.44, 61.61, 27.70.

HPLC: 45%B in 60 min, t_R = 17.4 min (A: H_2O+0.1%TFA; B: ACN+0.07%TFA). **MS:** calculated for $C_{18}H_{14}O_4N_2SF_4$: 430.4; found 543.1 [M-1H+TFA]$^-$.

Chapter 8

Bibliography

8 Bibliography

[1]   B. G. de la Torre, F. Albericio, *Molecules* **2020**, *25*, 2019–2021.

[2]   A. Henninot, J. C. Collins, J. M. Nuss, *J. Med. Chem.* **2018**, *61*, 1382–1414.

[3]   J. L. Lau, M. K. Dunn, *Bioorganic Med. Chem.* **2018**, *26*, 2700–2707.

[4]   S. Knauer, N. Koch, C. Uth, R. Meusinger, O. Avrutina, H. Kolmar, *Angew. Chemie - Int. Ed.* **2020**, *59*, 12984–12990.

[5]   M. Erak, K. Bellmann-Sickert, S. Els-Heindl, A. G. Beck-Sickinger, *Bioorganic Med. Chem.* **2018**, *26*, 2759–2765.

[6]   O. Al Musaimi, B. G. De La Torre, F. Albericio, *Green Chem.* **2020**, *22*, 996–1018.

[7]   QYResearch, "Global Peptide Therapeutics Sales Market Report 2020," **2020**.

[8]   ▮▮▮▮▮▮▮▮▮▮▮▮▮▮▮▮▮▮▮▮▮▮▮▮▮▮▮▮▮▮▮▮▮▮▮▮

[9]   J. M. Palomo, *RSC Adv.* **2014**, *4*, 32658–32672.

[10]   P. Anastas, N. Eghbali, *Chem. Soc. Rev.* **2010**, *39*, 301–312.

[11]   P. Palladino, D. A. Stetsenko, *Org. Lett.* **2012**, *14*, 6346–6349.

[12]   P. Brazeau, W. Vale, R. Burgus, N. Ling, M. Butcher, J. Rivier, R. Guillemin, *Science (80-.).* **1973**, *179*, 77–79.

[13]   G. Weckbecker, I. Lewis, R. Albert, H. A. Schmid, D. Hoyer, C. Bruns, *Nat. Rev. Drug Discov.* **2003**, *2*, 999–1017.

[14]   Y. Yamada, S. R. Post, K. Wang, H. S. Tager, G. I. Bell, S. Seino, *Proc. Natl. Acad. Sci.* **1992**, *89*, 251–255.

[15]   F. W. Kluxen, C. Bruns, H. Lübbert, *Proc. Natl. Acad. Sci.* **1992**, *89*, 4618–22.

[16]   I. M. Chapman, A. Helfgott, J. O. Willoughby, *J. Endocrinol.* **1991**, *128*, 369–374.

[17]   Y. C. Patel, T. Wheatley, *Endocrinology* **1983**, *112*, 220–225.

[18]   W. Bauer, U. Briner, W. Doepfner, R. Haller, R. Huguenin, P. Marbach, T. J. Petcher, J. Pless, *Life Sci.* **1982**, *31*, 1133–1140.

[19]   R. Z. Cai, B. Szoke, R. Lu, D. Fu, T. W. Redding, A. V. Schally, *Proc. Natl. Acad. Sci.* **1986**, *83*, 1896–1900.

[20]   W. A. Murphy, V. A. Lance, S. Moreau, J. P. Moreau, D. H. Coy, *Life Sci.* **1987**, *40*, 2515–2522.

[21]   C. Bruns, I. Lewis, U. Briner, G. Meno-Tetang, G. Weckbecker, *Eur. J. Endocrinol.* **2002**, *146*, 707–716.

[22]   R. Ramón Albalate, Síntesis Enantioselectiva de Aminoácidos No Naturales y Aplicación a La Síntesis de Péptidos Con Interés Farmacológico, Universitat de Barcelona, **2009**.

[23]   M. Gómez Caminals, Disseny, Síntesi i Avaluació Biològica de Nous Anàlegs de Somatostatina, Universitat de Barcelona, **2011**.

[24]   P. Martín-Gago, Synthesis of Highly Structured and Receptor-Selective Tetradecapeptidic Analogs of Somatostatin: Fine-Tuning the Non-Covalent Interactions among Their Aromatic Pablo Martín-Gago, Universitat de Barcelona, **2013**.

[25]   Á. Rol Rúa, Análogos de Somatostatina y Cortistatina. Efecto de Las Interacciones Aromáticas En Sus Estructuras y En La Actividad Biológica, Universitat de Barcelona, **2015**.

[26]   A. Escolà Jané, Somatostatin Analogues as Drug Delivery Systems for Receptor-Targeted Cancer Therapy, Universitat de Barcelona, **2018**.

[27]   R. Ramón, P. Martín-Gago, X. Verdaguer, M. J. Macias, P. Martin-Malpartida, J. Fernández-Carneado, M. Gomez-Caminals, B. Ponsati, P. López-Ruiz, M. A. Cortés, B. Colás, A. Riera, *ChemBioChem* **2011**, *12*, 625–632.

[28]   P. Martín-Gago, M. Gomez-Caminals, R. Ramón, X. Verdaguer, P. Martin-Malpartida, E. Aragón, J. Fernández-Carneado, B. Ponsati, P. López-Ruiz, M. A. Cortes, B. Colás, M. J. Maclas, A. Riera, *Angew. Chemie - Int. Ed.* **2012**, *51*, 1820–1825.

[29]   P. Martín-Gago, E. Aragón, M. Gomez-Caminals, J. Fernández-Carneado, R. Ramón, P. Martin-Malpartida, X. Verdaguer, P. López-Ruiz, B. Colás, M. A. Cortes, B. Ponsati, M. J. Macias, A. Riera, *Molecules* **2013**, *18*, 14564–14584.

[30]   P. Martín-Gago, R. Ramón, E. Aragón, J. Fernández-Carneado, P. Martin-Malpartida, X. Verdaguer, P. López-Ruiz, B. Colás, M. A. Cortes, B. Ponsati, M. J. Macias, A. Riera, *Bioorganic Med. Chem. Lett.* **2014**, *24*, 103–107.

[31]   P. Martin-Gago, A. Rol, T. Todorovski, E. Aragon, P. Martin-Malpartida, X. Verdaguer, M. Vallès Miret, J. Fernandez-Carneado, B. Ponsati, M. J. Maclas, A. Riera, *Sci. Rep.* **2016**, *6*, 1–9.

[32]   Á. Rol, T. Todorovski, P. Martin-Malpartida, A. Escolà, E. Gonzalez-Rey, E. Aragón, X. Verdaguer, M. Vallès-Miret, J. Farrera-Sinfreu, E. Puig, J. Fernández-Carneado, B. Ponsati, M. Delgado, A. Riera, M. J. Macias, *Nat. Commun.* **2021**, *12*, 1–15.

[33]   A. Parente Dueña, B. Ponsati Obiols, J. Fernández-Carneado, M. Gómez Caminals, R. Jordana i Lluch, *Peptide Ligands of Somatostatin Receptors*, **2010**, WO2010128098 A1.

[34]   J. Rivier, M. Brown, W. Vale, *Biochem. Biophys. Res. Commun.* **1975**, *65*, 746–751.

[35]   J. Farrera-Sinfreu, L. Matalonga Borrel, L. Gort Mas, R. Pascual Martínez, A. Ferrer Montiel, A. Ribes Rubió, B. Ponsati Obiols, *Bicalutamide Analogs or (S)-Bicalutamide as Exocytosis Activating Compounds for Use in the Treatment of a Lysosomal Storage Disorder or Glycogenosis*, **2019**, EP3086784B1.

[36]   K. D. James, N. N. Ekwuribe, *Tetrahedron* **2002**, *58*, 5905–5908.

[37]   F. M. Platt, A. D'Azzo, B. L. Davidson, E. F. Neufeld, C. J. Tifft, *Nat. Rev. Dis. Prim.* **2018**, *4*, 1–25.

[38]   R. B. Merrifield, *J. Am. Chem. Soc.* **1963**, *85*, 2149–2154.

[39]   M. Verlander, *Int. J. Pept. Res. Ther.* **2007**, *13*, 75–82.

[40]   A. A. Zompra, A. S. Galanis, O. Werbitzky, F. Albericio, *Future Med. Chem.* **2009**, *1*, 361–377.

[41]   J. H. Rasmussen, *Bioorganic Med. Chem.* **2018**, *26*, 2914–2918.

[42]   L. A. Carpino, G. Y. Han, *J. Org. Chem.* **1972**, 3404–3409.

[43] L. A. Carpino, G. Y. Han, *J. Am. Chem. Soc.* **1970**, *92*, 5748–5749.
[44] G. Barany, F. Albericio, *J. Am. Chem. Soc.* **1985**, *107*, 4936–4942.
[45] M. Muttenthaler, F. Albericio, P. E. Dawson, *Nat. Protoc.* **2015**, *10*, 1067–1083.
[46] W. König, R. Geiger, *Chem. Ber.* **1970**, *103*, 788–798.
[47] G. W. Anderson, J. E. Zimmerman, F. M. Callahan, *J. Am. Chem. Soc.* **1963**, *85*, 3039.
[48] R. Subirós-Funosas, R. Prohens, R. Barbas, A. El-Faham, F. Albericio, *Chem. - A Eur. J.* **2009**, *15*, 9394–9403.
[49] F. Albericio, *Curr. Opin. Chem. Biol.* **2004**, *8*, 211–221.
[50] B. G. de La Torre, D. Andreu, *J. Pept. Sci.* **2008**, *14*, 360–363.
[51] Y. E. Jad, A. Kumar, A. El-Faham, B. G. De La Torre, F. Albericio, *ACS Sustain. Chem. Eng.* **2019**, *7*, 3671–3683.
[52] D. Prat, A. Wells, J. Hayler, H. Sneddon, C. R. McElroy, S. Abou-Shehada, P. J. Dunn, *Green Chem.* **2015**, *18*, 288–296.
[53] K. C. Pugh, E. J. York, J. M. Stewart, *Int. J. Pept. Protein Res.* **1992**, *40*, 208–213.
[54] K. Hojo, M. Maeda, K. Kawasaki, *J. Pept. Sci.* **2001**, *7*, 615–618.
[55] K. Hojo, M. Maeda, K. Kawasaki, *Tetrahedron* **2004**, *60*, 1875–1886.
[56] K. Hojo, M. Maeda, T. J. Smith, E. Kita, F. Yamaguchi, S. Yamamoto, K. Kawasaki, *Chem. Pharm. Bull. (Tokyo).* **2004**, *52*, 422–427.
[57] K. Hojo, M. Maeda, K. Kawasaki, *Tetrahedron Lett.* **2004**, *45*, 9293–9295.
[58] A. S. Galanis, F. Albericio, M. Grøtli, *Org. Lett.* **2009**, *11*, 4488–4491.
[59] A. R. Katritzky, D. N. Haase, J. V Johnson, A. Chung, V. Uni, V. Gaines, R. C. J. C. Soc, P. Trans, *J. Org. Chem.* **2009**, 2028–2032.
[60] K. Hojo, H. Ichikawa, Y. Fukumori, K. Kawasaki, *Int. J. Pept. Res. Ther.* **2008**, *14*, 373–380.
[61] S. Knauer, T. M. L. Roese, O. Avrutina, H. Kolmar, *Method for Peptide Synthesis and Apparatus for Carrying out a Method for Solid Phase Synthesis of Peptides*, **2016**, WO2016050764.
[62] K. Hojo, A. Hara, H. Kitai, M. Onishi, H. Ichikawa, Y. Fukumori, K. Kawasaki, *Chem. Cent. J.* **2011**, *5*, 49.
[63] K. Hojo, H. Ichikawa, M. Maeda, S. Kida, Y. Fukumori, K. Kawasaki, *J. Pept. Sci.* **2007**, 493–497.
[64] K. Hojo, H. Ichikawa, A. Hara, M. Onishi, K. Kawasaki, Y. Fukumori, *Protein Pept. Lett.* **2012**, *19*, 1231–1236.
[65] K. Hojo, N. Shinozaki, A. Hara, M. Onishi, Y. Fukumori, H. Ichikawa, *Protein Pept. Lett.* **2013**, 1122–1128.
[66] K. Hojo, N. Shinozaki, Y. Nozawa, Y. Fukumori, H. Ichikawa, *Appl. Sci.* **2013**, *3*, 614–623.
[67] K. Hojo, N. Shinozaki, K. Hidaka, Y. Tsuda, Y. Fukumori, H. Ichikawa, J. D. Wade, *Amino Acids* **2014**, *46*, 2347–2354.
[68] J. D. Moseley, C. O. Kappe, *Green Chem.* **2011**, *13*, 794–806.
[69] A. De La Hoz, A. Díaz-Ortiz, P. Prieto, in *RSC Green Chem.*, Royal Society Of Chemistry, **2016**, pp. 1–33.
[70] C. J. Clarke, W. C. Tu, O. Levers, A. Bröhl, J. P. Hallett, *Chem. Rev.* **2018**, *118*, 747–800.
[71] C. M. Alder, J. D. Hayler, R. K. Henderson, A. M. Redman, L. Shukla, L. E. Shuster, H. F. Sneddon, *Green Chem.* **2016**, *18*, 3879–3890.
[72] A. Benazzouz, L. Moity, C. Pierlot, M. Sergent, V. Molinier, J. M. Aubry, *Ind. Eng. Chem. Res.* **2013**, *52*, 16585–16597.
[73] C. Capello, U. Fischer, K. Hungerbühler, *Green Chem.* **2007**, *9*, 927–93.
[74] G. A. Acosta, M. Del Fresno, M. Paradis-Bas, M. Rigau-DeLlobet, S. Côté, M. Royo, F. Albericio, *J. Pept. Sci.* **2009**, *15*, 629–633.
[75] F. P. Byrne, S. Jin, G. Paggiola, T. H. M. Petchey, J. H. Clark, T. J. Farmer, A. J. Hunt, C. Robert McElroy, J. Sherwood, *Sustain. Chem. Process.* **2016**, *4*, 7.
[76] D. S. MacMillan, J. Murray, H. F. Sneddon, C. Jamieson, A. J. B. Watson, *Green Chem.* **2013**, *15*, 596–600.
[77] Y. E. Jad, G. A. Acosta, S. N. Khattab, B. G. De La Torre, T. Govender, H. G. Kruger, A. El-Faham, F. Albericio, *Amino Acids* **2016**, *48*, 419–426.
[78] Y. E. Jad, G. A. Acosta, T. Govender, H. G. Kruger, A. El-Faham, B. G. De La Torre, F. Albericio, *ACS Sustain. Chem. Eng.* **2016**, *4*, 6809–6814.
[79] Y. E. Jad, T. Govender, H. G. Kruger, A. El-Faham, B. G. De La Torre, F. Albericio, *Org. Process Res. Dev.* **2017**, *21*, 365–369.
[80] A. Kumar, Y. E. Jad, A. El-Faham, B. G. de la Torre, F. Albericio, *Tetrahedron Lett.* **2017**, *58*, 2986–2988.
[81] A. Kumar, Y. E. Jad, J. M. Collins, F. Albericio, B. G. De La Torre, *ACS Sustain. Chem. Eng.* **2018**, *6*, 8034–8039.
[82] J. M. Collins, K. A. Porter, S. K. Singh, G. S. Vanier, *Org. Lett.* **2014**, *16*, 940–943.
[83] L. A. Carpino, E. Krause, C. D. Sferdean, M. Schümann, H. Fabian, M. Bienert, M. Beyermann, *Tetrahedron Lett.* **2004**, *45*, 7519–7523.
[84] S. B. Lawrenson, R. Arav, M. North, *Green Chem.* **2017**, *19*, 1685–1691.
[85] A. I. Adeleye, D. Patel, D. Niyogi, B. Saha, *Ind. Eng. Chem. Res.* **2014**, *53*, 18647–18657.
[86] J. Lopez, S. Pletscher, A. Aemissegger, C. Bucher, F. Gallou, *Org. Process Res. Dev.* **2018**, *22*, 494–503.
[87] J. Sherwood, H. L. Parker, K. Moonen, T. J. Farmer, A. J. Hunt, *Green Chem.* **2016**, *18*, 3990–3996.
[88] J. Pawlas, B. Antonic, M. Lundqvist, T. Svensson, J. Finnman, J. H. Rasmussen, *Green Chem.* **2019**, *21*, 2594–2600.
[89] A. R. Katritzky, Y. Zhang, S. K. Singh, *Synthesis (Stuttg).* **2003**, *6*, 2795–2798.
[90] A. R. Katritzky, K. Suzuki, S. K. Singh, *Synthesis (Stuttg).* **2004**, *5*, 2645–2652.
[91] A. R. Katritzky, P. Angrish, D. Hür, K. Suzuki, *Synthesis (Stuttg).* **2005**, 397–402.
[92] A. R. Katritzky, P. Angrish, K. Suzuki, *Synthesis (Stuttg).* **2006**, 411–424.
[93] R. G. Denkewalter, H. Schwam, R. G. Strachan, T. E. Beesley, D. F. Veber, E. F. Schoenewaldt, H. Barkemeyer, W. J. Paleveda, T. A. Jacob, R. Hirschmann, *J. Am. Chem. Soc.* **1966**, *88*, 3163–3164.
[94] C. A. G. N. Montalbetti, V. Falque, *Tetrahedron* **2005**, *61*, 10827–10852.
[95] R. De Marco, A. Tolomelli, A. Greco, L. Gentilucci, *ACS Sustain. Chem. Eng.* **2013**, *1*, 566–569.

[96]   V. Declerck, P. Nun, J. Martinez, F. Lamaty, *Angew. Chemie - Int. Ed.* **2009**, *48*, 9318–9321.

[97]   J. Bonnamour, T. X. Métro, J. Martinez, F. Lamaty, *Green Chem.* **2013**, *15*, 1116–1120.

[98]   J. E. Zadina, L. Hackler, L. J. Ge, A. J. Kastin, *Nature* **1997**, *386*, 499–502.

[99]   B. Henkel, L. Zhang, E. Bayer, *Liebigs Ann.* **1997**, 2161–2168.

[100] N. Thieriet, F. Guibé, F. Albericio, *Org. Lett.* **2000**, *2*, 1815–1817.

[101] A. Johansson, E. Åkerblom, K. Ersmark, G. Lindeberg, A. Hallberg, *J. Comb. Chem.* **2000**, *2*, 496–507.

[102] W. G. Gutheil, Q. Xu, *Chem. Pharm. Bull. (Tokyo).* **2002**, *50*, 688–691.

[103] A. D. Merg, R. Naik, G. C. Schatz, J. Slocik, M. G. Blaber, N. L. Rosi, *Langmuir* **2015**, *31*, 9492–9501.

[104] S. F. Andrade, B. G. Oliveira, L. C. Pereira, J. P. Ramos, A. R. Joaquim, M. Steppe, E. M. Souza-Fagundes, R. J. Alves, *Eur. J. Med. Chem.* **2017**, *138*, 13–25.

[105] J. Cornella, J. T. Edwards, T. Qin, S. Kawamura, J. Wang, C. M. Pan, R. Gianatassio, M. Schmidt, M. D. Eastgate, P. S. Baran, *J. Am. Chem. Soc.* **2016**, *138*, 2174–2177.

[106] A. Vaisburg, N. Bernstein, S. Frechette, M. Allan, E. Abou-Khalil, S. Leit, O. Moradei, G. Bouchain, J. Wang, S. H. Woo, M. Fournel, P. T. Yan, M. C. Trachy-Bourget, A. Kalita, C. Beaulieu, Z. Li, A. R. MacLeod, J. M. Besterman, D. Delorme, *Bioorganic Med. Chem. Lett.* **2004**, *14*, 283–287.

[107] S. Specklin, J. Cossy, *J. Org. Chem.* **2015**, *80*, 3302–3308.

[108] L. Wang, K. J. Hale, *Org. Lett.* **2015**, *17*, 4200–4203.

[109] R. M. Pater De, B. Lange De, *Method for Acylating a Cyclic Peptide*, **2020**, EP3230304B1.

[110] C. Kaduk, H. Wenschuh, M. Beyermann, K. Forner, L. A. Carpino, M. Bienert, *Lett. Pept. Sci.* **1996**, *2*, 285–288.

[111] M. Meguro, *Process of Preparing Peptides Using Diphenyl Phosphorylazide (DPPA)*, **1975**, US3873509.

[112] R. A. Hughes, S. P. Thompson, L. Alcaraz, C. J. Moody, *J. Am. Chem. Soc.* **2005**, *127*, 15644–15651.

[113] B. Vasantha, V. V Sureshbabu, *Indian J. Chem.* **2010**, *49B*, 812–817.

[114] V. V. Sureshbabu, H. S. Lalithamba, N. Narendra, H. P. Hemantha, *Org. Biomol. Chem.* **2010**, *8*, 835–840.

[115] F. Guillier, D. Orain, M. Bradley, *Chem. Rev.* **2000**, *100*, 3859.

[116] V. Martin, P. H. G. Egelund, H. Johansson, S. Thordal Le Quement, F. Wojcik, D. Sejer Pedersen, *RSC Adv.* **2020**, *10*, 42457–42492.

[117] C. Petrou, Y. Sarigiannis, *Peptide Synthesis: Methods, Trends, and Challenges*, Elsevier Ltd, **2018**.

[118] R. Behrendt, P. White, J. Offer, *J. Pept. Sci.* **2016**, *22*, 4–27.

[119] A. Isidro-llobet, A. Mercedes, F. Albericio, *Chem. Rev.* **2009**, 2455–2504.

[120] M. Amblard, J.-A. Fehrentz, J. Martinez, G. Subra, *Mol. Biotechnol.* **2006**, *33*, 239–54.

[121] O. Al Musaimi, Y. E. Jad, A. Kumar, J. M. Collins, A. Basso, B. G. de la Torre, F. Albericio, *Curr. Opin. Green Sustain. Chem.* **2018**, *11*, 99–103.

[122] K. Barlos, O. Chatzi, D. Gatos, G. Stavropoulos, *J. Pept. Protein Res.* **1991**, 513–520.

[123] R. K. Henderson, A. P. Hill, A. M. Redman, H. F. Sneddon, *Green Chem.* **2015**, *17*, 945–949.

[124] Bachem AG, *Solid Phase Peptide Synthesis*, **2020**.

[125] D. A. Stetsenko, P. Palladino, *Method and Compositions for Removing Acid-Labile Protecting Groups*, **2014**, WO2014033466 A1.

[126] L. A. Carpino, H. Shroff, S. A. Triolo, E. S. M. E. Mansour, H. Wenschuh, F. Albericio, *Tetrahedron Lett.* **1993**, *34*, 7829–7832.

[127] P. Palladino, V. Castelletto, A. Dehsorkhi, D. Stetsenko, I. W. Hamley, *Chem. Commun.* **2012**, *48*, 9774–9776.

[128] P. Palladino, V. Castelletto, A. Dehsorkhi, D. Stetsenko, I. W. Hamley, *Langmuir* **2012**, *28*, 12209–12215.

[129] O. Al Musaimi, Y. E. Jad, A. Kumar, A. El-Faham, J. M. Collins, A. Basso, B. G. De La Torre, F. Albericio, *Org. Process Res. Dev.* **2018**, *22*, 1809–1816.

[130]

[131]

[132]

[133]

[134]

[135]

[136]

[137]

[138]

[139]

[140]

[141]

[142]

[143]

[144]

[145]

[146]

[147] ██
██
████████████████████████

[148] ██
████████

[149] ██
████████

[150] ██
████████████████

[151] D. Teutonico, S. Montanari, G. Ponchel, *Expert Opin. Drug Deliv.* **2012**, *9*, 343–354.

[152] A. Van Gysel, F. Soeterbroeck, G. Vermeulen, *Acetonitrile Recycling Process*, **2005**, WO2005044783A2.

[153] T. Günther, G. Tulipano, P. Dournaud, C. Bousquet, Z. Csaba, H. J. Kreienkamp, A. Lupp, M. Korbonits, J. P. Castaño, H. J. Wester, M. Culler, S. Melmed, S. Schulz, *Pharmacol. Rev.* **2018**, *70*, 763–835.

[154] D. Hoyer, G. I. Bell, M. Berelowitz, J. Epelbaum, W. Feniuk, P. P. A. Humphrey, A. M. O'Carroll, Y. C. Patel, A. Schonbrunn, J. E. Taylor, T. Reisine, *Trends Pharmacol. Sci.* **1995**, *16*, 86–88.

[155] A. Janecka, M. Zubrzycka, T. Janecki, *J. Pept. Res.* **2001**, *58*, 91–107.

[156] G. Tulipano, S. Schulz, in *Eur. J. Endocrinol. Suppl.*, **2007**, pp. S3–S11.

[157] Y. Patel, *Front. Neuroendocrinol.* **1999**, *20*, 157–198.

[158] T. Stroh, A. C. Jackson, C. Dal Farra, A. Schonbrunn, J. P. Vincent, A. Beaudet, *Synapse* **2000**, *38*, 177–86.

[159] Q. Liu, A. Schonbrunn, *J. Biol. Chem.* **2001**, *276*, 3709–17.

[160] Z. Csaba, S. Peineau, P. Dournaud, *J. Mol. Endocrinol.* **2012**, *48*, DOI 10.1530/JME-11-0121.

[161] S. Jacobs, S. Schulz, *Mol. Cell. Endocrinol.* **2008**, *286*, 58–62.

[162] D. Nouel, G. Gaudriault, M. Houle, T. Reisine, J. P. Vincent, J. Mazella, A. Beaudet, *Endocrinology* **1997**, *138*, 296–306.

[163] G. Tulipano, R. Stumm, M. Pfeiffer, H. J. Kreienkamp, V. Höllt, S. Schulz, *J. Biol. Chem.* **2004**, *279*, 21374–21382.

[164] S. Lesche, D. Lehmann, F. Nagel, H. A. Schmid, S. Schulz, *J. Clin. Endocrinol. Metab.* **2009**, *94*, 654–61.

[165] A. Lehmann, A. Kliewer, T. Günther, F. Nagel, S. Schulz, *Mol. Endocrinol.* **2016**, *30*, 645–659.

[166] K. S. M. Smalley, J. A. Koenig, W. Feniuk, P. P. A. Humphrey, *Br. J. Pharmacol.* **2001**, *132*, 1102–1110.

[167] A. Petrich, A. Mann, A. Kliewer, F. Nagel, A. Strigli, J. C. Märtens, F. Pöll, S. Schulz, *Mol. Endocrinol.* **2013**, *27*, 671–682.

[168] S. Schulz, A. Lehmann, A. Kliewer, F. Nagel, *Br. J. Pharmacol.* **2014**, *171*, 1591–1599.

[169] J. P. Moreau, F. V. DeFeudis, *Life Sci.* **1987**, *40*, 419–437.

[170] W. Vale, C. Rivier, M. Brown, *Annu. Rev. Physiol.* **1977**, *39*, 473–527.

[171] W. Vale, J. Rivier, N. Ling, M. Brown, *Metabolism* **1978**, *27*, 1391–1401.

[172] B. H. Hirst, B. Shaw, C. A. Meyers, D. H. Coy, *Regul. Pept.* **1980**, *1*, 97–113.

[173] S. W. J. Lamberts, A. J. Van Der Lely, W. W. De Herder, L. J. Hofland, *N. Engl. J. Med.* **1996**, *334*, 255–260.

[174] R. Z. Cai, T. Karashima, J. Guoth, B. Szoke, D. Olsen, A. V. Schally, *Proc. Natl. Acad. Sci.* **1987**, *84*, 2502–2506.

[175] J. E. Taylor, A. E. Bogden, J. P. Moreau, D. H. Coy, *Biochem. Biophys. Res. Commun.* **1988**, *153*, 81–86.

[176] Y. C. Patel, C. B. Srikant, *Endocrinology* **1994**, *135*, 2814–2817.

[177] G. Weckbecker, U. Briner, I. Lewis, C. Bruns, *Endocrinology* **2002**, *143*, 4123–4130.

[178] G. Liapakis, C. Hoeger, J. Rivier, T. Reisine, *J. Pharmacol. Exp. Ther.* **1996**, *276*.

[179] M. Z. Strowski, R. M. Parmar, A. D. Blake, J. M. Schaeffer, *Endocrinology* **2000**, *141*, 111–117.

[180] E. E. Müller, V. Locatelli, D. Cocchi, *Physiol. Rev.* **1999**, *79*, 511–607.

[181] R. Guillemin, J. E. Gerich, *Annu. Rev. Med.* **1976**, *27*, 379–388.

[182] K. Sharma, C. B. Srikant, *Int. J. Cancer* **1998**, *76*, 259–266.

[183] J. Guillermet, N. Saint-Laurent, P. Rochaix, O. Cuvillier, T. Levade, A. V Schally, L. Pradayrol, L. Buscail, C. Susini, C. Bousquet, *Proc. Natl. Acad. Sci. U. S. A.* **2003**, *100*, 155–60.

[184] C.-Z. Qiu, C. Wang, Z.-X. Huang, S.-Z. Zhu, Y.-Y. Wu, J.-L. Qiu, *World J. Gastroenterol.* **2006**, *12*, 2011–5.

[185] T. Moody, D. Chan, J. Fahrenkrug, R. Jensen, *Curr. Pharm. Des.* **2003**, *9*, 495–509.

[186] A. V. Schally, *Cancer Res.* **1988**, *48*, 6977–6985.

[187] J. C. Reubi, *Endocr. Rev.* **2003**, *24*, 389–427.

[188] J. C. Reubi, U. Horisberger, C. E. Essed, J. Jeekel, J. G. H. Klijn, S. W. J. Lamberts, *Gastroenterology* **1988**, *95*, 760–763.

[189] J. C. Reubi, B. Waser, A. Schmassmann, J. A. Laissue, *Int. J. Cancer* **1999**, *81*, 376–386.

[190] W. E. Fisher, T. A. Doran, P. M. Ii, L. G. Boros, E. C. Ellison, W. J. Schirmer, *J. Natl. Cancer Inst.* **1998**, *90*, 322–324.

[191] T. Fischer, C. Doll, S. Jacobs, A. Kolodziej, R. Stumm, S. Schulz, *J. Clin. Endocrinol. Metab.* **2008**, *93*, 4519–24.

[192] A. Lupp, A. Hunder, A. Petrich, F. Nagel, C. Doll, S. Schulz, *Neuroendocrinology* **2011**, *94*, 255–64.

[193] A. Saveanu, M. Muresan, C. De Micco, D. Taieb, A.-L. Germanetti, F. Sebag, J.-F. Henry, L. Brunaud, A. Enjalbert, G. Weryha, A. Barlier, *Endocr. Relat. Cancer* **2011**, *18*, 287–300.

[194] M. S. Elston, G. Y. Meyer-Rochow, H. M. Conaglen, A. Clarkson, R. J. Clifton-Bligh, J. V Conaglen, A. J. Gill, *Hum. Pathol.* **2015**, *46*, 390–6.

[195] S. Schulz, S. U. Pauli, S. Schulz, M. Händel, K. Dietzmann, R. Firsching, V. Höllt, *Clin. Cancer Res.* **2000**, *6*, 1865–74.

[196] J. Guyotat, J. Champier, G. S. Pierre, A. Jouvet, P. Bret, C. Brisson, M. F. Belin, F. Signorelli, M. F. Montange, *J. Neurooncol.* **2001**, *51*, 93–103.

[197]   P. Cervera, C. Videau, C. Viollet, C. Petrucci, J. Lacombe, R. Winsky-Sommerer, Z. Csaba, L. Helboe, C. Daumas-Duport, J. C. Reubi, J. Epelbaum, *J. Neuroendocrinol.* **2002**, *14*, 458–471.

[198]   M. Remke, E. Hering, N. U. Gerber, M. Kool, D. Sturm, C. H. Rickert, J. Gerß, S. Schulz, T. Hielscher, M. Hasselblatt, A. Jeibmann, V. Hans, V. Ramaswamy, M. D. Taylor, T. Pietsch, S. Rutkowski, A. Korshunov, C.-M. Monoranu, M. C. Frühwald, *Childs. Nerv. Syst.* **2013**, *29*, 1253–62.

[199]   A. R. Albers, M. S. O'Dorisio, D. A. Balster, M. Caprara, P. Gosh, F. Chen, C. Hoeger, J. Rivier, G. D. Wenger, T. M. O'Dorisio, S. J. Qualman, *Regul. Pept.* **2000**, *88*, 61–73.

[200]   R. Srirajaskanthan, J. Watkins, L. Marelli, K. Khan, M. E. Caplin, *Neuroendocrinology* **2009**, *89*, 308–14.

[201]   V. Zamora, A. Cabanne, R. Salanova, C. Bestani, E. Domenichini, F. Marmissolle, N. Giacomi, J. O'Connor, G. Méndez, E. Roca, *Dig. Liver Dis.* **2010**, *42*, 220–225.

[202]   K. Okuwaki, M. Kida, T. Mikami, H. Yamauchi, H. Imaizumi, S. Miyazawa, T. Iwai, M. Takezawa, M. Saegusa, M. Watanabe, W. Koizumi, *Cancer* **2013**, *119*, 4094–102.

[203]   S. Mehta, P. R. de Reuver, P. Gill, J. Andrici, L. D'Urso, A. Mittal, N. Pavlakis, S. Clarke, J. S. Samra, A. J. Gill, *Medicine (Baltimore).* **2015**, *94*, e1281.

[204]   Z. R. Qian, T. Li, M. Ter-Minassian, J. Yang, J. A. Chan, L. K. Brais, Y. Masugi, A. Thiaglingam, N. Brooks, R. Nishihara, M. Bonnemarie, A. Masuda, K. Inamura, S. A. Kim, K. Mima, Y. Sukawa, R. Dou, X. Lin, D. C. Christiani, F. Schmidlin, C. S. Fuchs, U. Mahmood, S. Ogino, M. H. Kulke, *Pancreas* **2016**, *45*, 1386–1393.

[205]   Y. Wang, W. Wang, K. Jin, C. Fang, Y. Lin, L. Xue, S. Feng, Z. Zhou, C. Shao, M. Chen, X. Yu, J. Chen, *Oncol. Lett.* **2017**, *13*, 1165–1174.

[206]   H. Kajiwara, K. Hirabayashi, M. Miyazawa, N. Nakamura, T. Hirasawa, T. Muramatsu, M. Mikami, M. Yasuda, R. Y. Osamura, *Arch. Gynecol. Obstet.* **2009**, *279*, 521–525.

[207]   G. Mizutani, Y. Nakanishi, N. Watanabe, T. Honma, Y. Obana, T. Seki, S. Ohni, N. Nemoto, *Acta Histochem. Cytochem.* **2012**, *45*, 167–176.

[208]   I. Evangelou, C. Petraki, P. Msaouel, A. Scorilas, E. Sdrolia, G. Padazi, V. Koborozos, M. Koutsilieris, *Eur. J. Clin. Invest.* **2012**, *42*, 777–783.

[209]   M. Bläker, M. Schmitz, A. Gocht, S. Burghardt, M. Schulz, D. C. Bröring, A. Pace, H. Greten, A. De Weerth, *J. Hepatol.* **2004**, *41*, 112–8.

[210]   H. Reynaert, K. Rombouts, A. Vandermonde, D. Urbain, U. Kumar, P. Bioulac-Sage, M. Pinzani, J. Rosenbaum, A. Geerts, *Gut* **2004**, *53*, 1180–1189.

[211]   C. Verhoef, H. van Dekken, L. J. Hofland, P. E. Zondervan, J. H. W. de Wilt, R. van Marion, R. A. de Man, J. N. M. IJzermans, C. H. J. van Eijck, *Dig. Surg.* **2008**, *25*, 21–6.

[212]   M. Pilichowska, N. Kimura, M. Schindler, A. Suzuki, R. Yoshida, H. Nagura, *Endocr. Pathol.* **2000**, *11*, 57–67.

[213]   C. Orlando, C. C. Raggi, S. Bianchi, V. Distante, L. Simi, V. Vezzosi, S. Gelmini, P. Pinzani, M. C. Smith, A. Buonamano, E. Lazzeri, M. Pazzagli, L. Cataliotti, M. Maggi, M. Serio, *Endocr. Relat. Cancer* **2004**, *11*, 323–332.

[214]   U. Kumar, S. I. Grigorakis, H. L. Watt, R. Sasi, L. Snell, P. Watson, S. Chaudhari, *Breast Cancer Res. Treat.* **2005**, *92*, 175–186.

[215]   A. Frati, R. Rouzier, B. Lesieur, G. Werkoff, M. Antoine, A. Rodenas, E. Darai, E. Chereau, *Anticancer Res.* **2014**, *34*, 3997–4004.

[216]   S. Schulz, J. Schmitt, W. Weise, *Gynecol. Oncol.* **2003**, *89*, 385–390.

[217]   G. H. Hall, L. W. Turnbull, I. Richmond, L. Helboe, S. L. Atkin, *Br. J. Cancer* **2002**, *87*, 86–90.

[218]   D.-V. Matei, G. Renne, M. Pimentel, M. T. Sandri, L. Zorzino, E. Botteri, C. De Cicco, G. Musi, A. Brescia, F. Mazzoleni, V. Tringali, S. Detti, O. de Cobelli, *Clin. Genitourin. Cancer* **2012**, *10*, 164–73.

[219]   J. K. Hennigs, J. Müller, M. Adam, J. M. Spin, E. Riedel, M. Graefen, C. Bokemeyer, G. Sauter, H. Huland, T. Schlomm, S. Minner, *PLoS One* **2014**, *9*, e100469.

[220]   J. C. Reubi, B. Waser, J. C. Schaer, J. A. Laissue, *Eur. J. Nucl. Med.* **2001**, *28*, 836–46.

[221]   A. A. Sinisi, A. Bellastella, D. Prezioso, M. R. Nicchio, T. Lotti, M. Salvatore, D. Pasquali, *J. Clin. Endocrinol. Metab.* **1997**, *82*, 2566–9.

[222]   F. Kosari, J. M. A. Munz, C. D. Savci-Heijink, C. Spiro, E. W. Klee, D. M. Kube, L. Tillmans, J. Slezak, R. J. Karnes, J. C. Cheville, G. Vasmatzis, *Clin. Cancer Res.* **2008**, *14*, 1734–1743.

[223]   A. D. Herrera-Martínez, M. D. Gahete, R. Sánchez-Sánchez, R. O. Salas, R. Serrano-Blanch, Á. Salvatierra, L. J. Hofland, R. M. Luque, M. A. Gálvez-Moreno, J. P. Castaño, *Lung Cancer* **2017**, *109*, 128–136.

[224]   A. Lupp, F. Nagel, S. Schulz, *Regul. Pept.* **2013**, *183*, 1–6.

[225]   A. Lupp, F. Nagel, C. Doll, C. Röcken, M. Evert, C. Mawrin, W. Saeger, S. Schulz, *Neuroendocrinology* **2012**, *96*, 301–10.

[226]   F. Gabalec, M. Drastikova, T. Cesak, D. Netuka, V. Masopust, J. Machac, J. Marek, J. Cap, M. Beranek, *Physiol. Res.* **2015**, 369–377.

[227]   M. Lee, A. Lupp, N. Mendoza, N. Martin, R. Beschorner, J. Honegger, J. Schlegel, T. Shively, E. Pulz, S. Schulz, F. Roncaroli, N. S. Pellegata, *Endocr. Relat. Cancer* **2015**, *22*, 111–9.

[228]   D. Kaemmerer, T. Träger, M. Hoffmeister, B. Sipos, M. Hommann, J. Sänger, S. Schulz, A. Lupp, *Oncotarget* **2015**, *6*, 27566–79.

[229]   K. B. Song, S. C. Kim, J. H. Kim, D.-W. Seo, S.-M. Hong, K.-M. Park, D. W. Hwang, J. H. Lee, Y.-J. Lee, *Pancreas* **2016**, *45*, 187–92.

[230]   D. Kaemmerer, E. Specht, J. Sänger, R. M. Wirtz, M. Sayeg, S. Schulz, A. Lupp, *J. Clin. Endocrinol. Metab.* **2015**, *100*, 831–40.

[231]   W. Y. Zhao, C. Zhuang, J. Xu, M. Wang, Z. Z. Zhang, L. Tu, C. J. Wang, T. L. Ling, H. Cao, Z. G. Zhang, *Am. J. Transl.*

Res. **2014**, *6*, 831–840.

[232]   Y. Taniyama, T. Suzuki, Y. Mikami, T. Moriya, S. Satomi, H. Sasano, *Endocr. J.* **2005**, *52*, 605–611.

[233]   R. Panetta, Y. C. Patel, *Life Sci.* **1994**, *56*, 333–342.

[234]   K. Pazaitou-Panayiotou, E. T. Janson, T. Koletsa, V. Kotoula, M. Stridsberg, G. Karkavelas, G. Karayannopoulou, *Hormones* **2012**, *11*, 290–296.

[235]   H. Atkinson, J. A. England, A. Rafferty, V. Jesudason, K. Bedford, L. Karsai, S. L. Atkin, *Int. J. Exp. Pathol.* **2013**, *94*, 226–229.

[236]   S. Woelfl, S. Bogner, H. Huber, S. Salaheddin-Nassr, M. Hatzl, C. Decristoforo, I. Virgolini, M. Gabriel, *NuklearMedizin* **2014**, *53*, 179–185.

[237]   M. Herac, B. Niederle, M. Raderer, M. Krebs, K. Kaserer, O. Koperek, *APMIS* **2016**, *124*, 839–845.

[238]   S. Stollberg, D. Kämmerer, E. Neubauer, S. Schulz, I. Simonitsch-Klupp, B. Kiesewetter, M. Raderer, A. Lupp, *J. Cancer Res. Clin. Oncol.* **2016**, *142*, 2239–2247.

[239]   T. Ruuska, Y. Ramírez Escalante, S. Vaittinen, M. Gardberg, A. Kiviniemi, P. Marjamäki, J. Kemppainen, S. Jyrkkiö, H. Minn, *Acta Oncol.* **2018**, *57*, 283–289.

[240]   C. Lapa, H. Hänscheid, V. Wild, T. Pelzer, A. Schirbel, R. A. Werner, S. Droll, K. Herrmann, A. K. Buck, K. Lückerath, *Oncotarget* **2016**, *7*, 20033–20040.

[241]   C. Gardair, M. Samimi, A. Touzé, P. Coursaget, G. Lorette, A. Caille, E. Wierzbicka, A. Croué, M. Avenel-Audran, F. Aubin, R. Kerdraon, E. Estève, N. Beneton, S. Guyétant, *Neuroendocrinology* **2015**, *101*, 223–235.

[242]   M. Giusti, G. Gussoni, C. M. Cuttica, G. Giordano, *J. Clin. Endocrinol. Metab.* **1996**, *81*, 2089–2097.

[243]   R. J. Robbins, *J. Clin. Endocrinol. Metab.* **1997**, *82*, 15–17.

[244]   A. Colao, L. F. S. Grasso, A. Giustina, S. Melmed, P. Chanson, A. M. Prereira, R. Pivonello, *Nat. Rev. Dis. Prim.* **2019**, *5*, 1–17.

[245]   M. R. Gadelha, M. D. Bronstein, T. Brue, M. Coculescu, M. Fleseriu, M. Guitelman, V. Pronin, G. Raverot, I. Shimon, K. K. Lievre, J. Fleck, M. Aout, A. M. Pedroncelli, A. Colao, *Lancet Diabetes Endocrinol.* **2014**, *2*, 875–884.

[246]   A. Colao, M. D. Bronstein, P. Freda, F. Gu, C. C. Shen, M. Gadelha, M. Fleseriu, A. J. Van Der Lely, A. J. Farrall, K. Hermosillo Reséndiz, M. Ruffin, Y. Chen, M. Sheppard, *J. Clin. Endocrinol. Metab.* **2014**, *99*, 791–799.

[247]   B. M. K. Biller, A. B. Grossman, P. M. Stewart, S. Melmed, X. Bertagna, J. Bertherat, M. Buchfelder, A. Colao, A. R. Hermus, L. J. Hofland, A. Klibanski, A. Lacroix, J. R. Lindsay, J. Newell-Price, L. K. Nieman, S. Petersenn, S. Sonino, G. K. Stalla, B. Swearingen, M. L. Vance, J. A. H. Wass, M. Boscaro, in *J. Clin. Endocrinol. Metab.*, Endocrine Society, **2008**, pp. 2454–2462.

[248]   N. A. Tritos, N. A. Tritos, B. M. K. Biller, B. Swearingen, *Nat. Publ. Gr.* **2011**, *7*, 279–289.

[249]   R. A. Feelders, L. J. Hofland, *J. Clin. Endocrinol. Metab.* **2013**, *98*, 425–438.

[250]   C. de Bruin, R. A. Feelders, A. M. Waaijers, P. M. van Koetsveld, D. M. Sprij-Mooij, S. W. J. Lamberts, L. J. Hofland, *J. Mol. Endocrinol.* **2009**, *42*, 47–56.

[251]   K. Öberg, S. W. J. Lamberts, *Endocr. Relat. Cancer* **2016**, *23*, R551–R566.

[252]   S. J. Kim, J. W. Kim, S. W. Han, D. Y. Oh, S. H. Lee, D. W. Kim, S. A. Im, T. Y. Kim, D. Seog Heo, Y. J. Bang, *BMC Cancer* **2010**, *10*, DOI 10.1186/1471-2407-10-448.

[253]   L. B. Anthony, W. Martin, D. Delbeke, M. Sandler, *Digestion* **1996**, *57*, 50–53.

[254]   J. C. Yao, M. Hassan, A. Phan, C. Dagohoy, C. Leary, J. E. Mares, E. K. Abdalla, J. B. Fleming, J. N. Vauthey, A. Rashid, D. B. Evans, *J. Clin. Oncol.* **2008**, *26*, 3063–3072.

[255]   A. Rinke, H. H. Müller, C. Schade-Brittinger, K. J. Klose, P. Barth, M. Wied, C. Mayer, B. Aminossadati, U. F. Pape, M. Bläker, J. Harder, C. Arnold, T. Gress, R. Arnold, *J. Clin. Oncol.* **2009**, *27*, 4656–4663.

[256]   M. E. Caplin, M. Pavel, J. B. Ćwikła, A. T. Phan, M. Raderer, E. Sedláčková, G. Cadiot, E. M. Wolin, J. Capdevila, L. Wall, G. Rindi, A. Langley, S. Martinez, J. Blumberg, P. Ruszniewski, *N. Engl. J. Med.* **2014**, *371*, 224–233.

[257]   E. P. Krenning, W. A. P. Breeman, P. P. M. Kooij, J. S. Lameris, W. H. Bakker, J. W. Koper, L. Ausema, J. C. Reubi, S. W. J. Lamberts, *Lancet* **1989**, *333*, 242–244.

[258]   W. H. Bakker, R. Albert, C. Bruns, W. A. P. Breeman, L. J. Hofland, P. Marbach, J. Pless, D. Pralet, B. Stolz, J. W. Koper, S. W. J. Lamberts, T. J. Visser, E. P. Krenning, *Life Sci.* **1991**, *49*, 1583–1591.

[259]   W. H. Bakker, E. P. Krenning, J. C. Reubi, W. A. P. Breeman, B. Setyono-Han, M. de Jong, P. P. M. Kooij, C. Bruns, P. M. van Hagen, P. Marbach, T. J. Visser, J. Pless, S. W. J. Lamberts, *Life Sci.* **1991**, *49*, 1593–1601.

[260]   E. P. Krenning, D. J. Kwekkeboom, W. H. Bakker, W. A. P. Breeman, P. P. M. Kooij, H. Y. Oei, M. van Hagen, P. T. E. Postema, M. de Jong, J. C. Reubi, T. J. Visser, A. E. M. Reijs, L. J. Hofland, J. W. Koper, S. W. J. Lamberts, *Eur. J. Nucl. Med.* **1993**, *20*, 716–731.

[261]   E. P. Krenning, W. H. Bakker, P. P. M. Kooij, W. A. P. Breeman, H. Y. Oei, M. De Jong, J. C. Reubi, T. J. Visser, C. Bruns, D. J. Kwekkeboom, A. E. M. Reijs, P. M. Van Hagen, J. W. Koper, S. W. J. Lamberts, *J. Nucl. Med.* **1992**, *33*, 652–658.

[262]   J. A. Koenig, J. M. Edwardson, *Trends Pharmacol. Sci.* **1997**, *18*, 276–287.

[263]   B. Stolz, G. Weckbecker, P. M. Smith-Jones, R. Albert, F. Raulf, C. Bruns, *Eur. J. Nucl. Med.* **1998**, *25*, 668–674.

[264]   P. Antunes, M. Ginj, H. Zhang, B. Waser, R. P. Baum, J. C. Reubi, H. Maecke, *Eur. J. Nucl. Med. Mol. Imaging* **2007**, *34*, 982–993.

[265]   M. Schottelius, J. Šimeček, F. Hoffmann, M. Willibald, M. Schwaiger, H.-J. Wester, *EJNMMI Res.* **2015**, *5*, 22.

[266]   J. Strosberg, G. El-Haddad, E. Wolin, A. Hendifar, J. Yao, B. Chasen, E. Mittra, P. L. Kunz, M. H. Kulke, H. Jacene, D. Bushnell, T. M. O'Dorisio, R. P. Baum, H. R. Kulkarni, M. Caplin, R. Lebtahi, T. Hobday, E. Delpassand, E. Van Cutsem, A. Benson, R. Srirajaskanthan, M. Pavel, J. Mora, J. Berlin, E. Grande, N. Reed, E. Seregni, K. Öberg, M. L. Sierra, P. Santoro, T. Thevenet, J. L. Erion, P. Ruszniewski, D. Kwekkeboom, E. Krenning, in *N. Engl. J. Med.*, Massachussetts

Medical Society, **2017**, pp. 125–135.

[267] T. Brabander, W. A. Van Der Zwan, J. J. M. Teunissen, B. L. R. Kam, R. A. Feelders, W. W. De Herder, C. H. J. Van Eijck, G. J. H. Franssen, E. P. Krenning, D. J. Kwekkeboom, *Clin. Cancer Res.* **2017**, *23*, 4617–4624.

[268] I. Lewis, R. Albert, R. Kneuer, J. Pless, C. Simeon, S. Kerrad, D. Hoyer, C. Bruns, *J. Endocrinol. Invest.* **2005**, *28*, 15–20.

[269] B. Zlatopolskiy, E. Urusova, B. Neumaier, A. Vogg, S. Reske, *J. Nucl. Med.* **2007**, *48*.

[270] M. Fani, F. Braun, A. Mann, A. Kliewer, J. Kaufmann, W. Weber, H. Bouterfa, S. Schulz, H. Maecke, *J. Nucl. Med.* **2012**, *53*.

[271] F. Liu, T. Liu, X. Xu, X. Guo, N. Li, C. Xiong, C. Li, H. Zhu, Z. Yang, *Mol. Pharm.* **2018**, *15*, 619–628.

[272] F. Liu, H. Zhu, C. Li, X. Lin, C. Xiong, C. Li, Z. Yang, *J. Radioanal. Nucl. Chem.* **2016**, *307*, 1069–1075.

[273] F. Liu, X. Guo, T. Liu, X. Xu, N. Li, C. Xiong, C. Li, H. Zhu, Z. Yang, *ACS Med. Chem. Lett.* **2020**, *11*, 450.

[274] A. Tatsi, T. Maina, R. Cescato, B. Waser, E. P. Krenning, M. de Jong, P. Cordopatis, J. C. Reubi, B. A. Nock, *EJNMMI Res.* **2012**, *2*, 25.

[275] J. Clemente, B. Ponsati, G. Jodas, M. Canas, *Procedure for Obtaining the Somatostatin Analog, Octreotide*, **1999**, EP0953577A1.

[276] B. Ponsati, J. Fernández, J. Farrera-Sinfreu, A. Parente, *Cortistatin Analogues for the Treatment of Inflammatory and/or Immune Diseases*, **2014**, EP3046933A1.

[277] A. D. Herrera-Martínez, R. van den Dungen, F. Dogan-Oruc, P. M. Van Koetsveld, M. D. Culler, W. W. De Herder, R. M. Luque, R. A. Feelders, L. J. Hofland, *Endocr. Relat. Cancer* **2019**, *26*, 585–599.

[278] D. Hormaechea-Agulla, J. M. Jiménez-Vacas, E. Gómez-Gómez, F. L. López, J. Carrasco-Valiente, J. Valero-Rosa, M. M. Moreno, R. Sánchez-Sánchez, R. Ortega-Salas, F. Gracia-Navarro, M. D. Culler, A. Ibáñez-Costa, M. D. Gahete, M. J. Requena, J. P. Castaño, R. M. Luque, *FASEB J.* **2017**, *31*, 4682–4696.

[279] A. Ibáñez-Costa, E. Rivero-Cortés, M. C. Vázquez-Borrego, M. D. Gahete, L. Jiménez-Reina, E. Venegas-Moreno, A. de la Riva, M. Á. Arráez, I. González-Molero, H. A. Schmid, S. Maraver-Selfa, I. Gavilán-Villarejo, J. A. García-Arnés, M. A. Japón, A. Soto-Moreno, M. A. Gálvez, R. M. Luque, J. P. Castaño, *J. Endocrinol.* **2016**, *231*, 135–145.

[280] S. Pedraza-Arévalo, D. Hormaechea-Agulla, E. Gómez-Gómez, M. J. Requena, L. A. Selth, M. D. Gahete, J. P. Castaño, R. M. Luque, *Prostate* **2017**, *77*, 1499–1511.

[281] M. C. Vázquez-Borrego, F. L-López, M. A. Gálvez-Moreno, A. C. Fuentes-Fayos, E. Venegas-Moreno, A. D. Herrera-Martínez, C. Blanco-Acevedo, J. Solivera, T. Landsman, M. D. Gahete, A. Soto-Moreno, M. D. Culler, J. P. Castaño, R. M. Luque, *Neuroendocrinology* **2020**, *110*, 70–82.

[282] M. Shahbaz, F. Ruliang, Z. Xu, L. Benjia, W. Cong, H. Zhaobin, N. Jun, *World J. Surg. Oncol.* **2015**, *13*, 1–6.

[283] M. KARAVITAKIS, P. MSAOUEL, V. MICHALOPOULOS, M. KOUTSILIERIS, *Anticancer Res.* **2014**, *34*.

[284] M. Maas, L. Mayer, org Hennenlotter, G. Biol, V. St, S. Walz, M. Scharpf, T. Neumann, A. Stenzl, T. Todenh, **2020**, DOI 10.1016/j.urolonc.2020.07.005.

[285] N. Dizeyi, L. Konrad, A. Bjartell, H. Wu, V. Gadaleanu, J. Hansson, L. Helboe, P. A. Abrahamsson, *Urol. Oncol.* **2002**, *7*, 91–98.

[286] G. Halmos, A. V. Schally, B. Sun, R. Davis, D. G. Bostwick, A. Plonowski, *J. Clin. Endocrinol. Metab.* **2000**, *85*, 2564–2571.

[287] J. Niu, R. Hili, D. R. Liu, *Nat. Chem.* **2013**, *5*, 282–292.

[288] D. Kaemmerer, R. Schindler, F. Mußbach, U. Dahmen, A. Altendorf-Hofmann, O. Dirsch, J. Sänger, S. Schulz, A. Lupp, *BMC Cancer* **2017**, *17*, 1–14.

[289] M. D. Gahete, J. M. Jiménez-Vacas, E. Alors-Pérez, V. Herrero-Aguayo, A. C. Fuentes-Fayos, S. Pedraza-Arévalo, J. P. Castaño, R. M. Luque, *J. Endocrinol.* **2019**, *240*, R73–R96.

[290] S. Soriano, M. Castellano-Muñoz, A. Rafacho, P. Alonso-Magdalena, L. Marroquí, A. Ruiz-Pino, E. Bru-Tarí, B. Merino, E. Irles, M. Bello-Pérez, P. Iborra, S. Villar-Pazos, J. F. Vettorazzi, E. Montanya, R. M. Luque, Á. Nadal, I. Quesada, *Mol. Cell. Endocrinol.* **2019**, *479*, 123–132.

[291] M. C. Vazquez-Borrego, V. Gupta, A. Ibañez-Costa, M. D. Gahete, E. Venegas-Moreno, Á. Toledano-Delgado, D. A. Cano, C. Blanco-Acevedo, R. Ortega-Salas, M. A. Japon, A. Barrera-Martín, A. Vasiljevic, J. Hill, S. Zhang, H. Halem, J. Solivera, G. Raverot, M. A. Galvez, A. Soto-Moreno, M. Paez-Pereda, M. D. Culler, J. P. Castaño, R. M. Luque, *Clin. Cancer Res.* **2020**, *26*, 957–969.

[292] "Eurofins Scientific," can be found under https://www.eurofins.com/, **2021**.

[293] I. Lewis, W. Bauer, R. Albert, N. Chandramouli, J. Pless, G. Weckbecker, C. Bruns, *J. Med. Chem.* **2003**, *46*, 2334–2344.

[294] D. L. Medina, A. Ballabio, *Autophagy* **2015**, *11*, 970–971.

[295] K. Todkar, H. S. Ilamathi, M. Germain, *Front. Cell Dev. Biol.* **2017**, *5*, 106.

[296] C. Settembre, A. Fraldi, D. L. Medina, A. Ballabio, *Nat. Rev. Mol. Cell Biol.* **2013**, *14*, 283–296.

[297] A. Sun, *Ann. Transl. Med.* **2018**, *6*, 476.-476.

[298] G. Parenti, G. Andria, A. Ballabio, *Annu. Rev. Med.* **2015**, *66*, 471–486.

[299] R. H. Lachmann, F. M. Platt, *Expert Opin. Investig. Drugs* **2001**, *10*, 455–466.

[300] J. M. F. G. Aerts, C. E. M. Hollak, R. G. Boot, J. E. M. Groener, M. Maas, *J. Inherit. Metab. Dis.* **2006**, *29*, 449–456.

[301] J. A. Shayman, *Drugs Future* **2010**, *35*, 613–620.

[302] F. M. Platt, G. R. Neises, R. A. Dwek, T. D. Butters, *J. Biol. Chem.* **1994**, *269*, 8362–8365.

[303] H. Tucker, *Amide Derivatives*, **1984**, EP0100172.

[304] L. Thijs, R. Keltjens, B. Ettema, *Process for Making Bicalutamide and Intermediates Thereof*, **2003**, US20030073742A1.

[305] H. Tucker, G. J. Chesterson, *J. Med. Chem.* **1988**, *31*, 885–887.

[306] S. s. Jew, S. Terashima, K. Koga, *Tetrahedron* **1979**, *35*, 2337–2343.

[307] S.-S. Jew, S. Terashima, K. Koga, *Tetrahedron* **1979**, *35*, 2345–2352.

[308] J. T. Dalton, M. S. Steiner, R. Narayanan, S. Ahn, *A Method of Treating Androgen Receptor (AR)-Positive Breast Cancers with Selective Androgen Receptor Modulator (SARMS)*, **2014**, WO2014011220A2.

[309] B. Sörös, Z. Tuba, G. Gálik, Á. Bor, Á. Demeter, F. Trischler, J. Horváth, J. Brlik, *Process for the Synthesis of N-(4-Cyano-3-Trifluoromethylphenyl)-3-(4-Fluorophenylsulfonyl)-2-Hydroxy-2-Methyl-Propionamide*, **2001**, WO0100608A1.

[310] B.-Z. Dolitzky, O. Reany, J. Shammai, *Novel Process for Preparing and Isolating (Rac)-Bicalutamide and Its Intermediates*, **2004**, US20040044249A1.

[311] X. Zhou, J. Luo, J. Liu, S. Peng, G. J. Deng, *Org. Lett.* **2011**, *13*, 1432–1435.

[312] W. Chen, X. Zhou, F. Xiao, J. Luo, G. J. Deng, *Tetrahedron Lett.* **2012**, *53*, 4347–4350.

[313] G. Filippini, M. Silvi, P. Melchiorre, *Angew. Chemie - Int. Ed.* **2017**, *56*, 4447–4451.

[314] C. J. Li, B. M. Trost, *Proc. Natl. Acad. Sci. U. S. A.* **2008**, *105*, 13197–13202.

[315] ▇▇▇▇▇▇ ▇▇▇▇▇▇▇▇ ▇▇▇▇▇▇▇ ▇▇▇▇▇ ▇▇▇▇ ▇▇▇▇▇ ▇▇▇▇▇▇ ▇▇▇▇▇▇ ▇▇ ▇▇▇▇▇▇▇▇▇▇▇▇▇▇▇▇ ▇▇▇▇▇▇▇

Chapter 9

Annex

9 Annex

9.1 Green Solid-Phase Peptide Synthesis

9.1.1 Green solvent protocols

Table 9.1 Green SPPS protocols using 2-MeTHF or EtOAc[78]

	EtOAc / 2-MeTHF (protocol D)	2-MeTHF (protocol E)
1) Washing	1xEtOAc	1x2-MeTHF 3xEtOAc 1x2-MeTHF
2) Fmoc removal	20% piperidine/EtOAc 7 min	20% piperidine/2-MeTHF 7 min
3) Washing	1xEtOAc 1x2-MeTHF	1x2-MeTHF 3xEtOAc 1x2-MeTHF
4) Coupling	Fmoc-AA-OH/DIPCDI/OxymaPure (3:3:3 eq), 1h, 2-MeTHF	

Table 9.2 Green SPPS protocols using GVL (D) or NFM (E)[80]

	GVL (D)	NFM (E)
1) Washing	2xGVL	2xNFM
2) Fmoc removal	20% piperidine/GVL 1x1 min + 1x7 min	20% piperidine/NFM 1x1 min + 1x7 min
3) Washing	3xGVL	3xNFM
4) Coupling	Fmoc-AA-OH/DIPCDI/OxymaPure (3:3:3 eq), 1h	

Table 9.3 MW-assisted Green SPPS protocol with GVL[81]

	GVL (MW)
1) Fmoc removal	20% piperidine/GVL at 90ºC for 95 s
2) Coupling	Fmoc-AA-OH/DIPCDI/OxymaPure (5:5:5 eq) at 90ºC for 165s

Table 9.4 Green SPPS protocol with PC

	Propylene Carbonate (PC)
1) Washing	3xPC
2) Fmoc removal	20% piperidine/PC, 10 min + 20 min
3) Washing	3xPC
4) Coupling	Fmoc-AA-OH/HBTU/HOBt/DIEA (3: 3: 3: 6 eq), 2x1h, PC

Table 9.5 Green SPPS protocol using solvent mixtures of NBP/EtOAc[88]

	NBP/EtOAc
1) Washing	NBP/EtOAc 1:9, 45ºC, 4x5 min
2) Fmoc removal	5% NMPip in NBP/EtOAc 1:1, 45ºC, 2x15 min
3) Washing	NBP/EtOAc 1:9, 45ºC, 4x5 min
4) Coupling	Fmoc-AA-OH/DIPCDI/OxymaPure (1: 3: 1 eq) in NBP/EtOAc 1:1, 45ºC, 30 min

9.1.2 Green solvents

Table 9.6 Activation experiments with NFM

EXP	Resin	ACTIVATION	Pip-MP (%)
E3-60iii	MP1-TG	ACT8, GVL, 2x30 min	68.0
E3-61iv	MP1-TG	ACT8, PC, 2x30 min	69.3
E3-62i		ACT1, NFM, 2x1h	35.0
E3-62ii	MP1-TG	ACT3, NFM, 1x2h	49.2
E3-62iii		ACT6, NFM, 2x1h	29.7
E3-62iv		ACT8, NFM, 2x30 min	17.7

9.1.3 Screening of organic and inorganic bases

Table 9.7 Screening of tertiary amines

EXP	Resin	ACTIVATION	COUPLING	G-G-MP (%)	G-MP (%)
E1-90i	G-MP1-PS (E1-72)	ACT1, DCM, 2x2h	B + Et$_3$N	68.0	27.1
E1-92iv	G-MP1-PS (E1-72)	ACT1, DCM, 2x2h	B + DBU (1 eq)	19.4	36.5
E1-96i	G-MP1-PS (E1-94)	ACT1, DCM, 2x2h	B + Collidine	58.9	33.0
E1-99i	G-MP1-PS (E1-94)	ACT1, DCM, 2x2h	B + Me$_3$N	59.2	28.1
E1-99ii			B + Me$_3$N (5 eq)	60.7	28.4
E2-02i	G-MP1-PS (E1-94)	ACT1, DCM, 2x2h	B + LUT (5 eq)	57.8	35.2
E2-04i	G-MP1-PS (E1-94)	ACT1, DCM, 2x2h	B + NMM	59.7	36.4
E2-08i	G-MP1-PS (E1-94)	ACT1, DCM, 2x2h	B + DABCO	66.7	26.5
E2-10ii	G-MP1-PS (E1-94)	ACT1, DCM, 2x2h	B + NMPip (5 eq)	68.1	25.0
E2-63ii	G-MP1-PS (E2-52)	ACT3, DCM, 1x2h	B + Collidine (5 eq)	40.4	21.4
E2-63iv			B + LUT (5 eq)	37.6	21.3
E2-64i	G-MP1-PS (E2-52)	ACT3, DCM, 1x2h	B + NMM	45.6	19.3

Table 9.8 Experiments with inorganic bases

EXP	Resin	ACTIVATION	COUPLING	G-G-MP (%)	G-MP (%)
E2-27i	G-MP1-PS (E2-06i)	ACT1, DCM, 2x2h	B + NaHCO$_3$	69.8	24.0
E2-29i		ACT1, DCM, 2x2h	B + Na$_2$CO$_3$	68.9	24.1
E2-42iv		ACT1, DMF, 2x2h	B + NaHCO$_3$ (10 eq) + Na$_2$CO$_3$ (3 eq)	69.5	12.6
E2-46i	G-MP1-PS (E2-31)	ACT1, DMF, 2x2h	B + NaHCO$_3$ (1 eq) + Na$_2$CO$_3$ (10 eq)	72.4	9.0

9.1.4 Hydrolysis experiments

Table 9.9 Hydrolysis experiments

EXP	Resin	ACTIVATION	COUPLING	Pip-MP1 (%)				
				t_{0h}	t_{1h}	t_{3h}	t_{5h}	$t_{21.5h}$
E3-69i		ACT1, GVL, 2x1h	B + Et$_3$N (5eq)	60.9	27.3	18.8	16.1	0
E3-69ii			A	95.9	52.4	36.3	32.1	4.3
E3-77i		ACT3, PC, 1x2h	B + Et$_3$N (5eq)	93.5	72.8	64.7	60.1	52.2
E3-77ii	MP1-CM		A	98.2	85.1	78.9	75.7	62.9
E3-74i		ACT6, GVL, 2x1h	B + Et$_3$N (5eq)	47.6	11.0	8.9	6.0	3.8
E3-74ii			A	67.3	27.9	23.8	21.4	13.6
E3-73i		ACT8, DCM, 2x30 min	B + Et$_3$N (5eq)	24.3	6.6	0	0	0
E3-73ii			A	45.7	9.9	6.8	5.3	0

Table 9.10 Coupling rate experiments

EXP	Resin	ACTIVATION	COUPLING	G-MP1 (%)				
				t_{0h}	t_{1h}	t_{3h}	t_{5h}	$t_{21.5h}$
E3-78i		ACT1, GVL, 2x1h	B + Et$_3$N	45.8	82.5	81.9	81.9	81.9
E3-78ii			A	33.2	69.0	75.4	79.1	83.4
E3-81i		ACT3, PC, 1x2h	B + Et$_3$N	12.6	13.4	31.1	63.6	85.2
E3-81ii	MP1-CM		A	6.6	33.4	46.4	54.7	80.1
E3-79i		ACT6, GVL, 2x1h	B + Et$_3$N	50.1	70.8	69.7	70.7	70.5
E3-79ii			A	30.1	68.0	76.5	76.8	78.4
E3-80i		ACT8, DCM, 2x30 min	B + Et$_3$N	45.9	50.0	51.0	51.6	52.5
E3-80ii			A	40.4	45.7	48.4	51.9	52.6

9.2 Green solvent-mediated peptide acidolysis

9.2.1 Global cleavage/deprotection experiments

9.2.1.1 Standard procedures

Table 9.11 Mini-acidolysis experiments

Table 9.12 Mini-acidolysis experiments

#	Cocktail	Time (h)	Concentration (M)	ACMP1 (%)					
1									
2									
3									
5									
6									
7									
8									
9									
10									
11									
12									
13									
14									
15									
16									

9.3 Synthesis of Somatostatin Analogs

9.3.1 Development of Somatostatin analogs

Table 9.13 Synthesis of analogs A74 and A82

ID	Initial resin (g)	Final resin (g)	ΔMass (g)	Peptide mmol	Functionalization (mmol/g)
A74	2.0	7.18	5.18	1.82	0.91
A75	5.0	18.10	13.10	4.60	0.92
A76	2.5	10.59	8.09	2.89	1.15
A77	2.5	10.18	7.68	2.74	1.10
A78	2.5	10.88	8.38	2.99	1.20
A79	2.5	10.50	8.00	2.86	1.14
A80	2.5	10.40	7.90	2.82	1.13
A81	2.5	10.13	7.63	2.73	1.09
A82	2.0	7.52	5.52	1.92	0.96

Table 9.14 Oxidative cleavage and global deprotection of A74-A82

ID	OXIDATIVE CLEAVAGE		GLOBAL DEPROTECTION	
	Oxidized product (g)	Yield (%)	Crude (g)	Yield (%)
A74	5.60	107	3.11	102
A75	13.25	100	8.47	109
A76	8.04	132	5.59	118
A77	7.95	138	5.39	120
A78	7.52	119	4.87	99
A79	8.21	136	4.82	103
A80	8.40	141	5.85	127
A81	7.87	137	5.04	113
A82	5.66	122	3.92	120

Table 9.15 Purification and ion exchange of A74-A82

ID	PURIFICATION					ION EXCHANGE	
	Purification Method	Purification Column	Pure peptide (g)	Purity (%)	Recovery (%)	Acetate peptide (g)	Recovery (%)
A74	27%B in 30 min	MK9	0.73	98.6	23	0.66	91
A75	26%B in 30 min	MK9	2.77	98.5	32	2.29	84
A76	25%B in 30 min	NS17	0.80	99.3	14	0.69	86
A77	23%B in 35 min	NS17	1.63	99.3	31	1.43	88
A78	25%B in 30 min	NS17	0.81	96.9	17	0.70	87
A79	26%B in 25 min	NS17	2.03	97.7	42	1.78	88
A80	24%B in 28.5 min 25.5%B in 28.5-33 min	NS17	0.84	97.9	15	0.73	87
A81	24-36%B in 15 min 36%B in 15-32 min	NS17	0.85	98.2	17	0.68	81
A82	26%B in 25 min	NS17	0.81	99.5	21	0.71	87

9.3.2 Serum stability studies

Table 9.16 Stability studies of A46, A74 and A75

ID	Study	Method	Time points	Result (h)	Mean (h)
A46	**Previous[83a]**	20-80%B in 30 min	0h, 0.25h, 0.5h, 1h, 2h, 3h, 5h, 8h, 15.5h, 20h, 24h, 30h, 48h	24.6	-
	Previous[83b]	-	0h, 0.08h, 0.5h, 1h	0.45	-
	I	32%B in 30 min	0h, 0.25h, 0.5h, 0.75h, 1.0h	0.87	1.0
	II			1.11	
	III			1.08	
A74	**Previous[83b]**	-	0h, 0.08h, 0.17h, 0.5h, 1h, 2h, 8h, 30h, 48h	40.0	-
	I	31.5%B in 30 min	0h, 1h, 4h, 8h, 24h, 48h, 72h	56.1	-
	IIA		0h, 8h, 24h, 48h, 72h, 96h	43.6	53.8
	IIB			55.5	
	IIC			62.4	
A75	**I**	32%B in 30 min	0h, 3h, 6h, 24h, 72h, 96h	202.0	-
	IIA		0h, 72h, 120h, 168h, 240h, 288h	242.0	252.1
	IIB			241.2	
	IIC			273.2	

Table 9.17 Stability studies of A76 and A77

ID	Study	Method	Time points	Result (h)	Mean (h)
A76	**I**	30%B in 30 min	0h, 1h, 4h, 8h, 24h, 48h, 72h	2.6	-
	IIA		0h, 0.5h, 1.5h, 3h, 4h, 6h	1.0	1.1
	IIB			1.1	
	IIC			1.2	
A77	**I**	28%B in 30 min	0h, 1h, 4h, 8h, 24h, 48h, 72h	52.4	-
	IIA		0h, 8h, 24h, 48h, 72h, 96h	46.1	48.1
	IIB			49.9	
	IIC			48.3	

---

83 a) Performed by Dr. Marc Gómez[23]; b) Performed by Dr. Anna Escolà[26].

Table 9.18 Stability studies of A78 and A79

ID	Study	Method	Time points	Result (h)	Mean (h)
A78	I		0h, 1h, 4h, 8h, 24h, 48h, 72h	140.6	-
	IIA	30%B in 30 min		38.9	
	IIB		0h, 24h, 96h, 144h, 192h, 264h	35.4	36.7
	IIC			35.8	
A79	I		0h, 1h, 4h, 8h, 24h, 48h, 72h	331.6	-
	IIA	31%B in 30 min		520.4	
	IIB		0h, 96h, 168h, 264h, 336h, 408h, 480h	353.7	410.9
	IIC			358.6	

Table 9.19 Stability studies of A80 and A81

ID	Study	Method	Time points	Result (h)	Mean (h)
A80	I		0h, 1h, 4h, 8h, 24h, 48h, 72h	42.0	-
	IIA	28%B in 30 min		58.2	
	IIB		0h, 8h, 24h, 48h, 72h, 96h	55.7	56.7
	IIC			56.2	
A81	I		0h, 1h, 4h, 8h, 24h, 48h, 72h	104.2	-
	IIA	27.5%B in 30 min		164.5	
	IIB		0h, 24h, 96h, 120h, 144h, 192h	197.8	174.9
	IIC			162.4	

Table 9.20 Stability studies of A45 and A82

ID	Study	Method	Time points	Result (h)	Mean (h)
A45	**Previous[84]**	20-80%B in 30 min	0h, 0.25h, 0.5h, 1h, 2h, 3h, 5h, 8h, 15.5h, 20h, 24h, 30h, 48h	26.2	-
	I	32%B in 30 min	0h, 1h, 1.5h, 2h, 2.5h, 3h	1.5	-
A82	I		0h, 1h, 4h, 8h, 24h, 48h, 72h	75.0	-
	IIA	31%B in 30 min		112.3	
	IIB		0h, 24h, 48h, 72h, 80h, 96h, 104h	86.9	95.2
	IIC			86.5	

---

[84] Performed by Dr. Marc Gómez[23].

9.3.3 Metabolite studies
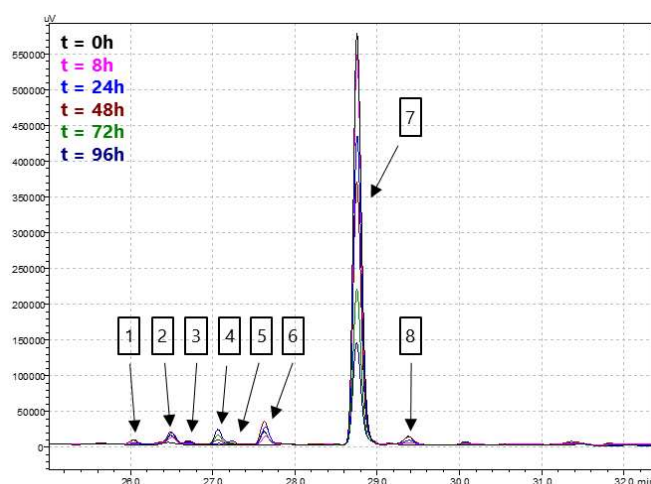
Figure 9.1 Metabolites of A74

Table 9.21 Metabolites of A74

#	t_R[85a] (min)	MS (amu)	Type of peak	MW (g/mol)	t_i[85b] (h)	Fragment Identification
1	25.3	776.2	$[M+2H]^{2+}$	1551.8	24	**des[D-Ala^1,Gly^2]-A74**
2	25.8	641.4	$[M+2H]^{2+}$	1282.5	8	**des[D-Trp^8,Lys^9,Thr^{10}]-A74**
3	26.0	685.4	$[M+2H]^{2+}$	685.8	24	**des[Asn^5,Phe^6,Msa^7,D-Trp^8,Lys^9,Thr^{10},Phe^{11}]-A74**
4	26.4	623.4	$[M+H]^+$	622.8	24	**Msa^7-D-Trp^8-Lys^9-Thr^{10}**
5	26.6	1031.5	$[M+H]^+$	1031.2	72	**Asn^5-Phe^6-Msa^7-D-Trp^8-Lys^9-Thr^{10}-Phe^{11}**
6	27.0	849.7	$[M+2H]^{2+}$	1698.0	8	**A74+H$_2$O (opening between Phe^6-Msa^7)**
7	28.2	840.9	$[M+2H]^{2+}$	1680.0	-	**A74**
8	28.8	1248.0	$[M+H]^+$	1247.5	24	**des[Asn^5,Phe^6,Msa^7]-A74**

Table 9.22 Metabolites of A76

#	t_R (min)	MS (amu)	Type of peak	MW (g/mol)	t_i (h)	Fragment Identification
1	13.2	755.3	$[M+2H]^{2+}$	1509.8	1.5	**des[D-Ala^1,Gly^2]-A76**
2	13.7	1567.4	$[M+H]^+$	1566.8	0	**des[D-Ala^1]-A76**
3	14.2	1047.0	$[M+H]^+$	1047.2	0.5	**des[Phe^6,Phe^7,Trp^8,Lys^9]-A76**
4	14.9	845.5	$[M+H]^+$	845.0	1.5	**des[Phe^7,Trp^8,Lys^9,Thr^{10},Phe^{11},Thr^{12}]-A76**
5	17.2	805.3	$[M+2H]^{2+}$	804.9	1.0	**des[Lys^4,Asn^5,Phe^6,Phe^7,Trp^8,Lys^9]-A76**
6	21.1	627.6	$[M+H]^+$	626.8	1.5	**Phe^6-Phe^7-Trp^8-Lys^9**
7	22.9	829.0	$[M+H]^+$	829.0	0	**Phe^7-Trp^8-Lys^9-Thr^{10}-Phe^{11}-Thr^{12}**
8	24.2	828.9	$[M+2H]^{2+}$	1656.0	0.5	**A76+H$_2$O (opening between Phe^7-Trp^8)**
9	25.0	916.9	$[M+H]^+$	916.0	0.5	**Phe^7-Trp^8-Lys^9-Thr^{10}-Phe^{11}-Thr^{12}-Ser^{13}**
10	25.9	869.6	$[M+H]^+$	869.0	0.5	**Lys^4-Asn^5-Phe^6-Phe^7-Trp^8-Lys^9**
11	27.1	819.8	$[M+2H]^{2+}$	1638.0	-	**A76**

---

[85] a) Retention time of the metabolite; b) Time point of the stability study in which the metabolite is detected.

Table 9.23 Metabolites of A77

#	t_R (min)	MS (amu)	Type of peak	MW (g/mol)	t_i (h)	Fragment Identification
1	15.5	1341.0	$[M+H]^+$	1341.5	24	des[D-Trp^8,Lys^9]-A77
2	16.2	976.6	$[M+H]^+$	727.9	0	Phe^6-Phe^7-D-Trp^8-Lys^9-Thr^{10}-Phe^{11}-Thr^{12}
3a	22.1	1194.4	$[M+H]^+$	1194.3	0	des[Phe^7,D-Trp^8,Lys^9]-A77
3b	22.2	1177.1	$[M+H]^+$	1177.3		Asn^5-Phe^6-Phe^7-D-Trp^8-Lys^9-Thr^{10}-Phe^{11}-Thr^{12}-Ser^{13}
4	32.7	581.4	$[M+H]^+$	580.7	8	Phe^7-D-Trp^8-Lys^9-Thr^{10}
5	32.9	845.2	$[M+H]^+$	845.0	24	des[Phe^7,D-Trp^8,Lys^9,Thr^{10},Phe^{11},Thr^{12}]-A77
6	33.6	829.3	$[M+H]^+$	829.0	8	Phe^7-D-Trp^8-Lys^9-Thr^{10}-Phe^{11}-Thr^{12}
7	34.5	704.5	$[M+H]^+$	703.8	24	des[Lys^4,Asn^5,Phe^6,Phe^7,D-Trp^8,Lys^9,Thr^{10}]-A77
8	34.6	1093.1	$[M+H]^+$	1093.2	8	des[Phe^7,D-Trp^8,Lys^9,Thr^{10}]-A77
9	35.1	1219.2	$[M+H]^+$	1219.4	24	des[Thr^{10},Phe^{11},Thr^{12},Ser^{13}]-A77
10	39.9	819.7	$[M+2H]^{2+}$	1637.9	-	A77
11	41.9	1061.7	$[M+H]^+$	1061.2	24	des[Asn^5,Phe^6,Phe^7,D-Trp^8]-A77

Table 9.24 Metabolites of A79

#	t_R (min)	MS (amu)	Type of peak	MW (g/mol)	t_i (h)	Fragment Identification
1	9.8	627.1	$[M+H]^+$	626.8	0	D-Phe^6-Phe^7-D-Trp^8-Lys^9
2	16.6	771.2	$[M+2H]^{2+}$	1541.8	336	des[Asn^5]-A79
3	17.2	754.6	$[M+2H]^{2+}$	1508.7	0	des[Phe^7]-A79
4	17.3	1047.2	$[M+H]^+$	1047.2	0	des[D-Phe^6,Phe^7,D-Trp^8,Lys^9]-A79
5	27.9	819.7	$[M+2H]^{2+}$	1637.9	-	A79
6	28.2	832.6	$[M+H]^+$	832.0	96	des[Asn^5,D-Phe^6,Phe^7,D-Trp^8,Lys^9,Thr^{10}]-A79
7	28.5	784.5	$[M+2H]^{2+}$	1568.8	0	des[Ser^{13}]-A79
8	28.6	842.0	$[M+H]^+$	842.0	96	Asn^5-D-Phe^6-Phe^7-D-Trp^8-Lys^9-Thr^{10}
9	29.1	1509.5	$[M+H]^+$	1509.8	168	des[D-Ala^1,Gly^2]-A79

Table 9.25 Metabolites of A80

#	t_R (min)	MS (amu)	Type of peak	MW (g/mol)	t_i (h)	Fragment Identification
1	13.3	624.3	$[M+2H]^{2+}$	1247.5	8	des[Asn^5,Phe^6,Phe^7]-A80
2	13.8	783.9	$[M+2H]^{2+}$	1566.8	0	des[D-Ala^1]-A80
3	14.5	754.6	$[M+2H]^{2+}$	1508.7	0	des[Phe^6]-A80
4	14.9	869.7	$[M+H]^+$	869.0	24	Lys^4-Asn^5-Phe^6-Phe^7-Trp^8-Lys^9
5	15.2	805.4	$[M+H]^+$	804.9	24	des[Lys^4,Asn^5,Phe^6,Phe^7,Trp^8,Lys^9]-A80
6	15.5	829.2	$[M+H]^+$	829.0	24	Phe^7-Trp^8-Lys^9-D-Thr^{10}-Phe^{11}-Thr^{12}
7	16.0	1218.0	$[M+H]^+$	1218.4	24	Lys^4-Asn^5-Phe^6-Phe^7-Trp^8-Lys^9-D-Thr^{10}-Phe^{11}-Thr^{12}
8	16.3	1240.3	$[M+H]^+$	1238.4	72	des[Trp^8,Lys^9,D-Thr^{10}]-A80
9	17.2	1047.2	$[M+H]^+$	1047.2	0	des[Phe^6,Phe^7,Trp^8,Lys^9]-A80
10	18.7	1413.1	$[M+H]^+$	1413.6	8	des[Lys^4,Asn^5]-A80
11	19.7	532.2	$[M+2H]^{2+}$	1063.2	8	Phe^6-Phe^7-Trp^8-Lys^9-D-Thr^{10}-Phe^{11}-Thr^{12}-Ser^{13}
12	26.0	819.7	$[M+2H]^{2+}$	1637.9	-	A80
13	26.2	784.9	$[M+2H]^{2+}$	1568.8	24	des[Ser^{13}]-A80

Table 9.26 Metabolites of A81

#	t_R (min)	MS (amu)	Type of peak	MW (g/mol)	t_i (h)	Fragment Identification
1	13.4	611.3	$[M+H]^+$	610.7	24	des[Phe^6,Phe^7,D-Trp^8,Lys^9,D-Thr^{10},Phe^{11},Thr^{12},Ser^{13}]-A81
2	13.8	685.0	$[M+H]^+$	684.8	24	des[Asn^5,Phe^6,Phe^7,D-Trp^8,Lys^9,D-Thr^{10},Phe^{11}]-A81
3	17.2	755.2	$[M+2H]^{2+}$	1509.8	0	des[D-Ala^1,Gly^2]-A81
4	22.2	989.5	$[M+H]^+$	989.1	24	Asn^5-Phe^6-Phe^7-D-Trp^8-Lys^9-D-Thr^{10}-Phe^{11}
5	23.3	1175.8	$[M+H]^+$	1175.3	24	des[Phe^6,Phe^7,D-Trp^8]-A81
6	24.5	799.4	$[M+H]^+$	798.9	96	des[Phe^6,Phe^7,D-Trp^8,Lys^9,D-Thr^{10},Phe^{11}]-A81
7	25.7	819.9	$[M+2H]^{2+}$	1637.9	-	A81
8a	25.8	869.8	$[M+H]^+$	869.0	24	Lys^4-Asn^5-Phe^6-Phe^7-D-Trp^8-Lys^9
8b	25.9	613.2	$[M+H]^+$	612.7	96	Asn^5-Phe^6-Phe^7-D-Trp^8
9	26.2	624.0	$[M+2H]^{2+}$	1247.5	96	des[Asn^5,Phe^6,Phe^7]-A81
10	27.4	1061.5	$[M+H]^+$	1061.2	96	des[Asn^5,Phe^6,Phe^7,D-Trp^8]-A81

Table 9.27 Metabolites of A82

#	t_R (min)	MS (amu)	Type of peak	MW (g/mol)	t_i (h)	Fragment Identification
1	12.7	884.8	$[M+H]^+$	884.0	48	Asn^5-Msa^6-Phe^7-D-Trp^8-Lys^9-Thr^{10}
2	13.1	988.1	$[M+H]^+$	988.1	0	des[Phe^7,D-Trp^8,Lys^9,Thr^{10},Phe^{11}]-A82
3	13.3	685.5	$[M+H]^+$	684.8	24	des[Asn^5,Msa^6,Phe7,D-Trp^8,Lys^9,Thr^{10},Phe^{11}]-A82
4	24.7	1132.0	$[M+H]^+$	1132.3	24	Asn^5-Msa^6-Phe7-D-Trp^8-Lys^9-Thr^{10}-Phe^{11}-Thr^{12}
5	25.0	682.2	$[M+H]^+$	681.8	48	D-Trp^8-Lys^9-Thr^{10}-Phe^{11}-Thr^{12}
6	26.1	1550.8	$[M+H]^+$	1550.8	24	des[Phe^7]-A82 or des[Phe^{11}]-A82
7	27.5	840.7	$[M+2H]^{2+}$	1680.0	-	A82

9.4 Synthesis of (*S*)-Bicalutamide

9.4.1 (*S*)-Bromoamide optimization

Table 9.28 Synthesis conditions of (S)-bromoamide (5-14) experiments

SYNTHESIS		E6-116	E6-130	E6-160	E6-168
(*S*)-bromoacid	Eq	1.2	1.2	1.2	1.2
(5-13)	Mass (g)	5.9	23.6	5.9	64.8
Aniline	Eq	1.0	1.0	1.0	1.0
(5-4)	Mass (g)	5.0	20.0	5.0	54.9
Stirring SOCl$_2$ (h)[86]		2.0	2.0	2.8	2.6
Stirring aniline (5-4) (min)[86]		10	10	20	30
Stirring Et$_3$N (min)[86]		10	10	10	30
Reflux time (h)		13	15	18	16

---

[86] Stirring time after the addition of the corresponding reagent.

Table 9.29 Purification conditions of (S)-bromoamide (5-14) experiments

PURIFICATION		E6-116	E6-130	E6-160	E6-168
Discoloration	**Time (h)**	18[87]	4.3[87]	4.0[88]	2.0[89]
1st Recrystallization	**Initial crude (g)**	10.3	-	11.7	134.2
	Toluene (mL)	10	25	7	70
	Product (g)	7.9	27.1	6.5	79.8
	Yield (%)	84	72	69	77
	Purity (%)[90]	98.95	-	98.73	99.20
	5-21 (%)	0	-	0	0
	5-30 (%)	0	-	0	0
2nd Recrystallization	**Solvent**	IPA/H_2O	IPA/H_2O	Toluene	-
	Product (g)	5.1	19.5	3.9	-
	Yield (%)	64	52	41	-
	Purity (%)	95.76	96.58	98.27	-
	5-21 (%)	0.13	0.07	0	-
	5-30 (%)	0.09	0.06	0	-
3rd Recrystallization	**Solvent**	IPA/H_2O	IPA/H_2O	-	-
	Product (g)	4.0	10.2	-	-
	Yield (%)	-	27	-	-
	Purity (%)	93.45	94.87	-	-
	5-21 (%)	0.64	0.54	-	-
	5-30 (%)	0.78	0.57	-	-

9.4.2 4-fluorobenzenesulfinate optimization

Table 9.30 Synthesis conditions of 4-fluorobenzenesulfinate (5-9) experiments

	SYNTHESIS	E6-124	E6-136	E6-174	E6-184	E6-188	E6-190
Sulfonyl (5-23)	**Eq**	1.0	1.0	1.0	1.0	1.0	1.0
	Mass(g)	20.0	10.0	30.0	10.0	10.0	205.0
	Distributor	Sigma-Aldrich		Fluorochem			T&W Group[91]
	Purity (%)	99.03		99.46			98.71
	5-28 (%)	0.96		Not detected			0.51
Eq Na_2SO_3		1.0	1.2	1.2	1.2	1.2	1.2
Eq Na_2CO_3		2.0	1.2	1.2	1.2	1.2	1.2
H_2O volumes		9	9	9	4.5	4.5	4.5
Heating time (h)		18	18	16	14.5	17	16.5

---

[87] Total time of discoloration performed at the same time as the recrystallizations with IPA/H_2O.

[88] Total time of discoloration performed at the same time as the recrystallizations with toluene.

[89] Discoloration time performed on the organic phase (EtOAc) of the work-up.

[90] (*S*)-bromoamide (**5-14**) HPLC: 45%B in 30 min (A: H_2O+0.1% TFA; B: ACN+0.07%TFA); t_R = 16.3 min.

[91] Although Fluorochem 4-fluoro sulfonyl (**5-23**) was selected as the best, we had already bought a big quantity of starting material from T&W Group. As a consequence, we used that 205.0 g batch from T&W Group only to increase the scale of the reaction.

Table 9.31 Purification conditions of 4-fluorobenzenesulfinate (5-9) experiments

PURIFICATION		E6-124	E6-136	E6-174	E6-184	E6-188	E6-190
EtOH	**Volume (mL)**	400	200	900	300	150	6000
	Stirring time (h)	1.3	0.5	1.0	1.5	1.5	16
ACN	**Volume (mL)**	100	75	170	90	90	1200
	Stirring time (h)	14	0.5	0.3	4.0	1.0	0.5
Product	**Mass (g)**	18.3	8.3	28.0	9.4	4.9	185.4
	Yield (%)	98	89	100	100	52	99
	Purity (%)[92]	97.70	98.03	-	99.90	-	98.97
	5-28 (%)	-	-	-	0	-	0.16

9.4.3 (*S*)-Bicalutamide optimization

Table 9.32 Synthesis conditions of (S)-bicalutamide (5-1) experiments

SYNTHESIS		E6-140	E6-156	E6-178	E6-186	E6-193	E6-195
(*S*)-bromoamide (5-14)	**Eq**	1.0	1.0	1.0	1.0	1.0	1.0
	Mass (g)	2.2	2.2	9.7	6.0	2.9	60.8
	Batch	E6-130		E6-168			
	Purity (%)	93.39		99.20			
Sulfinate (5-9)	**Eq**	3.0	5.0	5.4	3.0	3.0	3.0
	Mass (g)	3.4	5.7	27.5	9.4	4.5	94.5
	Batch	E6-124		E6-174	E6-184	E6-188	E6-190
	Purity (%)	97.31		-	99.89	-	98.97
	5-28 (%)	-		-	0	-	0.16
Eq TEBAC		1.1	1.1	2.0	1.1	1.1	1.1
Eq Na₂HPO₄		3.0	3.0	5.4	3.0	3.0	3.0
H₂O volumes		5.0	3.2	4.0	4.0	4.0	4.0
Temperatue (ºC)		115	110	100	80	100	100
Reflux time (h)		15	20	25	17	1	1

---

[92] Sulfinate (**5-23**) HPLC: 5-85%B in 20 min (A: H_2O+0.1%TFA; B: ACN+0.07%TFA); t_R = 11.7 min.

Table 9.33 Purification conditions of (S)-bicalutamide (5-1) experiments[93]

PURIFICATION		E6-140	E6-156	E6-178	E6-186	E6-193	E6-195
Work-up	**Procedure**	-	A + C	D	C	D	D
	Discoloration (h)	2.0	2.0	0.5	-	2.0	2.0
	Mass (g)	-	2.3	15.3	7.1	3.7	92.5
	Yield (%)	-	87	> 100	97	> 100	> 100
	Purity (%)	-	81.53	-	-	80.61	74.54
	5-27 (%)	-	0.51	-	-	0	0
	5-21 (%)	-	13.29	-	-	12.3	10.51
1st Recrystallization	**Procedure**	A	B	B	B	B	B
	Mass (g)	2.0	1.6	11.5	5.0	2.4	51.3
	Yield (%)	84	59	96	68	66	69
	Purity (%)	93.88	99.00	-	99.24	98.62	98.94
	5-27 (%)	0.56	0.57	-	0	0	0
	5-21 (%)	4.09	0.19	-	0.19	0.19	0.31
2nd Recrystallization	**Procedure**	B	-	B	-	-	-
	Mass (g)	1.7	-	11.1	-	-	-
	Yield (%)	63	-	92	-	-	-
	Purity (%)	99.22	-	99.90	-	-	-
	5-27 (%)	0.55	-	0	-	-	-
	5-21 (%)	0.08	-	0	-	-	-

9.4.4 Impurity B synthesis

Table 9.34 Synthesis and purification conditions of ortho-fluoro sulfinate (5-28) experiment

SYNTHESIS		E6-148	PURIFICATION		E6-148
***ortho*-fluoro sulfonyl (5-29)**	**Eq**	1.0	**EtOH**	**Volume (mL)**	140
	Mass(g)	4.5		**Stirring time (h)**	0.5
	Distributor	Sigma-Aldrich	**ACN**	**Volume (mL)**	40
	Purity (%)	100.00		**Stirring time (h)**	0.5
Eq Na$_2$SO$_3$		1.2	**Product**	**Mass (g)**	3.9
Eq Na$_2$CO$_3$		1.2		**Yield (%)**	93
H$_2$O volumes		9.0		**Purity (%)[94]**	99.69
Heating time (h)		22			

Table 9.35 Synthesis and purification conditions of impurity B (5-27) experiment

SYNTHESIS		E6-164	PURIFICATION		E6-164
(*S*)-bromoamide (5-14)	**Eq**	1.0	**Work-up**	**Procedure**	C
	Mass (g)	1.2			
	Batch	E6-130		**Mass (g)**	1.4
	Purity (%)	94.94			
***ortho*-fluoro sulfinate (5-28)**	**Eq**	3.0	**Column chromatography**	**Eluents**	Hexane/ EtOAc
	Mass	1.9			
	Batch	E6-148		**Mass (g)**	0.8
Eq TEBAC		1.1			
Eq Na$_2$HPO$_4$		3.0		**Yield (%)**	57
H$_2$O volumes		3.2			
Temperature (ºC)		100		**Purity (%)**	96.94
Reflux time (h)		20			

---

[93] **Procedure A**: discoloration/recrystallization using IPA/H$_2$O (same methodology as in the initial synthesis from section 5.3.1). **Procedure B**: recrystallization using IPA/H$_2$O (detailed in the text). **Procedure C**: product extraction with EtOAc. **Procedure D**: product extraction with EtOAc and discoloration with active carbon.
[94] *Ortho*-fluoro sulfinate (**5-28**) HPLC: 8%B in 30 min (A: H$_2$O+0.1%TFA; B: ACN+0.07%TFA); t$_R$ = 14.1 min

9.4.5 (*S*)-Bicalutamide recrystallization

Table 9.36 Final purification of (S)-bicalutamide (5-1)

FINAL PURIFICATION			E6-198					E7-058
	Batch	E6-140	E6-178	E6-186	E6-193	E6-195	E6-198	
Previous Batches	**Mass (g)**	1.3	8.0	4.9	2.2	51.3	65.7	
	Purity (%)	99.22	99.90	99.24	98.62	98.94	99.65	
	5-27 (%)	0.55	0	0	0	0	0	
	5-21 (%)	0.08	0	0.19	0.19	0.31	0	
	Total mass (g)	67.7						-
Recrystallization	**IPA/H$_2$O**	1:1.63						1:1.38
	Mass (g)	65.7						63.4
	Purity (%)	99.65						99.79
	5-27 (%)	0						0
	5-21 (%)	0						0
	Dehydratation *E/Z* **(5-31) (%)**	0.15						0.06
	(*S*)-bicalutamide + sulfinate (5-26) (%)	-						0.14